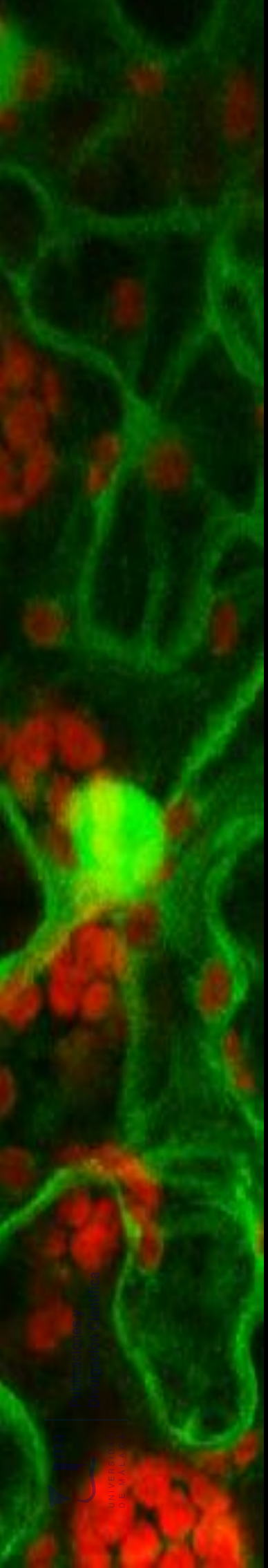

Universidad de Málaga
Dpto. Biología Celular, Genética y Fisiología
Área de Genética

Functional Analysis of *Pseudomonas savastanoi* pv. savastanoi Type III Secretion System Effectors

Mª del Pilar Castañeda Ojeda

TESIS DOCTORAL

Septiembre 2014

Publicaciones y
Divulgación Científica

AUTOR: María del Pilar Castañeda Ojeda

EDITA: Publicaciones y Divulgación Científica. Universidad de Málaga

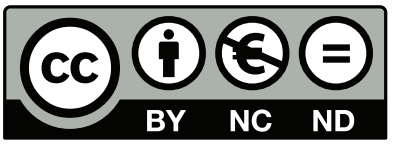

Memoria presentada por

Mª del Pilar Castañeda Ojeda

para optar al grado de Doctora por la Universidad de Málaga

Functional Analysis of *Pseudomonas savastanoi* pv. savastanoi Type III Secretion System Effectors

Directores:

Dr. Cayo J. Ramos Rodríguez

Catedrático. Área de Genética
Departamento de Biología Celular, Genética y Fisiología.
Universidad de Málaga
Instituto de Hortofruticultura Subtropical y Mediterránea "La Mayora" (IHSM)

Dra. Emilia López Solanilla

Profesora Titular Bioquímica y Biología Molecular.
Departamento de Biotecnología.
Universidad Politécnica de Madrid
Centro de Biotecnología y Genómica de Plantas (CBGP).

Universidad de Málaga
Málaga, 2014

COMITÉ EVALUADOR

Presidente

Dr. José Manuel Palacios Alberti
Departamento de Biotecnología
Centro de Biotecnología y Genómica de Plantas (CBGP)
Universidad Politécnica de Madrid

Secretario

Dr. Javier Ruíz Albert
Departamento de Biología Celular, Genética y Fisiología
Instituto de Hortofruticultura Subtropical y Mediterránea (IHSM)
Universidad de Málaga

Vocales

Dra. Carmen Beuzón López
Departamento de Biología Celular, Genética y Fisiología
Instituto de Hortofruticultura Subtropical y Mediterránea (IHSM)
Universidad de Málaga

Dra. Mª Trinidad Gallegos Fernández
Departamento de Protección Ambiental
Estación Experimental del Zaidín (CSIC), Granada

Dra. Lucia Jordá Miró
Departamento de Biotecnología
Centro de Biotecnología y Genómica de Plantas (CBGP)
Universidad Politécnica de Madrid

Suplentes

Dr. José Juan Rodríguez Herva
Departamento de Biotecnología
Centro de Biotecnología y Genómica de Plantas (CBGP)
Universidad Politécnica de Madrid

Dr. Francisco Cazorla López
Departamento de Microbiología
Instituto de Hortofruticultura Subtropical y Mediterránea (IHSM)
Universidad de Málaga

Área de Genética.
Departamento de Biología Celular, Genética y Fisiología.
Instituto de Hortofruticultura Subtropical y Mediterránea (IHSM).
Universidad de Málaga-Consejo Superior de Investigaciones Científicas.

Dr. **CAYO J. RAMOS RODRÍGUEZ**, Catedrático del Área de Genética del Departamento de Biología Celular, Genética y Fisiología de la Universidad de Málaga, y
Dra. **EMILIA LÓPEZ SOLANILLA**, Profesora Titular del Departamento de Biotecnología de la Universidad Politécnica de Madrid y Centro de Biotecnología y Genómica de Plantas (CBGP),

INFORMAN:

Que, **Mª DEL PILAR CASTAÑEDA OJEDA** ha realizado en este Departamento y bajo su dirección el trabajo titulado "Functional Analysis of *Pseudomonas savastanoi* pv. savastanoi Type III Secretion System Effectors", que constituye su memoria de Tesis Doctoral para aspirar al grado de Doctora en Biología.

Y para que así conste, y tenga los efectos que correspondan, en cumplimiento de la legislación vigente, extienden el presente informe.

En Málaga, a 7 de Julio de 2014.

Fdo. Cayo J. Ramos Rodríguez

Fdo. Emilia López Solanilla

A mis padres y hermanos

A Alejandro

AGRADECIMIENTOS

Ha llegado el momento de echar la vista atrás, de recordar todo lo que he vivido en esta etapa de mi vida que comenzó en Septiembre de 2008. En esa fecha se hacía realidad un sueño, comenzaba la aventura que supone una Tesis Doctoral. En aquel momento, bien es cierto, que no sabía toda la dedicación que iba a requerir ni la "montaña rusa" de emociones que viviría. En estos años, han sido muchas las cosas que he aprendido y muchos los momentos, buenos y no tan buenos, que he pasado en el laboratorio…pero como en toda gran aventura, no hay solo un protagonista; y ésta no hubiese sido posible llevarla a cabo sin esos grandes compañeros/amigos con los que he podido compartirla. Después de las muchas horas que pasamos en el laboratorio hemos llegado a formar una gran familia pero, como pasa en las mejores familias, hemos vivido todo tipo de emociones juntos: alguna que otra regañina y momentos de bajón, pero yo prefiero quedarme con todas las alegrías, risas y abrazos en grupo (que siempre vienen genial). Por ello quiero aprovechar este apartado de mi Tesis para agradecerles a todos ellos que formen parte de mi vida.

En primer lugar quiero agradecerle a Cayo, mi director de Tesis, que confiase en mí y me diese la oportunidad de formar parte de su grupo de investigación. Gracias por haberme guiado en mi carrera científica, por haber sabido encaminar esta Tesis y sacar una bonita historia. Gracias por encontrar qué era lo que más me gustaba y dirigir el trabajo en esa dirección. Y gracias por todo el tiempo que has invertido en enseñarme y en discutir resultados conmigo. Sin ti, este trabajo no sería lo que es ni yo la investigadora en la que me has convertido.

Así mismo, quiero darle las gracias a Emilia, mi otra directora de Tesis, por adoptarme en su grupo en todas las ocasiones que han sido necesarias y hacerme sentir un miembro más de él. Gracias por recibirme siempre con los brazos abiertos, por todo lo que me has enseñado y por estar siempre dispuesta a echarme una mano. Y, por supuesto, gracias por haberme cuidado tanto durante mis estancias en Madrid.

A mis compañeros de laboratorio, con los que tanto tiempo he pasado y tan buenos recuerdos me llevo. Gracias a Luis y a Mely por el tiempo que hemos compartido. Gracias a Isa*X* por todo lo que me enseñaste en mis comienzos en el laboratorio. A Clara, que aunque no hemos coincidido mucho, si que hemos tenido y seguiremos teniendo muchos ratitos de charlita. A IsaP (Pepa, Pepita, Pepis…), gracias por esa alegría con la que inundas todos los días el lab. A Eloy, nuestro sevillano "apretao", gracias por esas "peleillas" en el lab como consecuencia de los apodos *chonis* que nos pones y por estar siempre dispuesto a ayudar. A Chiara, mi italiana loca, con la que tanto me he reído en estos meses mientras intentaba enseñarme italiano y a la que tanto voy a echar de menos cuando se vuelva con la mafia *calabresa*. A Nachete, porque para mí sigues siendo parte de

nuestro laboratorio, gracias por ser como eres. Quién nos iba a decir cuando empezamos la carrera que acabaríamos siendo compañeros de lab…. A nuestros tres pequeños pupilos, Alba, Kim y Adri, gracias por esa energía renovada que traéis y el entusiasmo que mostráis ante todo lo que se os enseña. Y por último a la persona con la que más cosas he compartido, a mi Aragón; gracias por todos los momentos que hemos pasado juntas, porque siempre has estado ahí para ayudarme y escucharme, por los consejos que me has dado en todo este tiempo y por ser una gran amiga. Gracias también a mis otros compañeros de laboratorio, los del lab 285 del CBGP. Gracias a Mariela por su apoyo técnico en el laboratorio. A Pedro, mi sevillano favorito, por venir cada día con una gran sonrisa a darme un abrazo de buenos días y por amenizar las comidas contando chistes (que, aunque contados con gracia, la mayoría son malísimos…), pero sobre todo, gracias porque me llevo un gran amigo. Gracias a Chechu, por la minuciosidad con la que me has explicado las cosas y por estar dispuesto en todo momento a ayudarme y escucharme. Y sobre todo, a Isa, mi Fachima, gracias por compartir conmigo los momentos más divertidos de la Tesis y por ser el regalo más valioso que me llevo de esta etapa. Por último agradecer a Israel, que aunque no es parte de ninguno de mis dos grupos de investigación, ha sido para mí un gran apoyo durante mis estancias en Madrid. Gracias por todos esos ratos que hemos pasado fuera del CBGP, por contagiarme ese entusiasmo que tienes por nuestro trabajo, por aconsejarme cuando lo he necesitado y por saber sacarme una sonrisa cuando he tenido un mal día. En definitiva, gracias por ser como eres.

A los que forman parte del T3SS *group*: Adeli, gracias por todo el tiempo que hemos compartido en el lab y por estar siempre dispuesta ayudarme en lo profesional y en lo personal. A mi Ainhoichis, a la que echo mucho de menos, gracias por tu alegría, por los abrazos de madre y por esas "charletas" tan divertidas que tenemos. A Diego, poseedor durante poco tiempo del título *last mokey*, eres un gran descubrimiento. Gracias por todos los ratos de risas que hemos compartido y por tus visitas durante mi etapa de exilio para escribir la Tesis. Gracias por tu amistad y por animarme en todo momento. A Spy, *Chuck Norris of proteins, thanks for your good mood everyday and for being willing to help me*. A mi Josico, mi Abelino, mi amigo en todo momento…gracias por todos los buenos ratos que hemos compartido y que seguiremos compartiendo, por las discusiones científicas, los consejos sobre experimentos (¡aunque luego haga lo que me parezca!) y por hacer que ni la distancia sea capaz de distanciarnos.

Al chico del laboratorio del fondo, Luis, nuestro friki en mil y un aspectos. Gracias por hacerme reír siempre, por las comidas temáticas, los video-blogs y las sesiones de "Luis enseña, Luis divierte y Luis entretiene". Y a tu señora esposa, Laura, que es también parte de éste grupo. Gracias por estar también ahí.

Al resto de mis compañeros del área de Genética, a los que siguen por aquí y a los que ya se fueron, Nati, Juanjo, Inma O., Manolo, Tábata, Ana Luna…gracias por todos los momentos que hemos compartido.

A los profesores del área de Genética, Carmen, Javi, Eduardo, Araceli, Ana Grande, Enrique, Julia y Guillermo. Gracias por todo lo que me enseñasteis durante la carrera, por lo que he podido aprender de vosotros como científicos y por estar siempre dispuestos a echarme una mano. También a los profesores del departamento de Microbiología, Francis, Antonio, Alejandro, Juan Antonio Torés y Diego Romero. Así como, a los chicos del grupo de Micro: Guti, Victor, Jesús, Houda, Conchita, Carmen, Davinia, Laura, Nuria, Eva, María, Joaquín, Álvaro, Codina y, por supuesto a, Clau y David. Gracias por todas las charlas, los consejos y las ideas que me habéis dado en los seminarios de grupo. Sois un gran grupo.

A Pablo Rodríguez Palenzuela, gracias por sus consejos científicos, y a Pablo González Melendi, por sus consejos sobre microscopía y todas esas horas que nos hemos pasado en el confocal.

A David Navas, gracias por tu ayuda en todo lo relacionado con la microscopia. A Araceli Barceló y Eli Imbroda, por vuestra ayuda en el mantenimiento de las plantas. A Jose Manuel Pulido, por el cuidado que tiene con los invernaderos de "La Mayora" y de nuestros olivos adultos.

A mis amigos de fuera del laboratorio, Rocío, Manolo, Vero y María, gracias por estar siempre ahí, por intentar entender mi trabajo aunque a la mayoría os resultase difícil. A Cande, por su apoyo, porque siempre ha estado ahí para levantarme el ánimo y llevarme de cerves o de compras según el estado de ánimo. A Amparo, mi valenciana favorita, gracias por la sonrisa que consigues sacarme cada mañana con tu mail de "buenos días". Gracias por tu amistad y por tu apoyo incondicional. A Mar, porque han sido muchos los momentos que hemos compartido durante la carrera y el máster y, aunque la Tesis te llevó "*my-weapon-land*", siempre he podido contar contigo. Por último a mis mejores amigos, Tete e Inma, por estar siempre a mi lado, escucharme, animarme y quererme. Gracias por formar parte de mi vida y dejarme formar parte de la vuestra. Os quiero mucho.

A mi familia, porque sin entender muy bien a qué me dedico siempre me habéis preguntado por "Sebastián" y por cómo intentamos curar a los olivos. A mis padres, Pilar y Fernando, por darme la educación que me han dado y por los esfuerzos que han hecho para que hoy esté aquí escribiendo el último apartado del manuscrito de mi Tesis Doctoral. Gracias por animarme a que comenzase esta aventura y por inculcarme que con esfuerzo y perseverancia todo se consigue. A

mis hermanos, Fer, gracias por apoyarme en cada momento de mi vida y por tener siempre listo un “hermanita, claro que puedes”. Y a Elena, mi siamesa y compi de piso, gracias por todo lo que me has cuidado en este tiempo.

Y por último, a ti, Alejandro, que incluso en la distancia has vivido esta Tesis tan intensamente como yo. Gracias por estar a mi lado cada día durante estos 11 años, por apoyarme en cada momento, por decirme siempre lo orgulloso que estas de mí y por animarme a que siguiese adelante cuando he tenido ganas de tirar la toalla. Gracias por cada momento que hemos vivido juntos, por llenar mi vida de nuevos planes, de ilusión y de alegría. Y sobre todo por quererme como me quieres. Gracias por ésto y por todo. Te quiero.

"La ciencia se compone de errores,

que a su vez son los pasos hacia la verdad"

Julio Verne

Este trabajo ha sido financiado por los proyectos AGL2008-05311 y AGL2011-30343-C02-01 del Plan Nacional I+D del Ministerio de Economía y Competitividad (cofinanciado por FEDER) y por la Beca para la Formación de Personal Investigador (FPI) (2009-2013).

ÍNDICE

PREFACIO

Esta Tesis Doctoral se dirigió inicialmente al análisis genómico y funcional de los efectores del sistema de secreción tipo III de codificación plasmídica en *Pseudomonas savastanoi* pv. savastanoi NCPPB 3335. Durante el desarrollo de la misma, y derivado del establecimiento de diferentes colaboraciones, en paralelo se llevó a cabo el estudio de la interacción de comunidades bacterianas en el desarrollo y/o establecimiento de la tuberculosis del olivo, resultados que se publicaron en Passos da Silva et al., (2014). A su vez, se colaboró también en la identificación de cepas de *P. savastanoi* aisladas de plantas de *Mandevilla sanderi* (Dipladenia) que mostraban halos cloróticos en hojas y tumores en tallos (Eltlbany et al., 2012). Los resultados obtenidos en este sentido no se han incorporado en el cuerpo de esta Tesis Doctoral, si bien, las publicaciones científicas derivadas de los mismos, se han incluido en el Anexo 1.

Tras la secuenciación del genoma de *P. savastanoi* pv. savastanoi NCPPB 3335, la identificación del conjunto de posibles efectores codificados en la misma, y el establecimiento de esta cepa como modelo para el estudio de interacciones de *Pseudomonas* patógenas con plantas leñosas, esta Tesis se centro en el análisis funcional de los efectores del sistema de secreción tipo III. Los resultados obtenidos en este sentido se presentan en los tres capítulos incluidos en este documento. Así mismo, esta Tesis Doctoral incluye un apartado en el que se describe el material y métodos generales usados en los diferentes capítulos, si bien, cada capítulo incluye adicionalmente su material y métodos específicos. Este trabajo se realizó principalmente en la Universidad de Málaga, aunque durante su ejecución, se llevaron a cabo cuatro estancias de aproximadamente tres meses cada una en otros centros de investigación, tres en el grupo de la Dra. Emilia López Solanilla (Centro de Biotecnología y Genómica de Plantas, CBGP-UPM-INIA, Madrid), directora de esta Tesis Doctoral junto el Dr. Cayo Ramos de la Universidad de Málaga, y otra en el grupo del Dr. Rafael Giraldo (Centro de Investigaciones Biológicas, CSIC; Madrid). Recientemente, y en colaboración con el Dr. Jesús Murillo (Universidad Pública de Navarra), la Dra. Emilia López Solanilla y el Dr. Pablo Rodríguez Palenzuela, este último también perteneciente al CBGP (Madrid), se ha publicado un artículo en la revista *Molecular Plant-Microbe Interactions* (MPMI), titulado *Translocation and Functional Analysis of Pseudomonas savastanoi* pv. savastanoi NCPPB 3335 *Type III Secretion System Effectors Reveals Two Novel Effector Families of the Pseudomonas syringae Complex* (Matas et al., 2014). De este artículo, también incluido en el Anexo I, se han extraído los resultados relacionados con la interacción de siete efectores del sistema de secreción tipo III de *P. savastanoi* pv. savastanoi con los sistemas de defensa de la planta. Estos resultados se presentan en el capítulo 1 (***Chapter I***). Los resultados mostrados en los capítulos II y III (***Chapters* II and III**), se están preparando actualmente para su publicación.

ABBREVIATIONS

A

ANOVA: Analysis of variance
Ap: Ampicillin
A.tumefaciens: Agrobacterium tumefaciens
ASAP: A systematic annotation package

B

BLAST: Basic local alignment search tool
bp(s): Base pais(s)

C

cDNA: Complementary DNA
CFU: Coloni-forming units
CI: Competitive Index
Ck: cytokinin
Cm: Chloramphenicol
Cya: adenylate cyclase

D

DMSO: Dimethyl sulfoxide
dpi: days post-inoculation

E

E. coli: *Escherichia coli*
EDTA: Ethylenediaminetetraacetic acid

G

GFP: Green fluorescent protein
Gm: Gentamycin

H

h: hour(s)
Hop: hrp-dependent outer protein
HR: Hypersensitive response
hrc: hypersensitive response conserved
hrp: hypersensitive response and pathogenesis

I

IAA: Indole acetic acid

K

Kb: Kilobase
Km: Kanamycin
KB: King B medium

L

L: Litres
LB: Luria-Bertani

M

MEGA5: Molecular evolutionary genetics analysis
mL: Mililitre(s)
M: Molar
mM: Milimolar
min: Minute(s)

N

NCBI: National center for biotechnology information
NCPPB: National collection of plant pathogenic bacteria
Nf: Nitrofurantoin
ng: Nanograms
nt(s): Nucleotides

O

OD: Optical Density
o/n: Overnight
ORF: Open Reading Frame

P

PCR: Polymerase Chain Reaction
Pph: *Pseudomonas syringae* pv. phaseolicola
Psv: *Pseudomonas savastanoi* pv. savastanoi
Pto: *Pseudomonas syringae* pv. tomato
pv.: pathovar

Q

qRT-PCR: Quantitative Real time PCR

R

R gene: Resistance gene
Rif: Rifampicin
RNA: Ribonucleic acid
Rpm: Revolutions per minute

S

Sec: second(s)
Sm: Streptomycin
SOB: Super Optimal Broth medium
Sp: Spectinomycin

T

TAE: Tis-Acetate EDTA
TBE: Tris-Borate EDTA
Tc: Tetracycline
T3SS: Sistema de secreción tipo III
T3E: Efectores del T3SS

RESUMEN

Los efectores (T3E) del sistema de secreción tipo III (T3SS) son factores de virulencia esenciales en la interacción de bacterias fitopatógenas con sus hospedadores, debido a que: (i) promueven la penetración y permanencia del patógeno en el tejido del hospedador, (ii) interfieren con las respuestas de defensa de las plantas y (iii) facilitan el acceso a los nutrientes, promoviendo la proliferación y el crecimiento del patógeno (Gohre and Robatzek, 2008). La secuenciación y análisis de los genomas de diferentes cepas pertenecientes al complejo *Pseudomonas syringae*, ha permitido identificar el catálogo de T3E hipotéticos de cada una de ellas, así como clasificarlos en más de 60 familias génicas que constituyen el pangenoma de este relevante complejo de bacterias fitopatógenas (http://www.pseudomonassyringae.org/) (Baltrus et al., 2011; Lindeberg et al., 2012). Aunque la función concreta de la mayoría de los T3E identificados hasta la fecha en la interferencia con los mecanismos de defensa de la planta es aún desconocida, durante los últimos años se han producido grandes avances en el conocimiento del papel de los T3E del complejo *P. syringae* durante la interacción con plantas herbáceas. Estudios recientes, han establecido a *Pseudomonas savastanoi* pv. savastanoi NCPPB 3335 como una cepa modelo en el estudio de la interacción de este complejo bacteriano con plantas leñosas (Ramos et al., 2012). El análisis bioinformático del borrador del genoma de esta cepa identificó 33 posibles T3E (Rodriguez-Palenzuela et al., 2010; Ramos et al., 2012), cuya translocación a través del T3SS se demostró para 7 de ellos (AvrRpm2, HopA1, HopAA1, HopAZ1, HopBK1, HopBL1 y HopBL2) durante el desarrollo de esta Tesis Doctoral (Matas et al., 2014). Además, la secuenciación de los tres plásmidos de esta cepa reveló que los genes codificantes de los T3E HopAF1 y HopAO1 se localizan en los plásmidos pPsv48A y pPsv48B, respectivamente, codificándose en el cromosoma un homólogo de HopAF1 (HopAF1-2). Teniendo en cuenta estos antecedentes, el objetivo principal que se planteó en esta Tesis Doctoral fue el análisis funcional de los T3E de NCPPB 3335, prestando mayor atención a las familias HopAF y HopAO. Para llevar a cabo este objetivo general, se plantearon los siguientes abordajes: 1) estudiar la distribución de los efectores de las familias HopAF y HopAO en los patovares de *P. savastanoi* y *P. syringae*, 2) analizar la translocación a través del T3SS de NCPPB 3335 y el papel en virulencia de los efectores de las familias HopAF y HopAO y, 3) analizar la interacción con los sistemas de defensa de la planta de los siete efectores de NCPPB 3335 cuya translocación a través del sistema de secreción tipo III ha sido demostrada, así como de los pertenecientes a las familias HopAF y HopAO.

El análisis bioinformático y filogenético de las familias HopAF y HopAO permitió identificar que ambas se encuentran ampliamente distribuidas dentro del complejo *P. syringae*, si bien, *P. savastanoi* pv. savastanoi NCPPB 3335 codifica dos genes de la familia *hopAO* (*hopAO1* y *hopAO2*) y tres genes de la familia *hopAF* (dos copias del gen *hopAF1* y una del gen *hopAF1-2*). La filogenia de esta última familia reveló que el alelo *hopAF1* se codifica mayoritariamente en cepas patógenas de plantas leñosas. Análisis de translocación y transcripcionales validaron a los

T3E HopAF1, HopAF1-2, HopAO1 y HopAO2 como nuevos T3E del secretoma del T3SS de NCPPB 3335. Por otra parte, en este trabajo hemos demostrado que tanto los T3E AvrRpm2, HopBK1, HopBL1, HopBL2, HopAF1, HopAF1-2, HopAO1 y HopAO2, así como los efectores truncados HopAA1 y HopAZ1, interfieren con la respuesta de defensa primaria (PTI) de *Nicotiana tabacum*. Además, presentamos evidencias de que HopAZ1, HopBL1, HopAF1-2, HopAO1 y HopAO2 también inhiben la inmunidad mediada por efectores (ETI) en este mismo hospedador. Por otro lado, y utilizando fusiones traduccionales a la proteína verde fluorescente (GFP), hemos podido comprobar que los T3E HopAF1, HopAF1-2, HopAO1 y HopAO2 se localizan en la membrana plasmática de las células de *Nicotiana benthamiana*, así como que HopAO2 también se localiza en vesículas del aparato de Golgi.

Con el fin de averiguar el papel de los T3E HopAF1 y HopAO1 en la virulencia de NCPPB 3335 se construyeron mutantes simples de los mismos. La deleción del gen *hopAF1* del plásmido pPsv48A en NCPPB 3335 tuvo como consecuencia una ligera reducción en el tamaño de los tumores inducidos por este patógeno en plantas de olivo lignificadas, mientras que la deleción del gen *hopAO1* conllevó una clara disminución de la virulencia del mismo.

Los resultados incluidos en esta Tesis Doctoral, convierten a NCPPB 3335 en la cuarta cepa del complejo *P. syringae* cuyo secretoma del T3SS incluye un mayor número de T3E demostrados, y en la primera cepa aislada de un hospedador leñoso.

INTRODUCCIÓN GENERAL

1. *Pseudomonas syringae* y patógenos relacionados

El complejo formado por *Pseudomonas syringae* y especies relacionadas, entre las que se encuentra *Pseudomonas savastanoi*, está formado por un grupo de bacterias fitopatógenas Gram (-) con gran importancia desde el punto de vista económico y agrícola debido a la reaparición de enfermedades como el moteado del tomate (producido por *P. syringae* pv. tomato) y la aparición de nuevas enfermedades como el chancro del castaño de indias (producido por *P. syringae* pv. aesculi) (Mansfield et al., 2012). Los patovares (pv.) que conforman el complejo *P. syringae* presentan una gran variabilidad en cuanto a su capacidad de supervivencia epifita y rango de huésped, dado que infectan tanto plantas herbáceas como leñosas. Los síntomas que producen también son muy variados, pudiendo inducir moteados y necrosis en hojas, podredumbre de frutos, tumores y chancros en tallos, entre otros (Westcott and Horst, 1990; Bender et al., 1999; Fatmi et al., 2008).

Desde el año 1978 hasta la actualidad, la clasificación del género *Pseudomonas* ha sufrido numerosas modificaciones. En el año 1978, todas las cepas del género *Pseudomonas* patógenas de plantas, fluorescentes y oxidasa negativas se englobaron dentro de la especie *P. syringae* (Young et al., 1978). Posteriormente, se produjo una reclasificación de la especie *P. syringae*, atendiendo tanto a análisis bioquímicos, serológicos y patológicos, como a hibridaciones DNA-DNA llevadas a cabo entre cepas incluidas en *P. syringae* subespecie (subsp.) *syringae* y *P. syringae* subsp. *savastanoi*. Tras estas nuevas reordenaciones, *P. savastanoi* se elevó al rango de especie, dentro de la cual se incluyeron los pv. savastanoi (olivo), glycinea (soja), phaseolicola (judía), fraxini (fresno), nerii (adelfa) y retacarpa (retama) (Gardan et al., 1992; Young, 2004). En la actualidad, la mayor parte de la comunidad científica se refiere a los pv. phaseolicola y glycinea como *P. syringae* pv. phaseolicola (Pph) y *P. syringae* pv. glycinea (Pgy), respectivamente, siendo ampliamente aceptada la inclusión de los pv. savastanoi (Psv), nerii (Psn), retacarpa y fraxini dentro de la especie *P. savastanoi*. En este trabajo se ha empleado la nomenclatura aceptada por gran parte de la comunidad científica que, como se ha mencionado, incluye a los pv. phaseolicola y glycinea dentro de la especie *P. syringae*.

Actualmente, en el complejo *P. syringae* se incluyen más de 60 patovares según su especificidad de huésped y el origen de su aislamiento (Young, 2010; Parkinson et al., 2011). Además, el análisis de hibridaciones DNA-DNA entre patovares de *P. syringae* llevó a la clasificación de este complejo en 9 genomoespecies diferentes (Gardan et al., 1999; Scortichini and Marcelletti, 2014). Estos grupos taxonómicos concuerdan con los filogrupos en los que se han clasificado posteriormente los patovares de *P. syringae* y *P. savastanoi* mediante tipificación multilocus de secuencias (Baltrus et al., 2011). El uso de estas aproximaciones ha permitido emparentar filogenéticamente a *P. savastanoi* pv. savastanoi NCPPB 3335 con *P. syringae* pv.

aesculi (cepas 2250 y NCPPB 3681), *P. syringae* pv. tabaci ATC 11528 y *P. syringae* pv. phaseolicola 1448A (Sarkar and Guttman, 2004; Parkinson et al., 2011).

2. Pseudomonas savastanoi

En este trabajo, se incluyen en la especie *P. savastanoi* a cepas productoras de tumores o excrecencias en las partes aéreas de plantas leñosas. De este modo, el pv. savastanoi incluye cepas aisladas de tumores de olivo; el pv. nerii aislados de tumores de adelfa, el pv. retacarpa de tumores de retama y el pv. fraxini aislados de excrecencias en tallos de fresno (Figura 1). Recientemente, se ha descrito el aislamiento de cepas pertenecientes a la especie *P. savastanoi* de un nuevo huésped, *Mandevilla sanderi* (Dipladenia), las cuales inducen necrosis y halos cloróticos en hojas, así como tumores en el tallo de estas plantas. En este estudio, el aislado Ph3 procedente de *M. sanderi* se emparentó filogenéticamente con los pv. nerii y savastanoi (Eltlbany et al., 2012). Debido a la relevancia que tiene *P. savastanoi* pv. savastanoi en este trabajo, el resto de este apartado se dedica a los aspectos relacionados con la interacción de las cepas pertenecientes a este patovar con el olivo.

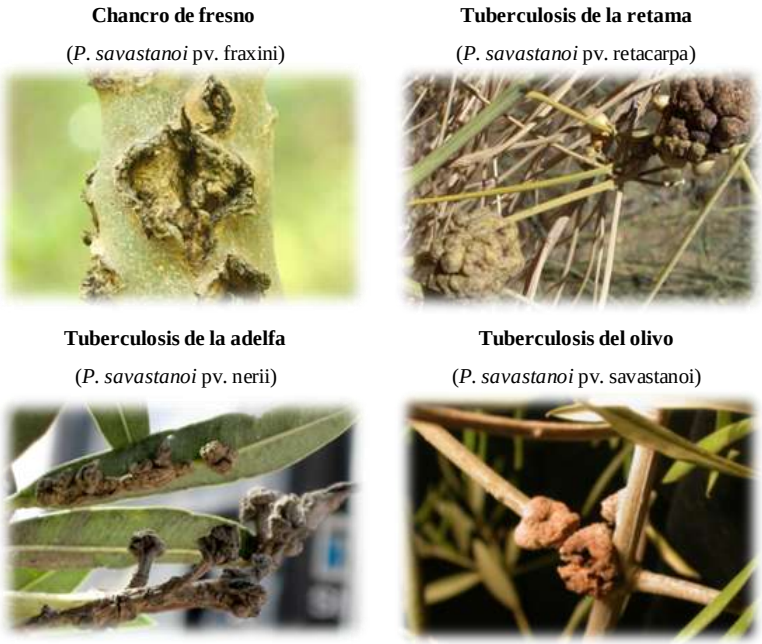

Figura 1. Sintomatología producida en la parte aérea de plantas leñosas infectadas por los diferentes patovares pertenecientes a la especie *P. savastanoi*.

2.1. Tuberculosis del olivo

La primera referencia histórica que se tiene de las enfermedades del olivo se encuentra en el libro *De Historia et de ausis plantarum* del filosofo griego Teofrasto (siglo IV a.C.). En él se

denomina tuberculosis o "verruga" del olivo, a la enfermedad producida en los olivos por Psv, también conocida como roña o agalla del olivo. Sin embargo, no es hasta 1887-1889 cuando Luigi Savastano describe la etiología bacteriana de la tuberculosis del olivo (Smith, 1920; Scortichini et al., 2004).

El termino tuberculosis hace referencia a los síntomas típicos de la enfermedad, que son tumores formados en troncos, ramas, brotes y, con menor frecuencia e intensidad, en las hojas, raíces y frutos de las plantas infectadas (Figura 2) (Kennelly et al., 2007). Los brotes y ramas jóvenes del olivo son las partes más afectadas. Los tumores formados son, generalmente, redondeados y de tamaño variable (desde mm a cm de diámetro). Tanto el vigor de los olivos, como el crecimiento y la producción de aceitunas, pueden verse moderada o severamente reducidos por la enfermedad (Schroth et al., 1973; Quesada et al., 2010).

La tuberculosis del olivo, es una enfermedad que se encuentra presente en casi todas las regiones olivícolas del mundo. Generalmente, su incidencia depende de la localización geográfica y de la variedad vegetal. Aunque actualmente no existe una estimación precisa de las pérdidas que ocasiona, se considera una de las enfermedades más importantes que afectan al cultivo del olivo (Young, 2004).

Figura 2. Sintomatología característica de la tuberculosis del olivo. Tumores producidos por *P. savastanoi* pv. savastanoi en una rama de olivo (A) y en una planta de olivo de un año de edad tras una infección artificial (B). Las flechas rojas indican la localización de algunos tumores presentes en la rama de olivo.

2.2. Ciclo de la enfermedad

Psv presenta un ciclo de vida epifítico/patógeno. En la etapa epífita, Psv coloniza la superficie de tallos y hojas por igual, alcanzando las mayores densidades bacterianas en los meses cálidos y lluviosos. La población se ve significativamente reducida en épocas calurosas y secas (Quesada et al., 2007). Además, se ha encontrado una relación directa entre el número de bacterias epífitas y el número de tumores desarrollados en los árboles infectados. Por otro lado, también se sabe que Psv es capaz de diseminarse a corta distancia (Quesada et al., 2009).

Durante la etapa patogénica, Psv se multiplica en los tejidos vegetales, alcanzando diferentes máximos poblacionales dependiendo de la susceptibilidad del cultivar (Varvaro and Surico, 1978). El aumento de la población bacteriana se traduce en una rápida proliferación del cambium y la

generación de un tumor, en el que se diferencian elementos del xilema y floema más o menos organizados (Surico, 1977). Cuando el tumor es viejo, las células vegetales pueden colapsar y formar cavidades que contienen gran cantidad de bacterias. Estas cavidades, alcanzan la superficie del tumor en forma de fisuras y favorece la salida de bacterias al exterior (Smith, 1920; Surico, 1977).

2.3. Control de la enfermedad

Los métodos más destacados para el control de esta enfermedad son los productos químicos de origen cúprico, habiéndose observado experimentalmente una reducción significativa en el número de tumores en plantas tratadas en comparación con los controles sin tratar (Quesada et al., 2010). Además, se ha descrito que la bacteriocina producida por *P. syringae* pv. ciccaronei es capaz de inhibir el crecimiento de Psv tanto en medio de cultivo como *in planta*, viéndose afectada la supervivencia del patógeno en las hojas y ramas de los árboles tratados (Lavermicocca et al., 2000; Lavermicocca et al., 2002). Por otro lado, también se ha abordado el control biológico de este patógeno utilizando *Pseudomonas* no patógenas y antagonistas de Psv aisladas de la rizosfera del olivo (Zadeh et al., 2008). Recientemente, una cepa de *Pseudomonas fluorescens* PICF7 aislada de raíz de olivo se ha descrito como agente efectivo en el biocontrol de la verticilosis (Mercado-Blanco et al., 2004) y potencial agente de biocontrol de la tuberculosis del olivo. Esta cepa, no es capaz de suprimir completamente el desarrollo de tumores inducidos por Psv, aunque su co-inoculación con el patógeno provoca una disminución de la población de Psv *in planta*, y en consecuencia, la formación de tumores con una disminución de los síntomas necróticos y una alteración de la colonización del tejido hiperplásico por el patógeno (Maldonado-González et al., 2013).

2.4. Factores de virulencia en *P. savastanoi*

Pese a que es conocido que la tuberculosis del olivo es de origen bacteriano desde hace más un siglo (Savastano, 1886), los factores moleculares que intervienen en la interacción de Psv con su huésped no se han estudiado tan exhaustivamente como en otros patovares del complejo *P. syringae*. Los factores de patogenicidad y virulencia mejor estudiados hasta le fecha en *P. savastanoi* son la síntesis y liberación en el tejido vegetal de las fitohormonas ácido indol-3-acético (IAA) y citoquininas (Ck) y el sistema de secreción tipo III (T3SS). Dada la relevancia de estos factores en el proceso de infección de olivo por Psv, en los apartados siguientes se describen de forma más detallada. Además, también se ha descrito que Psv presenta *in vitro* actividad celulasa, celobiasa, xilanasa y pectinasa (Magie, 1963). Estas actividades degradativas, se han propuesto como posible causa de la formación de cavidades o fisuras dentro de los tejidos tumorales, originadas por degradación de las paredes de las células vegetales (Wilson and Magie, 1964; Rodríguez-Moreno et al., 2009).

El análisis bioinformático del borrador del genoma de la cepa de Psv NCPPB 3335 permitió la identificación del arsenal de posibles factores de virulencia en este patógeno (Rodriguez-Palenzuela et al., 2010). Posteriormente, y utilizando un método de análisis genómico funcional, muchos de estos posibles factores de virulencia se confirmaron en nuestro grupo de investigación. En total, se identificaron 58 genes de NCPPB 3335 necesarios para la colonización de tumores de olivo, permitiendo la descripción de nuevos factores de virulencia en este patógeno. Además de genes implicados en el metabolismo requerido por NCPPB 3335 para colonizar el tejido vegetal, entre los que se encuentran los responsables de la biosíntesis de 9 de los 20 aminoácidos que componen las proteínas y de 3 vitaminas, se identificaron genes implicados en la degradación de compuestos aromáticos y en el transporte de compuestos abundantes en el apoplasto, como son el citrato, el glutamato y el sulfato. Entre los nuevos factores de virulencia descritos, cabe destacar los genes del sistema de secreción tipo II (T2SS) y tipo IV (T4SS), enzimas involucradas en la tolerancia y detoxificación de especies reactivas de oxígeno (ROS) y genes implicados en la biosíntesis de pared celular o en la regulación de los niveles del segundo mensajero di-GMPc (Matas et al., 2012).

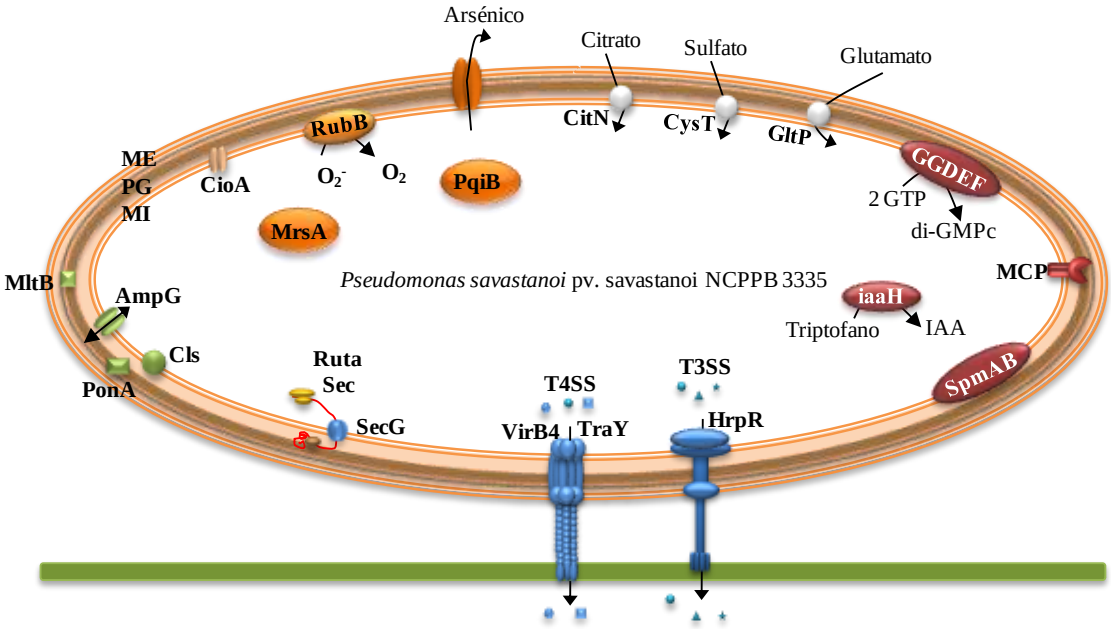

Figura 6. Representación esquemática de los mecanismos de virulencia en *Pseudomonas savastanoi* pv. savastanoi. ME, membrana externa; PG, peptidoglicano; MI, membrana interna; T3SS, sistema de secreción tipo III; T4SS, sistema de secreción tipo IV; MCP, quimioreceptores; GGDEF, proteínas con dominio GGDEF/EAL; IAA, ácido indol-3-acético. Adaptado de Matas et al., 2012.

2.4.1. Producción de fitohormonas en *P. savastanoi*

El IAA y las CK producidas por Psv inducen la división del tejido infectado, así como la diferenciación de células del parénquima en elementos traqueales del xilema y tubos cribosos del floema (Smidt and Kosuge, 1978; Comai and Kosuge, 1980, 1982; Surico et al., 1985; Morris, 1986; Iacobellis et al., 1994). La producción de IAA en *P. savastanoi* se lleva a cabo del siguiente modo: en primer lugar, el triptófano se convierte en indolacetamida (IAM) mediante la enzima triptófano monooxigenasa (codificada por el gen *iaaM*). Posteriormente, el IAM pasa a IAA mediante la actividad de la indolacetamida hidrolasa (producto del gen *iaaH*) (Magie, 1963; Kosuge et al., 1966). Además, los aislados de *P. savastanoi* pv. nerii son capaces de transformar el IAA en el conjugado IAA-lisina (IAA-Lys) mediante la actividad (indol-3-acetil-)-L-lisina sintetasa (codificada por el gen *iaaL*) (Hutzinger and Kosuge, 1968) (Figura 3).

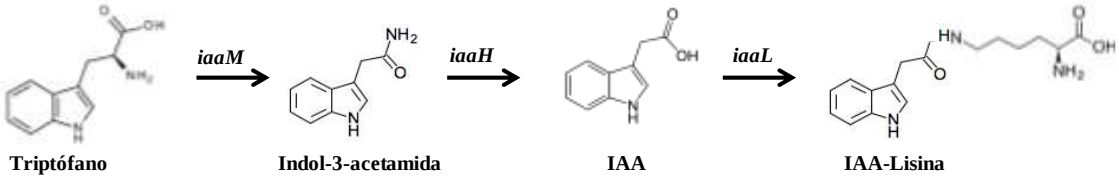

Figura 3. Ruta de biosíntesis de auxinas en cepas de *P. savastanoi*.

En concreto, la cepa de Psv NCPPB 3335 contiene dos alelos de los genes *iaaM* e *iaaH*, ambos organizados en forma de operón (*iaaMH*-1 e *iaaMH*-2) y de localización cromosómica (Pérez-Martínez et al., 2010; Rodríguez-Palenzuela et al., 2010). Estudios recientes han demostrado que solamente el operón *iaaMH*-1 contribuye a la cantidad total de IAA producido por NCPPB 3335. Además, mutantes en el operón *iaaMH*-1 o en los dos operones (mutante Δ*iaaMH*-1.2) presentan una disminución la virulencia de NCPPB 3335 en plantas de olivo, así como una disminución de la competitividad en planta en comparación con la cepa silvestre (Aragón et al., 2014).

Aunque la producción de Ck está extendida entre las bacterias fitopatógenas productoras de tumores (Morris, 1986), su ruta biosintética no ha sido caracterizada en detalle. Esta ruta parece constar de dos pasos: 1) mediante la enzima isopentenil transferasa se transforma el adenosín monofosfato (AMP) a isopentenil adenina e isopentenil adenosina y, 2) ambas moléculas sufren un proceso de hidroxilación originando trans-zeatina y trans-ribosilzeatina. En *P. savastanoi*, el único gen descrito en la producción de Ck es *ptz* (*Pseudomonas* trans zeatin) (Morris, 1986; Powell and Morris, 1986), de localización tanto plasmídica como cromosómica en aislados de olivo y adelfa (Macdonald et al., 1986; Powell and Morris, 1986; Iacobellis et al., 1994; Caponero et al., 1995; Pérez-Martínez et al., 2008). Estudios realizados en NCPPB 3335, cepa portadora de tres plásmidos de alto peso molecular (pPsv48A, pPsv48B y pPsv48C), demuestran que la cepa curada del plásmido pPsv48A, donde se localiza el gen *ptz*, induce síntomas atenuados en plantas

de olivo *in vitro*, aunque es capaz de multiplicarse en el interior de los tejidos de olivo de forma idéntica a la cepa silvestre (Bardaji et al., 2011).

En resumen, las fitohormonas juegan un papel muy importante en la virulencia de las bacterias fitopatógenas, incluida la cepa Psv NCPPB 3335 (Bardaji et al., 2011; Aragón et al., 2014). En el caso de NCPPB 3335, el IAA actúa también como molécula señalizadora, dado que su adición exógena a un cultivo de esta cepa conlleva una disminución de la expresión de genes del T3SS y un aumento de la expresión del sistema de secreción tipo VI (T6SS) (Aragón et al., 2014).

3. El sistema de secreción tipo III (T3SS)

El T3SS está presente en la mayoría de los patógenos Gram (-) de plantas y animales. Consiste en una jeringa molecular a través de la cual la bacteria inyecta proteínas, denominadas efectores (T3E), del citoplasma bacteriano al interior de la célula hospedadora (Fig. 4). Este sistema, se ha descrito como un factor de patogenicidad en *P. syrintae* pv. tomato DC3000 y muchas otras bacterias Gram (-). En ausencia del T3SS, no se produce la liberación de T3E, los cuales estimulan o interfieren con los procesos celulares del hospedador, dictando de esta manera los términos de la interacción bacteria-hospedador (Galan and Collmer, 1999; Buttner and He, 2009). En el caso de bacterias fitopatógenas, el T3SS está involucrado tanto en el desarrollo de enfermedades en hospedadores susceptibles como en el desencadenamiento de la muerte celular programada, también denominada respuesta hipersensible (HR), en hospedadores resistentes (Cornelis and Van Gijsegem, 2000). Las interacciones que se producen entre el patógeno y el hospedador se pueden clasificar en tres tipos: incompatible, compatible y *non-host*. En una interacción incompatible, el hospedador posee genes de resistencia (R) (Van der Biezen and Jones, 1998) cuyos productos proteicos reconocen, directa o indirectamente, a determinados T3E del patógeno, y en consecuencia, se induce la respuesta de defensa del hospedador (hospedador resistente) produciéndose una limitación del crecimiento del patógeno en la planta y el desencadenamiento de una HR. En una interacción compatible, al carecer el hospedador de genes R específicos (hospedador susceptible), el patógeno será capaz de infectar y se desarrollará una enfermedad (Dangl and Jones, 2001; Tao et al., 2003; Jones and Dangl, 2006). La interacción *non-host* entre bacterias y plantas hace referencia a la resistencia que muestra una especie de planta frente a todas las variantes genéticas de una bacteria que sí es patogénica en otras especies vegetales. En ocasiones esta interacción se acompaña de síntomas macroscópicos que en algunos casos son similares a la HR (Mysore and Ryu, 2004; Li et al., 2005b). Generalmente, este tipo de resistencia suele darse entre patógenos poco adaptados a hospedadores concretos, e implica a las barreras de defensa constitutivas de la planta, tal como la expresión de compuestos antimicrobianos o la rigidez de la pared celular, como a la activación de determinados elementos

de defensa (Kamoun et al., 1999; Heath, 2000; Thordal-Christensen, 2003; Nürnberger and Lipka, 2005; Gohre and Robatzek, 2008)

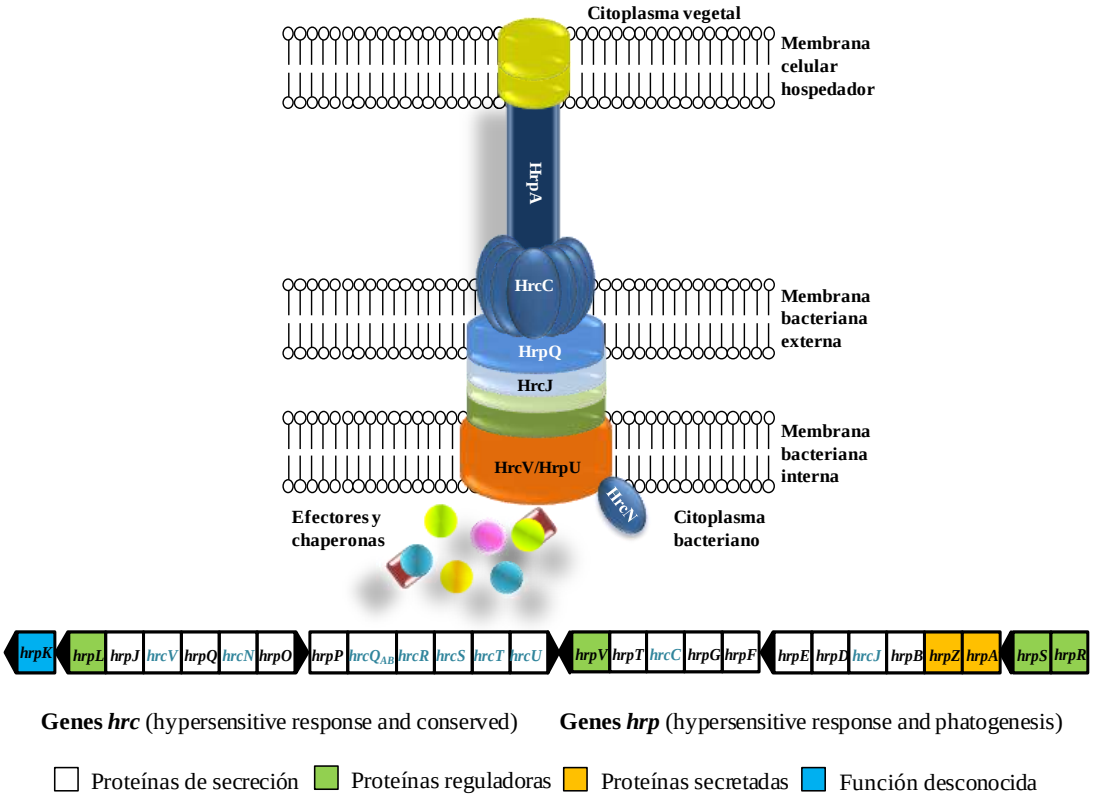

Figura 4. Esquema representativo de la estructura del sistema de secreción tipo III en *Pseudomonas syringae* (A). Distribución de los genes *hrp*/*hrc* en *P. syringae* , se representa el codificado por *P. syringae* pv. syringae 61, cuya organización es idéntica al de *P. syringae* pv. tomato DC3000 y *P. syringae* pv. syringae B728A. (B). Adaptado de Collmer y colaboradores (2000).

El T3SS está codificado por los genes *hrp* (*hypersensitive response and pathogenicity*) y *hrc* (*hypersensitive response and conserved*), conservándose los genes *hrc* en patógenos de plantas y animales. En *P. syringae*, los genes que codifican el T3SS se agrupan en una isla de patogenicidad que generalmente se localiza en el cromosoma bacteriano (Fig. 4) (Jackson et al., 1999; Alfano et al., 2000; Collmer et al., 2000). Además, los genes *hrp*/*hrc* se regulan tanto positiva como negativamente. La regulación positiva es dependiente de las proteínas HrpR y HrpS, que al formar el heterodímero activan la transcripción del factor sigma alternativo HrpL (Hutcheson et al., 2001; Ortíz-Martín et al., 2010a). HrpL actúa como activador de la expresión tanto de los genes *hrp*/*hrc* como de los genes codificadores de los T3E y sus chaperonas (Xiao et al., 1994; Xiao and Hutcheson, 1994). Además, la expresión del gen *hrpA*, que da lugar a la proteína estructural del pili Hrp, afecta positivamente a la expresión del operón *hrpRS*. Por otro lado, los genes *hrpV* y la proteasa Lon son los reguladores negativos de la expresión de los genes *hrp*/*hrc* (Xiao et al., 1994;

Grimm et al., 1995; Preston et al., 1998; Collmer et al., 2000; Wei et al., 2000; Hendrickson et al., 2000a; Hendrickson et al., 2000b; Bretz et al., 2002; Ortiz-Martín et al., 2010b).

En los últimos años, se ha descrito que Psv NCPPB 3335 contiene los genes necesarios que codifican un T3SS completo así como un conjunto de 22 genes que conforman un T3SS incompleto, al igual que ocurre en otras cepas del complejo *P. syringae* (por ejemplo, los patovares phaseolicola 1448A, pv. tabaci 11528 u oryzae 1_6). Este segundo T3SS parece no estar regulado por el factor de transcripción HrpL dado que no aparece precedido por las secuencias reguladoras que reconoce dicho factor (Rodriguez-Palenzuela et al., 2010). Además, la formación de tumores en plantas de olivo adultas se ha demostrado que depende de la funcionalidad del T3SS (Sisto et al., 2004; Pérez-Martinez et al., 2010). De este modo, un mutante por inserción de un mini-Tn5 en el gen *hrcC* (que codifica un elemento estructural de la jeringa del T3SS) de la cepa de Psv ITM 317, es incapaz de inducir la HR en plantas de tabaco y de formar tumores en plantas de olivo lignificadas (Sisto et al., 1999; Sisto et al., 2004). Comportamientos similares, se han observado en inoculaciones de plantas de olivo lignificadas con los mutantes de la cepa NCPPB 3335 afectados en los genes *hrpA* (Psv T3) o *hrpR* (Psv FAM-117) (Pérez-Martínez et al., 2010; Matas et al., 2012). Estudios de microscopia de epifluorescencia de los tumores generados en plantas de olivo cultivadas *in vitro* por las cepas Psv T3 y Psv FAM-117, marcadas con GFP, revelaron que las células mutantes no colonizan el tejido tumoral, quedando limitadas al punto de inoculación. En consecuencia, ambas cepas mutantes presentan una reducción de la virulencia en plantas de olivo y no son capaces de multiplicarse en el tejido vegetal (Pérez-Martínez et al., 2010; Matas et al., 2012).

3.1. El sistema de secreción tipo III y las respuestas de defensa de las plantas

Las cepas de *P. syringae* pueden suprimir la defensa basal que se induce en plantas sensibles tras el reconocimiento específico de los "patrones moleculares conservados" en las bacterias potencialmente patógenas, como la flagelina o el factor Tu de elongación (Tu-E). Este conjunto de moléculas se denomina genéricamente como PAMP o MAMP (del inglés, *Pathogen- or Microbial-associated Molecular Patterns*). De otro lado, las células vegetales poseen receptores transmembrana denominados PRR (del inglés, *Pattern Recognition Receptor*) dirigidos al reconocimiento de los PAMP (Zipfel, 2008). Tras el reconocimiento, se pone en marcha una cascada de transducción de señales que desencadena en la activación de genes de defensa, la producción de estrés oxidativo y el reforzamiento de la pared celular mediante la deposición de calosa. Este mecanismo de defensa, conocido como PTI (del inglés, *Pattern-Triggered Immunity*), tiene como objetivo detener la progresión del patógeno (Schwessinger and Zipfel, 2008) (Jones and Dangl, 2006). Para poder evadir la respuesta de defensa de la planta hospedadora, *P. syringae* dispone de una colección de T3E que inhiben la PTI. Estos T3E pueden interferir bien en el

reconocimiento de los PAMP por los PRR, en la transducción de señales o en el tráfico de vesículas inducido tras el reconocimiento de los PAMP. Todos estos mecanismos de señalización son necesario para inducir la respuesta de defensa tipo PTI y su inhibición tiene como resultado una ETS (del inglés, *Effector-Triggered Susceptibility*) (Jones and Dangl, 2006; Feng and Zhou, 2012) (Figura 5).

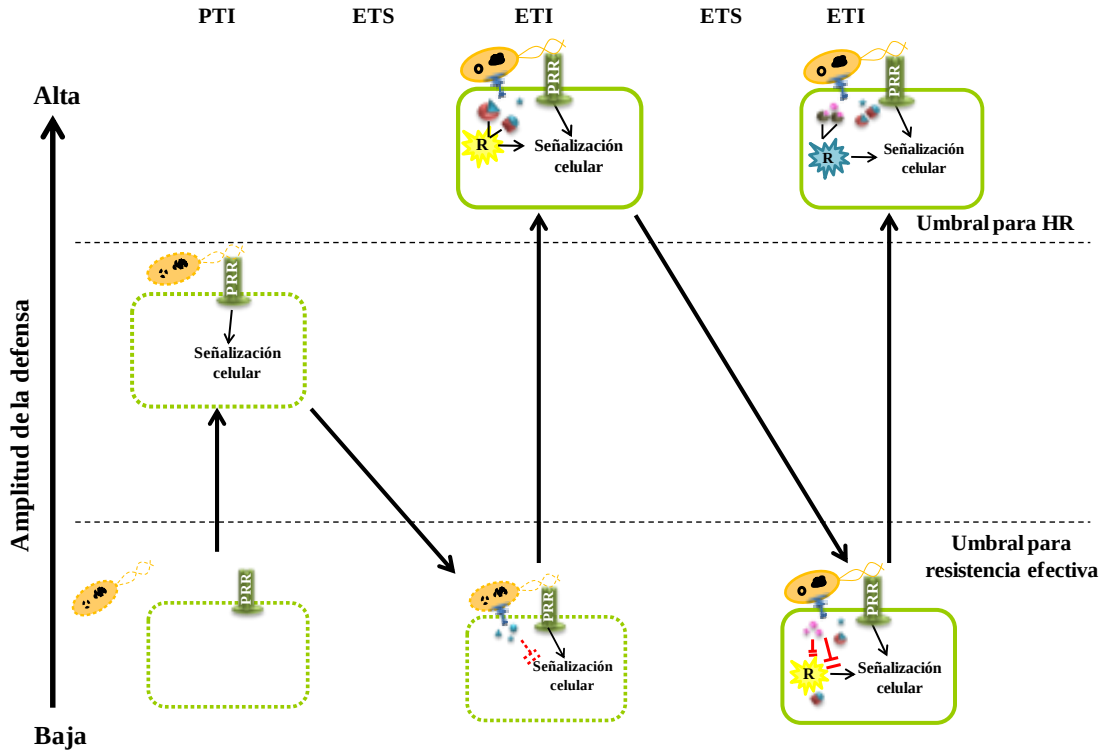

Figura 5. Esquema de las respuestas de defensa de la planta frente a patógenos. Modelo en zig-zag adaptado de Jones and Dangl, 2006.

Por otro lado, la planta es capaz de reconocer de forma directa la presencia de los T3E mediante las proteínas R, o indirectamnente la función de los mismos, desencadenando una respuesta de defensa denominada ETI (del inglés, *Effector-Triggered Immunity*) (Chisholm et al., 2006; Jones and Dangl, 2006). Este reconocimiento desencadena una respuesta de defensa más rápida e intensa que la PTI, y tiene como consecuencia la inducción de una HR en la zona de infección (Jones and Dangl, 2006). Sin embargo, este nivel de defensa también puede ser superado por la actividad de otros T3E capaces de interferir en el reconocimiento gen a gen (proteína R-T3E) o bien en la transducción de señales producida después del reconocimiento, inhibiendo de este modo la respuesta ETI y dando lugar a una nueva ETS. La Figura 5 representa el resultado "cuantitativo" de la inmunidad vegetal propuesto por Jones y Dangl en 2006 y denominado modelo Zig-Zag.

La continua interacción entre patógenos y huéspedes ha tenido como consecuencia que plantas y patógenos co-evolucionen. Entre las estrategias empleadas para la evolución del patógeno están: (i) la adquisición o pérdida de T3E por transferencia horizontal (Kim and Alfano, 2002; Arnold et al., 2003), y (ii) la patoadaptación. Esto último, consiste en la generación de pequeñas modificaciones en los T3E existentes, produciendo así un incremento de la virulencia del patógeno (Sokurenko et al., 1999; Sokurenko et al., 2004). Un ejemplo de patoadaptación en *P. syringae*, es el T3E *hopZ1*. Actualmente, se han encontrado tres formas funcionales y dos degeneradas por mutaciones patoadaptativas de este T3E (Ma et al., 2006). Por tanto, el resultado de la interacción planta-patógeno dependerá de la co-evolución del conjunto de T3E y proteínas R que estén implicados en dicha interacción.

3.2. Efectores del sistema de secreción tipo III

Los T3E son importantes en distintas fases de la interacción patógeno-hospedador porque: (i) promueven la penetración y permanencia del patógeno en el tejido del hospedador, (ii) suprimen la respuesta de defensa de la planta y (iii) facilitan el acceso a los nutrientes, proliferación y crecimiento del patógeno (Gohre and Robatzek, 2008). Actualmente, todos los T3E se conocen como Hop (del inglés, ***H**rp **o**uter **p**roteins*), salvo algunas familias de efectores que se conocen como proteínas de avirulencia (Avr) (por ejemplo AvrE), aunque también hay otras proteínas a las que se le han atribuido ambas designaciones (HopAB2/AvrPtoB) (Lindeberg et al., 2012). Los genes *avr*/*hop* pueden ser de localización cromosómica o plasmídica, aunque todos ellos comparten señales específicas en la región N-terminal de las proteínas que codifican, que les permiten translocarse a través del T3SS (Arnold et al., 2009), así como una secuencia promotora, denominadas Hrp-box (Figura 6), que responde al control del factor de transcripción HrpL (Xiao et al., 1994).

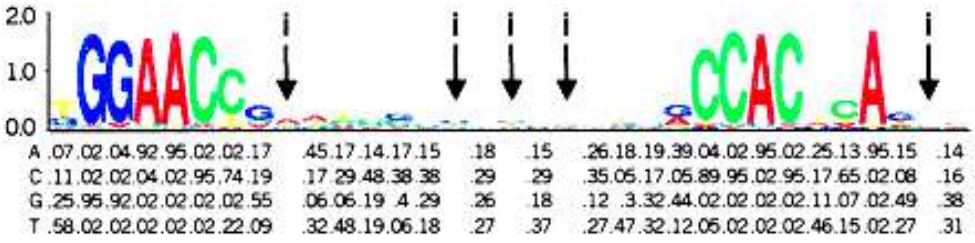

Figura 6. Secuencia consenso de los dominios Hrp-box. Esquema adaptado de Fouts et al., 2002 y Ferreira et al., 2006.

Actualmente, se dispone del catálogo de T3E hipotéticos codificados en los genomas de las, al menos, 35 *P. syringae* secuenciadas (Ver Table 1 en *Supplementary Material*). Los T3E identificados hasta la fecha en el pangenoma de *P. syringae* se agrupan en aproximadamente 60

familias génicas (http://www.pseudomonassyringae.org/) (Baltrus et al., 2011; Lindeberg et al., 2012). Aunque la función concreta de la mayoría de los T3E en la interferencia con los mecanismos de defensa de la planta es aún desconocida, se ha propuesto que el repertorio de T3E presentes en las bacterias fitopatógenas es uno de los factores más relevantes en la determinación de su rango de huésped (Baltrus et al., 2011).

3.2.1. Efectores del sistema de secreción tipo III en *P. savastanoi* pv. savastanoi NCPPB 3335

El análisis bioinformático del borrador del genoma de Psv NCPPB 3335 identificó inicialmente 30 T3E candidatos del T3SS, 19 de los cuales presentan un 65 % de identidad con T3E descritos previamente en otros patovares del complejo *P. syringae*. Además, y utilizando programas bioinformáticos dirigidos a la identificación de secuencias señales en el extremo N-terminal implicadas en el transporte de los T3E, así como la existencia de secuencias Hrp-box en las regiones promotoras de los genes anotados en este genoma, se identificaron 11 genes candidatos más no homólogos a ningún T3E descrito previamente, siendo 3 de ellos exclusivos de NCPPB 3335 (Rodriguez-Palenzuela et al., 2010). Revisiones posteriores de la secuencia del genoma de NCPPB 3335, permitieron descartar tres de estos 11 T3E no homólogos a otros T3E e identificar seis nuevos T3E candidatos (*hopAT1´*, *hopAZ1*, *hopF4*, *avrPto1*, *hopBL1 y hopBL2*) (Ramos et al., 2012; Matas et al., 2014). El repertorio de T3E de esta cepa, quedó así constituido por 33 candidatos (Tabla 1). Además, se determinó que NCPPB 3335, al igual que otras *P. syringae*, codifica variantes truncadas (o pseudogenes) de los T3E *hopAA1* y *hopAZ1* (Figura 7). Por otro lado, la secuenciación de los tres plásmidos de NCPPB 3335, confirmó que dos de los 33 T3E candidatos son de codificación plasmídica: *hopAF1* (pPsv48A) y *hopAO1* (pPsv48B) (Perez-Martinez et al., 2008; Bardaji et al., 2011).

Tabla 1. Efectores del sistema de secreción tipo III identificados en *P. savastanoi* pv. savastanoi NCPPB 3335.

ID-ASAP	Locus tag[a]	Pfam[b]	Nombre[c,d]	Referencias
AER-0005350	PSA3335_1360	PF11725	AvrE1	(Ramos et al., 2012)
AER-0005727	PSA3335_5082	PF11592	AvrPto1	(Ramos et al., 2012)
AER-0005728	PSA3335_5091	-----	**AvrRpm2**	(Ramos et al., 2012)
AER-0002657	PSA3335_5065	-----	**HopA1**	(Ramos et al., 2012)
AER-0000274	na	-----	**HopAA1**	(Ramos et al., 2012)
AER-0004725	PSA3335_2333	PF09046	HopAB1	(Rodríguez-Palenzuela et al., 2010)
AER-0000741	PSA3335_4315	PF15457	HopAE1	(Rodríguez-Palenzuela et al., 2010)
AER-0000968	PSA3335_1469	-----	HopAF1	(Ramos et al., 2012)
AER-0003643	PSA3335_1477	-----	HopAF1-2[#]	(Rodríguez-Palenzuela et al., 2010)
AER-0001776	PSA3335_2927	PF00150	HopAH2	(Rodríguez-Palenzuela et al., 2010)
AER-0000610	PSA3335_0875	PF14566	HopAO1[#]	(Rodríguez-Palenzuela et al., 2010)

Tabla 1. Efectores del sistema de secreción tipo III identificados en *P. savastanoi* pv. savastanoi NCPPB 3335 (continuación).

ID-ASAP	Locus tag[a]	Pfam[b]	Nombre[c,d]	Referencias
AER-0005024	PSA3335_4684	-----	HopAS1	(Rodríguez-Palenzuela et al., 2010)
AER-0005726	PSA3335_5084	-----	HopAT1'	(Ramos et al., 2012)
AER-0000625	PSA3335_5031	PF10791	HopAU1	(Rodríguez-Palenzuela et al., 2010)
AER-0001017	PSA3335_1783	-----	**HopAZ1'**	(Ramos et al., 2012)
AER-0000696	PSA3335_2068	PF13974	**HopBK1**	(Matas et al., 2014)
AER-0000509	PSA3335_0157	PF02902	**HopBL1**	(Matas et al., 2014)
AER-0003844	PSA3335_4544	PF02902	**HopBL2**	(Matas et al., 2014)
AER-0004681	PSA3335_4805	-----	HopD1	(Rodríguez-Palenzuela et al., 2010)
AER-0000629	PSA3335_0852	-----	HopG1	(Rodríguez-Palenzuela et al., 2010)
AER-0000168	PSA3335_4509	PF00226	HopI1	(Rodríguez-Palenzuela et al., 2010)
AER-0005351	PSA3335_1358	-----	HopM1'	(Rodríguez-Palenzuela et al., 2010)
AER-0004680	PSA3335_4804	PF01156	HopQ1	(Rodríguez-Palenzuela et al., 2010)
AER-0004685	PSA3335_4809	-----	HopR1	(Rodríguez-Palenzuela et al., 2010)
AER-0003015	PSA3335_2327	PF13485	HopV1	(Rodríguez-Palenzuela et al., 2010)
AER-0003833	PSA3335_5066	-----	HopW1'	(Rodríguez-Palenzuela et al., 2010)
AER-0000344	PSA3335_5061	-----	HP0344	(Rodríguez-Palenzuela et al., 2010)
AER-0000393	PSA3335_1416	-----	HP0393	(Rodríguez-Palenzuela et al., 2010)
AER-0001113	PSA3335_0894	PF07090	HP1113	(Rodríguez-Palenzuela et al., 2010)
AER-0001936	PSA3335_3242	None	HP3242	(Rodríguez-Palenzuela et al., 2010)
AER-0002597	PSA3335_0106	PF15184	HP2597	(Rodríguez-Palenzuela et al., 2010)
AER-0002714	PSA3335_2804	PF01565	HP2714	(Rodríguez-Palenzuela et al., 2010)
AER-0003934	PSA3335_1247	-----	HP3934	(Rodríguez-Palenzuela et al., 2010)

[a]na, no anotado; [b]Número de acceso de cada familia proteica en la base de datos pfam (http://pfam.xfam.org/); [c]Sombreado en gris aparecen los efectores cuya translocación fue analizada en Matas et al., 2014; [d]Nombres en negrita indican aquellos efectores cuya translocación se ha demostrado (Matas et al., 2014) ',pseudogenes hipotéticos; [#], genes de codificación plasmídica.

Recientemente, se han llevado a cabo ensayos de translocación a través del T3SS de Psv NCPPB 3335 de 12 de los 33 T3E candidatos codificados en el genoma de esta cepa. Tres de ellos (AvrRpm2, HopAA1, HopAZ1), son homólogos a proteínas de *P. syringae* cuya translocación en planta no había sido demostrada previamente. Además, se seleccionaron otros 8 candidatos que no tienen un homólogo en el genoma de la cepa filogenéticamente cercana a Psv, *P. syringae* pv. phaseolicola 1448A, incluyendo HopA1, y AER-0003934, un T3E candidato que muestra un homólogo en Pph 1448A. Los resultados demostraron la translocación a través del T3SS de NCPPB 3335 de 7 de los 12 candidatos seleccionados (AvrRpm2, HopA1, HopAA1, HopAZ1, HopBK1, HopBL1 y HopBL2). Por otra parte, estudios filogenéticos llevados a cabo con la secuencia de tres de estos siete efectores (HopBL1, HopBL2 y HopBK1), anotados en ese momento en los genomas de NCPPB 3335 y otras cepas del complejo *P. syringae* como proteínas hipotéticas, revelaron su pertenencia a 2 nuevas familias del T3E de este grupo de bacterias, HopBL y HopBK (Figura 8A y 8B). Adicionalmente, el análisis de dominios proteicos en estos 3 T3E reveló que HopBL1 y HopBL2 contienen el domino Pfam (http://pfam.xfam.org/) PF02902, correspondiente a la familia

de proteasas de SUMO (del inglés, *small ubiquitin-like modifier*) Ulp. HopBK1, HopBL1 y HopBL2 se codifican en la mayoría de las cepas de *P. savastanoi* pv. savastanoi y pv. nerii y en número reducido de otras cepas de *P. syringae* (Figura 8B). Además, de entre los genomas secuenciados hasta la fecha, HopBL1 y HopBL2 solamente se han detectado en cepas de *P. syringae* patógenas de plantas leñosas, lo que sugiere un papel relevante de los mismos en la interacción de *P. syringae* y *P. savastanoi* con plantas leñosas (Matas et al., 2014).

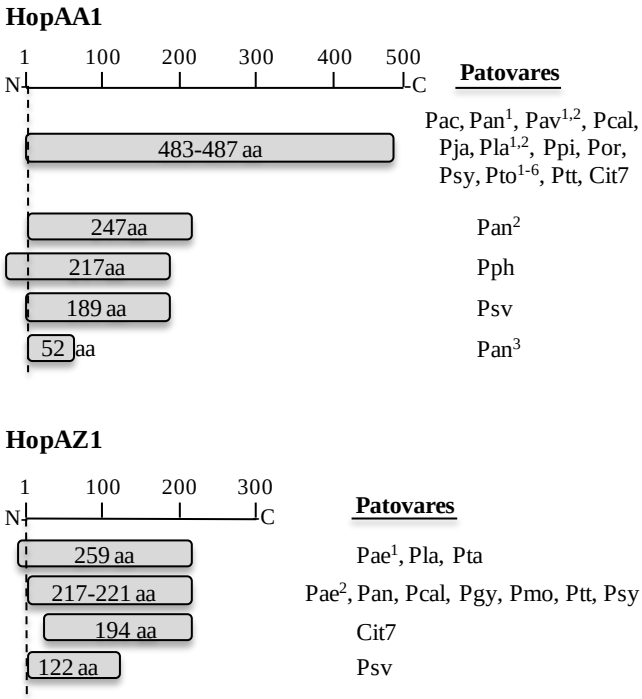

Figura 7. Mapa esquemático de los alelos de HopAA1 y HopAZ1 pertenecientes a distintos patovares del complejo *Pseudomonas syringae*. aa, residuos de aminoácidos codificados por cada gen. Abreviaturas de las cepas utilizadas en la construcción del esquema de HopAA1: Pac, pv. aceris MAFF 302273; Pan, pv. actinidiae MAFF 302091[1], ICMP 18884 (HopAA1-1)[2], ICMP 18884 (HopAA1-2)[3]; Pav, pv. avellanae BPIC 631 (HopAA1-1)[1] o BPIC 631 (HopAA1-2)[2]; Pcal, pv. alisalensis ES4326; Pja, pv. japonica MAFF 301072; Pla, pv. lachrymans MAFF 301315[1] o MAFF 302278[2]; Ppi, pv. pisi 1704B; Por, pv. orizae 1_6; Psy, pv. syringae 642; Pto, pv. tomato DC3000 (HopAA1-1)[1], DC3000 (HopAA1-1)[2], K40[3], Max13[4], NCPPB 1108[5] y T1[6]; Ptt, pv. aptata DSM 50252; Pph, pv. phaseolicola 1448A; Psv, pv. savastanoi NCPPB 3335. Y en la construcción del esquema de HopAZ1: Pae, pv. aesculi 0893-23 (NCPPB 3681)[1] y 2250[2]; Pta, pv. tabaci; Pla, pv. lachrymans MAFF 301315; Pcal, pv. alisalensis ES4326; Pan, pv. actinidae MAFF 302091; Pgy, pv. glycinea race4; Pmo, pv. mori MAFF 301020; Ptt, pv. aptata DSM 50252; Psy, pv. syringae FF5 y Psv, pv. savastanoi NCPPB 3335.

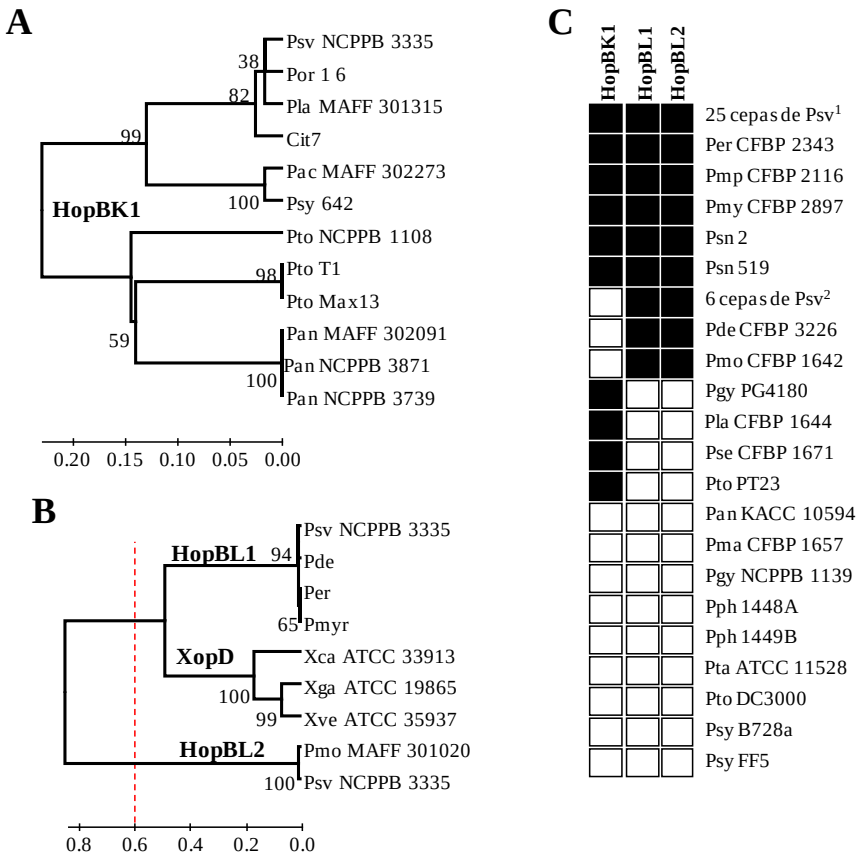

Figura 8. Distribución y filogenia de HopBK1, HopBL1 and HopBL2 entre patovares del complejo *Pseudomonas syringae*. Árbol filogenético realizado con las secuencias de proteínas de las cepas del complejo *P. syringae* de los efectores HopBK1 (**A**), HopBL1 and HopBL2 (**B**). HopBK1 está presente en *P. syringae* pv. actinidiae, conteniendo dos alelos con un 94 % identidad. Los porcentajes en los nodos y distancias evolutivas se indican en unidades de sustitución de aminoácidos por sitio. **C**, Distribución de los efectores *hopBK1*, *hopBL1* y *hopBL2* de *P. savastanoi* pv. savastanoi NCPPB 3335 en una colección de cepas del complejo *P. syringae* aisladas de plantas leñosas y herbáceas. Los cuadrados negros y blancos representan la presencia o ausencia, respectivamente, de señal de hibridación con cada efector analizado. [1], 25 cepas de *P. savastanoi* pv. savastanoi: B15.00; C2.01; C3.01; CFBP 2074; DAPP-PG722; IMC-2; ITM 317; IVIA 1628-3; IVIA 1629-1a; IVIA 1637-a; IVIA 1637-B3; IVIA 1649-1; IVIA 1651-C15; IVIA 1657-A2; IVIA 1657-B8; IVIA 2733-1a; IVIA 2743-3; NCPPB 64; NCPPB 1342; NCPPB 1344; NCPPB 3335; PVFi-1. [2], 6 cepas de *P. savastanoi* pv. savastanoi: CFBP 71; CFBP 1670; CFBP 1746; IMC-1; IVIA 1624-1b, NCPPB 1479.

Por tanto, aunque el repertorio de T3E candidatos del T3SS de Psv NCPPB 3335 es conocido, aún no se ha descrito la translocación *in planta* de todos ellos. Además, y tal y como ocurre en otras especies de bacterias fitopatógenas, la función de estos T3E durante el proceso de infección y su papel en la interferencia con los mecanismos de defensa de la planta es aún un área poco explorada.

OBJETIVOS

Los efectores (T3E) del sistema de secreción tipo III (T3SS) son esenciales para el establecimiento de las enfermedades producidas por bacterias fitopatógenas en huéspedes compatibles. Durante los últimos años, se han producido grandes avances en el conocimiento del papel de los T3E del complejo *Pseudomonas syringae* durante la interacción con plantas herbáceas. Recientemente, *Pseudomonas savastanoi* pv. savastanoi NCPPB 3335 se ha establecido como una cepa modelo en el estudio de la interacción de este complejo bacteriano con plantas leñosas (Ramos et al., 2012). El análisis bioinformático del borrador de la secuencia de nucleótidos del genoma de NCPPB 3335 identificó 33 posibles T3E (Rodríguez-Palenzuela *et al*., 2010; Ramos et al., 2012), cuya translocación a través del T3SS se ha demostrado para 7 de ellos (Matas et al., 2014). Por otro lado, la secuenciación de los tres plásmidos de esta cepa reveló que los genes codificantes de los T3E HopAF1 y HopAO1 se localizan en los plásmidos pPsv48A y pPsv48B, respectivamente, codificándose en el cromosoma un homólogo de HopAF1 (HopAF1-2). El objetivo principal de esta Tesis Doctoral ha sido el **análisis funcional de efectores del sistema de secreción tipo III de NCPPB 3335**, prestando mayor atención a los T3E de las familias HopAF y HopAO. Para ello se han llevado a cabo los siguientes objetivos específicos:

1- Estudiar la distribución de los efectores de las familias HopAF y HopAO en los patovares de *P. savastanoi* y *P. syringae*.
2- Analizar la translocación a través del sistema de secreción tipo III de *P. savastanoi* pv. savastanoi NCPPB 3335 de los efectores de las familias HopAF y HopAO.
3- Analizar la interacción con los sistemas de defensa de la planta de los siete efectores de *P. savastanoi* pv. savastanoi NCPPB 3335 cuya translocación a través del sistema de secreción tipo III ha sido demostrada, así como de los pertenecientes a las familias HopAF y HopAO codificados en el genoma de esta cepa.
4- Analizar el papel en virulencia de los efectores de las familias HopAF y HopAO de *P. savastanoi* pv. savastanoi NCPPB 3335.

GENERAL MATERIAL AND METHODS

The general material and methods used in the three different chapters of this PhD Thesis have been described in this section. Specific material and methods are included within each of the different chapters.

1. Bacterial strains, plasmids and growth conditions

The common strains and plasmids used in this study are described in Table 1 and Table2, respectively. The specific plasmids constructed appear in each corresponding chapter. Bacteria were grown at 37 ºC (*Escherichia coli*) or 28 ºC (*Pseudomonas savastanoi* pv. savastanoi NCPPB 3335 and *Pseudomonas syringae* pv. tomato DC3000D28E) with aeration in Luria-Bertani (LB) medium (Miller, 1972) or Super Optimal Broth (SOB) medium (2 % bactotriptone, 0.5 % yeast extract, 10 mM NaCl, 2.5 mM KCl, adjust pH to 7.0 with NaOH, autoclave to sterilize, and add 20 mM of $MgCl_2$ (before use)) (Hanahan, 1983). Solid and liquid media were supplemented, when required, with the appropriate antibiotics (Table 3).

Table 1. Strains used in this Thesis.

Strains[a]	Relevant characteristics	References
E. coli		
DH5α	*F -, ϕ80dlacZ M15, (lacZYA-argF) U169, deoR, recA1, endA, hsdR17 (rk - mk -), phoA, supE44, thi-1, gyrA96, relA1.*	(Hanahan, 1983)
XL1 Blue	*hsdR17, supE44, recA1, endA1, gyrA46, thi, relA1, lac/ F'* [*proAB*$^+$, *lacI*^{q}, *lacZ M15::*Tn10 (Tc^R)]	(Bullock et al., 1987)
GM2929	*F -, ara-14, leuB6, thi-1, tonA31, lacY1, tsx-78, galK2, galT22, glnV44, hisG4, rpsL136, xyl-5,mtl-1, dam13::Tn9, dcm-6, mcrB1, hsdR2, mcrA, recF143.* (Sp^R Cm^R).	(Palmer and Marinus, 1994)
Agrobacterium		
A. tumefaciens GV3101 (pMP90)	Carries Vir plasmid encoding T-DNA transfer machinery, Rif^R, Cm^R.	American Type Culture Collection 33970
Pseudomonas		
P. fluorescens 55 [pLN18] (Pf)	Containing 25 kb *P. syringae* pv. syringae 61 *hrc/hrp* cluster with *shcA* and *hopPsyA* replaced by an *nptII* cassette (Km^R) .	(Jamir et al., 2004)
P. savastanoi pv. nerii (Psn)		
2	Isolated from oleander	(Matas et al., 2009)
519	Isolated from oleander	(Surico et al., 1985)
P. savastanoi pv. savastanoi (Psv)		
NCPPB 3335	Wild-type strain isolated from olive	(Pérez-Martínez et al., 2007)
Psv-T3	Type III secretion mutant (Km^R)	(Pérez-Martinez et al., 2010)
NCPPB 3335 Δ*hrpL*	*hrpL* mutant derived from NCPPB 3335 (Km^R)	(Matas IM et al., 2014)

Table 1. Strains used in this Thesis (continued).

Strains[a]	Relevant characteristics	References
P. savastanoi pv. savastanoi (Psv)		
DAPP-PG722	Isolated from olive	(Hosni et al., 2011)
PVFi-1	Isolated from olive	(Iacobellis et al., 1993)
IMC-1	Isolated from olive	(Matas et al., 2009)
IMC-2	Isolated from olive	(Matas et al., 2009)
CFBP 1670	Isolated from olive	(Penyalver et al., 2000)
CFBP2074	Isolated from olive	(Penyalver et al., 2000)
CFBP 71	Isolated from olive	(Penyalver et al., 2000)
IVIA 1628-3	Isolated from olive	(Penyalver et al., 2000)
IVIA 1629-1a	Isolated from olive	(Penyalver et al., 2000)
IVIA 1624-1b	Isolated from olive	(Penyalver et al., 2000)
IVIA 1637-a	Isolated from olive	(Penyalver et al., 2000)
IVIA 1637-B3	Isolated from olive	(Penyalver et al., 2000)
IVIA 1649-1	Isolated from olive	(Penyalver et al., 2000)
IVIA 1651-C15	Isolated from olive	(Penyalver et al., 2000)
IVIA 1657-A2	Isolated from olive	(Penyalver et al., 2000)
IVIA 1657-B8	Isolated from olive	(Penyalver et al., 2000)
NCPPB 2327	Isolated from olive	(Penyalver et al., 2000)
NCPPB 1342	Isolated from olive	(Penyalver et al., 2000)
NCPPB 1344	Isolated from olive	(Penyalver et al., 2000)
NCPPB 1479	Isolated from olive	(Penyalver et al., 2000)
NCPPB 1506	Isolated from olive	(Penyalver et al., 2000)
NCPPB 64.	Isolated from olive	(Penyalver et al., 2000)
CFBP 1020	Isolated from olive	(Penyalver et al., 2000)
C2.01	Isolated from olive	(Pérez-Martínez et al., 2007)
B15.00,	Isolated from olive	(Pérez-Martínez et al., 2008)
C1.01	Isolated from olive	(Pérez-Martínez et al., 2008)
C3.01	Isolated from olive	(Pérez-Martínez et al., 2008)
IVIA2733-1a	Isolated from olive	(Quesada et al., 2008)
IVIA 2743-3	Isolated from olive	(Quesada et al., 2008)
ITM317	Isolated from olive	(Surico et al., 1985)
P. syringae pv. actinidiae (Pan)		
KACC10594	Isolated from kiwi	(Rees-George et al., 2010)
P. syringae pv. dendropanacis (Pde)		
CFBP 3226	Isolated from *Dendropanax*	(Gardan et al., 1999)
P. syringae pv. eriobotryae (Per)		
CFBP 2343	Isolated from loquat	(Gardan et al., 1999)
P. syringae pv. glycinea (Pgy)		
NCPPB 1139	Isolated from *Glycine javanica*	(Yamamoto et al., 2000)
PG4180	Isolated from soybean	(Mitchell, 1978)
P. syringae pv. lachrymans (Pla)		
CFBP 1644	Isolated from cucumber	(Gardan et al., 1999)
P. syringae pv. maculicola (Pma)		
CFBP1657	Isolated from cauliflower	(Gardan et al., 1999)

Table 1. Strains used in this Thesis (continued).

Strains[a]	Relevant characteristics	References
P. syringae pv. morsprunorum (Pmp)		
CFBP 2116	Isolated from tart cherry	(Gardan et al., 1999)
P. syringae pv. myricae (Pmy)		
CFBP 2897	Isolated from red bayberry	(Gardan et al., 1999)
P. syringae pv. phaseolicola (Pph)		
1448A	Isolated from bean	(Teverson, 1991)
1449B	Isolated from *Lablab purpureus*	(Taylor et al., 1996)
P. syringae pv. sesami (Pse)		
CFBP 1671	Isolated from sesame	(Gardan et al., 1999)
P. syringae pv. syringae (Psy)		
B728a	Isolated from bean	(Loper and Lindow, 1987)
FF5	Isolated from ornamental pear	(Sundin and Bender, 1993)
P. syringae pv. tabaci (Pta)		
ATCC 11528	Isolated from tobacco	(Studholme et al., 2009)
P. syringae pv. tomato (Pto)		
PT23	Isolated from tomato	(Bender and Cooksey, 1986)
DC3000	Isolated from tomato	(Cuppels, 1986)
DC3000D28E	*ΔhopU1-hopF2 ΔhopC1-hopH1*::FRT *ΔhopD1-hopR1*::FRT *ΔavrE-shcN ΔhopAA1-2-hopG1::*FRT *ΔhopI1 ΔhopAM1-1 ΔhopAF1*::FRT *ΔavrPtoB ΔavrPto ΔhopK1 ΔhopB1 ΔhopE1 ΔhopA1::*FRT *hopY1*::FRT pDC3000A− pDC3000B− (Sp^R)	(Cunnac et al., 2011)

[a]Cm^R, Km^R, Sp^R, Rif^R, and Tc^R indicate resistance to chloramphenicol, kanamycin, spectinomycin, rifampicin and tetracycline, respectively.

Table 2. Plasmids used in this Thesis.

Name	Description[a]	References
pGEM-T *easy*	Cloning vector containing ori f1 and *lac*Z (Amp^R)	(*Promega*, USA)
pGEM-T- KmFRT-*EcoR*I	Contains Km^R from pKD4 (Amp^R Km^R)	(Zumaquero et al., 2010)
pGEM-T- KmFRT-*BamH*I	Contains Km^R from pKD4 (Amp^R Km^R)	(Zumaquero et al., 2010)
pENTR/SD/D TOPO	Entry vector for Gateway cloning (Km^R, Cm^R)	(*Invitrogen Corp*.; California, USA)
pCPP3234	pVLT35::Gateway cassette-*cya* fusion, broad-host-range vector containing *tac* promoter and *lacI*^{q} (Sp^R, Str^R, Cm^R)	(Schechter et al., 2004)
pCPP5040	pML123::Gateway cassette, broad-host-range vector allowing for constitutive expression of inserts fused to a C-terminal HA tag from the *nptII* promoter (Gm^R, Cm^R)	(Lopez-Solanilla et al., 2004)
pGWB5	35S promoter, C-sGFP (35S promoter-R1-Cm^R-*ccdB*-R2-sGFP), Km^R, Hg^R	Invitrogen

[a]Ap^R, Cm^R, Km^R, Sp^R, Str^R and Hg^R, indicate resistance to ampicillin, chloramphenicol, kanamycin, spectinomycin, streptomycin and higromycin, respectively. *cya*, catalytic domain of *Bordetella pertusis* adenilate cyclase; HA tag, influenza hemagglutinin (HA) peptide YPYDVPDYA.

Table 3. Concentration (µg/ml) of selective and differentiating agents used in this Thesis.

Compounds	***E. coli strain***	***Pseudomonas* strains**
Ampicillin (Ap)	100	300
Kanamicyn (Km)		7
Gentamicin (Gm)	10	10
Spectomycin (Sp)	50	---
Nitrofurantoine (Nf)	---	25
Tetracycline (Tc)	10	10
X-Gal	40	40

2. Nucleic acids techniques.

2.1 RNA extraction and quantitative RT-PCR assays

Pure cultures of the wild-type *P. savastanoi* pv. savastanoi NCPPB 3335 and its Δ*hrpL* mutant were grown overnight in KB medium at 28 °C. The cells were diluted in fresh KB medium and incubated with shaking at 28 °C to an OD_{600} of 0.5. The sample was split into two. One half was pelleted, and freezed (for non-inducing condition) and the other half was pelleted, washed twice with 10 mM $MgCl_2$ and resuspended in the same volume of Hrp-inducing medium (Huynh et al., 1989) supplemented with 5 mM mannitol and 0.0006 % ferric citrate (Roine et al., 1997; Sambrook and Russell, 2001). After 6 h of incubation, the cells were pelleted and processed for RNA isolation using TriPure Isolation Reagent (Roche Applied Science, Mannheim, Germany) according to the manufacturer's instructions, except that the TriPure was preheated at 65 ºC, the lysis step was performed at 65 ºC, and BCP (Molecular Research Center, Cincinnati, Ohio, USA) was used instead of chloroform. Total RNA was treated with the RNAeasy kit (QIAGEN) as detailed by the manufacturer. The RNA concentration was determined spectrophotometrically, and its integrity was assessed by agarose gel electrophoresis. DNA-free total RNA was retrotranscribed to cDNA using the cDNA Reverse Transcription kit (Applied Biosystems, Foster City, CA, U.S.A.) and random hexamers. The primer efficiency tests, qRT-PCRs and confirmation of the specificity of the amplification reactions were performed as described previously (Vargas et al., 2011). The relative transcript abundance was calculated using the ΔΔ cycle-threshold (Ct) method (Livak and Schmittgen, 2001). Transcriptional data were normalized to the housekeeping gene *gyrA* using the Roche LightCycler 480 Software and are presented as the fold change in expression compared to the expression of each gene in the wild-type strain. The relative expression ratio was calculated as the difference in quantitative PCR threshold cycles (ΔCt = Ctgene of interest – CtgyrA). One PCR cycle represents a two fold difference in template abundance; therefore, fold-change values were calculated as $2^{-\Delta\Delta Ct}$ as previously described (Pfaffl,

2001; Rotenberg et al., 2006). Quantitative real-time PCRs (qRT-PCRs) were performed in triplicate.

2.2 DNA extraction and purification

Basic DNA and molecular techniques were performed following standard methods (Sambrook and Russell, 2001). Genomic DNA was extracted using the Jet Flex Extraction Kit (Genomed; Löhne, Germany). Plasmid DNA for cloning purposes was extracted using GenElute™ Plasmid Minsiprep Kit (Sigma-Aldrich, USA).

Routine plasmid clone analysis was carried out by a boiling based plasmid extraction that followed the method described previously (Holmes and Quigley, 1981), with some modifications. Cells from a 1.5 ml of an overnight (o/n) grown culture were centrifuged and resuspended into 110 µl of STETL (8 % sucrose, Triton X-100, 50 mM Tris pH 8, 50 mM EDTA, 0.5 mg/ml lisozyme). After boiling during 30 seconds, cells were centrifuged 15 minutes (min) in a microcentrifuge at maximum speed. The pellet was removed with a sterile toothpick, which was previously dipped into a 10 mg/ml RNAase solution. Following addition of 110 µl of isopropanol, cells were centrifuged 15 min as described above. The precipitate was air dried and resuspended into 25 µl of distilled water.

DNA gel-purification was carried out using GFX™ PCR DNA and Gel Band Purification Kit (GE Healthcare, UK).

2.3 DNA hybridization

DNA hybridization was performed following standard methods (Sambrook and Russell, 2001), using DIG-Nucleic Acid Detection kit (Roche; Mannheim, Germany), following the instructions provided by the manufacturer. DNA was transferred onto a nylon membrane by upward capillary transfer, and cross-linked by UV irradiation. Prehybridization and hybridization stages were carried out at 65 ºC. DNA probe was labeled by PCR reaction with chemiluminiscent digoxigenin-dNTPs using DIG Labelling Mix (Roche; Mannheim, Germany). The primers used to generate DNA probes are presented in specific tables within the different chapters.

2.4 Colony blots

To fix total DNA from the colonies, overnight cultures of *Pseudomonas* strains grown on LB microtiter plates were transferred onto nylon membranes placed on LB agar plates using a 48-pin

replicator (Sigma-Aldrich, Inc., St. Louis, MO, U.S.A.). Total DNA from the bacterial colonies was denatured on the membranes by alkaline lysis by placing a Whatman 3 MM paper soaked in denaturing solution (0.4 M NaOH) for 15 min on top of the colonies. The membranes were neutralized twice for 15 min in 1 M NaCl and 0.5 M tris, pH 7.2, then washed twice for 10 min in 2x SSC (1x SSC is 0.15 M NaCl plus 0.015 m sodium citrate). Finally, the DNA was cross-linked by UV fixation (Vilber Lourmat, Eberhardzell, Germany). DNA probes were amplified and labeled by PCR using primers and digoxigenin (DIG)-dNTPs from the Dig Labelling Mix kit (Roche Applied Science, Mannheim, Germany) and the appropriate DNA template. Hybridization was performed at 65 ºC using the DIG Nucleic Acid Detection Kit (Roche Applied Science, Mannheim, Germany) following the manufacturer's instructions.

2.5 DNA restriction, polymerization, and ligation procedures

Endonucleases from Takara corp. (Kaohsiung 802, Taiwan) were used according to the instructions provided by the manufacturer.

Go-Taq®DNA polymerase (Promega Cor.; Madison, EEUU) or Expand High Fidelity (Roche; Mannheim, Germany) was used as appropriate.

DNA ligation was performed using T4 DNA ligase (Takara biocorp; Kaohsiung 802, Taiwan). The concentration of the insert was calculated following the formula: [(100 ng of insert) (bps of insert)]/ bps of vector. Fragments were combined in 1:3 ratio of vector and insert.

2.6 DNA sequencing

The sequencing of DNA fragments or plasmids purified were carried out by Secugen (http://www.secugen.es/) or Stabvida (http://www.stabvida.com/).

2.7 Electrophoresis

Conventional agarose gel electrophoresis was used to confirm plasmid purifications, to visualize plasmids digestions, to prepare DNA fragments for Southern hybridization, to isolate DNA bands from agarose gels, etc. Agarose (Gellyphor® Euroclone; Siziano, Italy) was dissolved in Tris/Borate EDTA buffer (TBE) or Tris/Acetate EDTA buffer (TAE) for separated high weight plasmid from *P. savastanoi spp*. Syber ® Safe Gel Stain (Invitrogen; Carlsbad, California, USA) was added to visualize the DNA. Gels (0.8 % - 1.5 % agarose) were casted in a gel tank and electrophoresis was carried out in a horizontal tank containing TBE or TAE buffer. Gels were imaged using Image Lab™ software (Bio-Rad Laboratories SA; Madrid, Spain).

2.8 Transformation of bacterial strains

Plasmid were transformed into *E. coli* strains by heat-stock transformation (Hanahan, 1983). Therefore, high efficiency competent cells were prepared as described previously (Inoue et al., 1990). Pure culture of the *E. coli* strain was grown o/n in 5 mL of SOB medium at 28 °C. The cells were diluted 1000 times into 200 mL of fresh SOB medium and this fresh culture was grown with shaking at 22 ºC to an OD_{600} of 0.5. After 10 min incubation on ice, cells were centrifuged at 2500 g for 10 min at 4 ºC, and resuspended in 80 mL of ice-cold TB buffer (Pipes 10 mM, $CaCl_2$ 15 mM, KCl 250 mM, $MnCl_2$ 55 mM, pH 6.7, filtrated to sterilize). Cells were incubated 10 more min on ice, and centrifuged as before. Finally, the pellet resuspended in 20 mL of cold TB buffer and 1.5 mL of DMSO. Aliquots of 100 µl were kept at -80 ºC. The transformation was carried out mixing 100 µl of competent cells with plasmid DNA or ligation reactions. The mixture was incubated on ice for 30 min, transferred to 42 ºC and incubated for 45 sec (heat shock). Afterwards, 1 mL of SOB medium was added, and the transformation mixture was incubated with shaking for 2 h at 37 ºC. The cells were pelleted, and plated onto LB medium with the appropriated antibiotics.

For *Pseudomonas* spp. an electroporation protocol was carried out according the one described by (Choi et al., 2006). Briefly, a culture of the receptor strain, grown o/n in SOB medium, was centrifuged at 2500 g at room temperature during 3 min and resuspended in 300 mM sucrose solution three times. Competent cells were transformed by electroporation, and incubated in SOB medium for 2 h (for *P. syringae* pv. tomato DC3000D28E and *P.syringae* pv. phaseolicola) or 4 h (for *P. savastanoi* pv. savastanoi NCPPB 3335).

3. Construction of bacterial strains and plasmids

PCR products were cloned into the cloning vectors pGEM-T *easy* (Promega, USA) or pENTR/SD/TOPO (Invitrogen, California, USA) and sequenced prior to subcloning into the relevant broad-host-range or suicide vector. Using Gateway Technology, the genes of interest without a stop codon cloned in an entry vector can be transferred by recombination into a destination vector, creating an in-frame fusion. These genes were PCR amplified with specific primer pairs (indicated in each chapter) and cloned into plasmid pENTR/SD/D-TOPO (Invitrogen Cor., California, USA). DNA sequencing using the universal primers T7 and M13 confirmed the absence of mutations in the cloned DNA fragments. Expression clones were made by combining the pENTR plasmids with the desired expression vector and the LR clonase. The recombination reactions were performed as suggested by the manufacturer (Invitrogen Cor., California, USA). Three Gateway compatible expression vectors were used: (i) pCPP3234, a derivative of the broad

host range vector pVLT35 that employs a *tac* promoter to express inserted genes and generates hybrid proteins with a C-terminal Cya fusion for T3SS translocation studies (Schechter et al., 2004); and (ii) pCPP5040, a derivative of the broad-host-range vector pML123 (Labes et al., 1990), which expresses inserted genes from the *nptII* promoter and generates protein products with a C-terminal HA tag for expression in *Pseudomonas* spp.; (iii) pGWB5, which allows for 35S-regulated expression of insert genes and production of proteins with a C-terminal GFP fusion for expression in *A. tumefaciens* (Invitrogen)

To construct deletions mutants in *P. savastanoi* pv. savastanoi NCPPB 3335, DNA fragments of a 1.2 Kb corresponding to the 5' and 3' flanking regions of the ORF to be deleted, were amplified by three rounds of PCR using genomic DNA as a template as previously described (Zumaquero et al., 2010). The resulting product was A/T cloned into pGEM-T-*easy* (Table 2) and fully sequenced to discard mutations on flanking regions. The resulting plasmid was labeled with the *nptII*, Km resistance gene, obtained from pGEM-T-KmFRT-*BamH*I or pGEM-T-KmFRT-*EcoRI* (Table 2). For marker exchange mutagenesis, theses plasmids were transformed by electroparation into NCPPB 3335 as described previously (Pérez-Martínez et al., 2007). Transformants were selected on LB medium containing Km, and replica plates of the resulting colonies were made on LB-Ap plates to determine whether each transconjugant underwent plasmid integration (Ap^R) or allelic exchange (Ap^S). Southern blot analyses were carried to confirm that allelic exchange occurred at a single and correct position within the genome. For each mutant, two different probes were used, one corresponding to the gene deleted and the second corresponding to the *nptII* gene.

4. Phylogenetic analysis

The phylogenetic analyses of proteins were performed using aminoacidic sequences obtained from the NCBI (http://www.ncbi.nlm.nih.gov/) and the ASAP genome (http://www.genome.wisc.edu/tools/asap.htm) databases. Multiple alignments of the different proteins were performed with ClustalW (Larkin et al., 2007), and phylogenetic trees were obtained using the neighbor-joining method (Saitou and Nei, 1987). The percentage of replicate trees in which the associated taxa were clustered in the bootstrap test (10,000 replicate) was shown next to the branches. The phylogenetic analyses were conducted using MEGA5 (Tamura et al., 2011).

5. Translocation assay

Translocation assays were performed as previously described Schechter and collaborators (2004). This method is based on the construction of fusion proteins between identified T3E and the calmodulin-dependent Cya reporter domain. Electrocompetent *P. savastanoi* pv. savastanoi NCPPB 3335 and NCPPB 3335- T3 cells were transformated with Cya fusions, as previously described (Choi et al., 2006). Sp^R transformants were tested by PCR using a forward primer designed specifically for each T3E gene (indicated in corresponding chapter) and a reverse primer annealing to the *cya* gene (primer Cya-R135). Cya assays were performed in *Nicotiana tabacum* var. Newdel plants, as previously described (Schechter et al., 2004). *P. savastanoi* pv. savastanoi NCPPB 3335 and NCPPB 3335-T3 transformants carrying plasmids expressing T3E-Cya fusions were scraped off of the LB plates, washed twice and resuspended to an optical density at 600 nm (OD_{600}) of 0.5 (approximately 10^8 CFU/mL) in 5 mM morpholinoethanesulfonic acid (pH 5.5) and 100 µM isopropyl-thiogalactopyranoside (IPTG). Cell suspensions were injected into the fully expanded upper plant leaves using a 1 mL syringe. Leaf disks were collected at 6 h post-inoculation (hpi) with a 10 mm inner-diameter cork borer, frozen in liquid nitrogen, ground to a powder and suspended in 250 µl of 0.1 M HCl. The samples were incubated at -20 ºC overnight, and cAMP levels were determined using a 1:100 dilution of the samples and the Correlate-EIA cAMP immunoassay kit according to the manufacturer's directions (Assay Designs, Inc., Michigan, USA).

The Cya activity of the Cya fusion protein expressed in *E. coli* XL1Blue from pCPP3234 derivatives were assayed as previously reported (Schechter et al., 2004). Bacterial cells were grown in 5 mL of LB medium containing 100 µM IPTG to an OD_{600} of 0.6 to 0.8. The culture was centrifuged, and the pellet was washed and resuspended in sonication buffer (20 mM tris-HCl [pH 8.0] and 10 mM $MgCl_2$). The bacteria were sonicated with a microtip for 2 min, and the cellular debris was pelleted by centrifugation. Cya activity was determined in the presence or absence of bovine calmodulin (Calbiochem, Farmstadt, Germany) by using 5µl of each lysate (Sory and Cornelis, 1994).

6. Plant bioassays

6.1 Hypersensitive response and competitive index assays.

The *Nicotiana bentamiana* and *N. tabacum* (var. Newdel and var. Xanthi) plants used in this study were 5-7 and 4-6 weeks old, respectively. The plants were grown with a 16-h light/8-h dark photoperiod with day/night temperatures of 26 °C/22 °C. Bacterial suspensions in 10 mM $MgCl_2$

were inoculated into plant leaves using a blunt syringe. Assays with derivatives of *P. fluorescens* Pf55 [pLN18] were performed by injecting a bacterial suspension ($5x10^7$ CFU/mL) into *N. tabacum* var. Xanthi leaves using a blunt syringe. The injected areas were lightly marked on the back of the leaves. The bacterial inoculum levels differed among experiments. The bacterial levels *in planta* were determined by cutting three leaf disks with a boring tool (inner diameter: 10 mm) and placing the plant material in 1 mL of 10 mM $MgCl_2$. The disks were completely homogenized, and the resulting suspensions, containing the bacteria, were diluted and plated on LB-Sp plates (DC3000D28E) or LB-Sp-Gm plates (transformants containing pCPP5040 derivatives). *N. tabacum* var. Newdel plants were used for the HR assays. The leaves were infiltrated with bacterial suspensions (10^7 and 10^8 CFU/mL) of *P. syringae* pv. tomato DC3000D28E or its derivatives harboring plasmids expressing each of the different *P. savastanoi* pv. savastanoi T3E (Table 2). The generated symptoms, scored 48 h after inoculation, were captured with a high-resolution digital camera (Nikon DXM 1200, Nikon Corporation, Tokyo, Japan).

For competition assays, the *N. benthamiana* leaves were inoculated with mixed suspensions containing equal CFU (approximately 10^4 CFU/mL) of *P. syringae* pv. tomato DC3000D28E and each of its transformants carrying pCPP5040 derivatives expressing *P. savastanoi* pv. savastanoi T3E (Table 2). Input and ouput pools, assayed 1 and 6 h after inoculation, respectively, were plated onto LB-Sp and LB-Sp-Gm to select for DC3000D28E and the transformants with pCPP5040 derivatives, respectively. A competitive index (CI) was calculated by dividing the output ratio (CFU transformant : CFU DC3000D28E) by the input ratio (CFU transformant : CFU DC3000D28E). Competition indices of the transformant strains expressing *P. savastanoi* pv. savastanoi T3E versus DC3000D28E were normalized with respect to the CI obtained for DC3000D28E (pCPP5040). The CIs presented in each chapter represent the mean of three replicates demonstrating typical results from three independent experiments. The results were statistically analyzed using one-way ANOVA followed by post-hoc comparisons using Tukey test.

6. 2 Detection of ROS production and callose deposition

ROS production was observed after DAB staining (Thordal-Christensen et al., 1997) 4 h after inoculation with *P. fluorescens* Pf55 [pLN18] derivatives. Bacterial suspensions (10^8 CFU/mL) were inoculated into *N. tabacum* var. Xanthi leaves using a blunt syringe. Small pieces of tobacco leaves cut from around the injection area were placed into a syringe and stained by vacuum infiltration of a freshly prepared 1 mg/mL solution of DAB (Sigma-Aldrich D-8001, Sigma-Aldrich, Inc., St. Louis, MO, U.S.A.) in 8 mM HCl, pH 3.8. Chlorophyll was removed by submerging the leaves into a solution of ethanol/lactic acid/glycerol [3:1:1 (vol/vol/vol)] at 60 °C

and stored overnight at room temperature on water-soaked filter paper. At least ten biological replicates from each specimen were mounted on slides in a 50 % glycerol (vol/vol) solution and observed with a Nikon Eclipse E800 microscope (Nikon Corporation, Tokyo, Japan) under bright field. DAB staining produces an intensely brown precipitate at the sites of ROS production, which were next to the infection zone.

Callose deposition samples were developed 12 h after inoculation and stained as previously described (Guo et al., 2009). Chlorophyll was removed in 95 % (vol/vol) ethanol from small pieces of tobacco leaves, which were cut from around the injection area, and staining was performed in a 0.02 % (wt/vol) solution of aniline blue (Sigma-Aldrich #415049, Sigma-Aldrich, Inc., St. Louis, MO, U.S.A.) in 150 mM potassium phosphate, pH 9, for 1 h in the dark. At least ten biological replicates from each specimen were mounted in 50 % (vol/vol) glycerol on glass slides. Observations were conducted under UV-light excitation using the filter UV-2ª (EX 330-380, DM 400; BA 420) on a Nikon Eclipse E 800 microscope (Nikon Corporation, Tokyo, Japan).

ROS production and callose deposition were quantified as previously described (Rodríguez-Herva et al., 2012) with slight modifications. Up to four snapshots of each specimen from equivalent areas surrounding the wound (inoculation zone) were captured with a Nikon DXM1200 camera using the Nikon ACT-1 2.70 software. The same settings and a final magnification of 40X were applied to all the samples. After calibrating all the images using the scale bar included in each picture, DAB staining and aniline blue fluorescence were quantified using the program Visilog 6.3 (Noesis, Les Ulis, France). For this purpose, the characteristic brown color of the DAB precipitate and the specific blue fluorescence of callose deposition were separated by color deconvolution using the i_classification command. Then, the stained areas were quantified, and the results were expressed in mm^2. Five-six images per assay were analyzed, and statistical analyses were performed using one-way ANOVA followed by post-hoc comparisons using Tukey test.

CHAPTER I

Expression and functional analysis of *Pseudomonas savastanoi* pv. savastanoi NCPPB 3335 type III secretion system effectors

Results presented in this chapter are included in the following publication:

Matas, I.M., **Castañeda-Ojeda, M.P**., Aragón, I.M., Antúnez-Lamas, M., Murillo, J., Rodríguez-Palenzuela, P., López-Solanilla, E., and Ramos, C. (2014). Translocation and functional analysis of *Pseudomonas savastanoi* pv. savastanoi NCPPB 3335 type III secretion system effectors reveals two novel effector families of the *Pseudomonas syringae* complex. *Mol Plant Microbe Interact* 27(5):424-36.

INTRODUCTION

Type III secretion system (T3SS) effectors (T3E) delivered by bacterial pathogens are key elements for establishing infection. In bacterial plant pathogens, these proteins primarily interfere with the plant immune system at two main defense layers: pathogen-associated molecular pattern (PAMP)-triggered immunity (PTI) and effector-triggered immunity (ETI) (Chisholm et al., 2006; Jones and Dangl, 2006). A more detail explanation about the effect of these defense systems *in planta* is included in pages 43-44 in the General Introduction section (See *Introducción General*).

As it has been previously described (See *Introducción General*), bioinformatics analysis of the draft genome sequence of *P. savastanoi* pv. savastanoi NCPPB 3335 have allowed the identification of 33 putative T3E in the effector repertoire of this pathogen (Rodriguez-Palenzuela et al., 2010; Bardaji et al., 2011; Matas et al., 2014).

The translocation assays carried out previously in our group with 12 of the 33 putative T3E, showed that 7 of these T3E candidates are translocated into plant cells through the NCPPB 3335 T3SS (Matas et al., 2014) (Table 1). This study included three T3E for which translocation into plant cells has not been demonstrated for any other *P. syringae* strain (AvrRpm2, HopAA1, and HopAZ1); three novel T3E (HopBK1, HopBL1, and HopBL2) from two new effector families of the *P. syringae* complex (HopBK and HopBL); and HopA1 whose homolog in *P. syringae* pv. tomato DC3000 has been shown to be translocated into *Arabidopsis* leaves (Chang et al., 2005; Matas et al., 2014).

Table 1. *P. savastanoi* pv. savastanoi NCPPB 3335 type III effectors which translocation has been demonstrated using Cya fusions (Matas et al., 2014).

Name	Locus tag[a]	Pfam[b]	Reference	Homolg translocated in *P. syringae*[c]	Reference
AvrRpm2	PSA3335_5091	None	(Ramos et al., 2012)	nd	
HopA1	PSA3335_5065	None		+	(Chang et al., 2005)
HopAA1	na	None	(Ramos et al., 2012)	-	(Chang et al., 2005)
HopAZ1	PSA3335_1783	None	(Ramos et al., 2012)	nd	
HopBK1	PSA3335_2068	PF13974	(Rodríguez-Palenzuela et al., 2010)	nd	
HopBL1	PSA3335_0157	PF02902	(Matas et al., 2014)	nd	
HopBL2	PSA3335_4544	PF02902	(Matas et al., 2014)	nd	

[a]na, not available; [b]Accession number for the corresponding protein families at the pfam database (http://pfam.xfam.org/); [c]nd, not determined.

Due to the limited information available about the function of T3E proteins in the interaction of NCPPB 3335-plants, in this chapter, we study the expression dependency on HrpL and the ability to inhibit plant defense responses of the seven NCPPB 3335 T3E which translocation into plant cells has been demonstrated.

MATERIAL AND METHODS

Bacterial strains, plasmids and growth conditions

The strains and the specific plasmid used in this chapter are described in Table 2 and Table 3, respectively. *Pseudomonas* and *Escherichia coli* strains were grown at 28°C and 37ºC, respectively, using Luria-Bertani (LB) medium (Miller, 1972), King´s B (KB) medium (King et al., 1954) or Super Optimal Broth (SOB) medium (Hanahan, 1983). Solid and liquid media were supplemented, when required, with the following antibiotics (amounts reported in µg/ml) for the *Pseudomonas*/*E. coli* strains: ampicillin (Ap) 300/100, gentamicin (Gm) 10/10 and kanamycin (Km) 10/50.

Table 2. Bacterial strains used in this study.

Strain	Relevant characteristics	References
Pseudomonas		
P. savastanoi pv. savastanoi (Psv)		
NCPPB 3335	Wild-type strain isolated from olive	(Perez-Martinez et al., 2007)
NCPPB 3335-T3	Type III secretion mutant (Km^R)	(Perez-Martinez et al., 2010)
NCPPB 3335Δ*hrpL*	*hrpL* mutant derived from NCPPB 3335 (Km^R)	(Matas et al., 2014)
P. syringae pv. tomato (Pto)		
DC3000D28E	*ΔhopU1-hopF2 ΔhopC1-hopH1*::FRT *ΔhopD1-hopR1*::FRT *ΔavrE-shcN ΔhopAA1-2-hopG1::*FRT *ΔhopI1 ΔhopAM1-1 ΔhopAF1*::FRT *ΔavrPtoB ΔavrPto ΔhopK1 ΔhopB1 ΔhopE1 ΔhopA1::*FRT *hopY1::*FRT pDC3000A− pDC3000B− (Sp^R)	(Cunnac et al., 2011)
P. fluorescens 55 (Pf55) [pLN18]	Containing 25 kb *P. syringae* pv. syringae 61 *hrc/hrp* cluster with *shcA* and *hopPsyA* replaced by an *nptII* cassette (Km^R) .	(Jamir et al., 2004)

[a] Cm^R, Km^R, Tc^R and Gm^R indicate resistance to chloramphenicol, kanamycin, tetracycline and gentamicine, respectively.

Table 3. Plasmid used in this study.

Plasmid	Relevant characteristics	References
pENTR-*avrRpm2*	pENTR/D/SD TOPO::AER-0005728 (Km^R)	(Matas et al., 2014)
pENTR-*hopA1*	pENTR/D/SD TOPO::AER-0002657 (Km^R)	(Matas et al., 2014)
pENTR-*hopAA1*	pENTR/D/SD TOPO::AER-0000274 (Km^R)	(Matas et al., 2014)
pENTR-*hopAZ1*	pENTR/D/SD TOPO::AER-0001017 (Km^R)	(Matas et al., 2014)
pENTR-*hopBK1*	pENTR/D/SD TOPO::AER-0000696 (Km^R)	(Matas et al., 2014)
pENTR-*hopBL1*	pENTR/D/SD TOPO::AER-0000509 (Km^R)	(Matas et al., 2014)
pENTR- *hopBL2*	pENTR/D/SD TOPO::AER-0003844 (Km^R)	(Matas et al., 2014)
pEXP-*avrRpm2*	pCPP5040 expressing AER-0005728-HA tag (Gm^R)	This study
pEXP-*hopA1*	pCPP5040 expressing AER-0002657-HA tag (Gm^R)	This study
pEXP-*hopAA1*	pCPP5040 expressing AER-0000274-HA tag (Gm^R)	This study
pEXP-*hopAZ1*	pCPP5040 expressing AER-0001017-HA tag (Gm^R)	This study
pEXP- *hopBK1*	pCPP5040 expressing AER-0000696-HA tag (Gm^R)	This study
pEXP- *hopBL1*	pCPP5040 expressing AER-0000509-HA tag (Gm^R)	This study
pEXP-*hopBK2*	pCPP5040 expressing AER-0003844-HA tag (Gm^R)	This study

[a] Km^R and Gm^R indicate resistance to kanamycin and gentamicine, respectively.

Quantitative RT-PCR assays

qRT-PCR assays were performed as described at General Material and Methods section using oligonucleotides primers shown in Table 4.

Table 4. Primers used in this study.

Forward primers		Reverse primers	
Name[a]	Sequence	Name[a]	Sequence
avrPto-F295	GACAGGAGAGTCAGGAGTAAACC	*avrPto*-R430	GAAGTCGTCGTCAGAATCTG
iaaM-F293	GGCCTTTTCCACTACCTGAA	*iaaM*-R501	GCAACTAAAGAACCGCCTTC
hopBK1-F26	GCCGAGAGTGGATCAAGAAG	*hopBK1*-R139	ATCACTCAGTGCGTCGATCA
hopBL1-F1332	TCCAGCTTCGACCTTCAAC	*hopBL1*-R1514	AACGGCAGATTGTCCACAT
hopBL2-F1134	ACAGGGACGAAGGCTTGGA	*hopBL2*-R1241	CGGAGACATGGTGGATGGA

[a] F and R, forward and reverse primer, respectively. Numbers included after F and R in primers names correspond to the hybridization position of the 3 end of the primer in the corresponding ORF sequence.

Plant bioassays

The *N. bentamiana* and *N. tabacum* (var. Newdel and var. Xanthi) plants used in this study were inoculated as described at General Material and Methods section with *P. fluorescens* Pf55 [pLN18] or *P. syringae* pv. tomato DC3000D28E or its derivatives harboring plasmids expressing each of the different *P. savastanoi* pv. savastanoi T3E (Table 3).

RESULTS

HrpL-dependent expression of novel *P. savastanoi* T3SS effectors

To unveil the HrpL-dependent expression of the three hypothetical proteins identified as novel T3E of the *P. syringae* complex (HopBK1, HopBL1 and HopBL2), a Δ*hrpL P. savastanoi* pv. savastanoi NCPPB 3335 mutant was used (Matas et al., 2014). The expression of the *hopBK1*, *hopBL1* and *hopBL2* genes was analyzed using quantitative reverse-transcription polymerase chain reaction (qRT-PCR) with both the wild type and the NCPPB 3335 Δ*hrpL* mutant. In addition, the expression of the *avrPto1* gene and the *iaaM* gene (encoding tryptophan monooxygenase, involved in the biosynthesis of indoleacetic acid) was also tested as positive and negative controls, respectively. Under non-inducing conditions (cells grown in KB medium), the expression of the *hopBK1*, *hopBL1* and *hopBL2* genes was comparable in the Δ*hrpL* mutant and the wild-type strain (data not shown). However, six hours after the transfer of bacterial cells to Hrp-inducing medium, the expression of all three genes and the expression of the *avrPto1* gene decreased (0.002- to 0.4-fold) in the Δ*hrpL* mutant compared to the wild type, demonstrating an expression dependency on HrpL. As expected for the negative control, no reduction in the expression of the *iaaM* gene was observed under the same conditions (Fig. 1).

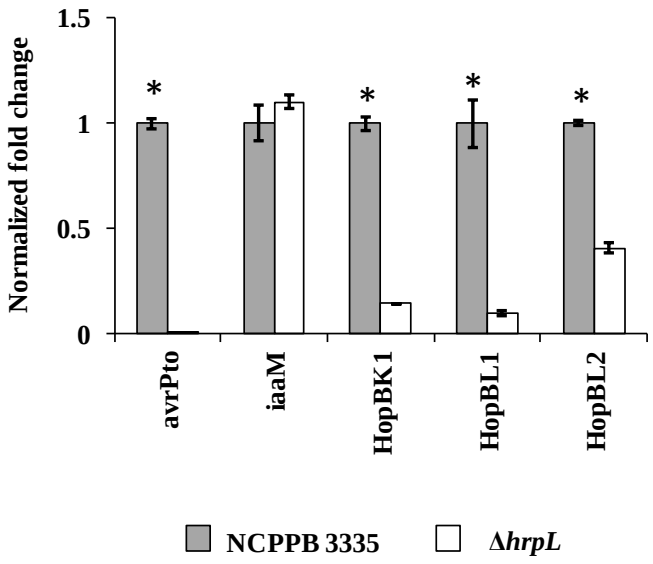

Figure. 1. HrpL-dependent expression of the *P. savastanoi* pv. savastanoi NCPPB 3335 novel T3SS effectors. Quantitative reverse-transcription polymerase chain reaction (qRT-PCR) with the indicated *P. savastanoi* pv. savastanoi NCPPB 3335 T3E genes in NCPPB 3335 Δ*hrpL* vs. NCPPB 3335 at 6 h after transfer to Hrp-inducing medium. The fold change was calculated after normalization using the *gyrA* gene as an internal control. The results represent the means from three independent experiments. The error bars represent the standard deviation. Asterisks indicate significant differences (P = 0.05) between the values obtained for the wild type and the Δ*hrpL* strains.

Heterologous expression of *P. savastanoi* T3SS effectors in the non-pathogen *Pseudomonas fluorescens* Pf55 expressing a cloned *P. syringae* Hrp system

T3E activities interfere with the innate immunity response of the plant at different levels. ROS production and callose deposition upon pathogen recognition are early plant defense responses. To test the ability of the seven *P. savastanoi* pv. savastanoi T3E analyzed in this study (Table 1) to attenuate these responses, we expressed their corresponding genes (see pCPP5040 derivatives, Table 3) in *Pseudomonas fluorescens* 55 (Pf55) [pLN18], which heterologously expresses a *P. syringae* T3SS, thus enabling the delivery of effector proteins into plant cells at levels characteristic of a natural infection (Jamir et al., 2004; Lopez-Solanilla et al., 2004; Oh et al., 2010; Rodríguez-Herva et al., 2012). For this purpose, *N. tabacum* leaves were used. PAMPs displayed by Pf55 generate a PTI response in inoculated plants, which is increased by the pLN18-encoded T3SS, as indicated by a higher ROS level than that induced by Pf55 without a T3SS (Oh et al., 2010). Figure 2 demonstrates that the ROS levels, determined by 3,3'-diaminobenzidine (DAB) staining, were significantly reduced by the expression of each of the seven T3E compared to the control strain Pf55 [pLN18] harboring an empty vector (Tukey test; $P \leq 0.01$) (Fig. 2A and 2B). Moreover, with the exception of HopA1, all the other T3E significantly reduced the levels of callose deposition compared to the control strain (Tukey test; $P \leq 0.01$) (Fig. 2C and 2D). These results suggest that these T3E interfere with the early responses associated with plant immunity.

Heterologous expression of *P. savastanoi* T3SS effectors in the functionally effectorless polymutant *P. syringae* pv. tomato DC3000D28E

To further analyze the individual roles of the *P. savastanoi* pv. savastanoi T3E when confronting the plant immune system, we constructed derivatives of the *P. syringae* pv. tomato DC3000D28E strain expressing each of the seven effectors from the pCPP5040 plasmid (Table 3). DC3000D28E is a polymutant of the model pathogen *P. syringae* pv. tomato DC3000 that harbors deletions in all 28 well-expressed effector genes. Thus, DC3000D28E is considered a functionally effectorless but otherwise wild type *in planta*. Although the wild-type strain DC3000 induces an ETI-like rapid plant cell death in *N. benthamiana* and *N. tabacum*, DC3000D28E has a reduced ability to induce this response and seems to elicit plant defenses that are T3SS-dependent and additional to basal PTI (Cunnac et al., 2011). This elicitation is explained by the fact that DC3000D28E has the wild-type complement of T3SS helper proteins (except HrpW1), and several of these proteins can elicit plant defenses and induce an HR response (Kvitko et al., 2007; Cunnac et al., 2011). Therefore, this strain is an excellent tool to investigate the role of heterologous effectors in amenable systems, such as *N. benthamiana* and *N. tabacum*. DC3000D28E derivatives expressing the selected T3E were compared with DC3000D28E

regarding their ability to elicit cell death in *N. tabacum* at two different inoculum levels, which were chosen to exceed the threshold typically needed to elicit cell death associated with ETI. Neither the polymutant strain DC3000D28E nor the derivatives expressing *P. savastanoi* pv. savastanoi T3E incited the HR response typical of the wild-type strain DC3000 at a bacterial dose of $2x10^7$ CFU/mL. However, with ten times more bacteria ($2x10^8$ CFU/mL), the polymutant strain stimulated an ETI-like response after 48 h of inoculation, which was partially or completely inhibited by the expression of the *P. savastanoi* pv. savastanoi proteins HopAZ1 and HopBL1, respectively (Fig. 3A and 3B). These results suggest that these two effectors participate in the inhibition of the plant defense response associated with the onset of programmed cell death.

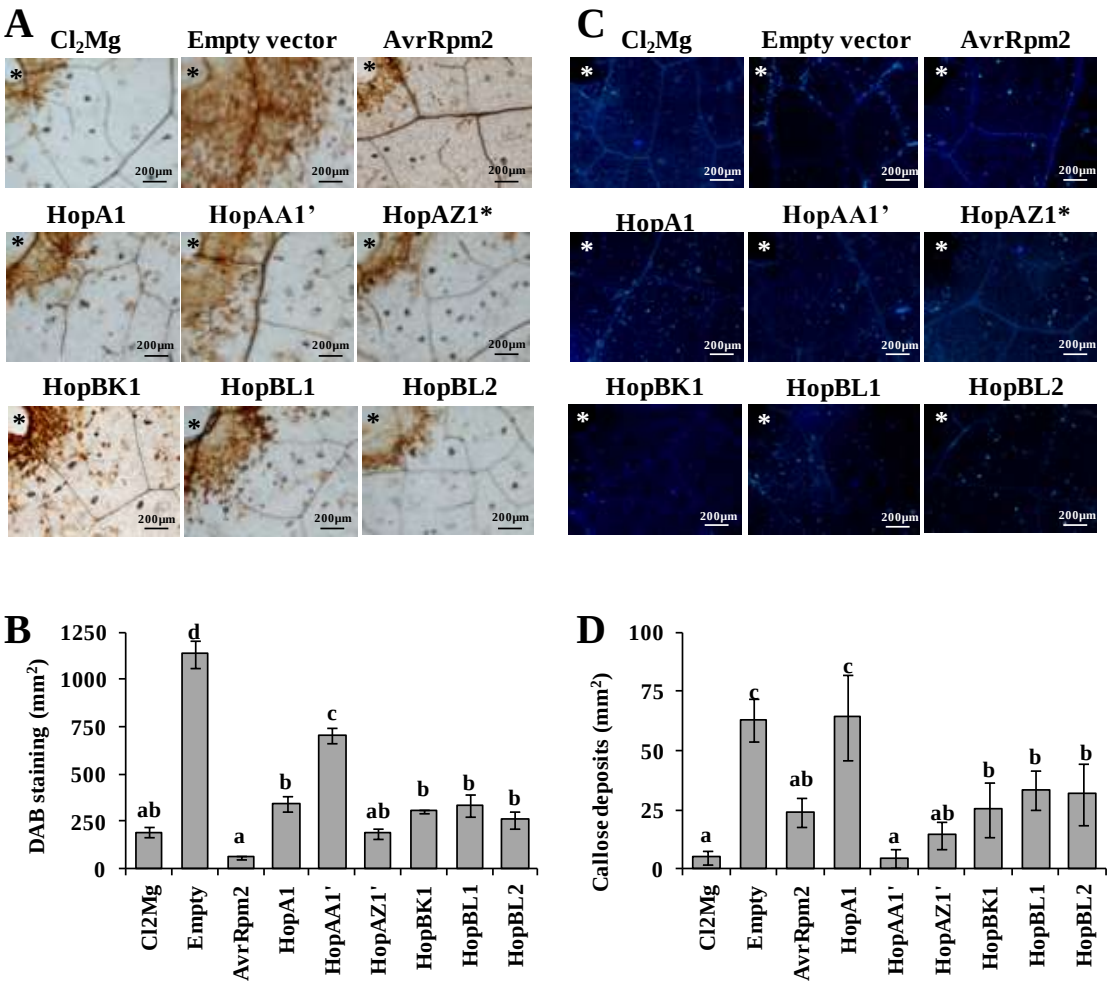

Figure 2. DAB staining and callose deposition in *N. tabacum* var. Xanthi leaves. Plants were challenged with *P. fluorescens* 55 [pLN18] harboring the pCPP5040 empty vector or the vectors expressing the indicated *P. savastanoi* pv. savastanoi NCPPB 3335 T3E. **A,** The DAB signal was quantified 4 h after infection and represented in a histogram (**B**). **C,** The callose deposition was assessed using aniline blue staining, quantified 12 h after infection and represented in a histogram (**D**). The asterisks in **A** and **C** indicate inoculation zones. For histograms, data are means ± standard error of the mean for at least five replicas; bars topped with the same letter represent values that are not significantly different using one-way ANOVA followed by post-hoc comparisons using Tukey test.

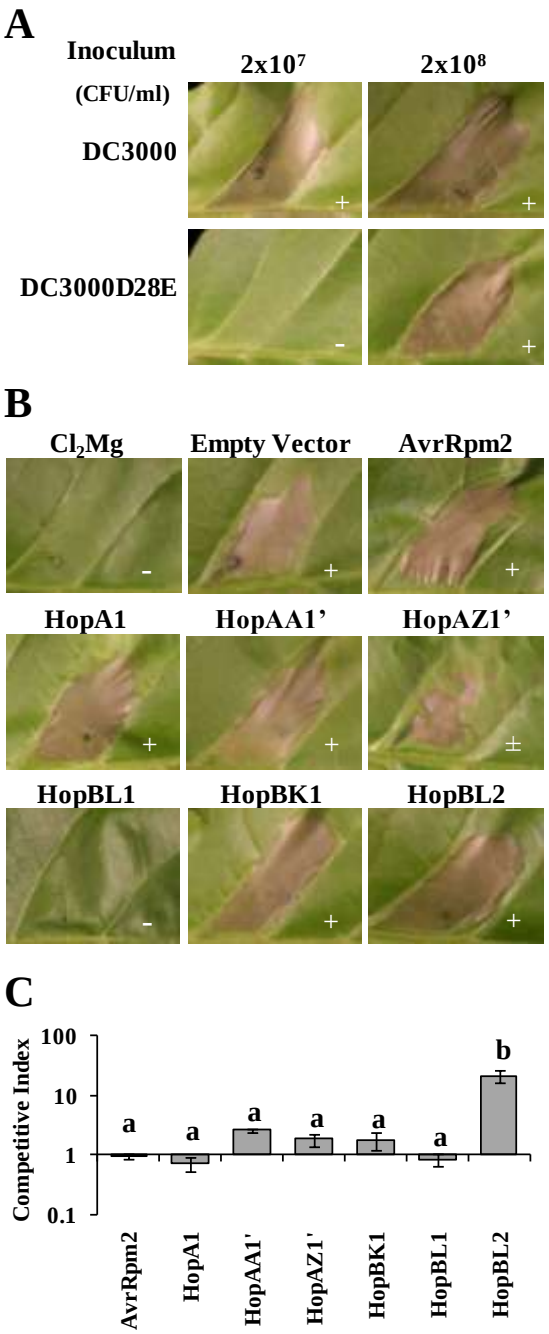

Figure. 3. Delivery of *P. savastanoi* pv. savastanoi T3SS effectors by functionally effectorless *P. syringae* pv. tomato DC3000D28E in *Nicotiana* leaves. **A,** Cell death response in *N. tabacum* var. Newdel leaves 48 h after inoculation with *P. syringae* pv. tomato strains DC3000 (wild type) or DC3000D28E cells suspended in $MgCl_2$ and adjusted to the indicated densities (in CFU/ml). **B,** Cell death response in *N. tabacum* var. Newdel leaves 48 h after inoculation with *P. syringae* pv. tomato DC3000D28E cells suspended in $MgCl_2$ carrying pCPP5040 (empty vector) derivatives expressing the indicated *P. savastanoi* pv. savastanoi NCPPB 3335 T3E (Table 3) adjusted to $2x10^8$ CFU/ml. Cell death response: +, positive; -, null; ±, partial. Each experiment was repeated at least three times with similar results. **C,** Competition assays in *N. benthamiana* leaves between *P. syringae* pv. tomato DC3000D28E and each of its transformants carrying pCPP5040 derivatives expressing the indicated *P. savastanoi* pv. savastanoi T3E. Competition indices (CI) were normalized with respect to the CI obtained for DC3000D28E vs. DC3000D28E expressing the empty vector (pCPP5040). Values are the mean ± standard error of the mean of three replicates demonstrating typical results from three independent experiments; bars topped with the same letter represent values that are not significantly different using one-way ANOVA followed by post-hoc comparisons using Tukey test.

The DC3000D28E strain has been shown to grow better *in planta* when coinoculated with a strain that is able to suppress plant immunity, such as DC3000Δ*hopQ1-1* (Cunnac et al., 2011). Therefore, this strain is considered an excellent tool for testing the ability of individual T3E to restore bacterial growth or to induce specific plant responses. To investigate the effect of the seven *P. savastanoi* pv. savastanoi T3E on the ability of DC3000D28E to colonize *N. benthamiana*, competition assays between the polymutant strain (DC3000D28E) and each derivative expressing the selected T3E were conducted. *N. benthamiana* leaves were infiltrated with a mixed inoculum (1:1) of DC3000D28E and each of the derivatives, and after 6 days, bacteria were recovered and viable cells were determined. The results presented in Figure 3C are expressed as the competition indices (CI) of the derivatives expressing each of the *P. savastanoi* pv. savastanoi T3E relative to the DC3000D28E strain. Interestingly, the expression of *P. savastanoi* pv. savastanoi HopBL2 in DC3000D28E significantly increased the competitiveness of the strain, which was reflected in a CI value (HopBL2/DC3000D28E) of 21.1. Expression of HopAA1 also increased the competitiveness of the strain, although at lower level (CI= 2.6) than HopBL2. These results suggest that these effectors inhibit plant defense responses.

DISCUSSION

The recent availability of complete and draft genome sequences for several *P. syringae* and *P. savastanoi* pathovars and the relevant advances in the development of bioinformatics tools led to a comprehensive catalog of candidate effector-repertoire for 19 different strains (Baltrus et al., 2011). Given that only nine new effector families were identified after the latest comparative genome-sequence analysis, it was suggested that the *P. syringae* complex effector super-repertoire could be nearly complete with 57 effector families (Baltrus et al., 2011; Lindeberg et al., 2012). However, translocation analysis of 12 *P. savastanoi* pv. NCPPB 3335 candidate T3E revealed two novel effector families of the *P. syringae* complex, HopBL and HopBK (Matas et al., 2014). Novel candidate effectors should be functionally characterized in relation to their expression dependency on HrpL and in the contex of a unified model for a two-layered immune system in plants (Block and Alfano, 2011; Lindeberg et al., 2012). In this study, we first demonstrated that the expression of the three novel T3E whose translocation across the *P. savastanoi* pv. savastanoi T3SS was previously demonstrated (Matas et al., 2014) were transcriptionally dependent on HrpL (Fig. 1).

The vast majority of the *P. syringae* pv. tomato DC3000 type III effectors have been demonstrated to suppress ETI, and many can also suppress PTI, suggesting that numerous type III effectors exert multiple activities or, alternatively, that common type III effector targets are utilized in pathways needed for ETI, PTI or both (Guo et al., 2009). Our results indicate that the seven *P. savastanoi* pv. savastanoi NCPPB 3335 T3E tested - AvrRpm2, HopA1, HopAA1, HopAZ1, HopBK1, HopBL1 and HopBL2 (Table 1) -, including the truncated versions of HopAA1 and HopAZ1, interfered with early responses associated with plant defense (Fig. 2). In addition, we demonstrated that HopAZ1 and HopBL1 also inhibited the ETI-like response incited by DC3000D28E in tobacco (Fig. 3).

Although all the tested T3E significantly reduced ROS production (Fig. 2), expression of HopA1 in Pf55 did not significantly reduce callose deposition under the conditions tested. The secretion of HopA1 via the T3SS in *P. syringae* pv. syringae 61 requires the ShcA chaperone (Dijk et al., 2002). Although a ShcA protein homolog has been annotated in the draft genome of *P. savastanoi* pv. savastanoi (AER-0002589), the expression analysis of this effector in this study did not include the NCPPB 3335 ShcA. Thus, we cannot exclude that this protein chaperone may also be necessary for full secretion and *in planta* activity of HopA1 in *P. savastanoi*. Conversely, HopA1 from *P. syringae* pv. syringae 61 has been demonstrated to elicit an HR in tobacco when expressed in *P. fluorescens* (Alfano and Collmer, 1996). In agreement with these authors, HopA1 expression in DC3000D28E did not suppress the HR response incited by DC3000D28E in tobacco.

DC3000D28E has been demonstrated to be suitable for testing the ability of T3E to restore bacterial growth and induce plant responses (Cunnac et al., 2011). Although the expression of *P. savastanoi* pv. savastanoi HopBL2 in DC3000D28E did not inhibit the ETI-like response induced at high cell doses by DC3000D28E in *N. tabacum*, HopBL2 expression in this strain significantly increased its competitiveness in *N. benthamiana* (Fig. 3C). Significant DC3000D28E growth restoration in *N. benthamiana* due to the expression of single DC3000 effectors was demonstrated for only AvrPto and AvrPtoB, but neither other effectors, such as HopM1, nor a set of several conserved effectors displayed this effect. Conversely, single DC3000 effectors promoted growth when combined with other effectors in DC3000D28E (Cunnac et al., 2011). Thus, our results suggest that the *P. savastanoi* pv. savastanoi HopBL2, which harbors a C-terminal XopD-like SUMO protease domain (Kim et al., 2011; Matas et al., 2014) and HopBL1, might be involved in the inhibition of the initial perception of pathogens. More specifically, XopD has been recently demonstrated to suppress the ethylene production required for anti-*Xanthomonas euvesicatoria* immunity (Kim et al., 2013). Although the current knowledge of specific T3E functions is limited, our results suggest that the seven *P. savastanoi* T3E analyzed here inhibited PTI, whereas HopAZ1 and HopBL1 also inhibited the ETI-like response. Moreover, and although truncated T3E (HopAA1 and HopAZ1) are generally considered as functionless pseudogenes (see Figure 6 in General Introduction), our results also demonstrate that the N-terminal region of the truncated versions of HopAA1 and HopAZ1 encoded by *P. savastanoi* pv. savastanoi NCPPB 3335 (Matas et al., 2014) are able to interfere with responses associated with plant defense (Fig 2 and Fig. 3). Although no function has been yet established for the HopAZ and HopAA T3E families, *P. syringae* pv. avellanae HopAZ1 is a promising candidate for modulating hazelnut host specificity (O'Brien et al., 2012). On the other hand, deletion of *hopAA1-1* in *P. syringae* pv. tomato significantly reduced the formation of necrotic speck lesions in tomato leaves (Munkvold *et al.*, 2009). Moreover, HopAA1 has been demonstrated to attenuate the innate immunity in *Arabidopsis* (Li et al., 2005a).

In summary, here we demonstrate that seven *P. savastanoi* pv. savastanoi NCPPB 3335 T3E, including HopBK1, HopBL1 and HopBL2, interfere with early responses associated with plant defense. In addition, we demonstrate that HopAZ1 and HopBL1 also inhibit the ETI-like response. Future studies should focus on elucidating the precise mechanisms and targets of these and other effectors that are included in the *P. syringae* pangenome and that specifically participate in the infection of woody plants.

CHAPTER II

Pseudomonas savastanoi **pv. savastanoi NCPPB 3335 encodes two members of the type III effector tyrosine phosphatase family HopAO, both involved in the suppression of plant immune responses**

INTRODUCTION

The detailed study of the type III secretion system (T3SS) effectors (T3E) has been tackled using as a model several strains of the plant pathogenic bacteria *Pseudomonas syringae*. As result of these analyses, the pangenome of *P. syringae* has been described to encode over 60 families of T3E effectors injected by the T3SS. Moreover, the effector repertoires of phylogenetically diverse strains are today defined by a pool of core effectors targeting antimicrobial vesicle trafficking and a larger set of variable effectors targeting kinase-based recognition processes (Lindeberg et al., 2012).

The T3E repertoire of *P. savastanoi* pv. savastanoi NCPPB 3335, a model pathogen for exploring bacterial infection of woody host, includes 33 T3E (Rodriguez-Palenzuela et al., 2010; Ramos et al., 2012; Matas et al., 2014). Among these T3E candidates, only two are homologs of *P. syringae* T3E with a previously demonstrated enzymatic function (Matas et al., 2014), i.e., HopAO1 and HopAB1, which tyrosine phosphatase (Underwood et al., 2007) and E3 ubiquitin ligase (Janjusevic et al., 2006) activities, respectively, has been proven in *P. syringae* pv. tomato DC3000.

Research on the HopAO1 function has revealed its relevant contribution to the virulence of *P. syringae* pv. tomato DC3000 in *Arabidopsis* (Bretz et al., 2003), its ability to suppress both the HR elicited by an avirulent *P. syringae* strain on *Nicotiana benthamiana* (Espinosa et al., 2003), and in the suppression of the innate immnuty induced by the PAMP flagellin in *Arabidopsis* (Underwood et al., 2007). Moreover, recent studies have shown that HopAO1 phosphatase activity reduces elongation factor Tu (EF-Tu) receptor EFR phosphorylation, interfering with the initiation of the immune response after pathogen recognition (Macho et al., 2014). The phylogenetic distribution of effector families in the *P. syringae* effector super-repertoire shows that T3E of the HopAO family are distributed among strains belonging to multi locus sequence typing (MLST) groups I and III established by Baltrus et al. (2011) (Lindeberg et al., 2012). However, this analysis did not consider other members of the HopAO1 family like the HopAO1 homolog encoded by *P. savastanoi* pv. savastanoi NCPBB 3335, also a group III strain.

In this study, we first identify a new member of the HopAO1 family encoded in the genome of NCPBB 3335 (HopAO2). We demonstrate the translocation into plant cells and the inhibition of plant defense responses by both HopAO1 and HopAO2, which are plasmid and chromosomally encoded, respectively. Analyses of the subcellular localization of these two T3E in *N. benthamiana* using effector fusions to the green fluorescent protein (GFP), suggest their localization to the plasma membrane and Golgi vesicles, respectively. Moreover, we demonstrate that a Δ*hopAO1* mutant of NCPBB 3335 exhibits a reduced fitness and virulence in olive plants.

MATERIAL AND METHODS

Bioinformatics analysis

Accession numbers of the protein sequences used for the construction of the phylogenetic trees shown in Figure 1 are in Table 1. Sequence alignment using ClustalW, determination of the optimal amino acid substitution model and phylogenetic tree construction were performed using MEGA5 (Tamura et al., 2011). Neighbor-joining and maximum-likelihood phylogenetic trees of the individual protein sequences were generated using MEGA5 with the optimal model (John-Taylor-Thornton model) and the option of complete deletion to eliminate positions containing gaps. Confidence levels for the branching points were determined using 10,000 bootstraps replicates.

Table 1. Accession numbers of the protein sequences used for the construction of the phylogenetic trees shown in Figure 1.

Protein/Strain[a]	Abbreviated pathovars name	Accession number[b]	Locus Tag
HopAO1			
aesculi 2250	Pae	WP_005734863.1	Psyrpa2_010100025464
mori MAFF 301020	Pmo	WP_005760287.1	PSYMO_39895
orizae 1 6	Por	WP_005888836.1	Psyrpo1_010100006516
savastanoi NCPPB 3335	Psv	YP_006961588.1	PSA3335_0875
tomato DC3000	Pto	NP_794465.1	PSPTO_4722
HopAO2			
savastanoi NCPPB 3335	Psv	GG774693.1	PSA3335_5047
actinidae MAFF 302091	Pan	WP_017684870.1	PSYAC_20366
maculicola ES4326	Pma	na	PMA4326_30047
mori MAFF 301020	Pmo	na	PSYMO_27904

[a] Indicated as pathovars of *Pseudomonas syringae*, with the exception of *P. savastanoi* pv. savastanoi. [b] Database - Hops, http://www.pseudomonas-syringae.org/home.html. na, not available in GenBank.

Bacterial strains, plasmids, culture media and growth conditions

Most bacterial strains and plasmids used in this chapter are described in Tables 2 and 3, respectively. Bacterial strains used for dot blot hybridization are described in the General Material and Methods section (Table 1). All *Pseudomonas* strains were grown in King´s B (KB) medium (King et al., 1954), Luria-Bertani (LB) medium (Miller, 1972), Hrp-inducing medium (HIM) (Huynh et al., 1989) or Super Optimal Broth (SOB) (Hanahan, 1983) at 28 ºC. *Escherichia coli* and *Agrobacterium tumefaciens* were grown in LB medium at 37 ºC or 28 ºC, respectively. When required, the medium was supplemented with ampicillin (Ap), 100 µg/mL; gentamicin (Gm), 10 µg/mL; kanamycin (Km), 10 or 50 µg/mL; rifampicin (Rf), 50 µg/mL; tetraciclin (Tc), 10 µg/mL or spectinomycin (Sp), 10 µg/mL.

Table 2. Bacterial strains used in this study.

Strains[a]	Relevant characteristics	References[b]
E. coli		
DH5α	*F -, ϕ80dlacZ M15, (lacZYA-argF) U169, deoR, recA1, endA, hsdR17 (rk - mk -), phoA, supE44, thi-1, gyrA96, relA1.*	(Hanahan, 1983)
XL1 Blue	*hsdR17, supE44, recA1, endA1, gyrA46, thi, relA1, lac/ F′* [*proAB*$^{+}$, *lacI*^{q}, *lacZ M15::*Tn10 (Tc^{R})]	(Bullock et al., 1987)
GM2929	*F -, ara-14, leuB6, thi-1, tonA31, lacY1, tsx-78, galK2, galT22, glnV44, hisG4, rpsL136, xyl-5,mtl-1, dam13::Tn9, dcm-6, mcrB1, hsdR2, mcrA, recF143*. (Sp^{R} Cm^{R}).	(Palmer and Marinus, 1994)
BL21(DE3)	*F-, ompT, gal, dcm, lon, hsdSB* (r_B^- m_B^-), *λ* (*DE3* [*lacI, lacUV5-T7, gene 1, ind1, sam7, nin5*])	Novagen
Agrobacterium		
A. tumefaciens GV3101 (pMP90)	Carries Vir plasmid encoding T-DNA transfer machinery, Rif^{R}, Cm^{R}.	ATCC 33970
Pseudomonas		
P. fluorescens 55 [pLN18] (Pf)	Containing 25 kb *P. syringae* pv. syringae 61 *hrc/hrp* cluster with *shcA* and *hopPsyA* replaced by an *nptII* cassette (Km^{R}) .	(Jamir et al., 2004)
P. savastanoi pv. savastanoi (Psv)		
NCPPB 3335	Wild-type strain isolated from olive	(Pérez-Martínez et al., 2007)
NCPPB 3335-T3	Type III secretion mutant (Km^{R})	(Pérez-Martinez et al., 2010)
Psv48 ΔAB	NCPPB 3335 cured of pPsv48A and pPsv48B	(Bardaji et al., 2011)
NCPPB 3335 Δ*hrpL*	*hrpL* mutant derived from NCPPB 3335 (Km^{R})	(Matas IM et al., 2014)
Δ*hopAO1*	*hopAO1* mutant derived from NCPPB 3335 (Km^{R})	This study
P. syringae pv. phaseolicola (Pph)		
1448A	Isolated from bean	(Teverson, 1991)
P. syringae pv. tomato (Pto)		
DC3000	Isolated from tomato	(Cuppels, 1986)
DC3000D28E	*ΔhopU1-hopF2 ΔhopC1-hopH1*::FRT *ΔhopD1-hopR1*::FRT *ΔavrE-shcN ΔhopAA1-2-hopG1::*FRT *ΔhopI1 ΔhopAM1-1 ΔhopAF1*::FRT *ΔavrPtoB ΔavrPto ΔhopK1 ΔhopB1 ΔhopE1 ΔhopA1::*FRT *hopY1::*FRT pDC3000A− pDC3000B− (Sp^{R})	(Cunnac et al., 2011)

[a]Cm^{R}, Km^{R}, Sp^{R}, Rif^{R}, and Tc^{R} indicate resistance to chloramphenicol, kanamycin, spectinomycin, rifampicin, and tetracycline, respectively. [b]ATCC, American Type Culture Collection.

Expression plasmids (Table 3) were generated using Gateway™ cloning technology (Invitrogen Cor, California, USA) as indicated in General Material and Methods section.

Construction of the Δ*hopAO1* (AER-0000610) mutant from *P. savastanoi* pv. savastanoi NCPPB 3335 was performed by marker exchange mutagenesis as previously described and the correct exchange of the *hopAO1* gene by the Km resistance cassette was determined by Southern blot analysis (General Material and Methods section).

Table 3. Plasmid used in this study.

Name	Description[a]	References
pGEM-T	Cloning vector containing ori f1 and *lacZ* (Amp^R)	(*Promega*, USA)
pGEM-T- KmFRT-*EcoR*I	Contains Km^R from pKD4 (Amp^R Km^R)	(Zumaquero et al., 2010)
pPCO2	pGEM-T derivates, contains 1.2 kb approx. on each side of the *hopAO1* gene (AER-0000610) (Ap^R)	This study
pPCO2-Km	pGEM-T derivates, contains 1.2 kb approx. on each side of the *hopAO1* gene (AER-0000610) interrupted by the kanamycin resistance gen *nptII* (Ap^R, Km^R)	This study
pENTR/D/SD TOPO	Entry vector for Gateway cloning (Km^R, Cm^R)	(*Invitrogen Corp*.; California, USA)
pENTR-*hopAO1*	pENTR/D/SD TOPO::AER-0000610 (Km^R)	This study
pENTR-*hopAO2*	pENTR/D/SD TOPO::AER-0000328 (Km^R)	This study
pCPP3234	pVLT35::Gateway cassette-Cya fusion, broad-host-range vector containing *tac* promoter and *lacI*^{q} (Sp^R, Str^R, Cm^R)	(Schechter et al., 2004)
pCYA-*hopAO1*	pCPP3234 expressing AER-0000610-Cya (Sp^R, Str^R)	This study
pCYA-*hopAO2*	pCPP3234 expressing AER-0000328-Cya (Sp^R, Str^R)	This study
pCPP5040	pML123::Gateway cassette, broad-host-range vector allowing for constitutive expression of inserts fused to a C-terminal HA tag from the *nptII* promoter (Gm^R, Cm^R)	(Lopez-Solanilla et al., 2004)
pEXP-*hopAO1*	pCPP5040 expressing AER-0000610-HA tag (Gm^R)	This study
pEXP-*hopAO2*	pCPP5040 expressing AER-0000328-HA tag (Gm^R)	This study
pGWB5	35S promoter, C-sGFP (35S promoter-R1-Cm^R-*ccdB*-R2-sGFP), Km^R, Hg^R	Invitrogen
pLOC-*hopAO1*	pGWB5 expressing AER-0000610-GFP (Km^R, Hg^R)	This study
pLOC-*hopAO2*	pGWB5 expressing AER-0000328-GFP (Km^R, Hg^R)	This study
pDEST42	pET Gateway™ compatible vector allowing for T7-regulated expression of a protein with a C-terminal His_6-V5 tag, Ap^R	Invitrogen
pPUR-*hopAO1*	pDEST42 expressing AER-0000610-6His tag (Ap^R)	This study
pPUR-*hopAO1*-Cys_{376}	pDEST42 expressing AER-0000610-Cys_{376}-6His tag (Ap^R)	This study
G-rk *CD3-967*	Contains the first 49 aa of GmMan1, soybean α-1,2-mannosidase I (as a Golgi-targeting sequence) fused to the mCherry RFP, Km^R	(Nelson et al., 2007)

[a] Ap^R, Cm^R, Km^R, Sp^R, Str^R, Hg^R and Tc^R indicate resistance to ampicillin, chloramphenicol, kanamycin, spectinomycin, streptomycin, higromycin and tetracycline, respectively. AER numbers indicate ASAP (http://www.genome.wisc.edu/tools/asap.htm) identification numbers for Psv NCPPB 3335 genes. *Cya*, catalytic domain of *Bordetella pertusis* adenilate cyclase; HA tag, influenza hemagglutinin (HA) peptide YPYDVPDYA.

Quantitative RT-PCR assays

qRT-PCR assays were performed as described in General Material and Methods section using oligonucleotides primers shown in Table 4.

Table 4. Primer used in this study.

Forward primers		Reverse primers	
Name[a]	**Sequence**	**Name**	**Sequence**
HopAO1 F-96	TCTCAGTCACAGCATTCC	HopAO1 R-366	GCTTACGATGTCGTACTC
Oligo P1	GTGTAGGCTGGAGCTGCTTC	Km R-768	TTGCATCAGCCATGATGG
hopAO1-F	TGGTTGTGAACGCATTTCCTC	*hopAO1*-R	GCATGAGATTCTTCGCGCA
hopAO2-F	TGCGTTTGATGGTGACCGA	*hopAO2*-R	ACCGCAATGGATATGTACCCG
TA-HopAO1 F	TGTCGCTTAAGATCCAGC	TA-HopAO1 R-93	CCCTATAGTGAGTCGGATCCG TTCCGAAGAATCAGAAC
TD-HopAO1-F20	GGATCCGACTCACTATAGG GACGGATGCCGAGGTTTG	TD-HopAO1 R	ACACGGTATGTACGTAGG
TOPO-610-F	CACCATGTATCCCCTGAAATCT	TOPO-610-R	TTCTGACGCTATTTTTGC
TOPO-328-F	CACCATGCCGAAATTTCCGTCA	TOPO-328-R	GTCAGCGTTGTTGAGAGG
CS-*hopAO1*-F	GAGTCGGTAGTTGTGCACTCTA ACGGCGGTCGC	CS-hopAO1-R	GCGACCGCCGTTAGAGTGC ACAACTACCGACTC
CS-*hopAO1*-C	AGTCGGTAGTTGTGCACTC	*Cya*	CAATCAGGCTGGTGGAATGG

[a] F and R, forward and reverse primer, respectively. Numbers included after F and R in primers names correspond to the hybridization position of the 3 end of the primer in the corresponding ORF sequence.

Subcellular localization of HopAO1 and HopAO2

Agrobacterium constructs (pGWB5-HopAO1-GFP and pGWB5-HopAO2-GFP) (Table 3) were made by Gateway technology (See Material and Methods section). The constructs used in the present study were introduced into *Agrobacterium tumefaciens* strain GV3101 by electroporation (Weigel and Glazebrook, 2002). Subcellular localization assays were performed as previously described (Rodríguez-Herva et al., 2012). Four leaves of *N. benthamiana* plants were infiltrated with the *A. tumefaciens* cultures using a 1 ml syringe. Fluorescence images were acquired using a confocal microscope (LEICA-Sp8). To confirm the subcellular localization of HopAO2, *N. benthamiana* leaves were co-infected with a *A. tumefaciens* strain expressing Golgi vesicles marker (G-rk) for co-localization studies (Nelson et al., 2007).

Phosphatase assays

His-tagged *P. savastanoi* pv. savastanoi NCPPB 3335 HopAO1 was generated using plasmids pENTR-*hopAO1* and pDEST42 (Table 3) as entry and destination vectors, respectively (See Material and Methods section). Site-directed mutagenesis was carried out on pENTR-*hopAO1* using the QuickChange II Site-Directed Mutagenesis Kit (Stratagene, USA) following the

supplier´s instructions. *E. coli* BL21 (DE3) cultures containing plasmids expressing wild type or mutant HopAO1-His6 (Table 3) were grown at 25 ºC to an OD_{600} of 0.5 and induced with 0.4 mM isopropyl β-D-thiogalactoside (IPTG) for 4 h. Cell were harvested by centrifugation at 5000 g for 15 min, and the pellets were frozen overnight at -20 ºC. Native HopAO1 was purified according to protocol 12 of the QIAexpressionist handbook (Qiagen). The same protocol was used for a protein extract of *E. coli* BL21 (DE3) and the resulting fraction was used as negative control.

Phosphatase activity was performed using the sensolyte fluorescein diphosphate (FDP) protein phosphatase assay kit (AnaSpec) according to the manufacturer's instructions. This kit provides a fluorogenic assay for measuring the activity of protein phosphatases that convert the FDP into fluorescein, which has a high extinction coefficient and emission quantum yield, therefore providing high assay sensitivity. Phosphatase assay was performed mixing 50 µl of a protein phosphatase-containing sample with 50 µl of FDP reaction solution. The reaction was incubated at 25 ºC for 30 min, and 50 µl of stop solution was added to stop the reaction. Fluorescence signal was measured using excitation/emission = 485 nm/535 nm. As a negative control, samples without phosphatase activity (distilled water) were used. The phosphatase activity for the control sublines was set at 100 %, and the respective values for the experiment subline were calculated with respect to that.

RESULTS

Identification and distribution of HopAO1 and HopAO2 T3SS effectors among *P. savastanoi* pv. savastanoi and related strains

Prediction of T3E genes in the draft genome sequence of *P. savastanoi* pv. savastanoi NCPPB 3335 previously allowed the identification of a HopAO1 homolog located in plasmid pPsv48B (Rodriguez-Palenzuela et al., 2010; Bardaji et al., 2011). In order to refine the identification of T3E belonging to the HopAO family encoded in the genome of NCPPB 3335, a BLASTp search was performed against the draft genome sequence of this strain using the entire coding sequence of HopAO2 from *P. syringae* pv. actinidiae MAFF302091 (accession number WP_017684870.1, locus tag PSYAC_20366). A chromosomally encoded candidate HopAO2 T3E was found in NCPPB 3335 (accession number GG774693.1, locus tag PSA3335_5047), which showed 93% amino acid identity (100 % cover) with its corresponding MAFF302091 homolog. Thus, NCPBB 3335 encodes two candidate T3E of the HopAO family. To our knowledge, codification of two diverse members of this family in the genome of the same strain has not been previously reported. Further analyses of the amino acids sequences of HopAO1 and HopAO2 showed that both of them harbors the conserved motif [LIVMF]HCxAGxxR[STC][STAG] (Fauman and Saper, 1996), characteristic of the protein tyrosine phosphatase (PTP) family.

With the aim of analyzing the prevalence of HopAO1 and HopAO2 homologs among other strains of the *P. syringae* complex, a broader BLASTp search was performed against the non-redundant protein sequence database using both coding sequences. Results revealed that the amino acid sequence of HopAO1 from *P. savastanoi* pv. savastanoi NCPPB 3335 is most similar to its homologs encoded by other *P. syringae* strains also isolated from woody host, i.e. *P. syringae* pv. aesculi and *P. syringae* pv. morsprunorum (Fig. 1A). Although a high identity was found among all available amino acids sequences of HopAO2 encoded by members of the *P. syringae* complex (88 % - 98 % identity, 100 % cover), *P. savastanoi* pv. savastanoi NCPPB 3335 HopAO2 resulted to be the most divergent (Fig. 1B). The accession number of the protein sequences used for the construction of the phylogenetic trees shown in Fig. 1A and Fig. 1B are presented in Table 1.

The *hopAO1* and *hopAO2 P. savastanoi* pv. savastanoi NCPPB 3335 T3E genes were used as probes in dot-blot hybridizations to ascertain their distribution among a collection of 31 *P. savastanoi* pv. savastanoi strains isolated in different countries, and among a selection of *P. syringae* strains isolated from either woody or herbaceous hosts (See Table S2 in Supplementary Material section). Results showed that 30 out of the 31 *P. savastanoi* pv. savastanoi strains, as well as *P. savastanoi* pv. nerii 2, *P. syringae* pv. morsprunorum CFBP 2116, *P. syringae* pv. myricae CFBP 2897, *P. syringae* pv. eriobotryae CFBP 2343 and *P. syringae* pv. glycinea PG4180 hybridized with both probes. Conversely, strains belonging to *P. syringae* pathovars

phaseolicola, syringae, lachrymans, dendropanacis, sesami, and alisalensis did not hybridize with any of these probes and where discarded for further analysis (Table S2 in Supplementary Material section).

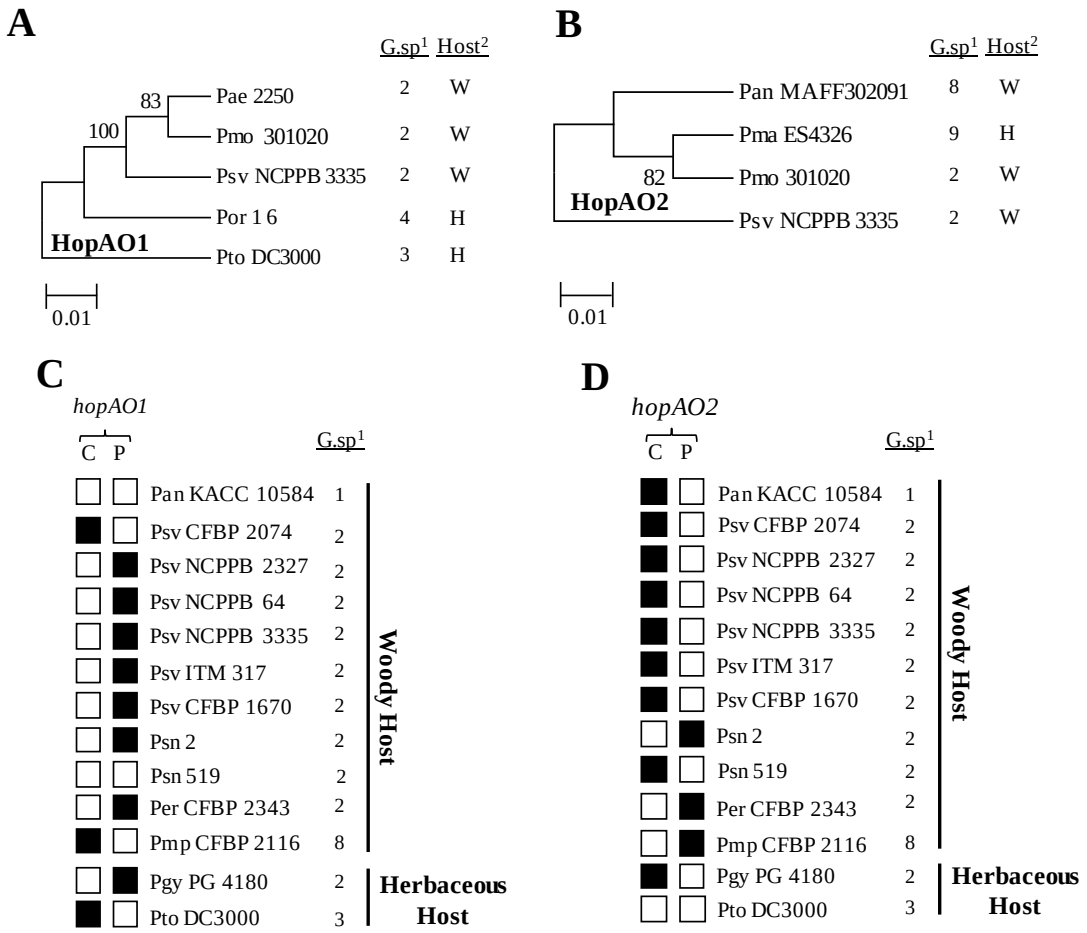

Figure 1. Distribution and phylogeny of HopAO1 and HopAO2 among pathovars of the *P. syringae* complex. Unrooted neighbor-joining tree of HopAO1 (**A**) and HopAO2 (**B**) proteins from strains of the *P. syringae* complex (see Table 1, for accession numbers). Bootstrap percentage values (10,000 repetitions) are shown on the branches, and evolutionary distances are given in units of amino acid substitutions per site. **C** and **D**, Distribution of the *P. savastanoi* pv. savastanoi NCPPB 3335 T3E genes *hopAO1* and *hopAO2* among a collection of strains from the *P. syringae* complex isolated from woody and herbaceous plant hosts. A colony blots analysis was performed using the indicated gene probes. The strains are indicated by their pathovar abbreviation (Table 2 in General Material and Methods section). Black and white squares represent the presence or absence, respectively, of strong hybridization signals with the indicated effectors for each strain analyzed. [1]G.sp, *P. syringae* genomospecies; [2]Host: W, woody host; H, herbaceous host.

Plasmid preparations and total DNA isolated from a selection of six *P. savastanoi* pv. savastanoi strains hybridizing with both *hopAO1* and *hopAO2* probes in the dot-blot analysis, as well as from all other strains hybridizing with at least one of the two probes (See Table S2 in Supplementary Material section) were analyzed by southern-blot hybridization to determine the localization of these genes on their replicons. While *hopAO1* was found to be plasmid encoded in

six out of the seven *P. savastanoi* pv savastanoi strains used, *hopAO2* was detected in the chromosome of all seven strains. In contrast, a random localization of *hopAO1* and *hopAO2* was found in the replicons of the remaining strains (Fig. 1C and 1D).

HopAO1 and HopAO2 are translocated via the *P. savastanoi* pv. savastanoi T3SS

An identifiable Hrp box (Fouts et al., 2002) was found in the 100 nucleotides upstream of the start codon of both *hopAO1* and *hopAO2* candidates from *P. savastanoi* pv. savastanoi NCPPB 3335 (Table 5).

Table 5. Occurrence of consensus Hrp-box sequences upstream of *hopAO1* and *hopAO2* genes from *P. savastanoi* pv. savastanoi NCPPB 3335.

Gene name	Hrp-box position[a]	Hrp-box sequence
CONSENSUS[b]		**BGGAACYHNNNNNNNNNNNNNNNCCACNHAG**
hopAO1	-86 to -55	CGGAACCCCACAAGCATTTAAGACCACGTAT
hopAO2	-60 to -29	TGGAACCGTTGGAGCCTATGCGCCCACGAAA

To determine whether the selected candidate effectors were T3SS substrates that could be translocated into plant cells, we constructed pCPP3234 derivatives (Table 3) expressing fusions of *Bordetella pertussis* adenylate cyclase (Cya) to the C terminus of full-length HopAO1 and HopAO2. In addition, a Cya fusion to the C terminus of T3E AvrRpm2 from NCPPB 3335 (Matas et al., 2014) was also included in these assays as positive control. This system, which is based in cyclic AMP (cAMP) production exclusively in the presence of eukaryotic calmodulin, has been widely used for analyzing the translocation of *P. syringae* T3E (Sory and Cornelis, 1994; Casper-Lindley et al., 2002; Schechter et al., 2004). *Nicotiana tabaccum* leaves were infiltrated with either *P. savastanoi* pv. savastanoi NCPPB 3335 or the strain NCPPB 3335-T3, a T3SS mutant derived from wild-type NCPPB 3335 (Pérez-Martínez et al., 2010), expressing each of the two constructed Cya fusions. As illustrated in Figure 2A, significant differences in cAMP production between the wild-type strain and the T3SS mutant strain were observed for AvrRpm2 and both T3E candidates tested —HopAO1, HopAO2—indicative of their translocation through the *P. savastanoi* pv. savastanoi T3SS.

Expression of *hopAO1* and *hopAO2* in *P. savastanoi* pv. savastanoi is HrpL-dependent

To unveil the HrpL-dependent expression of *hopAO1* and *hopAO2* in *P. savastanoi* pv. savastanoi NCPPB 3335, a Δ*hrpL* NCPPB 3335 mutant (Matas et al., 2014) was used. The expressions of the *hopAO1* and *hopAO2* genes were analyzed using quantitative reverse-

transcription polymerase chain reaction (qRT-PCR) with both the wild type and the NCPPB 3335 Δ*hrpL* mutant (Table 2). In addition, the expression of the *avrPto1* gene and the *iaaM* gene (encoding tryptophan monooxygenase, involved in the biosynthesis of indoleacetic acid) was also tested as positive and negative controls, respectively (Matas et al., 2014). Under inducing conditions (cells grown 6 hours in Hrp-inducing medium), the expression of the *avrPto1*, *hopAO1* and *hopAO2* genes decreased (0.01-, 0.4- and 0.02-fold, respectively) in the Δ*hrpL* mutant compared to the wild type, demonstrating an expression dependency on HrpL. As expected for the negative control, no reduction in the expression of the *iaaM* gene was observed under the same conditions (Fig. 2B).

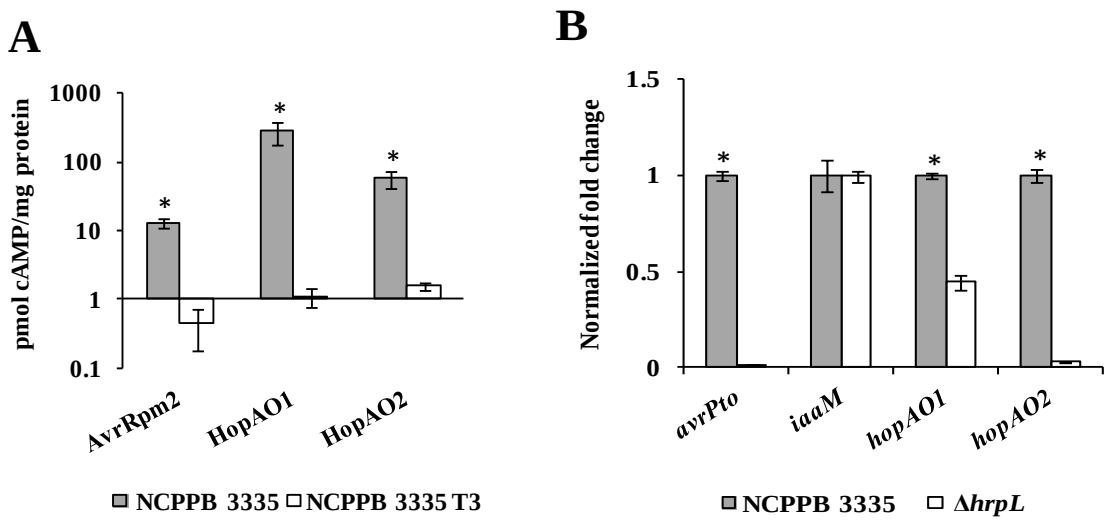

Figure 2. Translocation assay and HrpL-dependent expression of candidate *P. savastanoi* pv. savastanoi NCPPB 3335 T3E HopAO1 and HopAO2. **A,** Calmodulin- and Cya-dependent production of cAMP was used to measure the translocation of T3E-Cya fusions into plant cells. *N. tabacum* cv. Newdel plants were inoculated with *P. savastanoi* pv. savastanoi NCPPB 3335 or NCPPB 3335-T3 (T3SS mutant) expressing the indicated Hop-Cya fusions from pCPP3234 derivatives (Table 3). **B**, Quantitative reverse-transcription polymerase chain reaction (qRT-PCR) with HopAO1 and HopAO2 genes in NCPPB 3335 *ΔhrpL* vs. NCPPB 3335 at 6 h after transfer to Hrp-inducing medium. The fold change was calculated after normalization using the *gyrA* gene as an internal control. The values represent the mean and standard error for samples obtained in triplicate; similar results were obtained in multiple experiments. Asterisks indicate significant differences (P = 0.05) between the cAMP levels obtained for the NCPPB 3335 and NCPPB 3335-T3 strains (A) or the values obtained for the NCPPB 3335 and the *ΔhrpL* strains (B).

P. savastanoi pv. savastanoi NCPPB 3335 T3SS effectors HopAO1 and HopAO2 inhibit early plant defense responses in *N. tabaccum*.

Suppression of early plant defense responses, such as ROS production and callose deposition, by HopAO1 and HopAO2 was tested using the heterologous expression system *Pseudomonas fluorescens* 55 (Pf55) [pLN18] (Table 3). This system enables the delivery of effector proteins into plant cells through a heterologous expressed *P. syringae* T3SS (Jamir et al., 2004; Lopez-

Solanilla et al., 2004; Oh et al., 2010; Matas et al., 2014). PAMPs from Pf55 [pLN18] generate a PTI response in inoculated plants (Oh et al., 2010; Matas et al., 2014). This system has been previously used to demonstrate the suppression activity of PTI by other *P. savastanoi* NCPPB 3335 T3SS effectors (Matas et al., 2014). We expressed *P. savastanoi* pv. savastanoi T3E HopAO1 and HopAO2 (see pCPP5040 derivatives, Table 3) in Pf55 [pLN18]. After challenging *N. tabaccum* leaves with the derivative strains we analyzed ROS production and callose deposition. Figure 3 shows that the ROS levels, determined by 3,3'-diaminobenzidine (DAB) staining, were significantly reduced by the expression of HopAO1 or HopAO2 compared to the control strain Pf55 [pLN18] harboring an empty vector (Tukey test; $P \leq 0.01$) (Fig. 3A and C). Moreover, both T3E significantly reduced the levels of callose deposition compared to the control strain (Tukey test; $P \leq 0.01$) (Fig. 3B and 3D). Therefore, HopAO1 and HopAO2 are able to interfere with the early innate immunity responses of the plant.

P. savastanoi pv. savastanoi NCPPB 3335 T3SS effectors HopAO1 and HopAO2 inhibit programmed cell death in *N. tabaccum*

In order to determine the role of HopAO1 and HopAO2 in a scenario in which plant defenses are T3SS-dependent and additional to basal PTI, like the HR is, we expressed these two proteins in *P. syringae* pv. tomato strain DC3000D28E (Cunnac et al., 2011) (Table 3). This polymutant strain harbors deletions in all 28 well-expressed effector genes and is considered functionally effectorless but otherwise wild type *in planta*. The HR elicitation in *N. benthamiana* and *N. tabaccum* can be clarified by the fact that DC3000D28E has the wild-type complement of T3SS helper proteins (except HrpW1), and several of these proteins can elicit plant defenses and induce an HR response (Kvitko et al., 2007; Cunnac et al., 2011). We analyzed the ability of the DC3000D28E derivatives expressing HopAO1 or HopAO2 to elicit cell death in *N. tabaccum* compare with that of the DC3000D28E strain. After 48h of inoculation, the polymutant strain stimulated an ETI-like response which was partially and completely inhibited by the expression of the *P. savastanoi* pv. savastanoi NCPPB 3335 proteins HopAO1 and HopAO2, respectively (Fig. 4A). Results suggest that these two effectors participate in the inhibition of the plant defense response associated with the onset of programmed cell death.

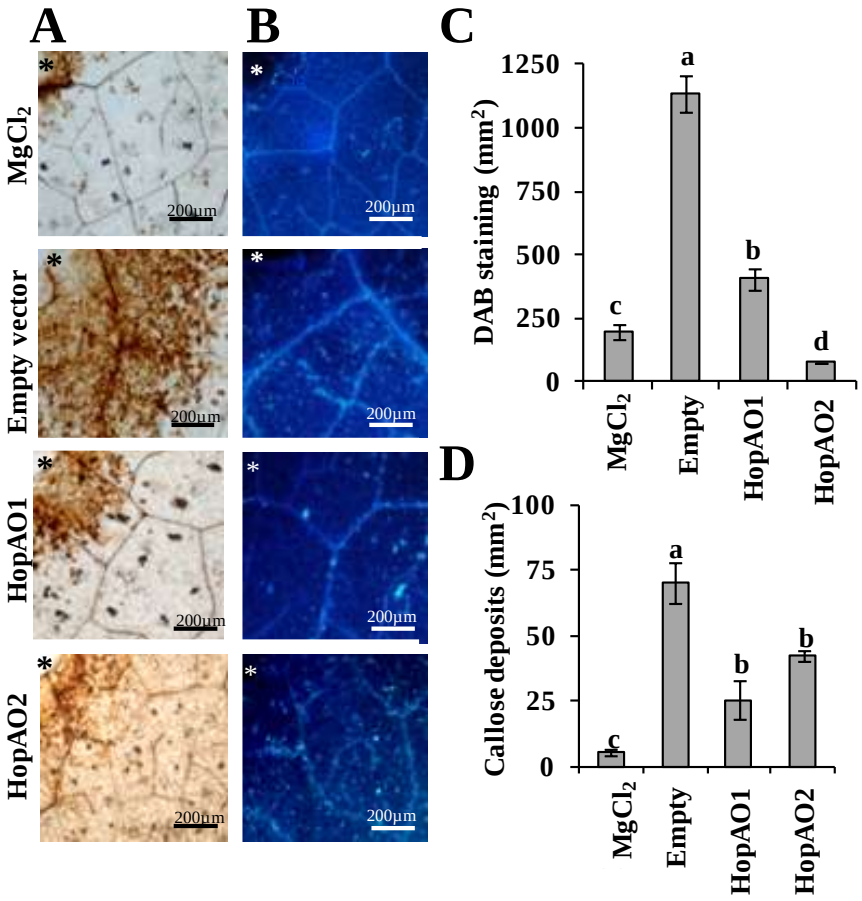

Figure 3. DAB staining, callose deposition in *N. tabacum* leaves. For DAB staining and callose deposition, plants were challenged with *P. fluorescens* 55 [pLN18] harboring the pCPP5040 empty vector or the vectors expressing the *P. savastanoi* pv. savastanoi NCPPB 3335 T3E HopAO1 or HopAO2 (Table 2) in *N. tabacum* vr. Xhanti. **A**, The DAB signal was quantified 4 h after infection and represented in a histogram (**C**). **B**, The callose deposition was assessed using aniline blue staining, quantified 12 h after infection and represented in a histogram (**D**). The asterisks in A and B indicate inoculation zones. For histograms, data are means ± standard error of the mean for at least five replicas; bars topped with the same letter represent values that are not significantly different using one-way ANOVA and Tukey test for multiple comparison (P=0.01). Each experiment was repeated at least three times with similar results.

DC3000D28E has been shown to grow better *in planta* when coinoculated with a strain that is able to suppress plant immunity, such as DC3000Δ*hopQ1-1* (Cunnac et al., 2011). The ability of HopAO1 and HopAO2 to restore growth of DC3000D28E *in planta* was tested in *N. benthamiana* leaves. For this purpose, competition assays between the polymutant strain (DC3000D28E) and each derivative expressing either HopAO1 or HopAO2 were conducted. *N. benthamiana* leaves were infiltrated with a mixed inoculum (1:1) of DC3000D28E and each of the derivatives, and after 6 days, bacteria were recovered and viable cells were determined. Interestingly, the expression of *P. savastanoi* pv. savastanoi HopAO1 or HopAO2 in DC3000D28E significantly increased the competitiveness of the strain, which was reflected in a CI value (HopAO1/DC3000D28E or HopAO2/DC3000D28E) of 2.14 and 1.82, respectively (Fig. 4B).

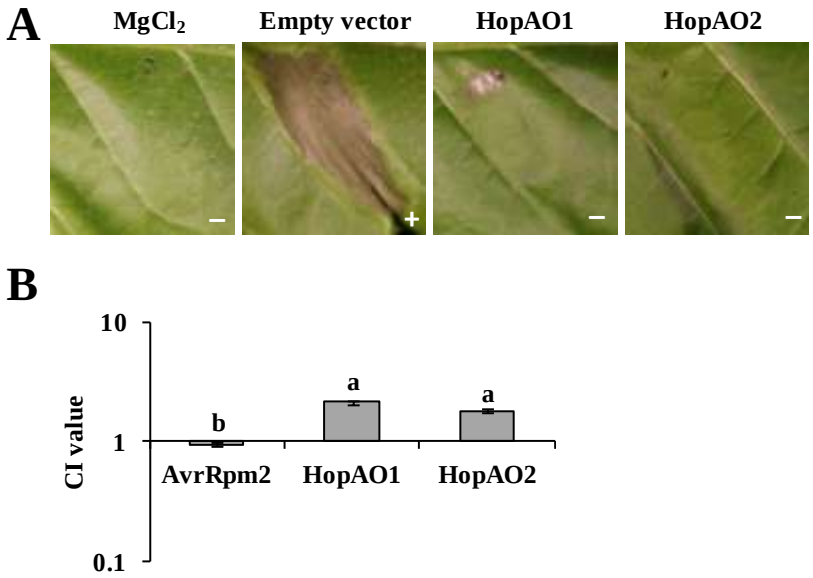

Figure 4. Delivery of *P. savastanoi* pv. savastanoi T3SS effectors HopAO1 and HopAO2 by functionally effectorless *P. syringae* pv. tomato DC3000D28E in *Nicotiana* leaves..**A**, Cell death responses in *N. tabacum* vr. Newdel leaves 48 h after inoculation with the polymutant *P. syringae* pv. tomato DC3000D28E. Cells were suspended in $MgCl_2$ carrying pCPP5040 (empty vector) derivatives expressing HopAO1 or HopAO2 (Table 3), adjusted to $2x10^8$ CFU/mL. This cell density was chosen to exceed the threshold typically needed to elicit cell death associated with ETI (Cunnac et al., 2011; Matas et al., 2014). **B**, Competition assay in *N. benthamiana* between *P. syringae* pv. tomato DC3000D28E and each of its derivatives expressing HopAO1 or HopAO2. CI were normalized with respect to the CI obtained for DC3000D28E versus DC3000D28E expressing the empty vector (pCPP5040). Values are the mean ± standard error of the mean of three replicates; bars topped with the same letter represent values that are not significantly different using one-way ANOVA followed by post-hoc comparision using the Tukey test. Cell death response: +, positive; -, null. Each experiment was repeated at least three times with similar results.

HopAO1 and HopAO2 localizes in the plasma membrane and Golgi vesicles, respectively, when transiently expressed in *N. benthamiana*

To further characterize the role of HopAO1 and HopAO2 *in planta*, GFP fusions to the C terminus of full-length T3E were cloned under control of a 35S promoter in a Gateway vector (pGWB5) (Table 3). Subsequently, the HopAO1-GFP and HopAO2-GFP fusion proteins were transiently expressed in *N. benthamiana* leaves using *Agrobacterium*-mediated gene transfer. At 48 h after infiltration, the plant tissue was analyzed using scanning laser confocal microscopy of epidermal cells on the abaxial leaf side.

The inspected cells showed the fluorescence signal of HopAO1-GFP associated with the plasma membrane. Moreover, distinct fluorescently labeled vesicles occurred underneath the cell membrane. In the case of HopAO2-GFP, cells exhibited some fluorescence in the plasma membrane and very clearly in intracellular punctuate structures (Fig. 5A) which could be associated with Golgi vesicles. To further analyze the HopAO2 location in these structures; we

coinfiltrated *N. benthamiana* leaves with the *Agrobacterium* derivatives expressing the HopAO2-GFP fusions and the known Golgi marker CD3-967 (Nelson et al., 2007) (Supplementary Table S4). Visualization of the infiltrated cells by confocal microscopy revealed the co-localization of HopAO2-GFP with G-RFP (Fig. 5B), suggesting the localization of HopAO2 in the vesicle trans-Golgi system of *N. benthamiana* cells.

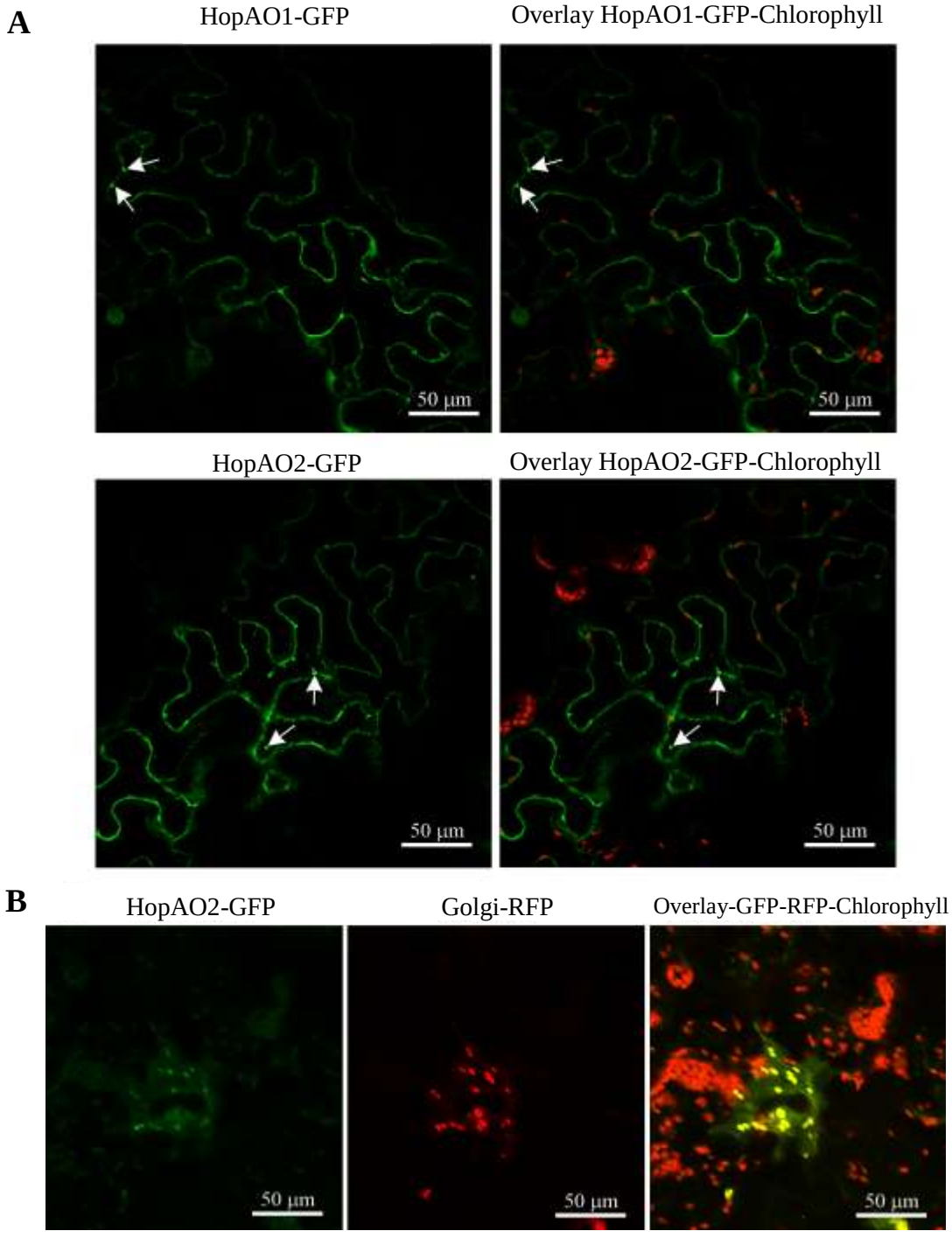

Figure 5. Subcellular localization of HopAO1 and HopAO2 in *Nicotiana benthamiana* leaves. **A**, Representative single-plane confocal images of HopAO1-GFP (top row) and HopAO2-GFP (bottom row). HopAO1 fluorescence is observed in patches attached to the plasma membrane (arrows). HopAO2 is seen in

cytoplasmic vesicles, close to the plasma membrane (arrows). The overlap of GFP fluorescence and chlorophyll autofluorescence is presented. **B**, Maximum projections of confocal stacks showing HopAO2-GFP (left), Golgi-RFP (middle) and overlay of GFP, RFP and chlorophyll autofluorescence (right).

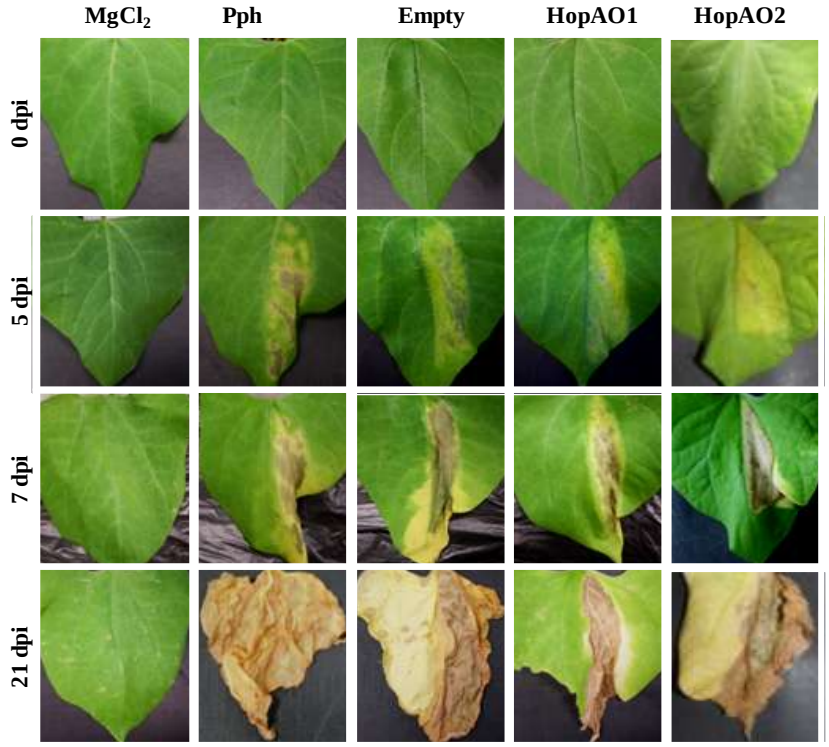

Figure 6. Monitoring of the infection of bean plants by *P. syringae* pv. phaseolicola 1448A (Pph) expressing *P. savastanoi* pv. savastanoi effectors HopAO1 or HopAO2. Symptoms induced on primary leaves of bean plants at 0, 5, 7 and 21 days post-inoculation (dpi) with $5x10^5$ CFU/mL of wild-type 1448A, or 1448A transformants containing the empty vector, or vectors expressing HopAO1 or HopAO2. Each experiment was repeated at least three times with similar results. Images show representative results.

Ectopic expressions of *P. savastanoi* pv. savastanoi HopAO1 in *P. syringae* pv. phaseolicola 1448A causes a delay of symptoms in bean-infected plants

To get more insights into the role of HopAO1 and HopAO2 during the confrontation with the plant defense mechanisms we analyzed the effect of their expression in the context of a compatible interaction. With that purpose we constructed *P. syringae* pv. phaseolicola 1448A derivatives expressing *P. savastanoi* pv. savastanoi NCPPB 3335 HopAO1 or HopAO2 from plasmid pCPP5040 (Table 3), which are not encoded in the genome of 1448A. Derivative strains were inoculated in the leaves of bean plants and symptoms development (water-soaked lesions surrounded by chlorosis) were recorder over time. *P. syringae* pv. phaseolicola 1448A and its derivative harboring the empty vector caused marked necrosis lesions at five days post-inoculation (dpi), while derivatives expressing HopAO1 and HopAO2 caused slight necrosis lesions at this time (Fig. 6). Moreover, it was observed that lesions incited by wild-type *P. syringae* pv.

phaseolicola 1448A and by its derivative harboring the empty vector started to expand outside the infection area at seven dpi. However, at this time the lesions caused by the strains expressing HopAO1 or HopAO2 appeared to be more restricted (Fig. 6). These results suggested a delay of symptom development caused by the expression of either HopAO1 or HopAO2 during the first week after infection. However, analysis of the progression of the symptoms at 21 dpi showed that only the expression of HopAO1 caused a consistent delay in symptoms development incited by 1448A.

HopAO1 is an active protein-tyrosine phosphatase

The HopAO T3E family is characterized on the basis of a conserved PTP domain (Bretz et al., 2003; Espinosa et al., 2003), which activity has been shown to be dependent on a cysteine located at position 378 of HopAO1 from *P. syringae* pv. tomato DC3000 (Bretz et al., 2003). To determine whether *P. savastanoi* pv. savastanoi NCPPB 3335 HopAO1 is also an active protein-tyrosine phosphatase, affinity-purified HopAO1-His_6 was used in a PTP *in vitro* assay performed under non-denaturing conditions. We also tested a site-directed HopAO1-His_6 mutant encoding a substitution of the PTP-related Cys_{376} by a Ser ($HopAO1_{C376S}$-His_6). FDF hydrolysis was clearly detected for wild-type HopAO1-His_6; however, the percentage of hydrolyzed FDF significantly decreased in the case of $HopAO1_{C376S}$-His_6 protein (Fig.7). Results demonstrate that the PTP activity shown *in vitro* by *P. savastanoi* pv. savastanoi NCPPB 3335 HopAO1 is dependent on its Cys_{376} amino acid residue.

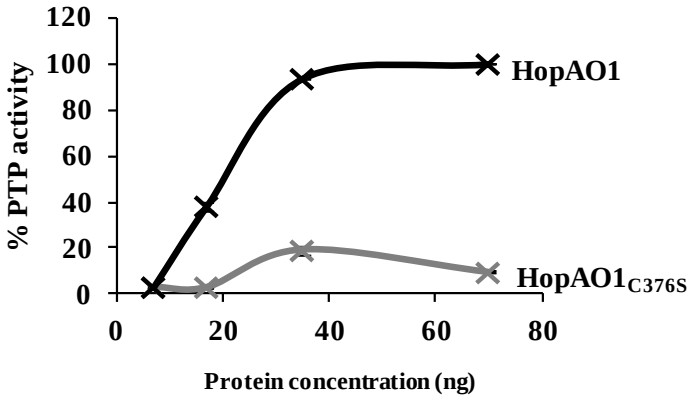

Figure 7. Protein tyrosine phosphatase (PTP) catalytic activity of *P. savastanoi* pv. savastanoi HopAO1. PTP activity was assayed using fluorescein diphosphate (FDP) as described in Material and Methods. Values were normalized to the PTP activity obtained for a negative control (see Material and Methods). The higher activity value obtained for wild-type HopAO1 (70 ng) was set to 100 %, and the activities of HopAO1 and $HopAO1_{C376S}$ obtained for all other protein concentrations were calculated with respect to this value. The results represent the means from three independent reactions.

A *P. savastanoi* pv. savastanoi NCPPB 3335 *hopAO1* mutant is hypovirulent in olive plants.

Artificial inoculation of olive plants with a *P. savastanoi* pv. savastanoi NCPPB 3335 mutant cured of plasmids pPsv48A and pPsv48B (strain Psv48ΔAB, Table 2), which encode T3E HopAF1 and HopAO1, respectively, has been reported to induce attenuated hyperplastic knots, also showing a slight necrosis (Bardaji et al., 2011). To investigate the relative contribution of HopAO1 to the development of symptoms in olive plants, a NCPPB 3335 Δ*hopAO1* mutant was constructed. In addition, complemented Psv48ΔAB and Δ*hopAO1* strains expressing HopAO1 (Table 3) were also constructed and inoculated in both *in vitro* micropropagated and lignified olive plants. In agreement with Bardaji et al (2011), Psv48ΔAB induced less severe knots than the wild-type strain in both plant systems (Fig. 8A, 8B and 8C). Interestingly, and although the size of the knots induced by the Δ*hopAO1* mutant at 28 dpi on the stem of *in vitro*-grown olive plants were not significantly different from those induced by the wild-type strain, they showed necrotic lesions similar to those developed in plants inoculated with the Psv48ΔAB mutant (Fig. 8A). In addition, the competitiveness of the Δ*hopAO1* mutant in this plant system was compromised compared with the wild-type strain (Fig. 8C). Also, the weight of the knots induced by the Δ*hopAO1* mutant in lignified olive plants, which also showed an increased necrosis, was significantly lower than those developed by the wild-type strain (Fig. 8B). Additionally, the knot volumes in olive plant infected with the Δ*hopAO1* mutant were approximately two times smaller of the knot volume developed in plants infected with the wild-type strain (data not shown). The ectopical expression of the *hopAO1* gene in both the Δ*hopAO1* mutant and the plasmid-cured strain Psv48ΔAB fully restored the wild type appearance of the knots in both plant systems (Fig. 8A and 8B). Complementation of the Δ*hopAO1* mutant also resulted in restoration of the competitiveness of the strain in olive plants (Fig. 8C). Together, all these results reveal a significant role of HopAO1 during the infection process of olive plants.

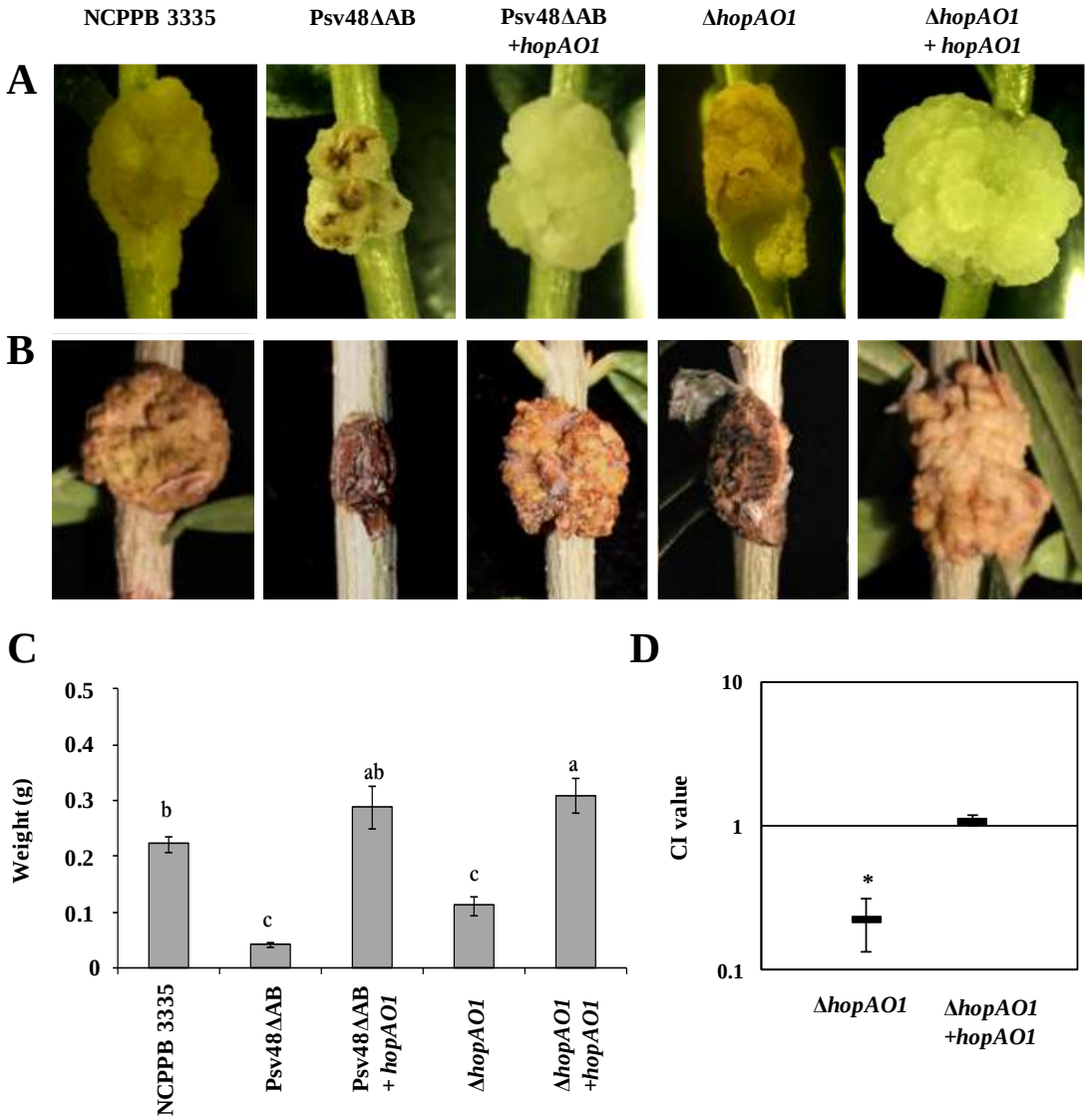

Figure 8. Role of the *hopAO1* gene in the virulence of *P. savastanoi* pv. savastanoi NCPPB 3335 in olive plants. Knots induced by the indicated strains on young micropropagated olive plants at 28 days post inoculation (dpi) (**A**) and in one year-old olive plants at 90 dpi (**B**). **C**, Weight of knots developed on lignified olive plants infected with the indicated strains. Knots weights are the means of six different knots. Statistical analyses were performed using one-way ANOVA. **D**, Competitive index for mixed inoculations of NCPPB 3335 and its derivative strains in micropropagated olive plants. The error bars indicate the standard error from the average of three different assays. The asterisks indicate values significantly different from one. Statistical analyses were performed using Student´s t-test with a threshold of P = 0.05. NCPPB 3335, wild-type strain; Pv48ΔAB, NCPPB 3335 cured of plasmids pPsv48A and pPsv48B; Pv48ΔAB + *hopAO1*, Pv48ΔAB expressing *hopAO1*; Δ*hopAO1*, NCPPB 3335 Δ*hopAO1* mutant; Δ*hopAO1* + *hopAO1*, Δ*hopAO1* expressing *hopAO1*.

DISCUSSION

Recent progresses in the analysis of T3E functions during the interaction of *P. syringae* strains with herbaceous hosts are opening a novel an exciting avenue in the study of bacterial virulence and plant defense response. However, knowledge on the infection of woody plants by strains belonging to the genus *Pseudomonas* lags far behind. Although *Pseudomonas* infection of woody hosts might share common features with their herbaceous relatives, it should be taken into account that the T3E repertoire of bacterial pathogens isolated from woody hosts, and their functions, might be conditioned by the specific characteristics of woody hosts. In fact, a recent functional analysis of *P. savastanoi* pv. savastanoi NCPPB 3335 T3E revealed that DNA sequences encoding HopBL1 and HopBL2 were uniquely detected in *P. savastanoi* pv. savastanoi and other *P. syringae* strains isolated from woody hosts, suggesting a relevant role of these two effectors in bacterial interactions with olive and other woody plants (Matas et al., 2014). In this work, we have analyzed the presence and function of two new members of the HopAO family encoded by this olive pathogen: HopAO1 and HopAO2.

The HopAO family is one of the most diverse T3E families of the *P. syringae* complex (Baltrus et al., 2011). Proteins belonging to this family share the presence of a tyrosine phosphatase domain, also found in NCPPB 3335 HopAO1 and HopAO2. Despite the codification of the *hopAO1* gene in a plasmid (Bardaji et al., 2011), the phylogeny of HopAO1 (Fig. 1A) is largely congruent with that of the *P. syringae* complex deduced from housekeeping genes (Ramos et al., 2012), suggesting that this protein is ancestral to the complex. On the other hand, clustering of HopAO2 from *P. syringae* pv. mori MAFF 301020 (genomospecies 2) with genomospecies 9 and 8 (Fig. 1B) provides evidence of horizontal transfer. However, only few *hopAO1* and *hopAO2* sequences are currently available at the Hop database (http://www.pseudomonas-syringae.org/). Further phylogenetic analysis including a higher number of sequences encoded by different *P. syringae* and *P. savastanoi* pathovars would be required to confirm these hypotheses. Although none of this two T3E are restricted to *P. syringae* pathovars infecting woody hosts, the widespread distribution and the simultaneous occurrence of these two effectors among *P. savastanoi* pv. savastanoi strains (Fig. 1C) suggests that both of them might play an important role during the interaction with olive plants. The phylogenetic analysis of these two T3E here described, together with the canonical characteristics which define *P. syringae* effector proteins, such are their translocation to plant cells (Fig. 2A) and their transcriptionally dependency on HrpL (Table 5, Fig. 2B), demonstrate that *P. savastanoi* pv. savastanoi NCPPB 3335 *hopAO1* and *hopAO2* genes codified bona fide T3E.

T3E proteins delivered into host cells by the T3SS of plant-pathogenic bacteria have a major role in promoting bacterial virulence and in the suppression of host defense responses (Mudgett, 2005; Grant et al., 2006; Underwood et al., 2007; Matas et al., 2014). Previous studies have shown

that the functionally effectorless strain *P. syringae* DC3000D28E is suitable for testing the ability of T3E to restore bacterial growth *in planta* and to modulate plant defense responses (Cunnac et al., 2011). Our results indicate that both HopAO1 and HopAO2 can interfere with the incitation of the ETI-like response induced by DC3000D28E in tobacco plants (Fig. 4). Also, expression of either HopAO1 or HopAO2 in DC3000D28E also increased the competitiveness of this strain in *N. benthamiana.* Growth restoration of DC3000D28E in *N. benthamiana* by the expression of single T3E in this strain has only been reported for *P. syringae* pv. tomato DC3000 AvrPto and AvrPtoB (Cunnac et al., 2011), as well as for *P. savastanoi* pv. savastanoi NCPPB 3335 HopBL2 (Matas et al., 2014). Thus, our results suggest that *P. savastanoi* pv savastanoi HopAO1 and HopAO2 might be involved in the inhibition of responses associated with the perception of bacterial pathogens. These results are in line with the observed delay in the onset of HR induced by *P. syringae* pv. phaseolicola in the non-host plant *N. tabaccum* when expressing *P. syringae* pv. tomato DC3000 HopAO1 (Espinosa et al., 2003).

P. syringae pv. tomato DC3000 HopAO1 has been recently demonstrated to directly interact and inactivate PRRs FLS2 and EFR (Macho et al., 2014). Both of these membrane-bound receptors (Gómez-Gómez and Boller, 2000; Zipfel et al., 2004; Zipfel et al., 2006), which are important for anti-bacterial immunity and recognize the bacterial PAMPs flagellin (flg22) and EF-Tu (elf18) (Boller and Felix, 2009). The subcellular localization of *P. savastanoi* pv. savastanoi NCPPB 3335 HopAO1 here identified in the host plasma membrane (Fig. 5) concurs with the localization of the host targets described for DC3000 HopAO1 (Macho et al., 2014). On the other hand, heterologous expression of NCPPB 3335 HopAO1 or HopAO2 in Pf55 resulted in the inhibition of callose deposition and ROS formation in *N. tabaccum* (Fig. 3A and 3B), phenotypes which among other response, are in agreement with those reported for the recognition of the host PRRs by DC3000 HopAO1 (Macho et al., 2014).Additionally, NCPPB 3335 HopAO2 was localized in Golgi vesicles (Fig. 5), indicating that this effector could interfere with vesicle trafficking, as it has been described for *P. syringae* pv. tomato DC3000 core T3E HopM1 (Nomura et al., 2006; Nomura et al., 2011) and AvrE (Nomura et al., 2011). Future research unveiling the plant target of this effector would allow a better understanding of its function in relation with the suppression of plant immune responses. It is noteworthy the fact that the two members of the HopAO family encoded by *P. savastanoi* pv. savastanoi NCPPB 3335 could be targeting the two distinct PTI processes, PAMP perception and vesicle trafficking, as is the case of the members of the *P. syringae* REGs (Redundant Effector Groups). The loss of the effectors in these groups is accompanied by a strong reduction in growth in *N. bethamiana* (Kvito et al., 2009).

The delay of symptoms in bean plants produced by the expression of HopAO1 and HopAO2 in *P. syringae* pv. phaseolicola 1448A (Fig. 6) is also consistent with the putative interference with

common steps in plant defense, like is the recognition of bacterial patterns or the vesicle trafficking associated with the production of antimicrobials compounds in response to pathogen detection. Both processes have been described as pivotal events in the defense response in plants and the results obtained are in line with the proposed idea that most of the effectors of the *P. syringae* complex can function as "generalists" in a broad range of plants (Lindeberg et al., 2012). In general, deletion of single effector genes do not often lead to a noticeable loss of virulence as measured by attenuation of bacterial growth and symptom development in infected tissue (Hauck et al., 2003). However, a *P. savastanoi* pv. savastanoi NCPPB 3335 mutant defective in *hopAO1* showed a reduced ability to grow in olive plants (Fig. 8). Similar results were previously reported for a *P. syringae* pv. tomato DC3000 *hopAO1* mutant in tomato leaves (Espinosa et al., 2003). Moreover, necrosis of the knot tissues induced by the NCPPB 3335 Δ*hopAO1* mutant resulted to be higher than that observed in plants infected with the wild-type strain (Fig. 8). We have previously reported that knots induced in olive plants by a NCPPB 3335 derivative (Psv48ΔAB) cured of plasmids pPsv48A (encoding T3E HopAF1) and pPsv48B (encoding HopAO1) showed an increased necrosis of knot tissues (Bardaji et al., 2011). Here we report that this phenotype could be fully restored by expression of HopAO1 in Psv48ΔAB (Fig. 8), further confirming its involvement in the interference of necrosis associated with disease development. Other reports showing an effect of T3E over the induction of necrosis associated with both compatible and incompatible interactions with plants have been previously described, as is the case of the *P. syringae* pv. tomato DC3000 HopN1 (Lopez-Solanilla et al., 2004). In relation to HopAO2, construction of a deletion mutant in the *P. savastanoi* pv. savastanoi NCPPB 3335 *hopAO2* gene by a double recombination event was not possible, as the nucleotide sequence of this gene is located near the end of a contig in the draft genome sequence of this strain (Rodriguez-Palenzuela et al., 2010). Thus, PCR amplification of the flaking regions of this gene was not possible. On the other hand, inactivation of this gene by plasmid insertion was also unsuccessful after several attempts. Complete sequencing of the genome of this strain would perhaps allow future construction of this mutant strain and analysis of its role in the virulence of this pathogen.

In summary, we report the translocation into plant cells and the *hrpL*-dependent expression of two new members of the effector repertoire of the olive pathogen *P. savastanoi* pv. savastanoi NCPPB 3335: HopAO1 and HopAO2. Our results also reveal that the *hopAO1* and *hopAO2* genes are widely distributed in *P. savastanoi* strains, suggesting a relevant function of these T3E genes during the interaction with olive plants, a role that was here demonstrated for *hopAO1*. Nevertheless, we demonstrate that both HopAO1 and HopAO2 interfere with early responses associated with plant defense. In the case of HopAO1, our results suggest that this interference could be mediated in a similar fashion to that described for DC3000 HopAO1 (Macho et al., 2014), as supported by its location in the plasma membrane. Location of HopAO2 in Golgi

vesicles also suggests a possible interference of this T3E with vesicle trafficking. Future experiments should focus in the analysis of the role in virulence of HopAO2 and in elucidating the targets in woody plants of these two effectors of the HopAO family.

CHAPTER III

Pseudomonas savastanoi **pv. savastanoi NCPPB 3335 encodes two diverse members of the type III secretion system effector family HopAF which differentially modulate plant immune responses**

INTRODUCTION

Recent research focused on the function of type III secretion system effectors (T3E) during bacterial infection of plants, have revealed relevant information about the composition of the T3E repertoire in *Pseudomonas savastanoi* pv. savastanoi NCPPB 3335 (Rodriguez-Palenzuela et al., 2010; Ramos et al., 2012; Matas et al., 2014). In addition, the latest contributions to this field have also revealed new data concerning the specific role of some T3E interfering with the plant defense responses (Matas et al., 2014; Chapter II).

Among the 34 T3E candidates identified in the genome of NCPPB 3335 (Rodriguez-Palenzuela et al., 2010; Ramos et al., 2012; Matas et al., 2014; Chapter II), two of them have been described to be plasmid encoded: HopAF1 (located in plasmid pPsv48A) and HopAO1 (located in plasmid pPsv48B) (Perez-Martinez et al., 2008; Bardaji et al., 2011). The role of the T3E family HopAO in NCPPB 3335, which also includes a chromosomally encoded member (HopAO2), is described in Chapter II of this PhD Thesis. In relation to pPsv48A, bioinformatics analysis of this plasmid revealed that it contains a putative T3E transposon, which has captured a chimeric DNA containing a fragment of the effector gene *hopAY1* fused to a *hopAF1* allele (Bardaji et al., 2011). Moreover, a chromosomally encoded *hopAF1-2* allele has been reported in *P. savastanoi* pv. savastanoi NCPPB 3335 (Rodriguez-Palenzuela et al., 2010; Matas et al., 2014).

HopAF family members are widely distributed among strains belonging to the multi locus sequence typing (MLST) groups I and III established by Baltrus et al. (2011). Moreover, this family is also present in approximately half of the MLTS group II strains, which have a smaller T3E repertoire than the other groups and lack many T3E families (Lindeberg et al., 2012). Members of the HopAF family can be very diverse in sequence and are located in a wide variety of genomic locations. Sequence differences among members of these families suggest that this class of T3E may be under different evolutionary pressures relative to the core T3E present in all sequenced genomes of the *Pseudomonas syringae* complex (Baltrus et al., 2011).

The function of the *P. syringae* pv. tomato DC3000 HopAF1 has been previously investigated (Li et al., 2005b; Cunnac et al., 2009). This T3E has been related with reduction of the expression of the *Arabidopsis* glycerol kinase NHO1, which is induced in response to flagellin and required for limiting the *in planta* growth of nonhost *Pseudomonas* bacteria (Li et al., 2005b; Cunnac et al., 2009). In addition, DC3000 HopAF1 is not able to suppress ETI-associated hypersensitive response (HR) cell death or elicit cell death in *Nicotiana* spp. (Cunnac et al., 2009). However, functional analysis of other members of the HopAF family, e.g. those encoded in the genome of *P. savastanoi* pv. savastanoi, has not been reported to date.

In the present study we identified an extra chromosomally encoded copy of the *hopAF1*gene in *P. savastanoi* pv. savastanoi NCPPB 3335. We demonstrate that both HopAF1 and HopAF1-2 are translocated into plant cells through the NCPPB 3335 T3SS. In addition, we analyze the role of

these two T3E in the inhibition of plant defense responses. Furthermore, we report their subcellular location in *Nicotiana benthamiana* leaves using T3E fusions to the green fluorescent protein (GFP).

MATERIAL AND METHODS

Bacterial strains, plasmids, media and growth conditions

Most bacterial strains and plasmids used in this study are described in Table 1 and 2, respectively. Bacterial strains used for dot blot hybridization are described at the General Material and Methods section (Table 1). All *Pseudomonas* strains were grown in King´s B (KB) medium (King et al., 1954), Luria-Bertani (LB) medium (Miller, 1972), Hrp-inducing medium (HIM) (Huynh et al., 1989) or Super Optimal Broth (SOB) medium (Hanahan, 1983) at 28 ºC. *Escherichia coli* and *Agrobacterium tumefaciens* strains were grown in LB medium at 37 ºC or 28 ºC, respectively. When required, the medium was supplemented with ampicillin (Ap), 100 µg/mL; gentamicin (Gm), 10 µg/mL; kanamycin (Km), 10 or 50 µg/mL; rifampicin (Rf), 50 µg/mL; tetraciclin (Tc), 10 µg/mL or spectinomycin (Sp), 10 µg/mL.

Table 1. Bacterial strains used in this study.

Strains[a]	Relevant characteristics	References[b]
E. coli		
DH5α	*F -, ϕ80dlacZ M15, (lacZYA-argF) U169, deoR, recA1, endA, hsdR17 (rk - mk -), phoA, supE44, thi-1, gyrA96, relA1.*	(Hanahan, 1983)
XL1 Blue	*hsdR17, supE44, recA1, endA1, gyrA46, thi, relA1, lac/ F'* [*proAB*$^+$, *lacI*^{q}, *lacZ M15::*Tn10 (Tc^R)]	(Bullock et al., 1987)
GM2929	*F -, ara-14, leuB6, thi-1, tonA31, lacY1, tsx-78, galK2, galT22, glnV44, hisG4, rpsL136, xyl-5,mtl-1, dam13::Tn9, dcm-6, mcrB1, hsdR2, mcrA, recF143.* (Sp^R Cm^R).	(Palmer and Marinus, 1994)
Agrobacterium		
A. tumefaciens GV3101 (pMP90)	Carries Vir plasmid encoding T-DNA transfer machinery, Rif^R, Cm^R.	ATCC 33970
Pseudomonas		
P. fluorescens 55 [pLN18] (Pf)	Containing 25 kb *P. syringae* pv. syringae 61 *hrc/hrp* cluster with *shcA* and *hopPsyA* replaced by an *nptII* cassette (Km^R) .	(Jamir et al., 2004)
P. savastanoi pv. savastanoi (Psv)		
NCPPB 3335	Wild-type strain isolated from olive	(Pérez-Martínez et al., 2007)
NCPPB 3335-T3	Type III secretion mutant (Km^R)	(Pérez-Martinez et al., 2010)
Psv48 ΔA	NCPPB 3335 cured of pPsv48A	(Bardaji et al., 2011)
NCPPB 3335 Δ*hrpL*	*hrpL* mutant derived from NCPPB 3335 (Km^R)	(Matas IM et al., 2014)
Δ*hopAF1*	*hopAF1* mutant derived from NCPPB 3335 (Km^R)	This study
P. syringae pv. tomato (Pto)		
DC3000D28E	*ΔhopU1-hopF2 ΔhopC1-hopH1*::FRT *ΔhopD1-hopR1*::FRT *ΔavrE-shcN ΔhopAA1-2-hopG1::*FRT *ΔhopI1 ΔhopAM1-1 ΔhopAF1*::FRT *ΔavrPtoB ΔavrPto ΔhopK1 ΔhopB1 ΔhopE1 ΔhopA1::*FRT *hopY1::*FRT pDC3000A− pDC3000B− (Sp^R)	(Cunnac et al., 2011)

[a]Cm^R, Km^R, Sp^R and Rif^R indicate resistance to chloramphenicol, kanamycin, spectinomycin and rifampicin, respectively. [b]ATCC, American Type Culture Collection.

Expression plasmids (Table 2) were generated using Gateway™ cloning technology (Invitrogen Corp, California, USA) as indicated in General Material and Methods section.

Construction of the Δ*hopAF1* (AER-0003643) mutant from *P. savastanoi* pv. savastanoi NCPPB 3335 was performed by marker exchange mutagenesis as previously described and the correct exchange of the *hopAF1* gene by the Km resistance cassette was determined by Southern blot analysis (General Material and Methods section).

Table 2. Plasmid used in this study.

Name[a]	Description[a]	References
pGEM-T	Cloning vector containing ori f1 and *lac*Z (Amp^R)	(*Promega*, USA)
pGEM-T- KmFRT-*BamHI*	Contains Km^R from pKD4 (Amp^R Km^R)	(Zumaquero et al., 2010)
pPCO1	pGEM-T derivates, contains 1.2 kb approx. on each side of the *hopAF1-2* gene (AER-0003643) (Ap^R)	This study
pPCO1-Km	pGEM-T derivates, contains 1.2 kb approx. on each side of the *hopAF1-2* gene (AER-0003643) interrupted by the kanamycin resistance gen *nptII* (Ap^R, Km^R)	This study
pENTR/D/SD TOPO	Entry vector for Gateway cloning (Km^R, Cm^R)	(*Invitrogen Corp*.; California, USA)
pENTR-*hopAF1*	pENTR/D/SD TOPO::AER-0003643 (Km^R)	This study
pENTR-*hopAF1-2*	pENTR/D/SD TOPO::AER-0000968 (Km^R)	This study
pCPP3234	pVLT35::Gateway cassette-Cya fusion, broad-host-range vector containing *tac* promoter and *lacI*^{q} (Sp^R, Str^R, Cm^R)	(Schechter et al., 2004)
pCYA-*hopAF1*	pCPP3234 expressing AER-0003643-Cya (Sp^R, Str^R)	This study
pCYA-*hopAF1-2*	pCPP3234 expressing AER-0000968-Cya (Sp^R, Str^R)	This study
pCPP5040	pML123::Gateway cassette, broad-host-range vector allowing for constitutive expression of inserts fused to a C-terminal HA tag from the *nptII* promoter (Gm^R, Cm^R)	(Lopez-Solanilla et al., 2004)
pEXP-*hopAF1*	pCPP5040 expressing AER-0003643-HA tag (Gm^R)	This study
pEXP-*hopAF1-2*	pCPP5040 expressing AER-0000968-HA tag (Gm^R)	This study
pGWB5	35S promoter, C-sGFP (35S promoter-R1-Cm^R-*ccdB*-R2-sGFP), Km^R, Hg^R	Invitrogen
pLOC-*hopAF1*	pGWB5 expressing AER-0003643-GFP (Km^R, Hg^R)	This study
pLOC-*hopAF1-2*	pGWB5 expressing AER-0000968-GFP (Km^R, Hg^R)	This study

[a]Ap^R, Cm^R, Km^R, Sp^R, Str^R and Hg^R indicate resistance to ampicillin, chloramphenicol, kanamycin, spectinomycin, streptomycin and higromycin, respectively. AER numbers indicate ASAP identification numbers for Psv NCPPB 3335 genes (http://www.genome.wisc.edu/tools/asap.htm). *Cya*, catalytic domain of *Bordetella pertusis* adenilate cyclase; HA tag, Influenza hemagglutinin peptide YPYDVPDYA.

Quantitative RT-PCR assays

qRT-PCR assays were performed as described in General Material and Methods section using oligonucleotides primers shown in Table 3.

Table 3. Primers used in this study.

Forward primers		Reverse primers	
Name[a]	**Sequence**	**Name**	**Sequence**
HopAF1 F-237	CTTATCAAGCAGAAAGACGG	HopAF1 R-536	AAGGGAGCAGATGGAATACG
Oligo P1	GTGTAGGCTGGAGCTGCTTC	Km R-768	TTGCATCAGCCATGATGG
hopAF1-F	GCGGATGCATTGAAACAGCT	*hopAF1*-R	AATAACAGCGCCCAGCAGAGT
hopAF1-2F	CACTGCGGAGGCATTGAAAA	*hopAF1*-2R	AGAATAACGGCGCCAAGCA
TA-HopAF1-F617	GCAACCTCATGGAGCGAC	TA-HopAF1 R353	CCCTATAGTGAGTCGGATCCG GTTGGACTTGGCACTG
TD-HopAF1-F6	GGATCCGACTCACTATAGGG CCAACACTAGGTGTAAC	TD-HopAF1 R293	GCTCATGTTTGGTGATCG
TOPO-968-F	CACCATGGGACTATGTATTTCA	TOPO-968-R	TAAAGCGACCAAATGCTT
TOPO-3643-F	CACCATGGGACTATGTATTTCA	TOPO-3643-R	GCCAGTCACCAAATGTTT
		Cya	CAATCAGGCTGGTGGAATGG

[a] F and R, forward and reverse primer, respectively. Numbers included after F and R in primers names correspond to the hybridization position of the 3' end of the primer in the corresponding ORF sequence.

Table 4. Accession number of the protein sequences used for the construction of the phylogenetic trees shown in Figure 2.

Strain[a]	**Abbreviated**	**Accession number**[b]	**Locus Tag**
aesculi 2250	Pae	WP_005730473.1	Psyrpa2_010100002225
aceris MAFF 302273	Pac	WP_003381937.1	PSYAR_11249
lachrymans M302278	Pla	WP_005746129.1	nd
lachrymans MAFF301315	Pla	EGH86579.1.	PLA107_25865
maculicola ES4326	Pma	WP_007248647.1	PMA4326_03644
mori MAFF 301020	Pmo	WP_005752338.1	PSYMO_39865
phaseolicola 1448A	Pph	YP_273699.1	PSPPH_1443
savastanoi NCPPB 3335	Psv HopAF1	EFI00483.1	PSA3335_1477
savastanoi NCPPB 3335	Psv HopAF1-2	YP_006961546.1	PSA3335_1469
syringae B728a	Psy	YP_236881.1	Psyr_3813
tomato DC3000	Pto	NP_791393.1	PSPTO_1568
tomato Max13	Pto	ZP_07233181	PsyrptM_010100019102
tomato NCPPB 1108	Pto	ZP_07256821	PsyrptN_010100005517
tomato T1	Pto	EEB59276.1.	PSPTOT1_4398
actinidae LV ICMP 18803	Pan LV HopAF1-1	na	A237_04053
actinidae LV ICMP 18803	Pan LV HopAF1-2	na	A237_28116
pisi 1704	Ppi	EGH45046.1.	PSYPI_22937

[a] Indicated as pathovars of *Pseudomonas syringae*, with the exception of *P. savastanoi* pv. savastanoi. [b] Database - Hops, http://www.pseudomonas-syringae.org/home.html. na, not available in GenBank.

Bioinformatics analysis

Accession numbers of the protein sequences used for the construction of the phylogenetic trees shown in Figure 2 are in Table 4. Sequence alignment using ClustalW, determination of the optimal amino acid substitution model and phylogenetic tree construction were performed using MEGA5 (Tamura et al., 2011). Neighbor-joining and maximum-likelihood phylogenetic trees of the individual protein sequences were generated using MEGA5 with the optimal model (John-Taylor-Thornton model) and the option of complete deletion to eliminate positions containing gaps. Confidence levels for the branching points were determined using 10,000 bootstraps replicates.

N-myristoylation sites (Maurer-Stroh et al., 2002) in HopAF1 and HopAF1-2 were identified using NMT program (http://mendel.imp.ac.at/myristate/SUPLpredictor.htm).

Subcellular localization

Agrobacterium constructs pGWB5-HopAF1-GFP and pGWB5-HopAF1-2-GFP (Table 2) were obtained by Gateway technology (See General Material and Methods section) and transformed into *A. tumefaciens* strain GV3101 by electroporation (Weigel and Glazebrook, 2002). Subcellular localization assays were performed as described by Rodríguez-Herva et al., (2012). The cells were grown in YEB medium (Vervliet et al., 1975) until exponential phase, pelleted and resuspended in MMA induction buffer (1 L of MMA: 4.4 g MS salt, 1 g MES, 2 % sucrose, pH 5.6) supplemented with acetosyringone to reach an optical density of 2.1-3.0. Cultures were incubated at room temperature for 1 h before infiltration. *A. tumefaciens* cultures were infiltrated into four leaves of *N. benthamiana* plants using a 1 ml syringe. At 48 h after inoculation, fluorescence images were acquired using a confocal microscope (Leica SP8).

RESULTS AND DISCUSSION

P. savastanoi pv. savastanoi NCPPB 3335 encodes three homolog sequences of the *hopAF* gene family.

Bioinformatics analysis of the draft genome sequence and the three plasmid complement of *P. savastanoi* pv. savastanoi NCPPB 3335, previously identified the *hopAF1* and *hopAF1-2* genes in plasmid pPsv48A and in the chromosome of this strain, respectively (Rodriguez-Palenzuela et al., 2010; Bardaji et al., 2011). A *hopAF* probe, 80 % identical with the sequence of *hopAF1-2*, and thus hybridizing with both *hopAF* alleles, was obtained by PCR using primers HopAF1 F-237 and HopAF1 R-536 (Table 3). The probe was labeled with digoxigenin (DIG) (General Material and Methods section). Total DNA isolated from wild-type NCPPB 3335 and from a NCPPB 3335 derivative cured of plasmid pPsv48A (Psv48ΔA) was digested with ClaI, which does not cut within the *hopAF1* or *hopAF1-2* genes, and hybridized with the *hopAF* probe. Two hybridization fragments of about 3.0 kb and 10.4 kb were obtained for NCPPB 3335 (Fig.1), corresponding to the *hopAF1* and *hopAF1-2* genes as deduced from the draft genome sequence of this strain (Rodriguez-Palenzuela et al., 2010). However, the 3.0-kb fragment was not observed for the Psv48ΔA sample, as expected for the loss of the pPsv48A-encoded *hopAF1* gene in this strain. Surprisingly, an unexpected fragment of approximately 9.4 kb was clearly observed for both NCPPB 3335 and Psv48ΔA (Fig. 1), indicating that NCPPB 3335 encodes three different nucleotide sequences hybridizing with the *hopAF1* probe. No additional *hopAF1*-like sequences were found in the complete plasmid sequences of NCPPB 3335 (Bardaji et al., 2011), suggesting the chromosomal codification of this additional sequence. Complete sequencing of the NCPPB 3335 genome would be necessary to confirm this hypothesis.

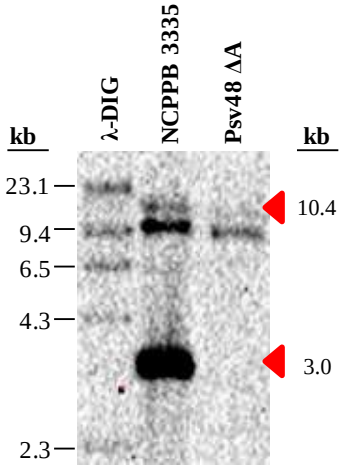

Figure 1. Detection of *hopAF*-like sequences in the genome of *P. savastanoi* pv. savastanoi NCPPB 3335 and derived strain Psv48ΔA. Southern blot analysis of ClaI-digested genomic DNA isolated from strains NCPPB 3335 and Psv48ΔA (cured of plasmid pPsv48A). Red arrows indicate hybridization fragments corresponding to the *hopAF1* and *hopAF1-2* genes (approximately 3.0 and 10.4 kb, respectively). The positions of molecular size markers (in kilobases, kb) are indicated to the left of the gel.

Distribution of HopAF1 among *P. savastanoi* pv. savastanoi and related strains

With the purpose of analyzing the presence of HopAF1 homologs among strains of the *Pseudomonas syringae* complex, a BLASTp search was performed against the non-redundant protein sequence database. The results revealed that NCPPB 3335 HopAF1 and HopAF1-2, which are 74 % identical (100% cover), are separated in different branches of the tree. The plasmid-encoded NCPPB 3335 HopAF1 is most similar to its homologs encoded by other *P. syringae* pathovars infecting woody hosts and belonging to genomospecies 2 and 3, like *P. syringae* pv. actinidae strains MAFF302091 and LV and *P. syringae* pv. mori MAFF301020, suggesting that this *hopAF1* allele could play a relevant role in bacterial interactions with woody host plants. However, NCPPB 3335 HopAF1 also clustered with that of *P. syringae* pv. lachrymans MAFF301315 (genomospecies 1), which causes angular leaf spot of cucumber (Bradbury, 1986). Conversely, NCPPB 3335 HopAF1-2 homologs are found in *P. syringae* strains isolated from either herbaceous or woody plants and belonging to genomospecies 1, 2, 3 and 9 (Fig. 2A). On the other hand, the phylogeny of these two members of the HopAF family is not congruent with the phylogeny of the *P. syringae* complex deduced from housekeeping genes (Ramos et al., 2012), suggesting the existence of horizontal transfer.

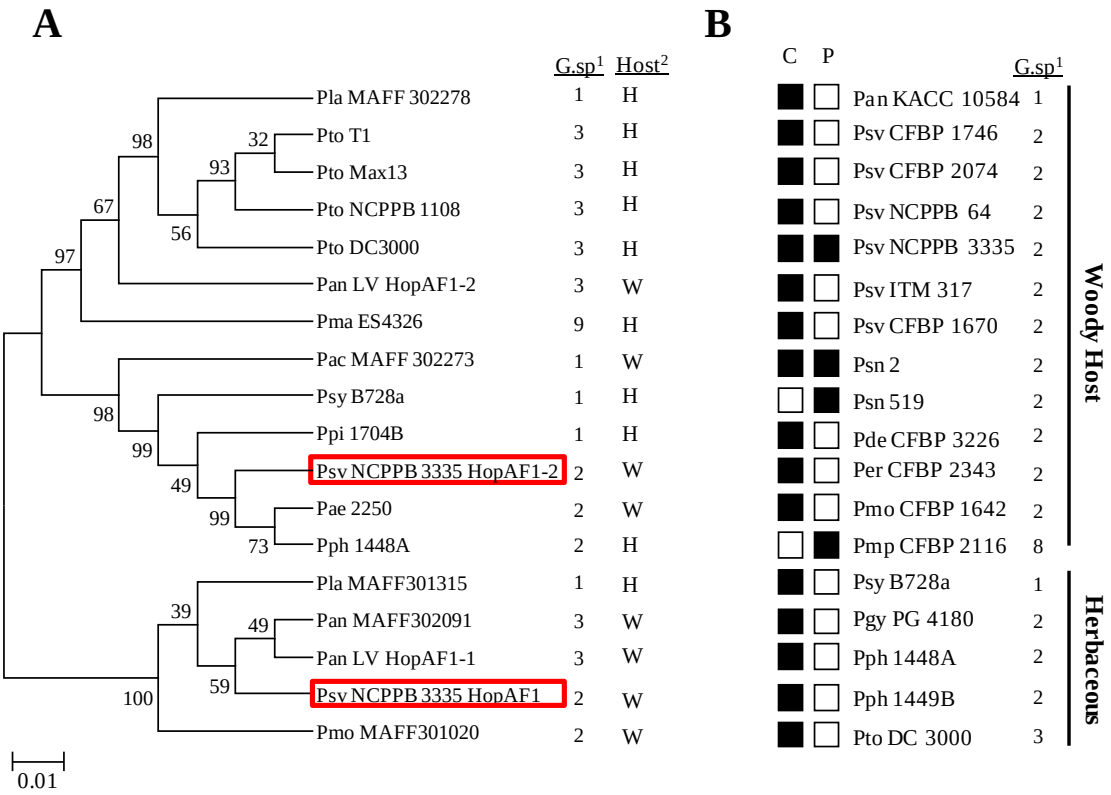

Figure 2. Distribution and phylogeny of the HopAF family in the *Pseudomonas syringae* complex. **A**, Unrooted neighbor-joining tree of HopAF proteins. The accession number of the protein sequences used for the construction of the phylogenetic tree is presented in Table 4. All amino acid sequences used are annotated as HopAF1 homologs, with the exception of *P. savastanoi* pv. savastanoi NCPPB 3335 HopAF1-2 and *P. syringae* pv. actinidae LV HopAF1-1 and HopAF1-2 (http://www.pseudomonas-

syringae.org/). Bootstrap percentage values (10,000 repetitions) are shown in the branches, and evolutionary distances are given in units of amino acid substitutions per site. **B**, Distribution of the *P. savastanoi* pv. savastanoi NCPPB 3335 T3E genes of the *hopAF* family among a collection of strains of the *P. syringae* complex isolated from woody and herbaceous plant hosts. A colony-blot analysis was performed using a *hopAF1* probe (Table S2 in Supplementary Material section). The strains are indicated by their pathovar abbreviation (Table 4). Black and white squares represent the presence or absence, respectively, of strong hybridization signals for each strain analyzed. [1]G.sp, genomospecies; [2]Host: W, woody host; H, herbaceous host.

To ascertain the distribution of *hopAF1*-like sequences among a collection of 31 *P. savastanoi* pv. savastanoi strains isolated in different countries and among a selection of *P. syringae* strains isolated from either woody and herbaceous host (see Table 1 in General Material and Methods section), a dot-blot hybridizations was performed using a *hopAF1* probe hybridizing with both *hopAF1* and *hopAF1-2*. A positive hybridization signal was obtained for 29 out of the 31 *P. savastanoi* pv. savastanoi strains analyzed, as well as for 16 out of the 22 *P. syringae* strains used (See Supplementary Material section, Table S2). Strains that did not hybridize with this probe where discarded for further analysis.

A collection of six *P. savastanoi* pv. savastanoi strains, two *P. savastanoi* pv. nerii isolates and 10 *P. syringae* strains hybridizing with the *hopAF1* probe in the dot-blot analysis were selected to determine the localization of *hopAF1*-related sequences in their replicons. Plasmid preparations and total DNA isolated from these 18 strains were analyzed by southern-blot hybridization using the *hopAF1* probe. The results revealed that, with the exception of *P. savastanoi* pv. nerii strain 519 y *P. syringae* pv. morsprunorum CFBP 2116, all other *P. savastanoi* and *P. syringae* strains analyzed encode at least one copy of the *hopAF1* gene in their chromosome. Besides *P. savastanoi* pv. savastanoi NCPPB 3335 and *P. savastanoi* pv. nerii strain 2 also contain a plasmid-encoded copy of this gene (Fig. 2B), further supporting the hypothesis that *hopAF1* has been horizontally transferred among strains of the *P. syringae* complex. In agreement with this hypothesis, Bardaji et al. (2011) reported that although the overall G+C content of the three plasmid complement of NCPPB 3335 is close to the 57.12% G+C of the NCPPB 3335 genome (Rodriguez-Palenzuela et al., 2010), they contained 22 CDS with less than 50% G+C that could have been acquired via horizontal gene transfer. The *hopAF1* gene (47.2% G+C) was identified among these CDS by these authors. Also, HopAF1 has been previously identified as a highly conserved T3E across *P. syringae* pathovars, reflecting a selective constraint more typical of core genes and suggesting that it plays a central role in the disease process (Sarkar et al., 2006). However, the HopAF family is not considered a core member of the *P. syringae* T3E super-repertoire, which is composed only by four members (AvrE, HopAA, HopI and HopM) (Baltrus et al., 2011; Lindeberg et al., 2012).

HrpL-dependent expression of the *P. savastanoi* pv. savastanoi T3SS effector genes *hopAF1* and *hopAF1-2*

An identifiable Hrp box sequence (Fouts et al., 2002) was found in the 290 nucleotides upstream of the start codon of the *P. savastanoi* pv. savastanoi NCPPB 3335 *hopAF1* and *hopAF1-2* genes (Table 5), suggesting that expression of these two T3E could be transcriptionally activated by HrpL. Similar Hrp box sequences were previously identified in the promoter sequences of several validated NCPPB 3335 T3E (Matas et al., 2014).

Table 5. Occurrence of consensus Hrp-box sequences upstream of the *P. savastanoi* pv. savastanoi NCPPB 3335 *hopAF1* and *hopAF1-2* genes.

Gene name	Location[a]	Hrp-box position[b]	Hrp-box sequence
CONSENSUS[c]			**BGGAACYHNNNNNNNNNNNNNNCCACNHAG**
hopAF1	P	-272 to -243	TGGAACTTTTTCTTGCCCGCTACCACCCAT
hopAF1-2	C	-287 to -257	TGGAACCGCTGAAGAGTTTTAGCCACTCAG

[a] Location: C, chromosomal and P, plasmid. [b] Coordinates are with respect to the annotated start codon of the CDS.
[c] Consensus Hrp box sequence (Fouts et al., 2002). Conserved sequences are highlighted in gray.

In order to test the HrpL-dependent expression of the NCPPB 3335 *hopAF1* and *hopAF1-2* genes, wild-type NCPPB 3335 and a NCPPB 3335 Δ*hrpL* mutant (Matas et al., 2014) were used. NCPPB 3335 Δ*hrpL* has been reported to be unable to elicit the hypersensitive response (HR) in *Nicotiana tabacum* plants or form knots in lignified olive plants (Matas et al., 2014). Expression analyses were performed under inducing conditions (cells grown for 6 h in HIM) using quantitative reverse-transcription polymerase chain reaction (qRT-PCR). Specific q-RT-PCR primers allowing differentiation between the *hopAF1* (primers *hopAF1*-F and *hopAF1*-R) and the *hopAF1-2* (primers *hopAF1-2F* and *hopAF1-2R*) genes were used (Table 3). The expression of the *hopAF1* and *hopAF1-2* genes decreased (0.29- and 0.14-fold, respectively) in the Δ*hrpL* mutant compared to the wild-type strain, demonstrating an expression dependency on HrpL (Fig. 3A). Using identical conditions to those reported in this analysis, Matas et al. (2014) recently demonstrated that expression of the NCPPB 3335 *avRPto1*, *hopBK1*, *hopBL1*, and *hopBL2* genes is also HrpL dependent. Also, an expression dependency on HrpL of the NCPPB 3335 *hopAO1* and *hopAO2* genes was demonstrated in this PhD Thesis using the same culture conditions (see Chapter II). However, expression of the *iaaM* gene (encoding tryptophan monooxygenase, involved in the biosynthesis of indoleacetic acid), which was used as negative control, was not reduced in the Δ*hrpL* mutant (Matas et al., 2014).

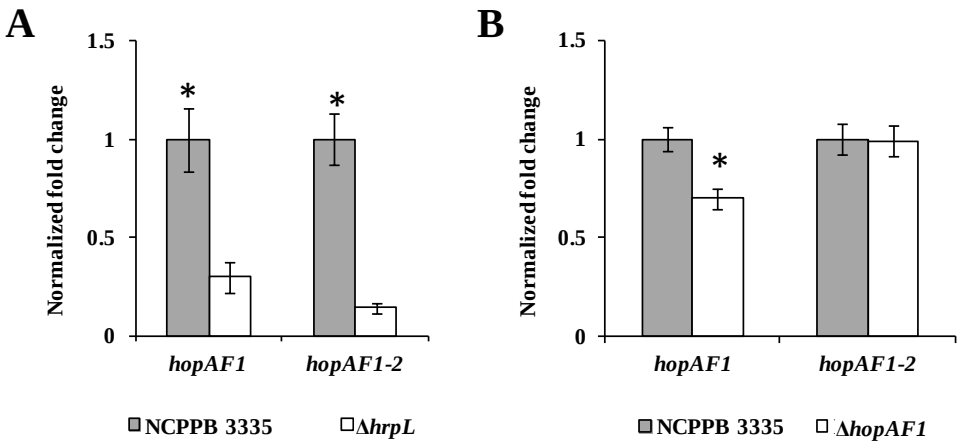

Figure 3. Transcriptional analysis of the *P. savastanoi* pv. savastanoi NCPPB 3335 *hopAF1* and *hopAF1-2* genes. Quantitative reverse-transcription polymerase chain reaction (qRT-PCR) with the indicated T3E genes in NCPPB 3335 versus NCPPB 3335 Δ*hrpL* (**A**) or NCPPB 3335 versus NCPPB 3335Δ*hopAF1* (**B**) at 6 h after transfer to Hrp-inducing medium. The fold change was calculated after normalization using the *gyrA* gene as an internal control. Results represent the means from three independent experiments. Error bars represent the standard deviation. Asterisks indicate significant differences (P = 0.05) between the expression values obtained for NCPPB 3335 and the mutant strains.

A NCPPB 3335 Δ*hopAF1* mutant was constructed by marker exchange mutagenesis (Zumaquero et al., 2010) and the loss of this plasmid-encoded gene was verified by Southern blot. As described above for strain Psv48ΔA (cured of pPsv48A) (Fig. 1), two DNA fragments hybridizing with the *hopAF* probe were observed in the Δ*hopAF1* mutant (data not shown), further supporting that NCPPB 3335 encoded three different *hopAF*-related sequences. Expression of the *hopAF1-2* gene was similar in the wild-type strain and the Δ*hopAF1* mutant, demonstrating that loss of plasmid-encoded *hopAF1* does not alter expression of *hopAF1-2* under the conditions tested (6 h after transfer to HIM). Unexpectedly, expression of the *hopAF1* gene was detected in the Δ*hopAF1* mutant using a *hopAF1*-specific primer. However, the expression decreased 0.31-fold in the Δ*hopAF1* mutant in comparison with the wild-type strain (Fig. 3B). These results suggest the existence of a second and transcriptionally active copy of the *hopAF1* gene encoded in the chromosome of NCPPB 3335. In fact, a DNA fragment of 840 bp was PCR amplified from the genome of Psv48ΔA using primers TOPO-968-F and TOPO-968-R (Table 3), which amplify specifically with the complete *hopAF1* ORF. Sequencing of these DNA fragments confirmed that this extra copy of the *hopAF1* gene is 100% identical to that encoded in plasmid pPsv48A. The plasmid-encoded NCPPB 3335 *hopAF1* gene has been shown to be a chimeric *hopAY1-hopAF1* allele captured by a putative effector transposon designated IS*Psy30* (Bardaji et al., 2011). Thus, it could be possible that one of the two copies of the *hopAF1* gene encoded in the NCPPB 3335 genome might have been originated by a true transposition event. Duplication of T3E genes within *P. syringae* genomes and association with mobile genetic elements has been previously related with ongoing insertions and deletions of T3E genes (Alfano and Collmer, 2004). Other examples of the duplication of T3E genes include *P. syringae* pv. maculicola M6 *hopX1* (Rohmer

et al., 2003), *P. syringae* pv. phaseolicola 1448A *hopW1-1* and *hopW1-2*, as well as *avrB4-1* and *avrB4-2* (Zumaquero et al., 2010) and *P. syringae* pv. tomato DC3000 *hopAA1-1* and *hopAA1-2*, and *hopAM1-1* and *hopAM1-2* (http://www.pseudomonas-syringae.org).

HopAF1 and HopAF1-2 are translocated through the *P. savastanoi* pv. savastanoi type III secretion system

To determine whether *P. savastanoi* pv. savastanoi NCPPB 3335 HopAF1 and HopAF1-2 could be translocated into plant cells via the T3SS, *Bordetella pertusis* adenylate cyclase (Cya) fusions to these two T3E were constructed as previously described (Matas et al., 2014). This system, based in cyclic AMP (cAMP) production exclusively in the presence of eukaryotic calmodulin, has been widely used for analyzing the translocation of *P. syringae* T3E (Sory and Cornelis, 1994; Casper-Lindley et al., 2002; Schechter et al., 2004). Wild-type NCPPB 3335 and NCPPB 3335-T3 (T3SS mutant, Table 1) (Perez-Martinez et al., 2010) expressing each of the two constructed Cya fusions (Table 2) were infiltrated in *N. tabacum* leaves. Significant differences in cAMP production between the wild type and the NCPPB 3335-T3 mutant were observed for both HopAF1 and HopAF1-2 (Fig. 4), indicative of their translocation through the NCPPB 3335 T3SS. These results, together with the expression dependency of these two T3E from HrpL (Fig. 3A), are in accordance with the characteristics required for the definition of T3E from the *P. syringae* complex (Lindeberg et al., 2005). Thus, HopAF1 and HopAF1-2 emerge as validated members of the *P. savastanoi* pv. savastanoi NCPPB 3335 T3SS secretome. We have previously reported the validation of another nine NCPPB 3335 T3E (Matas et al., 2014; chapter II of this PhD Thesis). Translocation and expression analysis allowing validation of T3E encoded by other strains of the *P. syringae* complex isolated from woody hosts has not been reported to date.

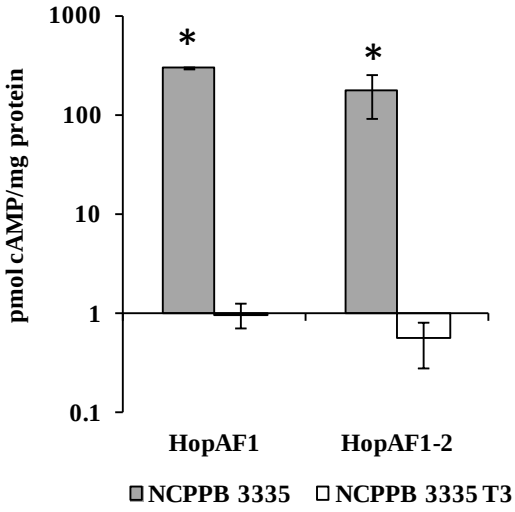

Figure 4. Translocation assay of *P. savastanoi* pv. savastanoi NCPPB 3335 HopAF1 and HopAF1-2. Calmodulin- and Cya-dependent production of cAMP was used to measure the translocation of T3E-Cya fusions into *N. tabacum* cv. Newdel plants. Plants were inoculated with *P. savastanoi* pv. savastanoi

NCPPB 3335 or NCPPB 3335-T3 (T3SS mutant) expressing the indicated Hop-Cya fusions from pCPP3234 derivatives (Table 2). The values represent the mean and standard error for samples obtained in triplicate; similar results were obtained in multiple experiments. Asterisks indicate significant differences (P = 0.05) between the cAMP levels obtained for the NCPPB 3335 and NCPPB 3335-T3 strains.

Role of the plasmid-encoded *hopAF1* gene in the virulence of *P. savastanoi* pv. savastanoi NCPPB 3335 in olive plants

We have previously reported that *P. savastanoi* pv. savastanoi strain Psv48ΔA (cured of plasmid pPsv48A, Table 1) induced less severe symptoms on the stems of the olive plants than the wild-type strain NCPPB 3335 (Bardaji et al., 2011). In order to determine the specific contribution to virulence of this plasmid-encoded gene, pathogenicity tests were performed in both *in vitro* micropropagated and lignified olive plants. In agreement with our previous results, Psv48ΔA induce attenuated hyperplastic knots, which also showed a premature necrosis of the tissue in both plant systems (Fig. 5A, 5B and 5C). In contrast, the sizes of the knots induced by the NCPPB 3335 Δ*hopAF1* mutant on the stem of *in vitro*-grown olive plants at 28 dpi were not significantly different from those induced by the wild-type strain (Fig. 5A and 5C). In addition, competition assays between the wild-type strain and the Δ*hopAF1* mutant in this plant system showed that these two strains were equally competitive (competition index no significantly different from 1.0), suggesting the existence of functional complementation by other T3E in the Δ*hopAF1* mutant. In fact, active transcription of the chromosomally encoded *hopAF1* and *hopAF1-2* genes was here reported for this strain (Fig. 3). Interestingly, the sizes of the knots induced by the Δ*hopAF1* mutant in lignified olive plants were in average slightly smaller, although no significantly different, than those induced by the wild-type strain (Fig. 5B and 5C). Complementation of the Δ*hopAF1* mutant with the *hopAF1* gene expressed from a constitutive promoter (*nptII* promoter, plasmid pCPP5040, Table 2), resulted in the formation of knots significantly larger and less necrotic than those induced by the wild-type strain, suggesting a relevant role of this T3E in the inhibition of plant defense responses. Furthermore, a Psv48ΔA derivative expressing the *hopAF1* gene (Table 2) induced knots similar in size and shape to those observed in *in vitro* olive plants infected with the wild-type strain (Fig. 5A). Conversely, complementation of knot size was not observed for this strain on lignified olive plants (Fig. 5B). Differences in the symptomatology induced by *P. savastanoi* pv. savastanoi T3SS mutants has been previously observed between in *in-vitro* grown and lignified olive plants. These differences, has been suggested to be likely due to the high susceptibility of the micropropagated plant material to this pathogen and to the ability of the T3SS mutants to produce indole-3-acetic acid (Perez-Martinez et al., 2010).

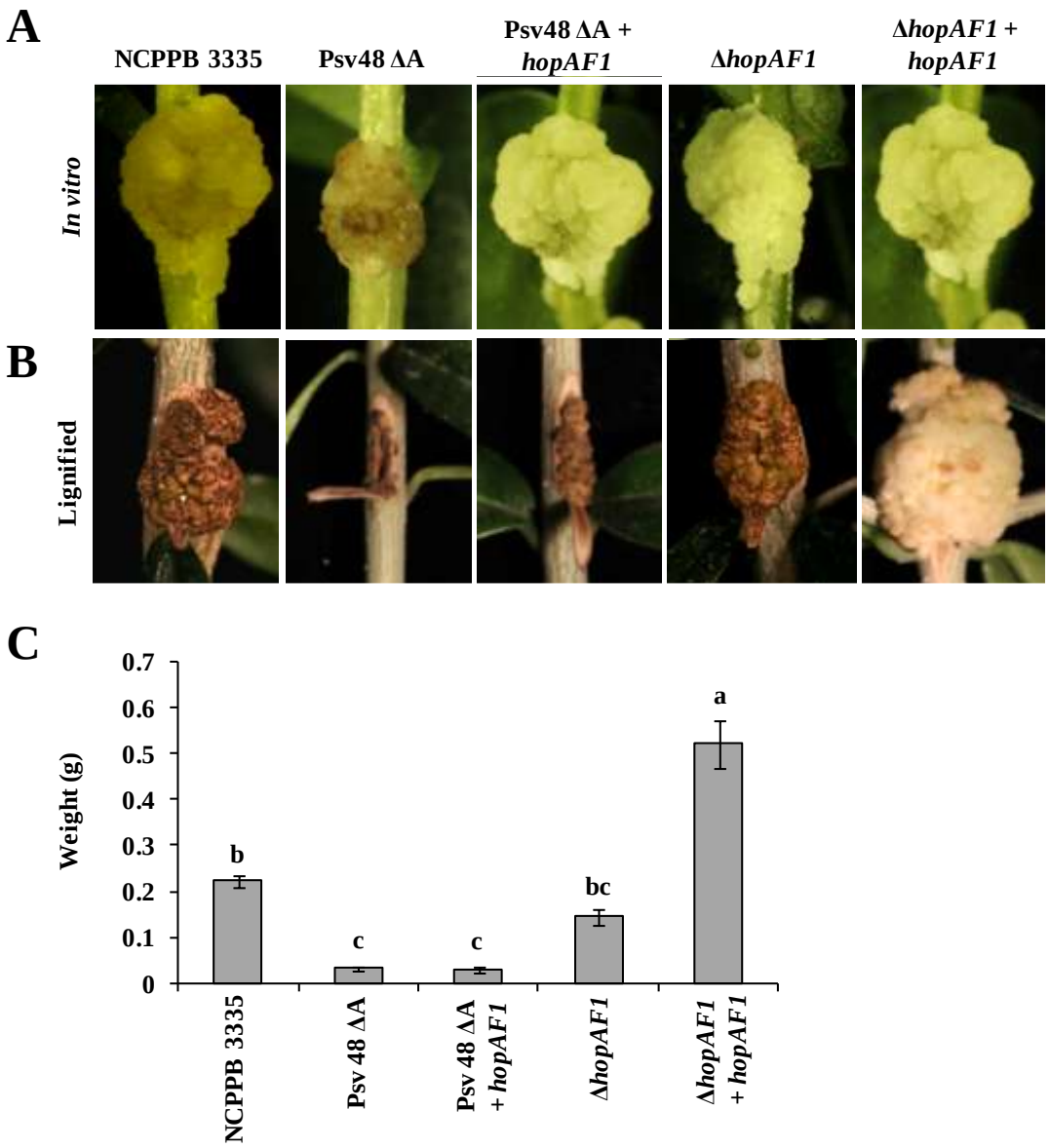

Figure 5. Virulence assay of *hopAF1* mutant on young micropropagated and lignified olive plants. Knots induced by the indicated strains on young micropropagated olive plants at 28 days post inoculation (dpi) (**A**) and in one year-old olive plants at 90 dpi (**B**). **C**, Weight of knots developed on lignified olive plants infected with the indicated strains. Knots weights are the means of six different knots. Statistical analyses were performed using one-way ANOVA followed by post-hoc comparisons using the Tukey test. The error bars indicate the standard error from the average of three different assays. Statistical analyses were performed using Student´s t-test with a threshold of P = 0.05. NCPPB 3335, wild-type strain; Pv48ΔA, NCPPB 3335 cured of plasmids pPsv48A; Pv48ΔA + *hopAF1*, Pv48ΔA expressing *hopAF1*; Δ*hopAF1*, NCPPB 3335 Δ*hopAF1* mutant; Δ*hopAF1* + *hopAF1*, Δ*hopAF1* expressing *hopAF1*.

T3E repertoires encoded by individual *P. syringae* strains compose a robust system that usually can tolerate loss of individual T3E because of high-level functional overlap among them (Cunnac et al., 2004). Thus, deletion of a single *P. syringae* T3E gene does not often lead to a noticeable loss of virulence, as measured by attenuation of bacterial growth and symptoms development in infected plants (Hauck et al., 2003). Nevertheless, deletion of other *P. savastanoi*

pv. savastanoi T3E genes such as *hopAO1* resulted in virulence reduction in olive plants (Chapter II of this PhD Thesis). Construction of a double *hopAF1* mutant, a single *hopAF1-2* mutant and a triple *hopAF1 hopAF1-2* mutant would be required to further study the role of the HopAF family in the virulence of *P. savastanoi* pv. savastanoi in olive plants. In this sense, we could not approach the replacement of the *hopAF1-2* gene by a Km cassette using the same strategy described here for the construction of the *hopAF1* mutant (Zumaquero et al., 2010), as the sequence of this gene is near the end of a contig in the draft genome sequence of NCPPB 3335 (Rodriguez-Palenzuela et al., 2010). Thus, primers allowing amplification of the genomic regions flanking the *hopAF1* gene could not be designed. On the other hand, disruption of this gene by plasmid integration yielded neither positive transformants. Complete sequencing of the genome of NCPPB 3335 would be required to address this question.

HopAF1 and HopAF1-2 differentially suppress physiological processes associated with PTI

The heterologous system *Pseudomonas fluorescens* 55 (Pf55) [pLN18], expressing a *P. syringae* T3SS (Jamir et al., 2004; Lopez-Solanilla et al., 2004; Oh et al., 2010; Matas et al., 2014), was used to analyze the effect of the expression of HopAF1 and HopAF1-2 over the incitation of plant associated defense responses as are ROS production and callose deposition. These two hallmarks were monitored after inoculation of *N. tabacum* leaves with Pf55 [pLN18] derivatives strains expressing either HopAF1 or HopAF1-2 (see pCPP5040 derivatives, Table 2). ROS levels, determined by 3-3´-diaminobenzidine (DAB) staining were significantly reduced by the expression of HopAF1 and HopAF1-2 compared to the control strains Pf55 [pLN18] harboring an empty vector (Fig. 6A and 6C) (Tukey test; $P \leq 0.01$). However, only HopAF1-2 reduced the levels of callose deposition compared to the control strain (Tukey test; $P \leq 0.01$) (Fig. 6B and 6D). These two defense markers are associated with the PTI incited upon pathogen attack (Boller and Felix, 2009). Although it has been reported that these two responses are usually associated, they belong to different categories regarding the timing of the process and they might be considered independent defense markers. While ROS production occurs during the early phase of PTI, callose deposition develops within longer periods of time (Nicaise et al., 2009; Henry et al., 2013). Moreover, both types of responses have been described to occur independently of plant resistant responses in some plant-pathogen interactions (Nishimura et al., 2003; Galletti et al., 2008; Segonzac et al., 2011). Our results are in line with the observed independency among these two processes, and show that HopAF1 interferes with early PTI-associated processes like ROS production, while HopAF1-2 suppress both early and late PTI defense responses. The description of specific *in planta* targets of these two effectors will shed light about the different pathways involved in the initiation of these responses.

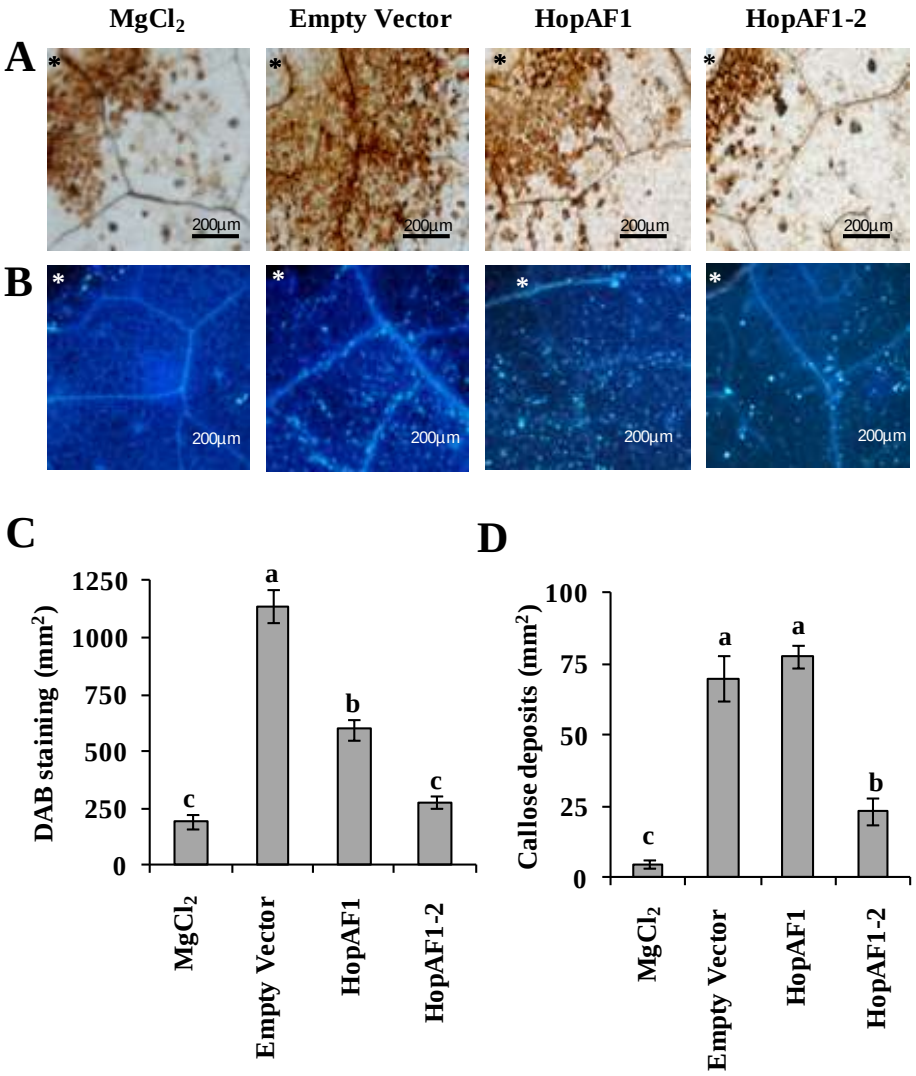

Figure 6. 3-3´-diaminobenzidine (DAB) staining and callose deposition in *N. tabacum* var. Xhanti leaves. Plants were challenged with *P. fluorescens* 55 [pLN18] harboring the pCPP5040 empty vector or the vectors expressing *P. savastanoi* pv. savastanoi NCPPB 3335 HopAF1 or HopAF1-2. **A**, DAB signal was quantified 4 h after inoculation, and **B**, callose deposition was detected by aniline blue staining and quantified 12 h after infection. **C** and **D**, quantification of DAB staining (ROS production) and callose deposition, respectively. For histograms, data are means ± standard error of the mean for at least five replicas; bars topped with the same letter represent values that are not significantly different using one-way ANOVA and Tukey test for multiple comparison (P=0.01). Each experiment was repeated at least three times with similar results.

ETI response induced by the effectorless polymutant *P. syringae* pv. tomato DC3000 is suppressed by HopAF1-2 but not by HopAF1

To further analyze the role of HopAF1 and HopAF1-2 in the interference of the ETI defense response, these two proteins were expressed individually from plasmid pCPP5040 (Table 2) in *P. syringae* pv. tomato DC3000D28E (Cunnac et al., 2011). This polymutant strains induce HR in *N. tabacum* and *N. benthamiana* (Kvitko et al., 2009; Cunnac et al., 2011). The DC3000D28E derivatives expressing *P. savastanoi* pv. savastanoi NCPPB 3335 HopAF1 or HopAF1-2 (See

Table 2) were inoculated in *N. tabacum* leaves. After 48 h, the polymutant strain stimulated an ETI-like response which was completely inhibited by the expression of the NCPPB 3335 HopAF1-2. However, expression of HopAF1 had no effect in the incited response (Fig. 7A). These results suggest that HopAF1-2 participate in the inhibition of the plant defense response associated with the onset programmed cell death. The results obtained with HopAF1 are in line with the reported involvement of its *P. syringae* pv. tomato DC3000 homolog in the suppression of PTI but not in the suppression of the ETI response (Li et al., 2005b; Cunnac et al., 2009).

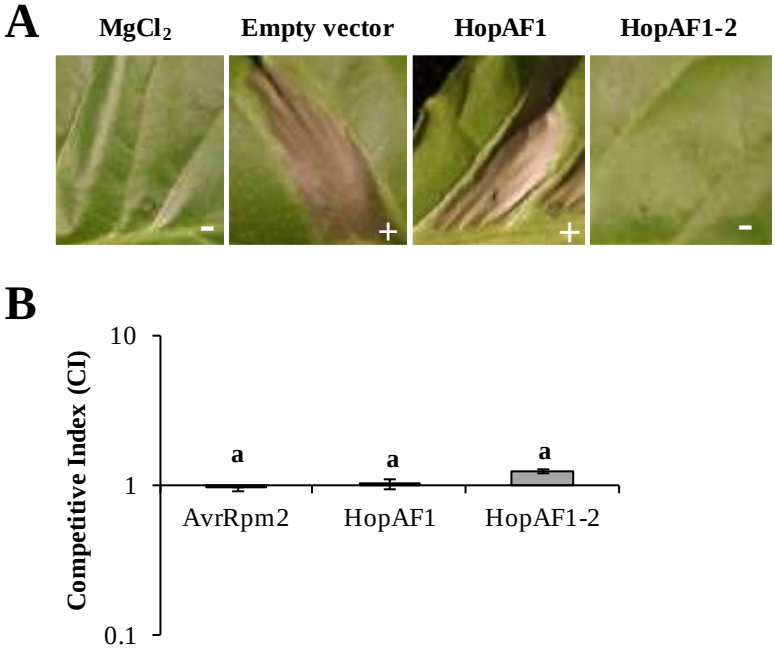

Figure 7. Delivery of HopAF1 and HopAF1-2 by functionally effectorless *P. syringae* pv. tomato DC3000D28E in *Nicotiana* leaves. **A**, Cell death response in *N. tabacum* var. Newdel leaves 48 h after inoculation with *P. syringae* pv. tomato DC3000D28E harboring pCPP5040 (empty vector) derivatives expressing HopAF1 or HopAF1-2. Bacterial cells were adjusted to 2 x 10^8 CFU/mL. Cell death response: +, positive; -, negative. Each experiment was repeated at least three times with similar results. **B**, Competition index (CI) between *P. syringae* pv. tomato DC3000D28E and the derivatives strains expressing HopAF1 or HopAF1-2 in *N. benthamiana*. CIs were normalized with respect to the CI obtained for DC3000D28E versus DC3000D28E expressing the empty vector. Values are the mean ± standard error of the mean of three replicates; bars topped with the same letter represent values that are not significantly different using one-way analysis of variance followed by post-hoc comparisons using the Tukey test.

To investigate the effect of HopAF1 and HopAF1-2 on the ability of DC3000D28E to colonize *N. benthamiana*, competition assays between the polymutant strain and its derivatives expressing these T3E were performed. Mixed inoculums (1:1) of DC3000D28E vs. each of the derivative strains were made and inoculated in *N. benthamiana* leaves. After 6 days, bacteria were recovered and viable cells were determined. None of the *P. savastanoi* T3E analyzed increased the competitiveness of the strain, which was reflected in a competitive index (CI) value of 1.02 and 1.24 for HopAF1/DC3000D28E and HopAF1-2/DC3000D28E, respectively (Fig. 7B).

Restoration of DC3000D28E growth by expression of NCPPB 3335 T3E has been only demonstrated to date for HopAO1, HopAO2 and HopBL1 (See chapter I and II).

Subcellular localization

In order to gain more information regarding the *in planta* behavior of HopAF1 and HopAF1-2, GFP fusions to C terminal full-length T3E were constructed in a Gateway vector (pGWB5) (Table 2) (See General Material and Methods). *N. benthamiana* leaves were infiltrated using *Agrobacterium*-mediated gene transfer transformed with these vectors. At 48 h after infiltration, abaxial epidermal cells were analyzed using scanning laser confocal microscopy. The results showed that the GFP fluorescence signal of HopAF1-GFP and HopAF1-2-GFP appears associated with the plasma membranes (Fig. 8).

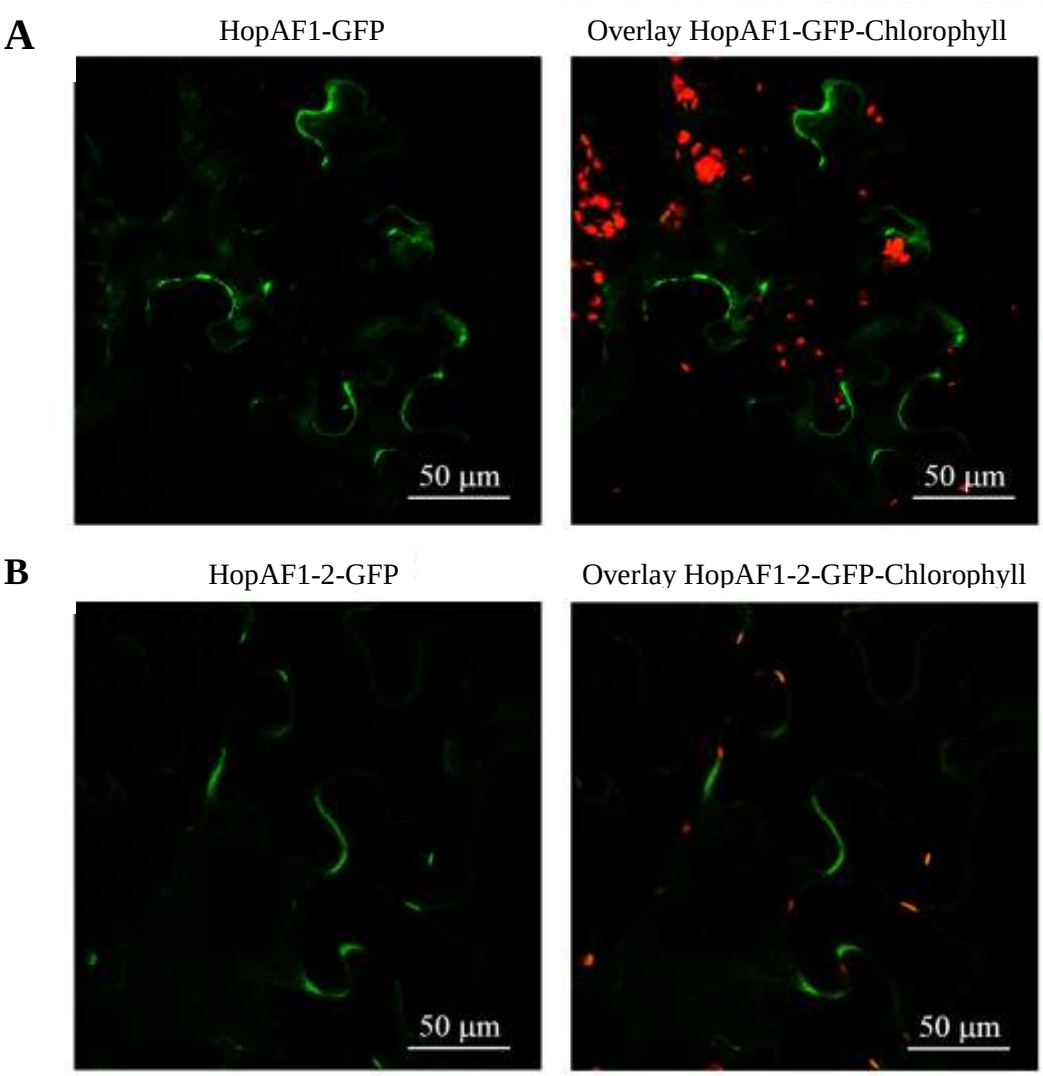

Figure 8. Subcellular localization of HopAF1 and HopAF1-2 in *Nicotiana benthamiana* leaves. **A**, Representative single-plane confocal images and overlap of GFP fluorescence and chlorophyll autofluorescence of HopAF1-GFP (A) or HopAF1-2 (**B**). In both cases fluorescence is observed in patches attached to the plasma membrane. Magnification bar: 50 µm.

Several *P. syringae* T3E have been shown to carry N-myristoylation signals required for their plasma membrane localization; i. e. AvrB, AvrPto, HopF2 and at least two alleles of the HopZ family (Nimchuk et al., 2000; Shan et al., 2000; Robert-Seilaniantz et al., 2006; Lewis et al., 2008). In agreement with the plasma membrane localization of NCPPB 3335 HopAF1 and HopAF2, a N-myristoylation site was found in these two proteins (Fig. 9) using NMT program (http://mendel.imp.ac.at/myristate/SUPLpredictor.htm).

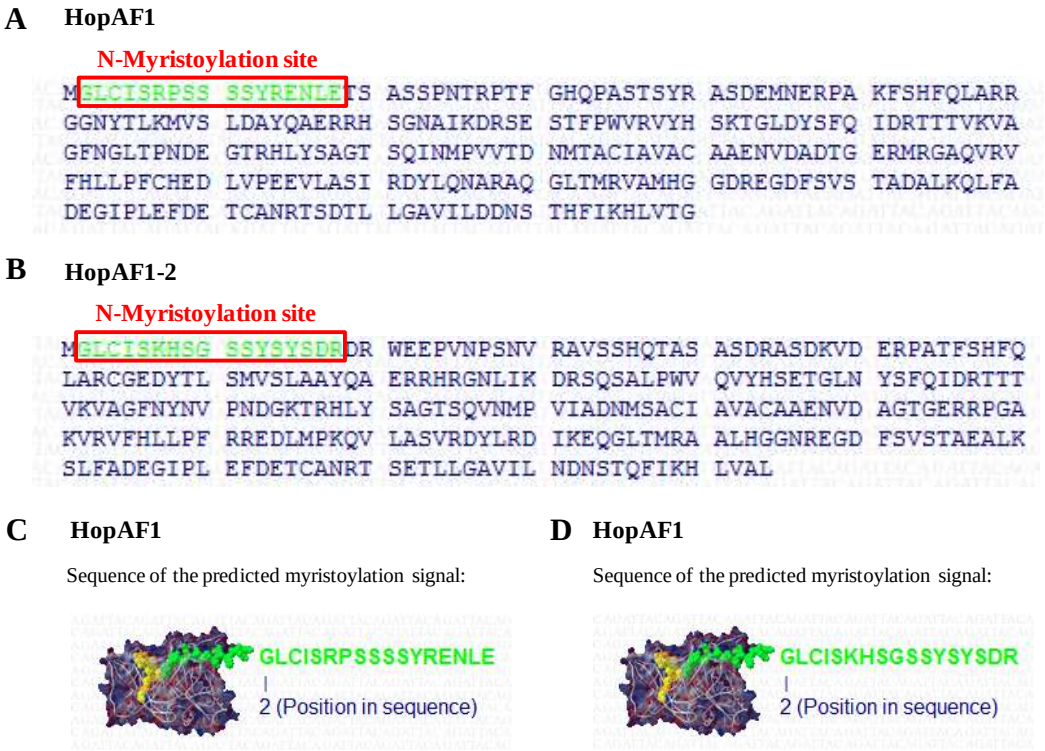

Figure 9. N-myristoylation site identified in *P. savastanoi* pv. savastanoi NCPPB 3335 HopAF1 and HopAF1-2. Myristoylation is the irreversible attachment of a myristoyl group to the N-terminal glycine residue of proteins that can act as a lipid anchor in biological membranes (Boutin, 1997). **A and B**, N-myristoylation site indicated in the amino acid sequences of HopAF1 and HopAF1-2, respectively, or in its tertiary structure (**C and D**).

Since the proper functioning of T3E is also likely to involve co-localization with targets within the host cell (Alfano and Collmer, 2004), it might be hypothesized that the interference with the plant defense machinery here observed for these two T3E could be produced during pathogen perception, which take place at the membrane level. This recognition even mediated by PRRs, includes the formation of protein complexes of different nature which initiate the transduction signal that triggers the defense response (Zipfel, 2008; Macho and Zipfel, 2014). Finding of the specific events interfered by these two NCPPB 3335 T3E will require further analysis regarding their biochemical function and their plant target during the interaction.

In summary, here we demonstrate that *P. savastanoi* pv. savastanoi NCPPB 3335 possess three copies of the *hopAF* gene family and validate HopAF1-2 and the plasmid-encoded HopAF1 as

T3E of the NCPPB 3335 T3SS secretome. Moreover, our results reveal that the *hopAF* gene family is widely distributed within *P. savastanoi* strains and other pathovars of the *P. syringae* complex. We demonstrate that HopAF1 and HopAF1-2, which localize in the host plasma membrane, differentially interfere with early responses associated with plant defense. Future experiments should focus in the construction of double and triple mutants affected in these T3E to further analyze their role in the virulence of *P. savastanoi* and related pathogens.

CONCLUDING REMARKS

Esta Tesis Doctoral se ha centrado en el análisis funcional de efectores (T3E) del sistema de secreción tipo III (T3SS) de *Pseudomonas savastanoi* pv. savastanoi NCPPB 3335, prestando mayor atención a los T3E de las familias HopAF y HopAO. Análisis bioinformáticos llevados a cabo sobre el borrador de la secuencia del genoma de NCPPB 3335 permitieron identificar 33 T3E candidatos (Rodriguez-Palenzuela et al., 2010; Ramos et al., 2012; Matas et al., 2014). Además, la secuenciación completa de los tres plásmidos nativos que posee NCPPB 3335, reveló que dos de estos T3E son de codificación plasmídica: HopAF1 (pPsv48A) y HopAO1 (pPsv48B) (Bardaji *et al.*, 2011). Durante el desarrollo de este trabajo, se demostró la translocación de 7 de los 33 T3E descritos hasta entonces en NCPPB 3335, de entre los cuales, 3 de ellos (HopBK1, HopBL1 y HopBL2) se propusieron como parte de dos nuevas familias de T3E incluidas en el pangenoma de *P. syringae* (Matas et al., 2014). Estos resultados, junto con la identificación de cajas Hrp-box en las regiones promotoras de los genes que los codifican y la demostración de su expresión dependiente del factor de transcripción HrpL (***Chapter I***), confirmaron que, de hecho, estos 3 efectores cumplen las características requeridas para la definición de T3E del complejo *Pseudomonas syringae* (Lindeberg et al., 2005).

En esta Tesis Doctoral, se han identificado dos nuevo T3E pertenecientes a las familias HopAO (HopAO2) y HopAF (probablemente similar a HopAF1). Además, se ha demostrado también la translocación y expresión dependiente de HrpL de 4 T3E pertenecientes a estas dos familias (*hopAF1*, *hopAF1-2*, *hopAO1* y *hopAO2*), pasando por tanto a formar parte del secretoma del T3SS de NCPPB 3335 comprobado experimentalmente (Tabla 1). Hasta la fecha, la demostración de la translocación de T3E del complejo *P. syringae* se había centrado principalmente en las 3 cepas cuyos genomas se habían secuenciado por completo: *P. syringae* patovar (pv.) tomato DC3000 (Buell et al., 2003), *P. syringae* pv. phaseolicola 1448A (Joardar et al., 2005) y *P. syringae* pv. syringae B728A (Feil et al., 2005). Todas estas cepas, se han aislado de plantas herbáceas. Los resultados incluidos en esta Tesis Doctoral, convierten a NCPPB 3335 en la cuarta cepa del complejo *P. syringae* cuyo secretoma del T3SS incluye un mayor número de T3E demostrados, y en la primera cepa aislada de un hospedador leñoso. En la Figura 1 se muestra un esquema del efecto en planta de los efectores de las familias HopAF y HopAO de *P. savastanoi* pv. savastanoi NCPPB 3335.

Tabla 1. Efecto en planta de las familias de efectores HopAF y HopAO de *P. savastanoi* pv. savastanoi NCPPB 3335 (***Chapter II and III***).

Ensayos	Efectores[a]			
	HopAF1	**HopAF1-2**	**HopAO1**	**HopAO2**
Translocación *N. tabacum*	+	+	+	+
Expresión dependiente de HrpL	+	+	+	+
Producción de ROS	↓	↓	↓	↓
Deposición de calosa	↓	≈	↓	↓
HR en *N. tabacum*	↓	≈	↓	↓
Competitividad D28E	≈	≈	↑	↑
Localización Subcelular	Membrana	Membrana	Membrana/ Endosomas	Membrana/ Vesículas Golgi
Virulencia	≈	nd	↓	nd

[a]HR, respuesta hipersensible; D28E, *Pseudomonas syringae* pv. tomato DC3000 delecionada de 28 efectores; + o -, indican si el resultado obtenido fue positivo o negativo, respectivamente. Flecha hacia arriba o hacia abajo, indican si en comparación con el control positivo el resultado obtenido fue un aumento o reducción, respectivamente. ≈, aproximadamente igual que el control positivo. nd, no determinado.

De entre los T3E de *P. savastanoi* pv. savastanoi NCPPB 3335 cuya translocación había sido demostrada previamente (Matas et al., 2014), o se ha demostrado en este trabajo (***Chapters II*** y ***III***), se ha conseguido describir la actividad enzimática para uno de ellos: HopAO1 (actividad tirosina fosfatasa, ***Chapter II***). Además, HopBL1 y HopBL2, miembros de una nueva familia de T3E del pangenoma de *P. syringae* (Matas et al., 2014), presentan el dominio Pfam (http://pfam.xfam.org/) PF02902 correspondiente a la familia de proteasas Ulp1, cuya actividad proteasa de SUMO está siendo verificada actualmente en colaboración con el Dr. Ruiz Albert (Universidad de Málaga). Estos efectores, se encuentran emparentados filogenéticamente con el T3E de *Xanthomonas* XopD, cuya actividad proteasa de SUMO se ha demostrado previamente (Hotson et al., 2003; Kay and Bonas, 2009). Hasta la fecha, no se ha asociado esta actividad con ningún otro T3E del género *Pseudomonas*.

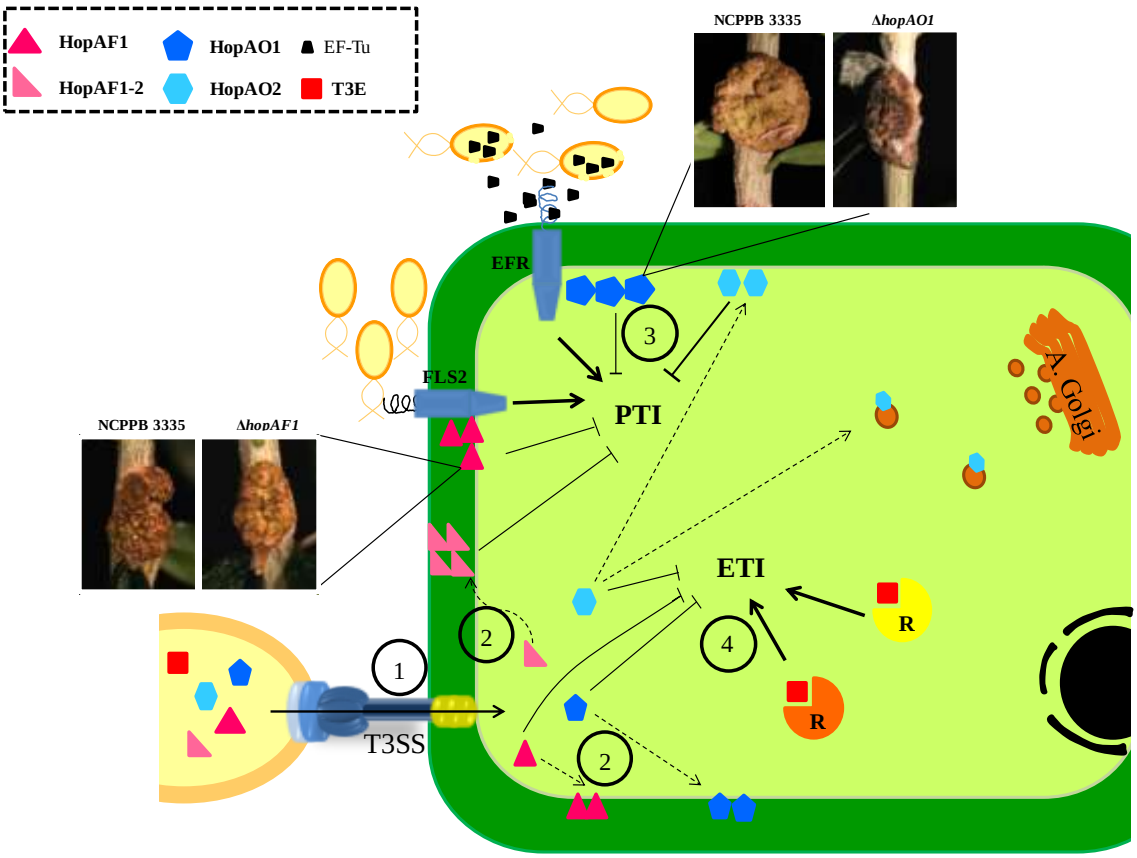

Figura 1. Representación gráfica del efecto en planta de los efectores de las familias HopAF y HopAO de *Pseudomonas savastanoi* pv. savastanoi NCPPB 3335. **(1)** NCPPB 3335 inyecta su batería de T3E al interior de la célula vegetal a través del T3SS. **(2)** Una vez en el interior de la célula, HopAO2 se localiza en vesículas del aparato de Golgi y los otros 4 T3E pertenecientes a estas dos familias se localizan en la membrana plasmática de la célula vegetal. **(3)** Estos 4 T3E, interfieren con las respuestas de defensa tempranas (PTI, *PAMP-triggered immunity*), y además, HopAF1-2, HopAO1 y HopAO2 también interfieren con la respuesta inducida por el reconocimiento de T3E (ETI, *Effector-triggered immunity*) **(4)**. En plantas de olivo, el mutante *hopAF1* induce la formación de tumores de un tamaño ligeramente inferior a los inducidos por la cepa silvestre, sin embargo, la deleción del gen *hopAO1*, no solo tiene como consecuencia la formación de tumores de menor tamaño, sino que además éstos muestran una necrosis temprana del tejido tumoral. HopAF1, triángulos fucsia; HopAF1-2, triángulos rosas; HopAO1, pentágonos azules, HopAO2, hexágonos celestes y; otros T3E, cuadrados rojos.

Durante las interacciones planta-patógeno, se desencadenan respuestas de defensa de la planta como consecuencia del reconocimiento de moléculas del patógeno muy conservadas en bacterias, como son la flagelina y el factor de elongación Tu (EF-Tu). Este reconocimiento, activa la respuesta de defensa temprana de la planta (PTI), lo que implica la producción de especies reactivas de oxígeno (ROS) y el engrosamiento de la pared celular mediante la deposición de calosa. Para evadir este tipo de respuestas, las bacterias patógenas poseen una batería de T3E que inyectan al interior de las células hospedadoras. Todos los T3E analizados en este trabajo interfieren con la formación de especies reactivas de oxígeno (ROS) y, salvo HopA1 y HopAF1, también reducen la deposición de calosa. Estos resultados indican que, en las condiciones

probadas, todos ellos son capaces de suprimir alguno de los marcadores asociados a la respuesta de defensa PTI (***Chapters I, II*** y ***III***). Además, HopAZ1, HopBL1, HopAO1 y HopAO2 también interfieren con la respuesta de defensa ETI (del inglés, *effector-triggered immunity*), producida como consecuencia del reconocimiento en el interior de la célula vegetal de los T3E o de su actividad. Resulta de gran interés que la expresión de HopBL2 y HopAO2 desde un derivado de *P. syringae* pv. tomato DC3000 carente de 28 T3E, DC3000D28E, induce un aumento de su competitividad. Este efecto, sugiere que ambos T3E, HopBL2, portador de un dominio proteasa de SUMO, y HopAO2, que posee un dominio con actividad tirosina fosfatasa, estarían involucrados en la supresión del reconocimiento inicial del patógeno (Figura 1).

En consonancia con la diana descrita para HopAO1 (Macho et al., 2014), su homólogo en NCPPB 3335 se localizó en este trabajo en la membrana de la célula vegetal, al igual que HopAO2, que también se localizó en vesículas del aparato de Golgi (***Chapter II***), dato que sugiere su participación en la interferencia con el tráfico de vesículas. Por otro lado, HopAF1 y HopAF1-2 también se localizaron en la membrana celular (***Chapter III***). Cabe mencionar, que recientemente hemos identificado en estos dos T3E una señal de N-miristoilación (Figura 8, ***Chapter III***), datos que apoyan su anclaje a la membrana.

Para profundizar en el conocimiento del papel de estos T3E en la interferencia de las respuestas de defensa de la planta, estudios futuros se dirigirán al análisis de sus actividades enzimáticas y de sus dianas en plantas de olivo, lo que abriría las puertas al análisis del papel de los T3E del complejo *P. syringae* durante la interacción con hospedadores leñosos.

CONCLUSIONES

1. El factor sigma alternativo HrpL activa la transcripción de los genes codificantes de los efectores del T3SS de *P. savastanoi* pv. savastanoi NCPPB 3335 HopAF1, HopAF1-2, HopAO1, HopAO2, HopBK1, HopBL1 y HopBL2.
2. Las proteínas HopAF1, HopAF1-2, HopAO1 y HopAO2 se translocan a través del T3SS de *P. savastanoi* pv. savastanoi NCPPB 3335. Estos resultados, unidos a su transcripción dependiente de HrpL, los revela como nuevos efectores del T3SS de este patógeno.
3. Los genes pertenecientes a las familias *hopAF* y *hopAO* están ampliamente distribuidos dentro del complejo *Pseudomonas syringae*; si bien, la filogenia de la familia HopAF separa a los efectores HopAF1 y HopAF1-2 de *P. savastanoi* pv. savastanoi NCPPB 3335 en dos ramas diferentes, agrupándose HopAF1 mayoritariamente con otras cepas patógenas de plantas leñosas.
4. *P. savastanoi* pv. savastanoi NCPPB 3335 codifica tres genes de la familia *hopAF* transcripcionalmente activos, dos de ellos codificantes del alelo *hopAF1*, localizados uno en el cromosoma y el otro en el plásmido pPsv48A, así como un alelo *hopAF1-2* de localización cromosómica.
5. Los efectores del T3SS AvrRpm2, HopBK1, HopBL1, HopBL2, HopAF1, HopAF1-2, HopAO1 y HopAO2, así como los efectores truncados HopAA1 y HopAZ1 interfieren con la respuesta de defensa primaria (PTI) de *Nicotiana tabacum*. HopAZ1, HopBL1, HopAF1-2, HopAO1 y HopAO2 también inhiben la inmunidad mediada por efectores (ETI) en este mismo hospedador.
6. La expresión de los efectores HopBL2 y HopAO2 en la cepa de *Pseudomonas syringae* pv. tomato DC3000 carente de 28 efectores (DC300028E) mejora su competitividad en *Nicotiana benthamiana*.
7. Los efectores HopAF1, HopAF1-2, HopAO1 y HopAO2 se localizan en la membrana plasmática de las células de *N. benthamiana*. Además, HopAO2 también se localiza en vesículas del aparato de Golgi de las células de este hospedador.
8. La expresión heteróloga de HopAO1 y HopAO2 en *Pseudomonas syringae* pv. phaseolicola 1448A induce un retraso en la aparición de síntomas asociados a la grasa de la judía.
9. El efector HopAO1 es una tirosina fosfatasa cuya actividad es dependiente del aminoácido Cys_{376} presente en el dominio catalítico.
10. La deleción del gen *hopAF1* del plásmido pPsv48A en *P. savastanoi* pv. savastanoi NCPPB 3335 tiene como consecuencia una ligera reducción en el tamaño de los tumores inducidos por este patógeno en plantas de olivo lignificadas, mientras que la deleción del gen *hopAO1* conlleva una clara disminución de la virulencia del mismo.

SUPPLEMENTARY MATERIAL

Table S1. *Pseudomonas savastanoi* and *P. syrinagae* strains sequenced to date**.**

Strains	References
Pseudomonas savastanoi	
pv. savastanoi NCPPB 3335	(Rodriguez-Palenzuela et al., 2010)
Pseudomonas syringae	
pv. tomato DC3000	(Buell et al., 2003)
pv. tomato T1	(Almeida et al., 2009)
pv. syringae B728A	(Feil et al., 2005)
pv. phaseolicola 1448A	(Joardar et al., 2005)
pv. tabaci ATCC 11528	(Baltrus et al., 2011)
pv. glycinea R4 (A29-2)	(Baltrus et al., 2011)
pv. mori MAFF 301020	(Baltrus et al., 2011)
pv. aesculi 0893_23	(Baltrus et al., 2011)
pv. lachrymans MAFF 301315	(Baltrus et al., 2011)
pv. lachrymans MAFF 302278PT	(Baltrus et al., 2011)
Cit 7	(Baltrus et al., 2011)
pv.aceris MAFF 302273PT	(Baltrus et al., 2011)
pv. pisi 1704B	(Baltrus et al., 2011)
pv.japonica MAFF 301072PT	(Baltrus et al., 2011)
pv. aptata DSM 50252	(Baltrus et al., 2011)
pv. maculicola ES4326	(Baltrus et al., 2011)
pv. morsprunorum MAFF 302280PT	(Baltrus et al., 2011)
pv. actinidiae MAFF 302091	(Baltrus et al., 2011)
pv. actinidiae J-35	(McCann et al., 2013)
pv. actinidiae NCPPB 3739	(Marcelletti et al., 2011)
pv. actinidiae NCPPB 3871	(Marcelletti et al., 2011)
pv. actinidiae CRA-FRU	(Marcelletti et al., 2011)
pv. aesculi 2250	(Green et al., 2010)
pv. aesculi NCPPB 3681	(Green et al., 2010)
pv. avellanae BP 631	(Scortichini et al., 2013)
pv. avellanae Ve013	(O'Brien et al., 2012)
pv. avellanae Ve037	(O'Brien et al., 2012)
pv. glycinea B076	(Qi et al., 2011)
pv. oryzae 1_6	(Reinhardt et al., 2009)
pv. phaseolicola 1644R	(Baltrus et al., 2012)
pv. syringae FF55	(Sohn et al., 2012)
pv. syringae 642	(Clarke et al., 2010)
pv. syringae B64	(Dudnik and Dudler, 2013)
pv. syringae B301D-R	(Dudnik and Dudler, 2014)

Table S2. Bacterial strains used in colony blot assays in chapter II and chapter III.

Strains	Relevant characteristics	Dot-blot hybridization[a]		References
		hopAF	*hopAO1/hop*	
P. savastanoi pv. nerii (Psn)				
2	Isolated from oleander	+	+/+	(Matas et al., 2009)
519	Isolated from oleander	+	-/+	(Surico et al., 1985)
P. savastanoi pv. savastanoi (Psv)				
NCPPB 3335	Isolated from olive	+	+/+	(Pérez-Martínez et al., 2007)
DAPP-PG722	Isolated from olive	+	+/+	(Hosni et al., 2011)
PVFi-1	Isolated from olive	+	+/+	(Iacobellis et al., 1993)
IMC-1	Isolated from olive	+	+/+	(Matas et al., 2009)
IMC-2	Isolated from olive	+	+	(Matas et al., 2009)
CFBP 1670	Isolated from olive	+	+/+	(Penyalver et al., 2000)
CFBP 2074	Isolated from olive	+	+/+	(Penyalver et al., 2000)
CFBP 71	Isolated from olive	+	+/+	(Penyalver et al., 2000)
IVIA 1628-3	Isolated from olive	+	+/+	(Penyalver et al., 2000)
IVIA 1629-1a	Isolated from olive	+	+/+	(Penyalver et al., 2000)
IVIA 1624-1b	Isolated from olive	+	+/+	(Penyalver et al., 2000)
IVIA 1637-a	Isolated from olive	+	+/+	(Penyalver et al., 2000)
IVIA 1637-B3	Isolated from olive	+	+/+	(Penyalver et al., 2000)
IVIA 1649-1	Isolated from olive	+	+/+	(Penyalver et al., 2000)
IVIA1651-C15	Isolated from olive	+	+/+	(Penyalver et al., 2000)
IVIA 1657-A2	Isolated from olive	+	+/+	(Penyalver et al., 2000)
IVIA 1657-B8	Isolated from olive	+	+/+	(Penyalver et al., 2000)
NCPPB 2327	Isolated from olive	+	+/+	(Penyalver et al., 2000)
NCPPB 1342	Isolated from olive	+	+/+	(Penyalver et al., 2000)
NCPPB 1344	Isolated from olive	+	+/+	(Penyalver et al., 2000)
NCPPB 1479	Isolated from olive	-	+/+	(Penyalver et al., 2000)
NCPPB 1506	Isolated from olive	+	+/+	(Penyalver et al., 2000)
NCPPB 64	Isolated from olive	+	+/+	(Penyalver et al., 2000)
CFBP 1020	Isolated from olive	-	-/+	(Penyalver et al., 2000)
P. savastanoi pv. savastanoi (Psv)				
C2.01	Isolated from olive	+	+/+	(Pérez-Martínez et al., 2007)
C2.01	Isolated from olive	+	+/+	(Pérez-Martínez et al., 2008)
B15.00	Isolated from olive	+	+/+	(Pérez-Martínez et al., 2008)
C1.01	Isolated from olive	+	+/+	(Pérez-Martínez et al., 2008)
C3.01	Isolated from olive	+	+/+	(Pérez-Martínez et al., 2008)
IVIA 2733-1a,	Isolated from olive	+	+/+	(Quesada et al., 2008)
IVIA 2743-3	Isolated from olive	+	+/+	(Quesada et al., 2008)
ITM317	Isolated from olive	+	+/+	(Surico et al., 1985)

Table S2. Bacterial strains used in colony blot assays in chapter II and chapter III (continued).

Strains	Relevant characteristics	Dot-blot hybridization[a]		References
		hopAF	*hopAO1/hopAO2*	
P. syringae pv. actinidiae (Pan)				
KACC10594	Isolated from kiwi	+	-/+	(Rees-George et al., 2010)
P. syringae pv. dendropanacis (Pde)				
CFBP 3226	Isolated from *Dendropanax*	+	`-/-	(Gardan et al., 1999)
P. syringae pv. eriobotryae (Per)				
CFBP 2343	Isolated from loquat	+	+/+	(Gardan et al., 1999)
P. syringae pv. glycinea (Pgy)				
NCPPB 1139	Isolated from *Glycine javanica*	+	-/-	(Yamamoto et al., 2000)
PG4180	Isolated from soybean	-	+/+	(Mitchell, 1978)
P. syringae pv. lachrymans (Pla)				
CFBP 1644	Isolated from cucumber	+	-/-	(Gardan et al., 1999)
P. syringae pv. maculicola (Pma)				
CFBP1657	Isolated from cauliflower	-	-/-	(Gardan et al., 1999)
P. syringae pv. morsprunorum (Pmp)				
CFBP 2116	Isolated from tart cherry	+	+/+	(Gardan et al., 1999)
P. syringae pv. myricae (Pmy)				
CFBP 2897	Isolated from red bayberry	+	+/+	(Gardan et al., 1999)
P. syringae pv. phaseolicola (Pph)				
1448A	Isolated from bean	+	-/-	(Teverson, 1991)
1449B	Isolated from *Lablab purpureus*	+	-/-	(Taylor et al., 1996)
P. syringae pv. sesami (Pse)				
CFBP 1671	Isolated from sesame	-	-/-	(Gardan et al., 1999)
P. syringae pv. syringae (Psy)				
B728a	Isolated from bean	+	-/-	(Loper and Lindow, 1987)
FF5	Isolated from ornamental pear	-	-/-	(Sundin and Bender, 1993)
P. syringae pv. tabaci (Pta)				
ATCC 11528	Isolated from tobacco	-	-/-	(Studholme et al., 2009)
P. syringae pv. tomato (Pto)				
PT23	Isolated from tomato	+	-/-	(Bender and Cooksey, 1986)
DC3000	Isolated from tomato	+	+/-	(Cuppels, 1986)
DC3000D28E	*ΔhopU1-hopF2* *ΔhopC1-hopH1*::FRT *ΔhopD1-hopR1*::FRT *ΔavrE-shcN* *ΔhopAA1-2-hopG1:*:FRT *ΔhopI1* *ΔhopAM1-1* *ΔhopAF1*::FRT *ΔavrPtoB* *ΔavrPto* *ΔhopK1* *ΔhopB1* *ΔhopE1* *ΔhopA1::*FRT *hopY1:*:FRT pDC3000A− pDC3000B− (Sp^R)	-	-/-	(Cunnac et al., 2011)

[a] + and - indicate the presence or absence, respectively, of strong hybridization signals with *hopAF*, *hopAO1* or *hopAO2* probes for each strain analyzed.

REFERENCES

Alfano, J.R., and Collmer, A. 1996. Bacterial pathogens in plants: life up against the wall. Plant Cell 8:1683-1698.

Alfano, J.R., and Collmer, A. 2004. Type III secretion system effector proteins: double agents in bacterial disease and plant defense. Annu Rev Phytopathol 42:385-414.

Alfano, J.R., Charkowski, A.O., Deng, W.L., Badel, J.L., Petnicki-Ocwieja, T., van Dijk, K., and Collmer, A. 2000. The Pseudomonas syringae Hrp pathogenicity island has a tripartite mosaic structure composed of a cluster of type III secretion genes bounded by exchangeable effector and conserved effector loci that contribute to parasitic fitness and pathogenicity in plants. Proc Natl Acad Sci U S A 97:4856-4861.

Almeida, N.F., Yan, S., Lindeberg, M., Studholme, D.J., Schneider, D.J., Condon, B., Liu, H.J., Viana, C.J., Warren, A., Evans, C., Kemen, E., MacLean, D., Angot, A., Martin, G.B., Jones, J.D., Collmer, A., Setubal, J.C., and Vinatzer, B.A. 2009. A draft genome sequence of *Pseudomonas syringae* pv. *tomato* T1 reveals a Type III effector repertoire significantly divergent from that of *Pseudomonas syringae* pv. *tomato* DC3000. Mol Plant Microbe Interact 22:52-62.

Aragón, I.M., Pérez-Martínez, I., Moreno-Pérez, A., Cerezo, M., and Ramos, C. 2014. New insights into the role of indole-3-acetic acid in the virulence of Pseudomonas savastanoi pv. savastanoi. FEMS Microbiology Letters:n/a-n/a.

Arnold, D.L., Pitman, A., and Jackson, R.W. 2003. Pathogenicity and other genomic islands in plant pathogenic bacteria. Mol Plant Pathol 4:407-420.

Arnold, R., Brandmaier, S., Kleine, F., Tischler, P., Heinz, E., Behrens, S., Niinikoski, A., Mewes, H.W., Horn, M., and Rattei, T. 2009. Sequence-based prediction of type III secreted proteins. PLoS Pathog 5:e1000376.

Baltrus, D.A., Nishimura, M.T., Dougherty, K.M., Biswas, S., Mukhtar, M.S., Vicente, J., Holub, E.B., and Dangl, J.L. 2012. The molecular basis of host specialization in bean pathovars of Pseudomonas syringae. Mol Plant Microbe Interact 25:877-888.

Baltrus, D.A., Nishimura, M.T., Romanchuk, A., Chang, J.H., Mukhtar, M.S., Cherkis, K., Roach, J., Grant, S.R., Jones, C.D., and Dangl, J.L. 2011. Dynamic evolution of pathogenicity revealed by sequencing and comparative genomics of 19 *Pseudomonas syringae* isolates. PLoS Pathog 7:e1002132.

Bardaji, L., Perez-Martinez, I., Rodriguez-Moreno, L., Rodriguez-Palenzuela, P., Sundin, G.W., Ramos, C., and Murillo, J. 2011. Sequence and role in virulence of the three plasmid complement of the model tumor-inducing bacterium *Pseudomonas savastanoi* pv. savastanoi NCPPB 3335. PLoS One 6:e25705.

Bender, C.L., and Cooksey, D.A. 1986. Indigenous plasmids in *Pseudomonas syringae* pv. tomato: conjugative transfer and role in copper resistance. J Bacteriol 165:534–541.

Bender, C.L., Alarcon-Chaidez, F., and Gross, D.C. 1999. Pseudomonas syringae phytotoxins: mode of action, regulation, and biosynthesis by peptide and polyketide synthetases. Microbiol Mol Biol Rev 63:266-292.

Block, A., and Alfano, J.R. 2011. Plant targets for Pseudomonas syringae type III effectors: virulence targets or guarded decoys? Curr Opin Microbiol 14:39-46.

Boller, T., and Felix, G. 2009. A renaissance of elicitors: perception of microbe-associated molecular patterns and danger signals by pattern-recognition receptors. Annu Rev Plant Biol 60:379-406.

Boutin, J.A. 1997. Myristoylation. Cell Signal 9:15-35.

Bradbury, J.F. 1986. Guide to Plant Pathogenic Bacteria. London, UK: CAB International Mycological Institute:154–177.

Bretz, J., Losada, L., Lisboa, K., and Hutcheson, S.W. 2002. Lon protease functions as a negative regulator of type III protein secretion in Pseudomonas syringae. Mol Microbiol 45:397-409.

Bretz, J.R., Mock, N.M., Charity, J.C., Zeyad, S., Baker, C.J., and Hutcheson, S.W. 2003. A translocated protein tyrosine phosphatase of *Pseudomonas syringae* pv. tomato DC3000 modulates plant defence response to infection. Mol Microbiol 49:389-400.

Buell, C.R., Joardar, V., Lindeberg, M., Selengut, J., Paulsen, I.T., Gwinn, M.L., Dodson, R.J., Deboy, R.T., Durkin, A.S., Kolonay, J.F., Madupu, R., Daugherty, S., Brinkac, L., Beanan, M.J., Haft, D.H., Nelson, W.C., Davidsen, T., Zafar, N., Zhou, L., Liu, J., Yuan, Q., Khouri, H., Fedorova, N., Tran, B., Russell, D., Berry, K., Utterback, T., Van Aken, S.E., Feldblyum, T.V., D'Ascenzo, M., Deng, W.L., Ramos, A.R., Alfano, J.R., Cartinhour, S., Chatterjee, A.K., Delaney, T.P., Lazarowitz, S.G., Martin, G.B., Schneider, D.J., Tang, X., Bender, C.L., White, O., Fraser, C.M., and Collmer, A. 2003. The complete genome sequence of the *Arabidopsis* and tomato pathogen *Pseudomonas syringae* pv. *tomato* DC3000. Proc Natl Acad Sci U S A 100:10181-10186.

Bullock, W.O., Fernandez, J.M., and Short, J.M. 1987. Xl1-Blue: a high efficiency plasmid transforming *recA Escherichia coli* strain with beta-galactosidase selection. Biotechniques 5:376-378.

Buttner, D., and He, S.Y. 2009. Type III protein secretion in plant pathogenic bacteria. Plant Physiol 150:1656-1664.

Caponero, A., Contesini, A.M., and Iacobellis, N.S. 1995. Population diversity of *Pseudomonas syringae* subsp. *savastanoi* on olive and oleander. Plant Pathol 44:848-855.

Casper-Lindley, C., Dahlbeck, D., Clark, E.T., and Staskawicz, B.J. 2002. Direct biochemical evidence for type III secretion-dependent translocation of the AvrBs2 effector protein into plant cells. Proc Natl Acad Sci U S A 99:8336-8341.

Clarke, C.R., Cai, R., Studholme, D.J., Guttman, D.S., and Vinatzer, B.A. 2010. *Pseudomonas syringae* strains naturally lacking the classical P. syringae hrp/hrc Locus are common leaf colonizers equipped with an atypical type III secretion system. Mol Plant Microbe Interact 23:198-210.

Collmer, A., Badel, J.L., Charkowski, A.O., Deng, W.L., Fouts, D.E., Ramos, A.R., Rehm, A.H., Anderson, D.M., Schneewind, O., van Dijk, K., and Alfano, J.R. 2000. *Pseudomonas syringae* Hrp type III secretion system and effector proteins. Proc Natl Acad Sci U S A 97:8770-8777.

Comai, L., and Kosuge, T. 1980. Involvement of plasmid deoxyribonucleic acid in indoleacetic acid synthesis in *Pseudomonas savastanoi*. J Bacteriol 143:950-957.

Comai, L., and Kosuge, T. 1982. Cloning characterization of *iaaM*, a virulence determinant of *Pseudomonas savastanoi*. J Bacteriol 149:40-46.

Cornelis, G.R., and Van Gijsegem, F. 2000. Assembly and function of type III secretory systems. Annu Rev Microbiol 54:735-774.

Cunnac, S., Lindeberg, M., and Collmer, A. 2009. *Pseudomonas syringae* type III secretion system effectors: repertoires in search of functions. Curr Opin Microbiol 12:53-60.

Cunnac, S., Occhialini, A., Barberis, P., Boucher, C., and Genin, S. 2004. Inventory and functional analysis of the large Hrp regulon in Ralstonia solanacearum: identification of novel effector proteins translocated to plant host cells through the type III secretion system. Mol Microbiol 53:115-128.

Cunnac, S., Chakravarthy, S., Kvitko, B.H., Russell, A.B., Martin, G.B., and Collmer, A. 2011. Genetic disassembly and combinatorial reassembly identify a minimal functional repertoire of type III effectors in *Pseudomonas syringae*. Proc Natl Acad Sci U S A 108:2975-2980.

Cuppels, D.A. 1986. Generation and Characterization of Tn5 Insertion Mutations in *Pseudomonas syringae* pv. tomato. Appl Environ Microbiol 51:323-327.

Chang, J.H., Urbach, J.M., Law, T.F., Arnold, L.W., Hu, A., Gombar, S., Grant, S.R., Ausubel, F.M., and Dangl, J.L. 2005. A high-throughput, near-saturating screen for type III effector genes from *Pseudomonas syringae*. Proceedings of the National Academy of Sciences of the United States of America 102:2549-2554.

Chisholm, S.T., Coaker, G., Day, B., and Staskawicz, B.J. 2006. Host-microbe interactions: shaping the evolution of the plant immune response. Cell 124:803-814.

Choi, K.H., Kumar, A., and Schweizer, H.P. 2006. A 10-min method for preparation of highly electrocompetent *Pseudomonas aeruginosa* cells: application for DNA fragment transfer between chromosomes and plasmid transformation. J Microbiol Methods 64:391-397.

Dangl, J.L., and Jones, J.D.G. 2001. Plant pathogens and integrated defence responses to infection. Nature 411:826-833.

Dijk, K.v., Tam, V.C., Records, A.R., Petnicki-Ocwieja, T., and Alfano, J.R. 2002. The ShcA protein is a molecular chaperone that assists in the secretion of the HopPsyA effector from the type III (Hrp) protein secretion system of *Pseudomonas syringae*. Mol Microbiol 44:1469-1481.

Dudnik, A., and Dudler, R. 2013. Non contiguous-finished genome sequence of *Pseudomonas syringae* pathovar syringae strain B64 isolated from wheat. Stand Genomic Sci 8:420-429.

Dudnik, A., and Dudler, R. 2014. Genome and Transcriptome Sequences of *Pseudomonas syringae* pv. syringae B301D-R. Genome Announc 2.

Eltlbany, N., Prokscha, Z.Z., Castaneda-Ojeda, M.P., Krogerrecklenfort, E., Heuer, H., Wohanka, W., Ramos, C., and Smalla, K. 2012. A new bacterial disease on Mandevilla sanderi caused by *Pseudomonas savastanoi* -- lessons learned for bacterial diversity studies. Appl Environ Microbiol 78:8492-8497.

Espinosa, A., Guo, M., Tam, V.C., Fu, Z.Q., and Alfano, J.R. 2003. The *Pseudomonas syringae* type III-secreted protein HopPtoD2 possesses protein tyrosine phosphatase activity and suppresses programmed cell death in plants. Mol Microbiol 49:377-387.

Fatmi, M.C., Iacobellis, N.S., Mansfield, J., Murillo, J., Schaad, N.W., and Ullrich, M. 2008.
Pseudomonas syringae Pathovars and Related Pathogens - Identification, Epidemiology and Genomics

Fauman, E.B., and Saper, M.A. 1996. Structure and function of the protein tyrosine phosphatases. Trends Biochem Sci 21:413-417.

Feil, H., Feil, W.S., Chain, P., Larimer, F., DiBartolo, G., Copeland, A., Lykidis, A., Trong, S., Nolan, M., Goltsman, E., Thiel, J., Malfatti, S., Loper, J.E., Lapidus, A., Detter, J.C., Land, M., Richardson, P.M., Kyrpides, N.C., Ivanova, N., and Lindow, S.E. 2005. Comparison of the complete genome sequences of *Pseudomonas syringae* pv. syringae B728a and pv. tomato DC3000. Proc Natl Acad Sci U S A 102:11064-11069.

Feng, F., and Zhou, J.M. 2012. Plant-bacterial pathogen interactions mediated by type III effectors. Curr Opin Plant Biol 15:469-476.

Fouts, D.E., Abramovitch, R.B., Alfano, J.R., Baldo, A.M., Buell, C.R., Cartinhour, S., Chatterjee, A.K., D'Ascenzo, M., Gwinn, M.L., Lazarowitz, S.G., Lin, N.C., Martin, G.B., Rehm, A.H., Schneider, D.J., Van Dijk, K., Tang, X., and Collmer, A. 2002. Genomewide identification of *Pseudomonas syringae* pv. tomato DC3000 promoters controlled by the HrpL alternative sigma factor. Proc Natl Acad Sci U S A 99:2275-2280.

Galan, J.E., and Collmer, A. 1999. Type III secretion machines: bacterial devices for protein delivery into host cells. Science 284:1322-1328.

Galletti, R., Denoux, C., Gambetta, S., Dewdney, J., Ausubel, F.M., De Lorenzo, G., and Ferrari, S. 2008. The AtrbohD-mediated oxidative burst elicited by oligogalacturonides in Arabidopsis is dispensable for the activation of defense responses effective against Botrytis cinerea. Plant Physiol 148:1695-1706.

Gardan, L., Bollet, C., Abu Ghorrah, M., Grimont, F., and Grimont, P.A.D. 1992. DNA relatedness among the pathovar strains of *Pseudomonas syringae* subsp. *savastanoi* Janse (1982) and proposal of *Pseudomonas savastanoi* sp. nov. Int J Syst Bacteriol 42:606-612.

Gardan, L., Shafik, H., Belouin, S., Broch, R., Grimont, F., and Grimont, P.A.D. 1999. DNA relatedness among the pathovars of *Pseudomonas syringae* and description of *Pseudomonas tremae* sp. nov. and *Pseudomonas cannabina* sp. nov. (*ex* Sutic and Dowson 1959). Int J Syst Bacteriol 49:469-478.

Gohre, V., and Robatzek, S. 2008. Breaking the barriers: microbial effector molecules subvert plant immunity. Annu Rev Phytopathol 46:189-215.

Gómez-Gómez, L., and Boller, T. 2000. FLS2: An LRR Receptor–like Kinase Involved in the Perception of the Bacterial Elicitor Flagellin in Arabidopsis. Molecular Cell 5:1003-1011.

Grant, S.R., Fisher, E.J., Chang, J.H., Mole, B.M., and Dangl, J.L. 2006. Subterfuge and manipulation: Type III effector proteins of phytopathogenic bacteria. Annu Rev Microbiol 60:425-449.

Green, S., Studholme, D.J., Laue, B.E., Dorati, F., Lovell, H., Arnold, D., Cottrell, J.E., Bridgett, S., Blaxter, M., Huitema, E., Thwaites, R., Sharp, P.M., Jackson, R.W., and Kamoun, S. 2010. Comparative Genome Analysis Provides Insights into the Evolution and Adaptation of *Pseudomonas syringae* pv. aesculi on *Aesculus hippocastanum*. PLoS One 5:e10224.

Grimm, C., Aufsatz, W., and Panopoulos, N.J. 1995. The hrpRS locus of Pseudomonas syringae pv. phaseolicola constitutes a complex regulatory unit. Mol Microbiol 15:155-165.

Guo, M., Tian, F., Wamboldt, Y., and Alfano, J.R. 2009. The majority of the type III effector inventory of *Pseudomonas syringae* pv. tomato DC3000 can suppress plant immunity. Mol Plant Microbe Interact 22:1069-1080.

Hanahan, D. 1983. Studies on transformation of *Escherichia coli* with plasmids. J Mol Biol 166:557-580.

Hauck, P., Thilmony, R., and He, S.Y. 2003. A *Pseudomonas syringae* type III effector suppresses cell wall-based extracellular defense in susceptible Arabidopsis plants. Proc Natl Acad Sci U S A 100:8577-8582.

Heath, M.C. 2000. Nonhost resistance and nonspecific plant defenses. Current Opinion in Plant Biology 3:315-319.

Hendrickson, E.L., Guevera, P., and Ausubel, F.M. 2000a. The alternative sigma factor RpoN is required for hrp activity in *Pseudomonas syringae* pv. maculicola and acts at the level of *hrpL* transcription. J Bacteriol 182:3508-3516.

Hendrickson, E.L., Guevera, P., Penaloza-Vazquez, A., Shao, J., Bender, C., and Ausubel, F.M. 2000b. Virulence of the phytopathogen *Pseudomonas syringae* pv. maculicola is *rpoN* dependent. J Bacteriol 182:3498-3507.

Henry, E., Yadeta, K.A., and Coaker, G. 2013. Recognition of bacterial plant pathogens: local, systemic and transgenerational immunity. New Phytologist 199:908-915.

Holmes, D.S., and Quigley, M. 1981. A rapid boiling method for the preparation of bacterial plasmids. Anal Biochem 114:193-197.

Hosni, T., Moretti, C., Devescovi, G., Suárez-Moreno, Z.R., Fatmi, M.B., Guarnaccia, C., Pongor, S., Onofri, A., Buonaurio, R., and Venturi, V. 2011. Sharing of quorum-sensing signals and role of interspecies communities in a bacterial plant disease. ISME J 5:1857-1870.

Hotson, A., Chosed, R., Shu, H., Orth, K., and Mudgett, M.B. 2003. *Xanthomonas* type III effector XopD targets SUMO-conjugated proteins in planta. Mol Microbiol 50:377-389.

Hutcheson, S.W., Bretz, J., Sussan, T., Jin, S., and Pak, K. 2001. Enhancer-binding proteins HrpR and HrpS interact to regulate hrp-encoded type III protein secretion in *Pseudomonas syringae* strains. J Bacteriol 183:5589-5598.

Hutzinger, O., and Kosuge, T., eds. 1968. 3-Indoleacetyl-r-L-lysine, a new conjugate of 3-indoleacetic acid produced by *Pseudomonas savastanoi*. The Runge Press Ltd., Ottawa, Canada.

Huynh, T.V., Dahlbeck, D., and Staskawicz, B.J. 1989. Bacterial blight of soybean: regulation of a pathogen gene determining host cultivar specificity. Science 245:1374-1377.

Iacobellis, N.S., Sisto, A., and Surico, G. 1993. Occurrence of unusual strains of *Pseudomonas syringae* subsp. savastanoi on olive in central Italy. Bull. OEPP. 23:429–435.

Iacobellis, N.S., Sisto, A., Surico, G., Evidente, A., and DiMaio, E. 1994. Pathogenicity of *Pseudomonas syringae* subsp. *savastanoi* mutants defective in phytohormone production. J Phytopathol 140:238–248.

Inoue, H., Nojima, H., and Okayama, H. 1990. High efficiency transformation of *Escherichia coli* with plasmids. Gene 96:23-28.

Jackson, R.W., Athanassopoulos, E., Tsiamis, G., Mansfield, J.W., Sesma, A., Arnold, D.L., Gibbon, M.J., Murillo, J., Taylor, J.D., and Vivian, A. 1999. Identification of a pathogenicity island, which contains genes for virulence and avirulence, on a large native plasmid in the bean pathogen *Pseudomonas syringae* pathovar phaseolicola. Proc Natl Acad Sci U S A 96:10875-10880.

Jamir, Y., Guo, M., Oh, H.S., Petnicki-Ocwieja, T., Chen, S., Tang, X., Dickman, M.B., Collmer, A., and Alfano, J.R. 2004. Identification of *Pseudomonas syringae* type III effectors that can suppress programmed cell death in plants and yeast. Plant J 37:554-565.

Janjusevic, R., Abramovitch, R.B., Martin, G.B., and Stebbins, C.E. 2006. A bacterial inhibitor of host programmed cell death defenses is an E3 ubiquitin ligase. Science 311:222-226.

Joardar, V., Lindeberg, M., Jackson, R.W., Selengut, J., Dodson, R., Brinkac, L.M., Daugherty, S.C., DeBoy, R., Durkin, A.S., Giglio, M.G., Madupu, R., Nelson, W.C., Rosovitz, M.J., Sullivan, S., Crabtree, J., Creasy, T., Davidsen, T., Haft, D.H., Zafar, N., Zhou, L.W., Halpin, R., Holley, T., Khouri, H., Feldblyum, T., White, O., Fraser, C.M., Chatterjee, A.K., Cartinhour, S., Schneider, D.J., Mansfield, J., Collmer, A., and Buell, C.R. 2005. Whole-genome sequence analysis of *Pseudomonas syringae* pv. phaseolicola 1448A reveals divergence among pathovars in genes involved in virulence and transposition. J Bacteriol 187:6488-6498.

Jones, J.D., and Dangl, J.L. 2006. The plant immune system. Nature 444:323-329.

Kamoun, S., Huitema, E., and Vleeshouwers, V.G. 1999. Resistance to oomycetes: a general role for the hypersensitive response? Trends Plant Sci 4:196-200.

Kay, S., and Bonas, U. 2009. How *Xanthomonas* type III effectors manipulate the host plant. Current Opinion in Microbiology 12:37-43.

Kennelly, M.M., Cazorla, F.M., de Vicente, A., Ramos, C., and Sundin, G.W. 2007. *Pseudomonas syringae* diseases of fruit trees. Progress toward understanding and control. Plant Disease 91:4-17.

Kim, J.F., and Alfano, J.R. 2002. Pathogenicity islands and virulence plasmids of bacterial plant pathogens. Curr Top Microbiol Immunol 264:127-147.

Kim, J.G., Taylor, K.W., and Mudgett, M.B. 2011. Comparative analysis of the XopD type III secretion (T3S) effector family in plant pathogenic bacteria. Mol Plant Pathol 12:715-730.

Kim, J.G., Stork, W., and Mudgett, M.B. 2013. *Xanthomonas* type III effector XopD desumoylates tomato transcription factor SlERF4 to suppress ethylene responses and promote pathogen growth. Cell Host Microbe 13:143-154.

King, E.O., Ward, M.K., and Raney, D.E. 1954. Two simple media for the demonstration of pyocyanin and fluorescin. J Lab Clin Med 44:301-307.

Kosuge, T., Heskett, M.G., and Wilson, E.E. 1966. Microbial synthesis and degradation of indole-3-acetic acid. I. The conversion of L-tryptophan to indole-3-acetamide by an enzyme system from *Pseudomonas savastanoi*. J Biol Chem 241:3738-3744.

Kvitko, B.H., Ramos, A.R., Morello, J.E., Oh, H.S., and Collmer, A. 2007. Identification of harpins in *Pseudomonas syringae* pv. tomato DC3000, which are functionally similar to HrpK1 in promoting translocation of type III secretion system effectors. J Bacteriol 189:8059-8072.

Kvitko, B.H., Park, D.H., Velasquez, A.C., Wei, C.F., Russell, A.B., Martin, G.B., Schneider, D.J., and Collmer, A. 2009. Deletions in the repertoire of *Pseudomonas syringae* pv. tomato DC3000 type III secretion effector genes reveal functional overlap among effectors. PLoS Pathog 5:e1000388.

Labes, M., Puhler, A., and Simon, R. 1990. A new family of RSF1010-derived expression and lac-fusion broad-host-range vectors for gram-negative bacteria. Gene 89:37-46.

Larkin, M.A., Blackshields, G., Brown, N.P., Chenna, R., McGettigan, P.A., McWilliam, H., Valentin, F., Wallace, I.M., Wilm, A., Lopez, R., Thompson, J.D., Gibson, T.J., and Higgins, D.G. 2007. Clustal W and Clustal X version 2.0. Bioinformatics 23:2947-2948.

Lavermicocca, P., Lonigro, S.L., Valerio, F., Evidente, A., and Visconti, A. 2002. Reduction of olive knot disease by a bacteriocin from *Pseudomonas syringae* pv. ciccaronei. Appl Environ Microbiol 68:1403-1407.

Lavermicocca, P., Valerio, F., Evidente, A., Lazzaroni, S., Corsetti, A., and Gobbetti, M. 2000. Purification and characterization of novel antifungal compounds from the sourdough *Lactobacillus plantarum* strain 21B. Appl Environ Microbiol 66:4084-4090.

Lewis, J.D., Abada, W., Ma, W., Guttman, D.S., and Desveaux, D. 2008. The HopZ family of Pseudomonas syringae type III effectors require myristoylation for virulence and avirulence functions in Arabidopsis thaliana. J Bacteriol 190:2880-2891.

Li, C., Potuschak, T., Colon-Carmona, A., Gutierrez, R.A., and Doerner, P. 2005a. *Arabidopsis* TCP20 links regulation of growth and cell division control pathways. Proc Natl Acad Sci U S A 102:12978-12983.

Li, X., Lin, H., Zhang, W., Zou, Y., Zhang, J., Tang, X., and Zhou, J.M. 2005b. Flagellin induces innate immunity in nonhost interactions that is suppressed by Pseudomonas syringae effectors. Proc Natl Acad Sci U S A 102:12990-12995.

Lindeberg, M., Cunnac, S., and Collmer, A. 2012. *Pseudomonas syringae* type III effector repertoires: last words in endless arguments. Trends Microbiol 20:199-208.

Lindeberg, M., Stavrinides, J., Chang, J.H., Alfano, J.R., Collmer, A., Dangl, J.L., Greenberg, J.T., Mansfield, J.W., and Guttman, D.S. 2005. Proposed guidelines for a unified nomenclature and phylogenetic analysis of type III Hop effector proteins in the plant pathogen *Pseudomonas syringae*. Mol Plant Microbe Interact 18:275-282.

Livak, K.J., and Schmittgen, T.D. 2001. Analysis of relative gene expression data using real-time quantitative PCR and the 2−ΔΔCT method. Methods 25:402-408.

Loper, J.E., and Lindow, S.E. 1987. Lack of evidence for in situ fluorescent pigment production by *Pseudomonas syringae* pv. syringae on bean leaf surfaces. Phytopathology 77:1449-1454.

Lopez-Solanilla, E., Bronstein, P.A., Schneider, A.R., and Collmer, A. 2004. HopPtoN is a *Pseudomonas syringae* Hrp (type III secretion system) cysteine protease effector that suppresses pathogen-induced necrosis associated with both compatible and incompatible plant interactions. Mol Microbiol 54:353-365.

Ma, W., Dong, F.F., Stavrinides, J., and Guttman, D.S. 2006. Type III effector diversification via both pathoadaptation and horizontal transfer in response to a coevolutionary arms race. PLoS Genet 2:e209.

Macdonald, E.M., Powell, G.K., Regier, D.A., Glass, N.L., Roberto, F., Kosuge, T., and Morris, R.O. 1986. Secretion of Zeatin, Ribosylzeatin, and Ribosyl-1" -Methylzeatin by *Pseudomonas savastanoi*: Plasmid-Coded Cytokinin Biosynthesis. Plant Physiol 82:742-747.

Macho, A.P., and Zipfel, C. 2014. Plant PRRs and the Activation of Innate Immune Signaling. Molecular Cell 54:263-272.

Macho, A.P., Schwessinger, B., Ntoukakis, V., Brutus, A., Segonzac, C., Roy, S., Kadota, Y., Oh, M.H., Sklenar, J., Derbyshire, P., Lozano-Duran, R., Malinovsky, F.G., Monaghan, J., Menke, F.L., Huber, S.C., He, S.Y., and Zipfel, C. 2014. A Bacterial Tyrosine Phosphatase Inhibits Plant Pattern Recognition Receptor Activation. Science.

Magie, A.R. 1963. Physiological factors involved in tumor production by the oleander knot pathogen, *Pseudomonas savastanoi*. Ph.D. Thesis. University of California.

Maldonado-González, M.M., Prieto, P., Ramos, C., and Mercado-Blanco, J. 2013. From the root to the stem: interaction between the biocontrol root endophyte Pseudomonas fluorescens PICF7 and the pathogen *Pseudomonas savastanoi* NCPPB 3335 in olive knots. Microbial Biotechnology 6:275-287.

Mansfield, J., Genin, S., Magori, S., Citovsky, V., Sriariyanum, M., Ronald, P., Dow, M., Verdier, V., Beer, S.V., Machado, M.A., Toth, I., Salmond, G., and Foster, G.D. 2012. Top 10 plant pathogenic bacteria in molecular plant pathology. Mol Plant Pathol 13:614-629.

Marcelletti, S., Ferrante, P., Petriccione, M., Firrao, G., and Scortichini, M. 2011. *Pseudomonas syringae* pv. actinidiae draft genomes comparison reveal strain-specific features involved in adaptation and virulence to Actinidia species. PLoS One 6:e27297.

Matas, I.M., Lambertsen, L., Rodriguez-Moreno, L., and Ramos, C. 2012. Identification of novel virulence genes and metabolic pathways required for full fitness of *Pseudomonas savastanoi* pv. savastanoi in olive (Olea europaea) knots. New Phytol.

Matas, I.M., Pérez-Martínez, I., Quesada, J.M., Rodríguez-Herva, J.J., Penyalver, R., and Ramos, C. 2009. *Pseudomonas savastanoi* pv. savastanoi contains two *iaaL* paralogs, one of

which exhibits a variable number of a trinucleotide (TAC) tandem repeat. Appl Environ Microbiol 75:1030-1035.

Matas, I.M., Castañeda-Ojeda, M.P., Aragón, I.M., Antúnez-Lamas, M., Murillo, J., Rodríguez-Palenzuela, P., López-Solanilla, E., and Ramos, C. 2014. Translocation and Functional Analysis of *Pseudomonas savastanoi* pv. savastanoi NCPPB 3335 Type III Secretion System Effectors Reveals Two Novel Effector Families of the Pseudomonas syringae Complex. Mol Plant Microbe Interact 27:424-436.

Maurer-Stroh, S., Eisenhaber, B., and Eisenhaber, F. 2002. N-terminal N-myristoylation of proteins: refinement of the sequence motif and its taxon-specific differences. Journal of Molecular Biology 317:523-540.

McCann, H.C., Rikkerink, E.H.A., Bertels, F., Fiers, M., Lu, A., Rees-George, J., Andersen, M.T., Gleave, A.P., Haubold, B., Wohlers, M.W., Guttman, D.S., Wang, P.W., Straub, C., Vanneste, J., Rainey, P.B., and Templeton, M.D. 2013. Genomic Analysis of the Kiwifruit Pathogen *Pseudomonas syringae* pv. actinidiae Provides Insight into the Origins of an Emergent Plant Disease. PLoS Pathog 9:e1003503.

Mercado-Blanco, J., Rodríguez-Jurado, D., Hervás, A., and Jiménez-Díaz, R.M. 2004. Suppression of *Verticillium* wilt in olive planting stocks by root-associated fluorescent *Pseudomonas* spp. . Biol Control 30: 474–486.

Miller, J.H. 1972. Experiments in molecular genetics. Cold Spring Harbor Laboratory, Cold Spring Harbor, NY.

Mitchell, R.E. 1978. Halo blight of beans: Toxin production by several *Pseudomonas phaseolicola* isolates. Physiol. Plant Pathol. 13:37-49.

Morris, R.O. 1986. Genes specifying auxin and cytoquinin biosynthesis in phytopathogens. Ann Rev Plant Physiol 37:509-538.

Mudgett, M.B. 2005. New insights to the function of phytopathogenic bacterial type III effectors in plants. Annu Rev Plant Biol 56:509-531.

Munkvold, K.R., Russell, A.B., Kvitko, B.H., and Collmer, A. 2009. *Pseudomonas syringae* pv. tomato DC3000 type III effector HopAA1-1 functions redundantly with chlorosis-promoting factor PSPTO4723 to produce bacterial speck lesions in host tomato. Mol Plant Microbe Interact 22:1341-1355.

Mysore, K.S., and Ryu, C.-M. 2004. Nonhost resistance: how much do we know? Trends in Plant Science 9:97-104.

Nelson, B.K., Cai, X., and Nebenfuhr, A. 2007. A multicolored set of in vivo organelle markers for co-localization studies in Arabidopsis and other plants. Plant J 51:1126-1136.

Nicaise, V., Roux, M., and Zipfel, C. 2009. Recent advances in PAMP-triggered immunity against bacteria: pattern recognition receptors watch over and raise the alarm. Plant Physiol 150:1638-1647.

Nimchuk, Z., Marois, E., Kjemtrup, S., Leister, R.T., Katagiri, F., and Dangl, J.L. 2000. Eukaryotic fatty acylation drives plasma membrane targeting and enhances function of several type III effector proteins from *Pseudomonas syringae*. Cell 101:353-363.

Nishimura, M.T., Stein, M., Hou, B.H., Vogel, J.P., Edwards, H., and Somerville, S.C. 2003. Loss of a callose synthase results in salicylic acid-dependent disease resistance. Science 301:969-972.

Nomura, K., DebRoy, S., Lee, Y.H., Pumplin, N., Jones, J., and He, S.Y. 2006. A Bacterial Virulence Protein Suppresses Host Innate Immunity to Cause Plant Disease. Science 313:220-223.

Nomura, K., Mecey, C., Lee, Y.N., Imboden, L.A., Chang, J.H., and He, S.Y. 2011. Effector-triggered immunity blocks pathogen degradation of an immunity-associated vesicle traffic regulator in *Arabidopsis*. Proc Natl Acad Sci U S A 108:10774-10779.

Nürnberger, T., and Lipka, V. 2005. Non-host resistance in plants: new insights into an old phenomenon. Mol Plant Pathol 6:335-345.

O'Brien, H.E., Thakur, S., Gong, Y., Fung, P., Zhang, J., Yuan, L., Wang, P.W., Yong, C., Scortichini, M., and Guttman, D.S. 2012. Extensive remodeling of the Pseudomonas

syringae pv. avellanae type III secretome associated with two independent host shifts onto hazelnut. BMC Microbiol 12:141.

Oh, H.S., Park, D.H., and Collmer, A. 2010. Components of the *Pseudomonas syringae* type III secretion system can suppress and may elicit plant innate immunity. Mol Plant Microbe Interact 23:727-739.

Ortiz-Martín, I., Thwaites, R., Mansfield, J.W., and Beuzón, C.R. 2010b. Negative Regulation of the Hrp Type III Secretion System in Pseudomonas syringae pv. phaseolicola. Mol Plant Microbe Interact 23:682-701.

Ortíz-Martín, I., Thwaites, R., Macho, A.P., Mansfield, J.W., and Beuzón, C.R. 2010a. Positive regulation of the Hrp type III secretion system in *Pseudomonas syringae* pv. phaseolicola. Mol Plant Microbe Interact 23:665-681.

Palmer, B.R., and Marinus, M.G. 1994. The dam and dcm strains of *Escherichia coli*--a review. Gene 143:1-12.

Parkinson, N., Bryant, R., Bew, J., and Elphinstone, J. 2011. Rapid phylogenetic identification of members of the *Pseudomonas syringae* species complex using the rpoD locus. Plant Pathol 60:338-344.

Penyalver, R., García, A., Ferrer, A., Bertolini, E., and López, M.M. 2000. Detection of *Pseudomonas savastanoi* pv. savastanoi in olive plants by enrichment and PCR. Appl Environ Microbiol 66:2673-2677.

Perez-Martinez, I., Rodriguez-Moreno, L., Matas, I.M., and Ramos, C. 2007. Strain selection and improvement of gene transfer for genetic manipulation of *Pseudomonas savastanoi* isolated from olive knots. Res Microbiol 158:60-69.

Perez-Martinez, I., Zhao, Y., Murillo, J., Sundin, G.W., and Ramos, C. 2008. Global genomic analysis of *Pseudomonas savastanoi* pv. savastanoi plasmids. J Bacteriol 190:625-635.

Perez-Martinez, I., Rodriguez-Moreno, L., Lambertsen, L., Matas, I.M., Murillo, J., Tegli, S., Jimenez, A.J., and Ramos, C. 2010. Fate of a *Pseudomonas savastanoi* pv. savastanoi type III secretion system mutant in olive plants (Olea europaea L.). Appl Environ Microbiol 76:3611-3619.

Pérez-Martinez, I., Rodriguez-Moreno, L., Lambertsen, L., Matas, I.M., Murillo, J., Tegli, S., Jimenez, A.J., and Ramos, C. 2010. Fate of a *Pseudomonas savastanoi* pv. savastanoi type III secretion system mutant in olive plants (Olea europaea L.). Appl Environ Microbiol 76:3611-3619.

Pérez-Martínez, I., Rodríguez-Moreno, L., Matas, I.M., and Ramos, C. 2007. Strain selection and improvement of gene transfer for genetic manipulation of *Pseudomonas savastanoi* isolated from olive knots. Res Microbiol 158:60-69.

Pérez-Martínez, I., Zhao, Y., Murillo, J., Sundin, G.W., and Ramos, C. 2008. Global genomic analysis of *Pseudomonas savastanoi* pv. savastanoi plasmids. J Bacteriol 190:625-635.

Pfaffl, M.W. 2001. A new mathematical model for relative quantification in real-time RT-PCR. Nucleic Acids Res 29:e45.

Powell, G.K., and Morris, R.O. 1986. Nucleotide sequence and expression of a *Pseudomonas savastanoi* cytokinin biosynthetic gene: homology with *Agrobacterium tumefaciens tmr* and *tzs* loci. Nucleic Acids Res 14:2555-2565.

Preston, G., Deng, W.L., Huang, H.C., and Collmer, A. 1998. Negative regulation of hrp genes in Pseudomonas syringae by HrpV. J Bacteriol 180:4532-4537.

Qi, M., Wang, D., Bradley, C.A., and Zhao, Y. 2011. Genome Sequence Analyses of *Pseudomonas savastanoi* pv. glycinea and Subtractive Hybridization-Based Comparative Genomics with Nine *Pseudomonads*. PLoS One 6:e16451.

Quesada, J.M., García, A., Bertolini, E., López, M.M., and Penyalver, R. 2007. Recovery of *Pseudomonas savastanoi* pv. savastanoi from symptomless shoots of naturally infected olive trees. Int Microbiol 10:77-84.

Quesada, J.M., Pérez-Martínez, I., Ramos, C., López, M.M., and Penyalver, R. 2008. IS53: an insertion element for molecular typing of *Pseudomonas savastanoi* pv. savastanoi. Res Microbiol 159:207-215.

Quesada, J.M., Penyalver, R., Pérez-Panadés, J., Salcedopa, C.I., Carbonell, E.A., and López, M.M. 2009. Dissemination of *Pseudomonas savastanoi* pv. savastanoi populations and subsequent appearance of olive knot disease. Plant Pathogen 59:262-269.

Quesada, J.M., Penyalver, R., Pérez-Panadés, J., Salcedo, C.I., Carbonell, E.A., and López, M.M. 2010. Comparison of chemical treatments for reducing epiphytic *Pseudomonas savastanoi* pv. savastanoi populations and for improving subsequent control of olive knot disease. Crop Protection 29:1413-1420.

Ramos, C., Matas, I.M., Bardaji, L., Aragon, I.M., and Murillo, J. 2012. *Pseudomonas savastanoi* pv. savastanoi: some like it knot. Mol Plant Pathol 13:998-1009.

Rees-George, J., Vanneste, J.L., Cornish, D.A., Pushparajah, I.P.S., Yu, J., Templeton, M.D., and Everett, K.R. 2010. Detection of *Pseudomonas syringae* pv. actinidiae using polymerase chain reaction (PCR) primers based on the 16S–23S rDNA intertranscribed spacer region and comparison with PCR primers based on other gene regions. Plant Pathology 59:453-464.

Reinhardt, J.A., Baltrus, D.A., Nishimura, M.T., Jeck, W.R., Jones, C.D., and Dangl, J.L. 2009. *De novo* assembly using low-coverage short read sequence data from the rice pathogen Pseudomonas syringae pv. oryzae. Genome Res 19:294-305.

Robert-Seilaniantz, A., Shan, L., Zhou, J.M., and Tang, X. 2006. The *Pseudomonas syringae* pv. tomato DC3000 type III effector HopF2 has a putative myristoylation site required for its avirulence and virulence functions. Mol Plant Microbe Interact 19:130-138.

Rodríguez-Herva, J.J., González-Melendi, P., Cuartas-Lanza, R., Antúnez-Lamas, M., Río-Alvarez, I., Li, Z., López-Torrejón, G., Díaz, I., del Pozo, J.C., Chakravarthy, S., Collmer, A., Rodríguez-Palenzuela, P., and López-Solanilla, E. 2012. A bacterial cysteine protease effector protein interferes with photosynthesis to suppress plant innate immune responses. Cell Microbiol 14:669-681.

Rodríguez-Moreno, L., Jiménez, A.J., and Ramos, C. 2009. Endopathogenic lifestyle of *Pseudomonas savastanoi* pv. savastanoi in olive knots. Microbial Biotechnology 2:476-488.

Rodriguez-Palenzuela, P., Matas, I.M., Murillo, J., Lopez-Solanilla, E., Bardaji, L., Perez-Martinez, I., Rodriguez-Moskera, M.E., Penyalver, R., Lopez, M.M., Quesada, J.M., Biehl, B.S., Perna, N.T., Glasner, J.D., Cabot, E.L., Neeno-Eckwall, E., and Ramos, C. 2010. Annotation and overview of the *Pseudomonas savastanoi* pv. savastanoi NCPPB 3335 draft genome reveals the virulence gene complement of a tumour-inducing pathogen of woody hosts. Environ Microbiol 12:1604-1620.

Rohmer, L., Kjemtrup, S., Marchesini, P., and Dangl, J.L. 2003. Nucleotide sequence, functional characterization and evolution of pFKN, a virulence plasmid in *Pseudomonas syringae* pathovar maculicola. Mol Microbiol 47:1545-1562.

Roine, E., Saarinen, J., Kalkkinen, N., and Romantschuk, M. 1997. Purified HrpA of *Pseudomonas syringae* pv. tomato DC3000 reassembles into pili. FEBS Lett 417:168-172.

Rotenberg, D., Thompson, T.S., German, T.L., and Willis, D.K. 2006. Methods for effective real-time RT-PCR analysis of virus-induced gene silencing. J Virol Methods 138:49-59.

Saitou, N., and Nei, M. 1987. The neighbor-joining method: a new method for reconstructing phylogenetic trees. Mol Biol Evol 4:406-425.

Sambrook, J., and Russell, D. 2001. Molecular cloning: a laboratory manual. Cold Spring Harbor Laboratory Press, Cold Spring Harbor New York, USA.

Sarkar, S.F., and Guttman, D.S. 2004. Evolution of the core genome of *Pseudomonas syringae*, a highly clonal, endemic plant pathogen. Appl Environ Microbiol 70:1999-2012.

Sarkar, S.F., Gordon, J.S., Martin, G.B., and Guttman, D.S. 2006. Comparative genomics of host-specific virulence in *Pseudomonas syringae*. Genetics 174:1041-1056.

Savastano, L. 1886. Le maladies de l'olivier et la tuberculose en particuler. Comp Rend Acad Agr France:103-114.

Scortichini, M., and Marcelletti, S. 2014. Definition of plant pathogenic *Pseudomonas* genomospecies of the *Pseudomonas syringae* complex through a phylogenomic approach. Phytopathology.

Scortichini, M., Rossi, M.P., and Salerno, M. 2004. Relationship of genetic structure of *Pseudomonas savastanoi* pv. savastanoi populations from Italian olive trees and patterns of host genetic diversity. Plant Pathol 53:491-497.

Scortichini, M., Marcelletti, S., Ferrante, P., and Firrao, G. 2013. A Genomic Redefinition of *Pseudomonas avellanae* species. PLoS One 8:e75794.

Schechter, L.M., Roberts, K.A., Jamir, Y., Alfano, J.R., and Collmer, A. 2004. Pseudomonas syringae type III secretion system targeting signals and novel effectors studied with a Cya translocation reporter. J Bacteriol 186:543-555.

Schroth, M.N., Osgood, J.W., and Miller, T.D. 1973. Quantitative assessment of effect of olive knot disease on olive yield and quality. Phytopathology 63:1064-1065.

Schwessinger, B., and Zipfel, C. 2008. News from the frontline: recent insights into PAMP-triggered immunity in plants. Curr Opin Plant Biol 11:389-395.

Segonzac, C., Feike, D., Gimenez-Ibanez, S., Hann, D.R., Zipfel, C., and Rathjen, J.P. 2011. Hierarchy and roles of pathogen-associated molecular pattern-induced responses in Nicotiana benthamiana. Plant Physiol 156:687-699.

Shan, L., Thara, V.K., Martin, G.B., Zhou, J.M., and Tang, X. 2000. The *Pseudomonas* AvrPto protein is differentially recognized by tomato and tobacco and is localized to the plant plasma membrane. Plant Cell 12:2323-2338.

Sisto, A., Cipriani, M.G., and Morea, M. 2004. Knot formation caused by *Pseudomonas syringae* subsp. *savastanoi* on Olive plants is *hrp*-dependent. Phytopathology 94:484-489.

Sisto, A., Morea, M., Zaccaro, F., Palumbo, G., and Iacobellis, N.S. 1999. Isolation and characterization of *Pseudomonas syringae* subsp. *savastanoi* mutants defective in hypersensitive response elicitation and pathogenicity. J Phytopathol 147:321-330.

Smidt, M., and Kosuge, T. 1978. The role of indole-3-acetic acid accumulation by alphamethyl tryptophan-resistant mutants of *Pseudomonas savastanoi* in gall formation in oleander. Physiol Plant Pathol 13:203-214.

Smith, E.F. 1920. An introduction to bacterial diseases of plants. in: S.W. Company, ed., Philadelphia.

Sohn, K.H., Jones, J.D., and Studholme, D.J. 2012. Draft genome sequence of *Pseudomonas syringae* pathovar syringae strain FF5, causal agent of stem tip dieback disease on ornamental pear. J Bacteriol 194:3733-3734.

Sokurenko, E.V., Hasty, D.L., and Dykhuizen, D.E. 1999. Pathoadaptive mutations: gene loss and variation in bacterial pathogens. Trends in Microbiology 7:191-195.

Sokurenko, E.V., Feldgarden, M., Trintchina, E., Weissman, S.J., Avagyan, S., Chattopadhyay, S., Johnson, J.R., and Dykhuizen, D.E. 2004. Selection Footprint in the FimH Adhesin Shows Pathoadaptive Niche Differentiation in *Escherichia coli*. Mol Biol Evol 21:1373-1383.

Sory, M.P., and Cornelis, G.R. 1994. Translocation of a hybrid YopE-adenylate cyclase from *Yersinia enterocolitica* into HeLa cells. Mol Microbiol 14:583-594.

Studholme, D.J., Ibanez, S.G., MacLean, D., Dangl, J.L., Chang, J.H., and Rathjen, J.P. 2009. A draft genome sequence and functional screen reveals the repertoire of type III secreted proteins of *Pseudomonas syringae* pv. tabaci 11528. BMC Genomics 10:395.

Surico, G. 1977. Histological observations on olive knots. Phytopathol. Mediterr. 16:109-125.

Surico, G., Iacobellis, N.S., and Sisto, A. 1985. Studies on the role of indole-3-acetic acid and cytokinins in the formation of knots on olive and oleander plants by *Pseudomonas syringae* pv. savastanoi. Physiol Plant Pathol 26:309-320.

Tamura, K., Peterson, D., Peterson, N., Stecher, G., Nei, M., and Kumar, S. 2011. MEGA5: molecular evolutionary genetics analysis using maximum likelihood, evolutionary distance, and maximum parsimony methods. Mol Biol Evol 28:2731-2739.

Tao, Y., Xie, Z., Chen, W., Glazebrook, J., Chang, H.S., Han, B., Zhu, T., Zou, G., and Katagiri, F. 2003. Quantitative nature of *Arabidopsis* responses during compatible and

incompatible interactions with the bacterial pathogen *Pseudomonas syringae*. Plant Cell 15:317-330.

Taylor, J.D., Teverson, D.M., Allen, D.J., and Pastor-Corrales, M.A. 1996. Identification and origin of races of *Pseudomonas syringae* pv. phaseolicola from Africa and other bean growing areas. Plant Pathology 45:469-478.

Teverson, D.M. (1991). Genetics of pathogenicity and resistance in the halo-blight disease of beans in Africa (Birmingham, UK: University of Birmingham).

Thordal-Christensen, H. 2003. Fresh insights into processes of nonhost resistance. Current Opinion in Plant Biology 6:351-357.

Thordal-Christensen, H., Zhang, Z., Wei, Y., and Collinge, D.B. 1997. Subcellular localization of H_2O_2 in plants, H_2O_2 accumulation in papillae and hypersensitive response during barley-powdery mildew interaction. Plant J 11:1187-1194.

Underwood, W., Zhang, S., and He, S.Y. 2007. The *Pseudomonas syringae* type III effector tyrosine phosphatase HopAO1 suppresses innate immunity in *Arabidopsis thaliana*. Plant J 52:658-672.

Van der Biezen, E.A., and Jones, J.D. 1998. Plant disease-resistance proteins and the gene-for-gene concept. Trends Biochem Sci 23:454-456.

Vargas, P., Felipe, A., Michan, C., and Gallegos, M.T. 2011. Induction of *Pseudomonas syringae* pv. tomato DC3000 MexAB-OprM multidrug efflux pump by flavonoids is mediated by the repressor PmeR. Mol Plant Microbe Interact 24:1207-1219.

Varvaro, L., and Surico, G. 1978. Comportamento di diverse cultivars di olivo Olea europaea L. alla inoculazione artificiale con *Pseudomonas savastanoi* (EF Smith) Stevens. Phytopathol Mediterr 17:174-178.

Vervliet, G., Holsters, M., Teuchy, H., Van Montagu, M., and Schell, J. 1975. Characterization of different plaque-forming and defective temperate phages in *Agrobacterium*. J Gen Virol 26:33-48.

Wei, W., Plovanich-Jones, A., Deng, W.L., Jin, Q.L., Collmer, A., Huang, H.C., and He, S.Y. 2000. The gene coding for the Hrp pilus structural protein is required for type III secretion of Hrp and Avr proteins in *Pseudomonas syringae* pv. tomato. Proc Natl Acad Sci U S A 97:2247-2252.

Weigel, D., and Glazebrook, J. 2002. How to transform Arabidopsis. In Arabidopsis: A Laboratory Manual. Cold Spring Harbor, NY, USA:119–140.

Westcott, C., and Horst, R.K. 1990. Westcott´s plant disease handbook. Van Nostrand Reinhold, New York:p. 953.

Wilson, E.E., and Magie, A.R. 1964. Systemic invasion of the host plant by the tumor inducing bacterium, *Pseudomonas savastanoi*. Phytopathology 54:577–579.

Xiao, Y., and Hutcheson, S.W. 1994. A single promoter sequence recognized by a newly identified alternate sigma factor directs expression of pathogenicity and host range determinants in *Pseudomonas syringae*. J Bacteriol 176:3089-3091.

Xiao, Y., Heu, S., Yi, J., Lu, Y., and Hutcheson, S.W. 1994. Identification of a putative alternate sigma factor and characterization of a multicomponent regulatory cascade controlling the expression of *Pseudomonas syringae* pv. syringae Pss61 hrp and hrmA genes. J. Bacteriol. 176:1025-1036.

Yamamoto, S., Kasai, H., Arnold, D.L., Jackson, R.W., Vivian, A., and Harayama, S. 2000. Phylogeny of the genus *Pseudomonas:* intrageneric structure reconstructed from the nucleotide sequences of *gyrB* and *rpoD* genes. Microbiology 146 (Pt 10):2385-2394.

Young, J.M. 2004. Olive knot and its pathogens. Australas Plant Pathol 33:33-39.

Young, J.M. 2010. Taxonomy of *Pseudomonas syringae*. J Plant Pathol 92:S1.5-S.14.

Young, J.M., Dye, D.W., Bradbury, J.F., Panagopoulos, C.G., and Robbs, C.F. 1978. A proposed nomenclature and classification for plant pathogenic bacteria. New Zeal J Agr Res 21:153-177.

Zadeh, H.R., Khavazi, K., Asgharzadeh, A., Hosseinimazinani, M., and de Mot, R. 2008. Biocontrol of *Pseudomonas savastanoi*, causative agent of olive knot disease: antagonistic

potential of non-pathogenic rhizosphere isolates of fluorescent *Pseudomonas*. Comm Appl Biol Sci Ghent University 73:199-203.

Zipfel, C. 2008. Pattern-recognition receptors in plant innate immunity. Curr Opin Immunol 20:10-16.

Zipfel, C., Robatzek, S., Navarro, L., Oakeley, E.J., Jones, J.D., Felix, G., and Boller, T. 2004. Bacterial disease resistance in Arabidopsis through flagellin perception. Nature 428:764-767.

Zipfel, C., Kunze, G., Chinchilla, D., Caniard, A., Jones, J.D.G., Boller, T., and Felix, G. 2006. Perception of the Bacterial PAMP EF-Tu by the Receptor EFR Restricts *Agrobacterium*-Mediated Transformation. Cell 125:749-760.

Zumaquero, A., Macho, A.P., Rufian, J.S., and Beuzon, C.R. 2010. Analysis of the role of the type III effector inventory of *Pseudomonas syringae* pv. phaseolicola 1448a in interaction with the plant. J Bacteriol 192:4474-4488.

ANEXO I:

OTRAS PUBLICACIONES

AEM
Journals.ASM.org

A New Bacterial Disease on *Mandevilla sanderi*, Caused by *Pseudomonas savastanoi*: Lessons Learned for Bacterial Diversity Studies

Namis Eltlbany,[a,d] Zsa-Zsa Prokscha,[a] M. Pilar Castañeda-Ojeda,[c] Ellen Krögerrecklenfort,[a] Holger Heuer,[a] Walter Wohanka,[b] Cayo Ramos,[c] and Kornelia Smalla[a]

Julius Kühn-Institut, Federal Research Centre for Cultivated Plants (JKI), Institute for Epidemiology and Pathogen Diagnostics, Braunschweig, Germany[a]; Geisenheim Research Center, Section Phytomedicine, Geisenheim, Germany[b]; Área de Genética, Facultad de Ciencias, Universidad de Málaga, Instituto de Hortofruticultura Subtropical y Mediterránea La Mayora (IHSM-UMA-CSIC), Málaga (Spain)[c]; and Suez Canal University, Faculty of Agriculture, Ismailia, Egypt[d]

Leaf lesions of *Mandevilla sanderi* were shown to be caused by *Pseudomonas savastanoi*. While BOX fingerprints were similar for *P. savastanoi* isolates from different host plants, plasmid restriction patterns and sequencing of plasmid-located pathogenicity determinants revealed that *Mandevilla* isolates contained similar plasmids distinct from those of other isolates. A *repA*-based detection method was established.

The ornamental plant *Mandevilla sanderi* (*Dipladenia sanderi* [family *Apocynaceae*]) originating from Middle and South America has become increasingly popular over the last decade, mainly because of its copiously formed red flowers. In 2008, breeders of *Mandevilla sanderi* observed for the first time large necrotic lesions with chlorotic rings on leaves and tumor formation on stems (see Fig. 1). The potential causal agents isolated from the lesions of leaves of diseased plant material were identified initially by metabolic profiling (Biolog) as *Pseudomonas savastanoi* pv. glycinea or pv. nerii (data not shown), pathogens of soybean (*Glycine max*) or oleander (*Nerium oleander*), respectively. Stem and leaf inoculation of healthy *Mandevilla* plants with these isolates indeed caused identical symptoms (Fig. 1) fulfilling Koch's postulates.

P. savastanoi strains are *Gammaproteobacteria* which belong to genomospecies 2 of the *Pseudomonas syringae* complex (6). Although the species *P. savastanoi* was established only in 1992 (5), sequencing of the genomes and plasmids of several *P. syringae* and *P. savastanoi* isolates reinforced the discussion about the taxonomic affiliation of *P. savastanoi*, as the core genome is clearly shared by *P. syringae* and *P. savastanoi* strains. Several pathovars of *P. savastanoi* infect woody plants, e.g., *P. savastanoi* pv. savastanoi is known as an important pathogen of olive trees (*Olea europaea*) in the Mediterranean area (11). The typical symptoms of olive knot disease, the formation of tumors in the stem and branches, were already described by Theobrast Eresos in the year 300 BC. The disease causes massive yield losses, and breeding for tolerant varieties is the main strategy to overcome the commercial losses due to infections with *P. savastanoi* pv. savastanoi (16).

Taking into account that other known hosts of *P. savastanoi* are oleander (*Nerium oleander*) and privet (*Liguster vulgare*), leaf and stem inoculations of *Mandevilla* isolates were done also on oleander, olive, and privet plants. Nine weeks after inoculation, the response patterns of oleander were similar to those observed on *Mandevilla* plants; however, while no symptoms were observed for olive plants, privet plants displayed only leaf lesions (unpublished results). Thus, it was hypothesized that the most likely causal agent of the novel bacterial disease of *Mandevilla sanderi* might have originated from infested oleander plantations in the vicinity of the *Mandevilla sanderi*-producing companies in the South of France. To shed light on this hypothesis, *P. savastanoi* isolates from *Mandevilla sanderi* were characterized and compared to isolates originating from olive trees, oleander, jasmine, and privet (information on the isolates, their hosts, and their geographical origins is given in Table 1). Furthermore, we aimed to use this information as the basis for the development of a sensitive and specific method for detection and differentiation of the pathogen from total community DNA.

The *P. savastanoi* strains used in this study (Table 1) were grown on King's B agar medium (12) and incubated for 2 days at 28°C. A loop full of freshly grown bacterial cell material was resuspended in 1 ml 0.85% NaCl and harvested by centrifugation for 5 min at 13,000 × *g*. This step was repeated once or twice to reduce slime due to copiously produced exopolysaccharides. Crude cell lysates were obtained using a Qiagen genomic DNA extraction kit (Qiagen, Hilden, Germany). The DNA was extracted using a silica-based kit (silica bead DNA extraction kit; Thermo Scientific, St. Leon-Rot, Germany). Checking the DNA yields under conditions of UV transillumination after agarose gel electrophoresis and ethidium bromide staining revealed the presence of both plasmid and genomic DNA in all strains. 16S rRNA gene fragments amplified from genomic DNA (Table 2) and digested with AluI-MspI or Hin6I-Bsh1236I displayed identical restriction patterns for the subset of strains (Ph1 to Ph16) tested, suggesting that these strains most likely belong to the same species (data not shown). The 16S rRNA gene sequence was determined for all seven isolates from *Mandevilla sanderi* (Ph2 to Ph8). All sequences were 100% identical. Phylogenetic analysis of partial nucleotide sequences (1,413 bp) of the 16S rRNA gene showed that the isolates from *Mandevilla sanderi* clustered together with those of *P. savastanoi* pv. nerii (ITM313) and *P. savastanoi* pv. savastanoi (NCPPB 3335)(Fig. 2).

Received 29 June 2012 **Accepted** 21 September 2012
Published ahead of print 28 September 2012
Address correspondence to Kornelia Smalla, kornelia.smalla@jki.bund.de.
Supplemental material for this article may be found at http://aem.asm.org/.

doi:10.1128/AEM.02049-12

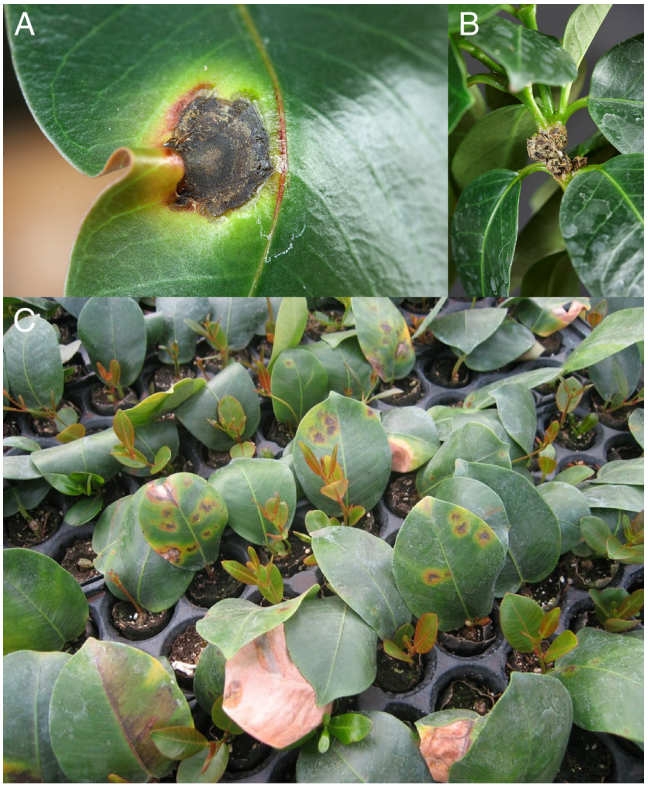

FIG 1 Symptoms caused by *Pseudomonas savastanoi* on leaves (A and C) and stems (B) of *Mandevilla sanderi*.

Subsequently, BOX-PCR fingerprints were generated for all isolates as previously described (18). Interestingly, the BOX-PCR fingerprints generated showed high similarity and were almost identical, independently of the strain's host and geographical origin (see Fig. S1 in the supplemental material). Highly similar BOX-PCR patterns were also obtained for olive isolates Ph12, Ph13, and Ph37 to Ph45 (data not shown). While the resolution of ARDRA (amplified ribosomal DNA restriction analysis) is at the genus or species level, BOX-PCR fingerprints have a much finer level of resolution. BOX-PCR fingerprinting is a powerful tool for strain differentiation in medical microbiology, epidemiology, and microbial ecology (10). The PCR products resolved by gel electrophoresis represent a genomic DNA fingerprint pattern that is assumed to be unique for each bacterial strain and isolate (10, 19). While BOX-PCR fingerprint patterns are stable over many generations, they are affected by polymorphism, rearrangements, recombination, or acquisition of foreign DNA (10). On the basis of the BOX-PCR fingerprints, it was concluded that the *P. savastanoi* strains were highly similar with respect to genomic diversity, indicating that the strains infecting *Mandevilla sanderi* might have originated from diseased or latently infested olive or oleander trees.

However, another picture emerged when plasmid DNA extracted from all isolates by means of a Qiagen plasmid minikit (Qiagen, Hilden, Germany) was analyzed. Plasmid DNA left undigested or digested with Bst1107I and PstI enzymes (Fermentas) was analyzed in 0.8% or 1% agarose gels, respectively. All strains contained plasmids and displayed multiple plasmid restriction patterns. The Bst1107I-plus-PstI restriction patterns of isolates from *Mandevilla sanderi* were distinct from those of all other strains. Moreover, plasmid restriction patterns of isolates from olive trees and oleander displayed high diversity, most likely due

TABLE 1 Bacterial strains and isolates used in this study

Isolate	Species (strain name)	Host plant	Origin	Reference or source
Ph1	*Pseudomonas savastanoi* pv. glycinea (DSMZ 19341)	*Olea europaea*	Yugoslavia	5
Ph2	*Pseudomonas savastanoi* (B202)	*Mandevilla sanderi*	France	This study
Ph3	*Pseudomonas savastanoi* (B203)	*Mandevilla sanderi*	France	This study
Ph4	*Pseudomonas savastanoi* (B204)	*Mandevilla sanderi*	France	This study
Ph5	*Pseudomonas savastanoi* (B205;H16931.1)	*Mandevilla sanderi*	Germany	This study
Ph6	*Pseudomonas savastanoi* (B205;H16931.2)	*Mandevilla sanderi*	Germany	This study
Ph7	*Pseudomonas savastanoi* (16973)	*Mandevilla sanderi*	Germany	This study
Ph8	*Pseudomonas* sp. (B209)	*Mandevilla sanderi*	France	This study
Ph9	*Pseudomonas* sp. (B211)	*Nerium oleander*	Germany	This study
Ph10	*Pseudomonas* sp. (B213)	*Nerium oleander*	Germany	This study
Ph11	*Pseudomonas* sp. (B215)	*Nerium oleander*	Germany	This study
Ph12	*Pseudomonas savastanoi* (B217)	*Olea europaea*	Amendolare, Italy	This study
Ph13	*Pseudomonas savastanoi* (B218)	*Olea europaea*	Bari, Italy	This study
Ph14	*Pseudomonas savastanoi* (B219)	*Nerium oleander*	Italy	This study
Ph15	*Pseudomonas savastanoi* (B220)	*Liguster vulgare*	Bari, Italy	This study
Ph16	*Pseudomonas savastanoi* (B221)	*Jasminum* sp.	Greece	This study
Ph37	*Pseudomonas savastanoi* (IVIA 1628–3/Psv29)	*Olea europaea*	Spain	17
Ph38	*Pseudomonas savastanoi* (NCPPB 2327–3/Psv31)	*Olea europaea*	Italy	17
Ph39	*Pseudomonas savastanoi* (IVIA 1657-b8/Psv32)	*Olea europaea*	Spain	17
Ph40	*Pseudomonas savastanoi* (CFBP 2074/Psv35)	*Olea europaea*	Algeria	17
Ph41	*Pseudomonas savastanoi* (NCPPB/Psv37)	*Olea europaea*	Portugal	17
Ph42	*Pseudomonas savastanoi* (NCPPB 1344/Psv47)	*Olea europaea*	United States	17
Ph43	*Pseudomonas savastanoi* (NCPPB 3335–3/Psv48)	*Olea europaea*	France	17
Ph44	*Pseudomonas savastanoi* (CFBP 1670/Psv62)	*Olea europaea*	Italy	17
Ph45	*Pseudomonas savastanoi* (ITM 317/Psv416)	*Olea europaea*	Serbia	17

TABLE 2 Primers, probes, and PCR conditions used in this study

Target	Primer	Sequence (5′–3′)	Annealing temp (°C)	Product size (bp)	Probe(s) generated from strain	Reference
BOX	BOX_A1R	CTACGGCAAGGCGACGCTGACG	53			14
repA	repA-F1	AGCTTCAAGAYCAGGGMAA	55	1,100	Ph4	13
	repA-R2	ARRTCCATCARYCGGTCRAA				
16S rRNA gene	U8-27	AGAGTTTGATC(AC)TGGCTCAG	56	1,506		9
	R1494	CTACGG(T/C)TACCTTGTTACGAC				
iaaM	iaaM-F	CATATGTATGACCATTTTAATTCACCC	57	1,674	Ph3, Ph38	17
	iaaM-R	GGTACCTTAATAGCGATAGGAGGC				
iaaL	iaaL-F	GGCACCAGCGGCAACATCAA	66	456	Ph3	17
	iaaL-R	CGCCCTCGGAACTGCCATAC				
hopAB1	hopAB1-F	GCCCGCCTCGCAGACTCAT	63	700	Ph3, Ph38	17
	hopAB1-R	CTGCGCGGATATCATTCACAACTT				
hopAF1	hopAF1-F	CTTATCAAGCAGAAAGACGG	55	339	Ph3, Ph43	17
	hopAF1-R	AAGGGAGCAGATGGAATACG				
hopAO1	hopAO1-F	TCTCAGTCACAGCATTCC	60	305	Ph43	17
	hopAO1-R	GCTTACGATGTCGTACTC				

to the presence of two or more plasmids (Fig. 3A). In fact, olive isolates Ph37 to Ph45 have been reported to contain at least two to six different native plasmids (17). The Southern-blotted plasmid restriction digests were subsequently hybridized with different digoxigenin (DIG)-labeled probes, which were obtained from plasmid-borne genes in *P. syringae* strains (25) or *P. savastanoi* strains (17). The probes were generated by PCR under the primer system, plasmid template DNA, and PCR conditions detailed in Table 2 and subsequent DIG labeling according to the manufacturer's instructions (Roche, Mannheim, Germany). Hybridization of Southern-blotted plasmid restriction digests was performed with the *repA* probe generated with *Mandevilla* isolate Ph4 according to the method of Götz et al. (7). The *repA* hybridization patterns of all *Mandevilla* isolates were identical and clearly distinct from the hybridization patterns of all other *P. savastanoi* isolates (Fig. 3B). Three strongly hybridizing fragments and two smaller fragments with less hybridization intensity were observed for all isolates from *Mandevilla sanderi*. While the *repA* probe was generated from *Mandevilla sanderi* isolate Ph4, all other probes used in this study were generated with DNA of olive tree isolates Ph38 and Ph43 and of *Mandevilla sanderi* isolate Ph3. The DIG-labeled probe for *iaaM*, coding for tryptophan-2-monooxygenase, an enzyme involved in the biosynthesis of indole-3-acetic acid (IAA), was generated from Ph38 and Ph3, whereas the probe for *iaaL* (IAA-lysine-synthase) was generated from Ph3. The *iaaM* and *iaaL* probes hybridized with the same restriction fragment size for all PstI/Bst1107I-digested plasmids of *Mandevilla* isolates (see Fig. S2A and D in the supplemental material). In agreement with previously reported data (17, 25), these probes hybridized with plasmid DNA from all oleander strains; however, only 2 of the 12 olive isolates tested hybridized with the *iaaM* probe. The sizes of the hybridization fragments obtained for *Mandevilla* isolates were similar to the sizes of the fragments detected for all samples giving a hybridization signal (see Fig. S2A and D in the supplemental material). These results clearly show that both the *iaaM* and *iaaL* genes are carried on plasmids in all *Mandevilla* isolates tested.

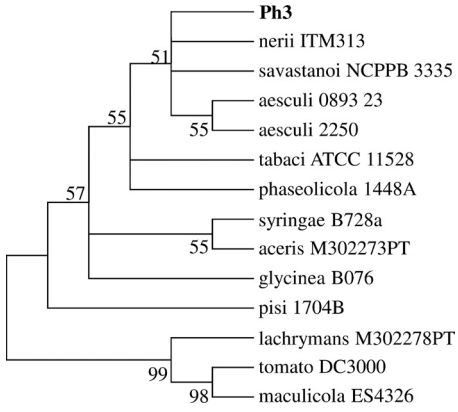

FIG 2 Phylogenetic analysis of partial nucleotide sequences of the 16S rRNA gene from strains of the *P. syringae* complex. All strains included in the tree are identified by their pathovar and strain names. Neighbor-joining trees were constructed using 14 nucleotide sequences (1,413 bp). See Fig. 4 for methodology and Table S3 in the supplemental material for locus tags.

Several genes encoding type III secretion system (T3SS) effectors have been reported to be carried on plasmids in *P. syringae* and *P. savastanoi* strains. However, different strains isolated from the same host largely differ in the number and type of T3SS effectors carried on their plasmids (17, 25). This was not the case for *Mandevilla* isolates, as identical fragment sizes were also observed for the Southern blot hybridizations performed with the DIG-labeled *hopAF1* gene probes (see Fig. S2C in the supplemental material) obtained from strain Ph43 or strain Ph3 as the template DNA and tested against plasmids from *Mandevilla* isolates. In addition, the sizes of the two hybridizing fragments observed for the isolates from *Mandevilla* were different from those of the isolates from all other strains analyzed. Only 4 of 12 isolates from olive and all 3 oleander isolates hybridized with the *hopAF1* probe. No hybridization signal was observed for isolates from privet and jasmine (see Fig. S2C in the supplemental material). The similarity in the gene content of the plasmids of all *Mandevilla* isolates was further confirmed using *hopAO1* and *hopAB1* probes. The *hopAO1* and the *hopAB1* probes did not hybridize with any of them. In contrast, the numbers and sizes of the plasmid fragments hybridizing with these probes largely differed among the remain-

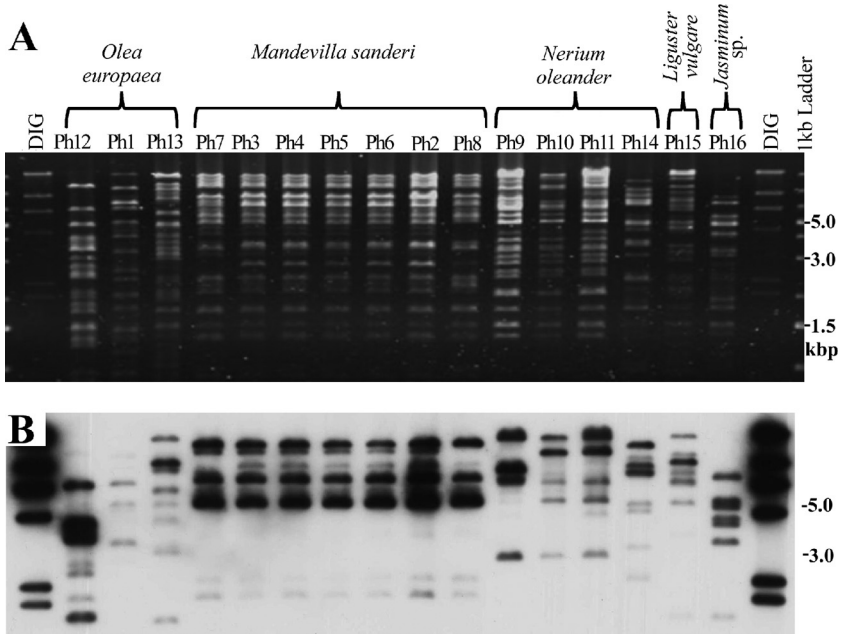

FIG 3 Restriction profiles of plasmid DNA determined with enzymes Bst1107I and PstI (A); hybridization of the Southern blot with a *repA* probe derived from *Mandevilla* isolate Ph4 (B). 1 kb, DNA molecular weight marker Generuler Plus DNA Ladder (Fermentas, St. Leon-Rot, Germany). DIG, DNA molecular weight marker VI (DIG labeled) (Roche, Mannheim, Germany).

ing *P. savastanoi* isolates (see Fig. S2B in the supplemental material; data not shown for the *hopAB1* probe), as expected from a variable distribution of plasmid-carried T3SS effector genes in these strains. The restriction patterns and hybridizations showed that all *P. savastanoi* isolates from *Mandevilla* isolates carried indigenous plasmids which belong to the pPT23A family and share the replication gene *repA*. However, these plasmids were clearly distinct from the plasmids carried by the other *P. savastanoi* isolates from all other host plants (Fig. 3). Plasmids belonging to the pPT23A family are assumed to contribute to host specificity and pathogenicity. Recently, the sequence and role in virulence of plasmids carried by the tumor-inducing *Pseudomonas savastanoi* pv. savastanoi NCPPB 3335 bacterium were determined (1). At least some of the genes involved in the biosynthesis of virulence factors such as *iaaM*, *iaaL*, and *hopAF1* identified on the plasmid complement of the olive tree NCPPB 3335 isolate could be also amplified on the plasmid DNA from the *P. savastanoi* isolates from *Mandevilla sanderi*. Amplicons obtained were cloned using pGEM-T Easy vector (Promega Corporation, Madison, WI), and two clones per gene fragment were sent for sequencing.

In a phylogenetic analysis of *repA*, the three plasmids of *P. savastanoi* pv. savastanoi NCPPB 3335 clustered with diverse plasmids from other *P. savastanoi* olive isolates (group C of *repA* sequences), although they were separated from plasmids isolated from other pathovars of the genomospecies 2 included in group A of *repA* sequences (1). In fact, the *repA* sequence from the *Mandevilla* Ph3 isolate clustered closely to the *repA* sequences of a plasmid from *P. savastanoi* pv. glycinea race 4, which belongs to group A (Fig. 4A). However, a phylogenetic analysis of *iaaL* (Fig. 4B) showed that the sequence of this gene from Ph3 clustered together with that from *P. savastanoi* pv. nerii PLVM2 and with one of the alleles (*iaaL-1*) of pv. savastanoi NCPPB 3335 (15, 20), suggesting that they share a recent common origin. Phylogenetic analyses were also performed for *hopAF1* and *iaaM* sequences (see Fig. S3A and B in the supplemental material, respectively). In both cases, the sequences from *Mandevilla* isolate Ph3 clustered together with those of *P. savastanoi* pv. savastanoi NCPPB 3335. Furthermore, the *iaaM* sequence from Ph3 also clustered in the same branch as that from *P. savastanoi* pv. nerii PLVM2 (see Fig. S3B in the supplemental material), providing further support for the idea of a recent common origin for all these plasmid-carried sequences. The sequence data have been submitted to the DDBJ/EMBL/GenBank databases (see below).

PCR-based system for detection of *P. savastanoi* in isolates from *Mandevilla sanderi*. PCR amplicons with the primers repA-F1 targeting the *repA* gene of pPT23A-like plasmids and repA-R2 targeting a downstream region of *repA* (13) were obtained from most *P. savastanoi* isolates (Fig. 5A). Only the amplicons generated from *Mandevilla* isolates had a size of approximately 1,100 bp and hybridized with the *repA* probe derived from the *Mandevilla* isolate Ph4 (strain B204) (see Fig. 5B). The 5′ sequence of the amplicon was 98.7% identical to the *repA* 3′ fragment of the pPT23A-like pREP601 plasmid (13). The system was successfully used to detect the pathogen in total community DNA extracted from leaf and tumor material of plants inoculated with strain Ph4 (data not shown). The hybridization method is an important means to increase not only the sensitivity but also the specificity of detection. While the *repA* PCR provides fast and specific detection of *P. savastanoi* isolates from *Mandevilla sanderi*, the application of the detection system in combination with hybridization can be also used to detect the pathogen in DNA directly extracted from plant material or soil.

Lessons learned for bacterial diversity studies. Although the ARDRA and BOX-PCR fingerprints indicated that the isolates originating from various diseased plant species and different geographic origins showed high genomic similarity, comparison of

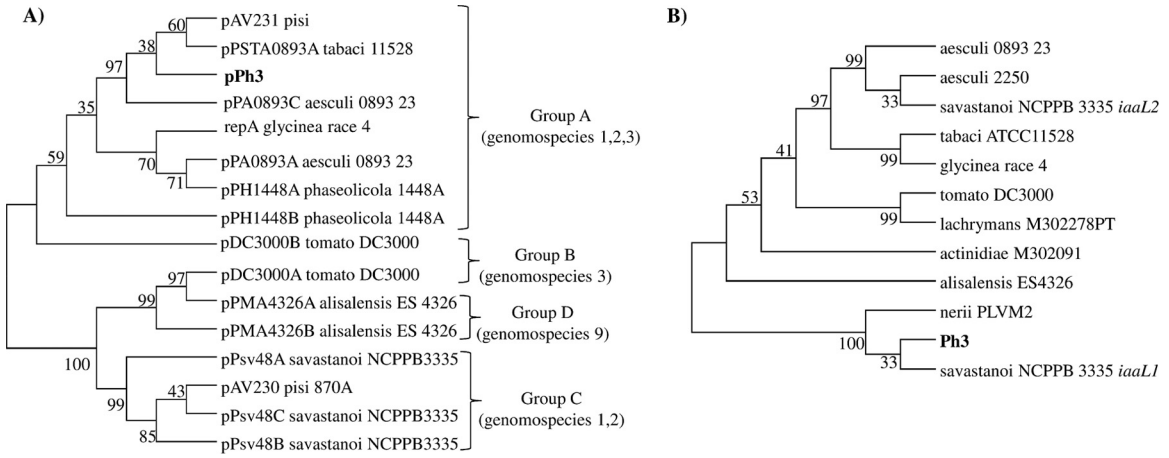

FIG 4 Phylogenetic analysis of partial nucleotide sequences of the *repA* (A) and *iaaL* (B) genes from strains of the *P. syringae* complex. The evolutionary history was inferred by the neighbor-joining method (21) using MEGA5 (23); evolutionary distances were computed in numbers of nucleotide substitutions per site. Strains included in the *repA* and *iaaL* trees are identified by their plasmid, pathovar, and strain names and by pathovar and strain names, respectively. Sequences from *Mandevilla* isolate Ph3 (in bold) (Table 1) were amplified using the primers indicated in Table 2. The topologies were identical for trees produced by the minimum evolution and maximum parsimony methods. The percentages of replicate trees in which the associated taxa clustered together in the bootstrap test (10,000 replicates) are shown next to the branches (4). The trees were constructed with published genome sequences plus those from Ph3. Neighbor-joining trees were constructed using (A) 16 nucleotide sequences from the *repA* gene (330 bp) and (B) 11 nucleotide sequences from the *iaaL* gene (356 bp); all positions containing gaps and missing data were eliminated using the option of complete deletion. Nucleotide sequences corresponding to the *P. syringae* complex were downloaded from NCBI, and their locus tags are included in Table S1 (*repA*) and Table S2 (*iaaL*) in the supplemental material.

plasmids of these isolates showed clear differences and allowed us to withdraw our research hypothesis that the new bacterial disease observed for *Mandevilla sanderi* is caused by strains from olive or oleander. The plasmids present in the *Mandevilla sanderi* isolates seemed to be unique, and we hypothesize that properties contributing to the interaction with the host are carried on the mobilome. However, only the plasmid sequence can provide more insights. This study not only provides insights into the diversity of *P. savastanoi* isolates from woody host plants but also is an example illustrating the resolution level of 16S rRNA gene-based bacterial diversity studies. The analysis of 16S rRNA gene fragments amplified from total community DNA by cloning and sequencing or fingerprinting methods such as terminal restriction fragment analysis, denaturing gradient gel electrophoresis, phylochip analysis, or pyrosequencing analysis has provided fascinating insights into the diversity of bacterial communities in rhizosphere and bulk soils over the last 2 decades. The effects of the soil type, the plant species, or the cultivar on the composition of bacterial communities were unraveled (2, 3, 22, 24). In particular, ultradeep amplicon sequencing techniques promise dramatically improved

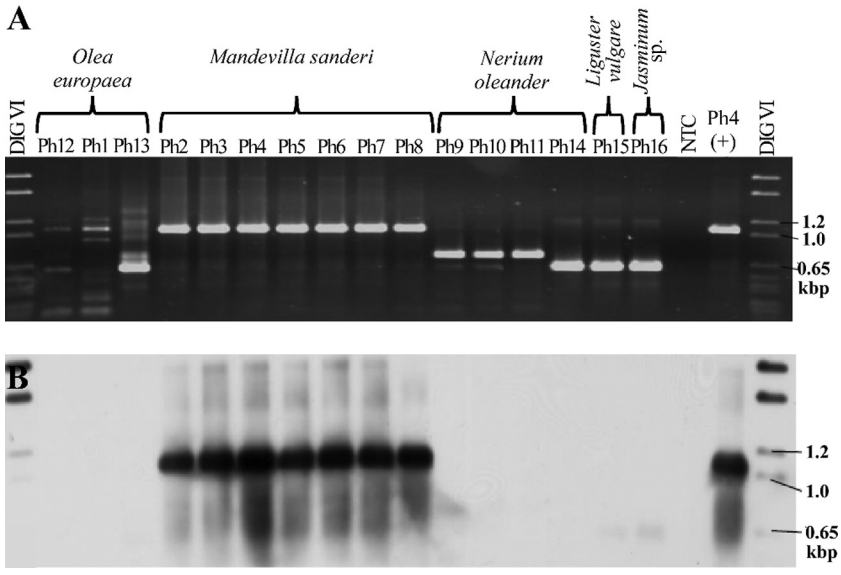

FIG 5 PCR amplicons of *Pseudomonas savastanoi* and *Pseudomonas* sp. from different host plants (see Table 1) with the primers repA-F1 targeting the *repA* gene of pPT23A-like plasmids and repA-R2 targeting a downstream region of *repA* (A) and hybridization with a *repA* probe derived from *Mandevilla* isolate Ph4 (+) (see Table 2) (B). NTC, no-target control. DIG VI, DNA molecular weight marker VI (DIG labeled) (Roche, Mannheim, Germany).

resolution. However, microbial ecologists need to be aware of the caveats and limitations with respect to bacterial diversity studies based on 16S rRNA genes or other genes belonging to the core gene pool. Despite the challenges encountered in studying the mobilome, we need to realize the important contribution of the mobilome for bacterial diversification, adaptation to changing environments, and the ability to colonize new ecological niches or interact with plants (8).

Nucleotide sequence accession numbers. The strain Ph3 sequence data have been submitted to the DDBJ/EMBL/GenBank databases under accession numbers JX227983 to JX227986 and JX678983.

ACKNOWLEDGMENTS

The research was supported by the German Federal Ministry of Food, Agriculture and Consumer Protection and Spanish Plan Nacional I+D+i grant AGL2011-30343-C02-01, cofinanced by FEDER.

REFERENCES

1. **Bardaji L, et al.** 2011. Sequence and role in virulence of the three plasmid complement of the model tumor-inducing bacterium *Pseudomonas savastanoi* pv. savastanoi NCPPB 3335. PLoS One **6**:e25705. doi:10.1371/journal.pone.0025705.
2. **Costa R, et al.** 2007. *Pseudomonas* community structure and antagonistic potential in the rhizosphere: insights gained by combining phylogenetic and functional gene-based analyses. Environ. Microbiol. **9**:2260–2273.
3. **Costa R, et al.** 2006. Effects of site and plant species on rhizosphere community structure as revealed by molecular analysis of microbial guilds. FEMS Microbiol. Ecol. **56**:236–249.
4. **Felsenstein J.** 1985. Confidence limits on phylogenies: an approach using the bootstrap. Evolution **39**:783–791.
5. **Gardan L, et al.** 1992. Evidence for a correlation between auxin production and host plant species among strains of *Pseudomonas syringae* subsp. savastanoi. Appl. Environ. Microbiol. **58**:1780–1783.
6. **Gardan L, et al.** 1999. DNA relatedness among the pathovars of *Pseudomonas syringae* and description of *Pseudomonas tremae* sp. nov. and *Pseudomonas cannabina* sp. nov. (ex Sutic and Dowson 1959). Int. J. Syst. Bacteriol. **49**:469–478.
7. **Götz A, et al.** 1996. Detection and characterization of broad-host-range plasmids in environmental bacteria by PCR. Appl. Environ. Microbiol. **62**:2621–2628.
8. **Heuer H, Abdo Z, Smalla K.** 2008. Patchy distribution of flexible genetic elements in bacterial populations mediates robustness to environmental uncertainty. FEMS Microbiol. Ecol. **65**:361–371.
9. **Heuer H, Kopmann C, Binh CT, Top EM, Smalla K.** 2009. Spreading antibiotic resistance through spread manure: characteristics of a novel plasmid type with low %G+C content. Environ. Microbiol. **11**:937–949.
10. **Ishii S, Sadowsky MJ.** 2009. Applications of the rep-PCR DNA fingerprinting technique to study microbial diversity, ecology and evolution. Environ. Microbiol. **11**:733–740.
11. **Kennelly MM, Cazorla FM, de Vicente A, Ramos C, Sundin GW.** 2007. *Pseudomonas syringae* diseases of fruit trees: progress toward understanding and control. Plant Dis. **91**:4–17.
12. **King EO, Ward MK, Raney DE.** 1954. Two simple media for the demonstration of pyocyanin and fluorescin. J. Lab. Clin. Med. **44**:301–307.
13. **Ma ZH, et al.** 2007. Phylogenetic analysis of the pPT23A plasmid family of *Pseudomonas syringae.* Appl. Environ. Microbiol. **73**:1287–1295.
14. **Martin B, et al.** 1992. A highly conserved repeated DNA element located in the chromosome of *Streptococcus pneumoniae.* Nucleic Acids Res. **20**:3479–3483.
15. **Matas IM, et al.** 2009. *Pseudomonas savastanoi* pv. savastanoi contains two *iaaL* paralogs, one of which exhibits a variable number of a trinucleotide (TAC) tandem repeat. Appl. Environ. Microbiol. **75**:1030–1035.
16. **Penyalver R, et al.** 2006. Factors affecting *Pseudomonas savastanoi* pv. savastanoi plant inoculations and their use for evaluation of olive cultivar susceptibility. Phytopathology **96**:313–319.
17. **Pérez-Martínez I, Zhao Y, Murillo J, Sundin GW, Ramos C.** 2008. Global genomic analysis of *Pseudomonas savastanoi* pv. savastanoi plasmids. J. Bacteriol. **190**:625–635.
18. **Rademaker JLW, de Bruijn FJ.** 1997. Characterization and classification of microbes by rep-PCR genomic fingerprinting and computer assisted pattern analysis, p 151–171. *In* Caetano-Anollés G, Gresshoff PM (ed), DNA markers: protocols, applications and overviews. John Wiley and Sons, New York, NY.
19. **Rademaker JL, et al.** 2000. Comparison of AFLP and rep-PCR genomic fingerprinting with DNA-DNA homology studies: *Xanthomonas* as a model system. Int. J. Syst. Evol. Microbiol. **50**:665–677.
20. **Rodríguez-Palenzuela P, et al.** 2010. Annotation and overview of the *Pseudomonas savastanoi* pv. savastanoi NCPPB 3335 draft genome reveals the virulence gene complement of a tumour-inducing pathogen of woody hosts. Environ. Microbiol. **12**:1604–1620.
21. **Saitou N, Nei M.** 1987. The neighbor-joining method: a new method for reconstructing phylogenetic trees. Mol. Biol. Evol. **4**:406–425.
22. **Smalla K, et al.** 2001. Bulk and rhizosphere soil bacterial communities studied by denaturing gradient gel electrophoresis: plant-dependent enrichment and seasonal shifts revealed. Appl. Environ. Microbiol. **67**:4742–4751.
23. **Tamura K, et al.** 2011. MEGA5: molecular evolutionary genetics analysis using maximum likelihood, evolutionary distance, and maximum parsimony methods. Mol. Biol. Evol. **28**:2731–2739.
24. **Weinert N, et al.** 2011. PhyloChip hybridization uncovered an enormous bacterial diversity in the rhizosphere of different potato cultivars: many common and few cultivar-dependent taxa. FEMS Microbiol. Ecol. **75**:497–506.
25. **Zhao Y, Ma Z, Sundin GW.** 2005. Comparative genomic analysis of the pPT23A plasmid family of *Pseudomonas syringae.* J. Bacteriol. **187**:2113–2126.

Microbiology (2014), **160**, 556–566 **DOI** 10.1099/mic.0.074468-0

Bacterial multispecies studies and microbiome analysis of a plant disease

Daniel Passos da Silva,[1] Maria Pilar Castañeda-Ojeda,[3] Chiaraluce Moretti,[2] Roberto Buonaurio,[2] Cayo Ramos[3] and Vittorio Venturi[1]

Correspondence
Vittorio Venturi
venturi@icgeb.org

[1]International Centre for Genetic Engineering and Biotechnology, Trieste, Italy

[2]Dipartimento di Scienze Agrarie e Ambientali, Università degli Studio di Perugia, Perugia, Italy

[3]Instituto de Hortofruticultura Subtropical y Mediterránea 'La Mayora', Universidad de Málaga-Consejo Superior de Investigaciones Científicas (IHSM-UMA-CSIC), Área de Genética, Facultad de Ciencias, Campus de Teatinos, Málaga, Spain

Although the great majority of bacteria found in nature live in multispecies communities, microbiological studies have focused historically on single species or competition and antagonism experiments between different species. Future directions need to focus much more on microbial communities in order to better understand what is happening in the wild. We are using olive knot disease as a model to study the role and interaction of multispecies bacterial communities in disease establishment/development. In the olive knot, non-pathogenic bacterial species (e.g. *Erwinia toletana*) co-exist with the pathogen (*Pseudomonas savastanoi* pv. *savastanoi*); we have demonstrated cooperation among these two species via quorum sensing (QS) signal sharing. The outcome of this interaction is a more aggressive disease when co-inoculations are made compared with single inoculations. *In planta* experiments show that these two species co-localize in the olive knot, and this close proximity most probably facilitates exchange of QS signals and metabolites. *In silico* recreation of their metabolic pathways showed that they could have complementing pathways also implicating sharing of metabolites. Our microbiome studies of nine olive knot samples have shown that the olive knot community possesses great bacterial diversity; however. the presence of five genera (i.e. *Pseudomonas*, *Pantoea*, *Curtobacterium*, *Pectobacterium* and *Erwinia*) can be found in almost all samples.

Received 25 October 2013
Accepted 2 January 2014

INTRODUCTION

Most bacterial research in plant pathology thus far, with the exception of crown gall caused by *Agrobacterium tumefaciens*, has focused most commonly on herbaceous plant diseases rather than woody plant diseases (Mansfield *et al.*, 2012). In recent years, the olive plant bacterial pathogen *Pseudomonas savastanoi* pv. *savastanoi* has begun to be studied, developing as a new model for woody plant disease (Rodríguez-Moreno *et al.*, 2008, 2009; Rodríguez-Palenzuela *et al.*, 2010). Olive trees (*Olea europaea* L.) infected by *Pseudomonas savastanoi* pv. *savastanoi* develop overgrowths, referred to as galls, knots or tumours, mainly on the aerial parts of the plants, with their incidence being rare on leaves and fruits. The productivity of olive trees infected with *Pseudomonas savastanoi* pv. *savastanoi* is reduced and no effective treatment is yet in place (Matas *et al.*, 2012; Quesada *et al.*, 2010; Ramos *et al.*, 2012; Schroth *et al.*, 1973; Young, 2004). The few studies of *Pseudomonas savastanoi* pv. *savastanoi* virulence have implicated type III secretion, phytohormones and quorum sensing (QS) as being involved in the disease process (Hosni *et al.*, 2011; Iacobellis *et al.*, 1994; Pérez-Martínez *et al.*, 2010; Surico *et al.*, 1985). A recent signature-tagged mutagenesis screening resulted in the identification of numerous other mechanisms associated with the virulence of *Pseudomonas savastanoi* pv. *savastanoi* (Matas *et al.*, 2012).

Interestingly, several other bacterial species have been isolated within the olive knot that are harmless or non-pathogenic to the olive plant (Moretti *et al.*, 2011; Ouzari *et al.*, 2008; Rojas *et al.*, 2004). The possible role of these *Pseudomonas savastanoi* pv. *savastanoi* co-residents in the olive knot has recently been addressed; isolates of *Pantoea agglomerans* and *Erwinia toletana* are believed to create multispecies communities with *Pseudomonas savastanoi* pv. *savastanoi*. More specifically, our laboratory has reported

Abbreviations: AHL, *N*-acylhomoserine lactone; CTAB, cetyltrimethylammonium bromide; QS, quorum sensing; RFP, red fluorescent protein.

One supplementary table and two supplementary figures are available with the online version of this paper.

previously that disease progression and knot volume was increased significantly by co-inoculation of *Pseudomonas savastanoi* pv. *savastanoi* with *E. toletana*. In addition, it was shown that *E. toletana* and *Pantoea agglomerans* could rescue *in planta* a QS mutant of *Pseudomonas savastanoi* pv. *savastanoi* by exogenously providing *N*-acylhomoserine lactone (AHL) signals to *Pseudomonas savastanoi* pv. *savastanoi*. The main conclusions drawn from that work were the exchange/sharing of QS AHL signals between *E. toletana*, *Pantoea agglomerans* and *Pseudomonas savastanoi* pv. *savastanoi*, and the synergistic effect on the disease when *E. toletana* and *Pseudomonas savastanoi* pv. *savastanoi* were co-inoculated in olive plants. Cell numbers of both *E. toletana* and *Pseudomonas savastanoi* pv. *savastanoi* increase when co-inoculated, providing further evidence of mutualism and interspecies interactions (Hosni *et al.*, 2011). *Pseudomonas savastanoi* pv. *savastanoi* is believed to grow as a biofilm inside the olive knot (Rodríguez-Moreno *et al.*, 2009), and questions that therefore arise are how are *E. toletana* and *Pseudomonas savastanoi* pv. *savastanoi* distributed spatially inside the olive knot, and how are they organized with respect to each other? Multispecies interactions within bacterial consortia are now beginning to be studied, and factors such as metabolic sharing, biofilm formation and chemical signalling are thought to play important roles (Hosni *et al.*, 2011; Kolenbrander *et al.*, 2010; Kuramitsu *et al.*, 2007; Ramsey *et al.*, 2011).

Recent research efforts are beginning to highlight the importance of social and molecular behaviour in multispecies bacterial communities (Duan *et al.*, 2003; Hosni *et al.*, 2011; Kim *et al.*, 2008; Kolenbrander *et al.*, 2010; Korgaonkar *et al.*, 2013; Kuramitsu *et al.*, 2007; Maldonado-González *et al.*, 2013; Mitri *et al.*, 2011; Ramsey *et al.*, 2011; Stolyar *et al.*, 2007). For example, in human oral bacteria, synergistic interactions occur via a mechanism of metabolite cross-feeding where the commensal *Streptococcus gordonii* degrades glucose generating L-lactate, which is then used by the pathogen *Aggregatibacter actinomycetemcomitans* (Ramsey *et al.*, 2011). Another interesting finding demonstrated the effect of the resident oropharyngeal microflora on the incoming human fibrocystic opportunistic pathogen *Pseudomonas aeruginosa*, where it was shown that the presence of the resident bacteria enhances pathogenicity most probably by chemical signalling (Duan *et al.*, 2003). More recently, it was also reported that recognition of peptidoglycan of Gram-positive bacteria is a cue and results in increased expression of virulence factors in *Pseudomonas aeruginosa* (Korgaonkar *et al.*, 2013). These kinds of examples of multispecies interactions among bacteria are likely to increase dramatically in the future.

Research on interactions that involve more than two species will be challenging using current microbiology methods. However, with the decreasing cost of techniques such as metagenomics, metatranscriptomics and metabolomics, these are rapidly becoming the preferred tools for addressing which bacteria are present in a niche, which genes are expressed when, and how this gene expression reflects on the metabolites present. Environments such as the ocean and soils are currently being characterized extensively with regard to their bacterial composition, and other complex niches like plants (Sessitsch *et al.*, 2012) and humans (Human Microbiome Project Consortium, 2012; Maurice *et al.*, 2013; Wang *et al.*, 2011) are now also being studied.

Olive knot disease caused by *Pseudomonas savastanoi* pv. *savastanoi* provides a niche for studying bacterial multispecies interaction in disease as we have shown that *Pseudomonas savastanoi* pv. *savastanoi* interacts with resident bacteria such as *E. toletana*. In this study, we investigated bacterial localization during the course of *in vitro* generated olive knots caused by co-inoculations of *Pseudomonas savastanoi* pv. *savastanoi* and *E. toletana*. The study of a possible metabolic interaction between these two species was evaluated *in silico*. Finally, the microbiome of nine naturally occurring olive knots from different regions of Italy was analysed to determine the composition of their bacterial community.

METHODS

Bacterial strains and growth conditions. *Pseudomonas savastanoi* pv. *savastanoi* DAPP-PG 722 and *E. toletana* DAPP-PG 735, and their derivatives DAPP-PG 722–GFP and DAPP-PG 735–DsRedExpress, were routinely grown at 28 °C in Luria–Bertani (LB) broth. When required, antibiotics were added in the following concentrations: nitrofurantoin, 50 μg ml^{-1}, and kanamycin, 100 μg ml^{-1}. *Escherichia coli* DH5α was grown at 37 °C in LB broth and when appropriate antibiotics were added in the following concentrations: ampicillin, 100 μg ml^{-1}, and kanamycin, 50 μg ml^{-1}.

Pseudomonas savastanoi pv. *savastanoi* and *E. toletana* were tested for growth on minimal M9 medium with sole carbon and nitrogen sources. Co-inoculations of *E. toletana* and *Pseudomonas savastanoi* pv. *savastanoi* were performed on M9 minimal medium containing a sole carbon source as follows: *E. toletana* and *Pseudomonas savastanoi* pv. *savastanoi* were grown overnight in rich media, and cells were then pelletted and washed twice in M9 medium without a carbon source. *E. toletana* and *Pseudomonas savastanoi* pv. *savastanoi* were then resuspended in M9 medium, and these cultures were used as inocula into an M9 medium with a unique carbon source. Amounts of *Pseudomonas savastanoi* pv. *savastanoi* and *E. toletana* that were inoculated resulted in OD_{600} 0.05 for each isolate, meaning that the mixed culture had OD_{600} 0.1. Bacterial growth was monitored constantly by measuring OD_{600} and by plating on rich media.

The biodegradation of aromatic acids by *E. toletana* and *Pseudomonas savastanoi* pv. *savastanoi* was analysed by reverse-phase HPLC, using a Varian 9010 solvent delivery system equipped with a Varian 9050 UV/vis detector. *E. toletana* and *Pseudomonas savastanoi* pv. *savastanoi* were grown in M9 minimal medium supplemented with 0.1 % of the aromatic acid. Samples were withdrawn from cultures after growth and centrifuged at 12 000 ***g***. The supernatant was diluted 100-fold into methanol and filtered through 0.2 μm filters; 10 μl samples were loaded on a 5 μm spherical C18 reverse-phase column (Supelcosil LC18 150 × 4.6 mm; Supelco), and eluted with 35 % methanol and 65 % water with 0.1 % acetic acid at a flow rate of 0.8 ml min^{-1}. The eluted metabolites were detected at 280 nm.

Construction of pBBR2GFP and pBBR2DsRedExpress plasmids. Digestion of pBK-miniTn*7*-*gfp*1 (Koch *et al.*, 2001) and

miniTn*7*(Km, Sm) $P_{A1/04/03}$-DsRedExpress-a (Lambertsen *et al.*, 2004) with *Not*I yielded fragments of 2 kb that were blunt-ended by treatment with DNA polymerase I. Fragments were cloned into pBBR1MCS5 (Kovach *et al.*, 1995) digested with *Sma*I. To generate pBBR2-GFP and pBBR2-DsRedExpress, the cassette was then transferred to pBBR1MCS2 using *Cla*I/*Spe*I restriction enzymes. The resulting plasmids were maintained in *E. coli* DH5α and transferred to *Pseudomonas savastanoi* pv. *savastanoi* or *E. toletana* by triparental conjugation by using the helper strain *E. coli* DH5α (pRK2013).

Plant infection and isolation of bacteria from olive knots. *O. europaea* plants derived from seeds germinated *in vitro* (collected originally from an 'Arbequina' plant) were micropropagated and rooted as described previously (Rodríguez-Moreno *et al.*, 2008) in Driver Kuniyuki Walnut (DKW) medium (Driver & Kuniyuki, 1984). Rooted explants were transferred to DKW medium without hormones and kept for at least 2 weeks in a growth chamber at 25 °C with a 16 h photoperiod prior to infection. The olive plants used for *in vitro* studies were 60–80 mm long (stem diameter 1–2 mm) and contained three to five internodal fragments. Micropropagated olive plants were wounded by excision of an intermediate leaf and infected in the stem wound with a bacterial suspension under sterile conditions. For this purpose, bacterial lawns were grown for 48 h on LB plates and resuspended in 10 mM $MgCl_2$. The concentration of the bacterial cells was adjusted to OD_{600} 0.1 for single inoculations, corresponding to ~10^8 c.f.u. ml^{-1}. For co-inoculations, a mixed bacterial suspension containing ~10^8 c.f.u. ml^{-1} of each species was prepared. The plant wounds were infected with 2 μl of the resulting cell suspension. The plants were then incubated in a growth chamber at 25 °C with a 16 h photoperiod and a light intensity of 35 μmol m^2 s^{-1}. At different time points, *Pseudomonas savastanoi* pv. *savastanoi* and *E. toletana* cells were recovered from the infected explants and spotted onto LB plates as described previously (Maldonado-González *et al.*, 2013). Population densities were calculated from at least three replicates. The morphology of the olive plants infected with bacteria was visualized using a stereoscopic microscope (Leica MZ FLIII).

Real-time monitoring of bacterial infection by epifluorescence microscopy and CLSM. To visualize bacterial infection within knots in real-time, whole knots were examined directly with a stereoscopic fluorescence microscope at 3, 14, 21 and 28 days post-inoculation (p.i.) (Leica MZ FLIII) equipped with a 100 W mercury lamp, a GFP2 filter (excitation 480/40 nm; emission 510LP nm) and a red fluorescent protein (RFP) filter (excitation 546/10 nm; emission 570LP nm). Images were captured using a high-resolution digital camera (Nikon DXM 1200). To visualize bacterial infection within the knots of the olive plants with CLSM, the knots were sampled 28 days p.i. at 1 cm above and below the inoculation point. These samples were fixed and embedded in agarose as described previously (Rodríguez-Moreno *et al.*, 2009). Samples were fixed overnight at 4 °C in 2.5 % paraformaldehyde prepared in 0.1 M phosphate buffer, pH 7.4. The fixed samples were then transferred into 2.5 % paraformaldehyde with an ascending gradient of 10, 20 and 30 % sucrose for 10, 20 and 30 min, respectively. Finally, samples were embedded in 7 % low-melting-point agarose and cooled to 4 °C. Sections (40 and 60 μm) were cut from the knot samples using a vibrating microtome (Leica CM1325). Fluorescence of the bacterial cells within knot sections was visualized by epifluorescence microscopy using a Nikon Microphot FXA microscope. For confocal microscopy, we used an inverted CLSM (TCS-NT; Leica) equipped with detectors and filters that detect simultaneously green and red fluorescence. Images of green fluorescence were acquired at an excitation wavelength of 488 nm and an emission wavelength of 500–550 nm, whilst red fluorescence emission was recorded in the interval between 575 and 625 nm. The images were acquired by sequential scan analysis and processed using Leica LAS AF Lite software.

SavCyc, TolCyc and SavtolCyc creation and availability. Metabolic pathways were recreated using the software Pathway Tools (Karp *et al.*, 2010). The Pathological input file was prepared according to the instructions in the Pathway Tools (version 16.5) user's guide by feeding the software with the latest annotated files of *Pseudomonas savastanoi* pv. *savastanoi* and *E. toletana* (Passos da Silva *et al.*, 2013; Rodríguez-Palenzuela *et al.*, 2010) draft genomes, and merged files of the *Pseudomonas savastanoi* pv. *savastanoi*/*E. toletana* draft genomes. Initial builds of the *Pseudomonas savastanoi* pv. *savastanoi*, *E. toletana* and joined *Pseudomonas savastanoi* pv. *savastanoi*/*E. toletana* metabolic pathways were named SavCyc, TolCyc and SavtolCyc, respectively, using the default reference database, MetaCyc. MetaCyc pathways were included as the reference pathways (Caspi *et al.*, 2012). No manual curation was performed on the created databases. Created databases are available via Pathway Tools software and at ftp://ftp.icgeb.org/pub/tmp/Passos.

Sample collection and processing for metagenomics. Young knots were collected from diseased 'Frantoio', 'Cima di Mola' and 'Oliva Rossa' olive trees grown in Umbria (Central Italy) and Apulia (South Italy). Genomic DNA was isolated from 1 g fresh-weight knots using a cetyltrimethylammonium bromide (CTAB) plant DNA extraction protocol. Briefly, knots (these were not sterilized as they are porous and *Pseudomonas savastanoi* pv. *savastanoi* is known to be localized mainly near the surface) were ground to a fine powder in liquid nitrogen within a cooled mortar. The ground tissue was mixed with 6 ml ice-cold extraction buffer (100 mM Tris/HCl, pH 8.0, 500 mM NaCl, 50 mM EDTA, 10 mM β-mercaptoethanol) and transferred to a 15 ml Falcon tube. After addition of 0.8 ml 10 % SDS and incubation at 65 °C for 30 min, 2 ml ice-cold 5/3 KAc solution (5 M acetic potassium; glacial acetic acid) were added. The suspension was centrifuged for 10 min at 5000 ***g*** at 4 °C and the supernatant was filtered through a paper filter (S&S 595). After 2-propanol precipitation and centrifugation for 10 min at 10 000 ***g*** at room temperature, the pellet was dissolved in 400 μl TE (10 mM Tris/HCl, pH 8.0, 1 mM EDTA) and RNase (20 mg ml^{-1}) treatment was performed for 20 min at room temperature. After incubation for 15 min at 65 °C with CTAB buffer [0.2 M Tris/HCl, pH 7.5, 2 M NaCl, 0.05 M EDTA, 2 % (w/v) CTAB], two chloroform/isoamylic alcohol (24 : 1) extractions were performed. Nucleic acid was precipitated from the aqueous layer by the addition of an equal volume of ethanol (96 %). After centrifugation, the pellet was washed with 70 % (v/v) ethanol, air-dried and resuspended in 110 μl nuclease-free water.

Bacterial 16S rRNA PCR amplification and pyrosequencing. The PCR strategy was carried out by GATC Biotech (Konstanz) as follows. First 16S rRNA PCR for the V1/V3 region using primers 27F (AGAGTTTGATCCTGGCTCAG) and 534R (ATTACCGCGGCTGC-TGG) was performed. The PCR conditions used were: denaturation at 98 °C for 30 s, followed by 25 cycles at 98 °C 10 s, 56 °C 30 s, 72 °C 10 s and a final extension at 72 °C per 1 min. Next, PCR products were column purified, and a second PCR was performed to add the sequencing adaptors and multiplex identifiers. The PCR conditions for the second PCR were the same as above, except only five amplification cycles were performed. The library was sequenced on a Roche GS FLX following standard protocols from Roche.

Metagenomics data analysis. Unassembled reads were uploaded to the open-access MG-RAST server (http://metagenomics.anl.gov/) (Meyer *et al.*, 2008). Analyses were performed using the MG-RAST pipeline applying the RDP dataset. Results were imported into an Excel (Microsoft) spreadsheet curated manually for graphical presentation and table creation. Alpha diversity was estimated using the MG-RAST metagenomics analysis server using the same sequencing reads for classification. Results are based on RDP using a maximum *E*-value of 1e–2, a minimum identity of 80 %, and a minimum alignment length of 50 bp applying Bray–Curtis distance

and ward clustering. Data were normalized based on MG-RAST version 3.0. Sequences obtained during this study were deposited for public access in the MG-RAST server under the accession numbers 4516653.3, 4516654.3, 4516655.3, 4516656.3, 4516657.3, 4516658.3, 4516659.3, 4516660.3 and 4516661.3.

RESULTS

Pseudomonas savastanoi pv. *savastanoi* and *E. toletana* cells co-localized in the olive knot

Our laboratory has reported previously that the *Pseudomonas savastanoi* pv. *savastanoi* bacterial pathogen and the *E. toletana* bacterial resident share AHL QS signals in the olive knot, and when co-inoculated lead to a more aggressive disease as seen in a larger knot-size and larger population sizes in hyperplasic tissue for both bacterial species (Hosni *et al.*, 2011). In order to obtain an insight into this interspecies interaction between a pathogen and a harmless resident bacteria, *Pseudomonas savastanoi* pv. *savastanoi* and *E. toletana* cells were co-inoculated in *in vitro* micropropagated olive plants. Localization of bacteria was followed in real-time throughout knot development using stereoscopic epifluorescence microscopy combined with fluorescent tagging of *Pseudomonas savastanoi* pv. *savastanoi* DAPP-PG 722 and *E. toletana* DAPP-PG 735 with GFP and DsRedExpress, respectively (Figs 1, S1 and S2, available in the online Supplementary Material). Acquired images showed that when inoculated alone, *E. toletana* was not visible (the red observed was mostly autofluorescence of the plant) (Fig. 1c). In contrast, when *E. toletana* was co-inoculated with *Pseudomonas savastanoi* pv. *savastanoi*, *E. toletana* cells were abundant and visible at the inoculation site (Fig. 1a). In addition, in co-inoculation, epifluorescence revealed that *E. toletana* was distributed throughout the knot and the distribution of *E. toletana* matched the position of *Pseudomonas savastanoi* pv. *savastanoi*. Pathogen distribution as observed with epifluorescence did not show any significant alteration in the knot when inoculated alone compared with when co-inoculated with *E. toletana* (Fig. 1a, b). To further study the localization and distribution of the two species expressing autofluorescent proteins in the knot, transversal transections made via vibratome sectioning of the knot were analysed by CLSM (Fig. 2). This allowed exploration of the inner localization and distribution of *Pseudomonas savastanoi* pv. *savastanoi* and *E. toletana* within the knot without the necessity of further manipulation or staining of the samples. It was observed that *E. toletana*–DsRedExpress bacterial cells were localized in the vicinity of *Pseudomonas savastanoi* pv. *savastanoi*–GFP cells, suggesting that *E. toletana* strictly requires the close presence of *Pseudomonas savastanoi* pv. *savastanoi* for growth and persistence in the olive knot (Fig. 2a, b). In both single and co-inoculations (Fig. 2c, a, respectively), *Pseudomonas savastanoi* pv. *savastanoi* was present mainly on the surface or in the outer regions of the knots, as was reported to be its common location by Maldonado-González *et al.* (2013).

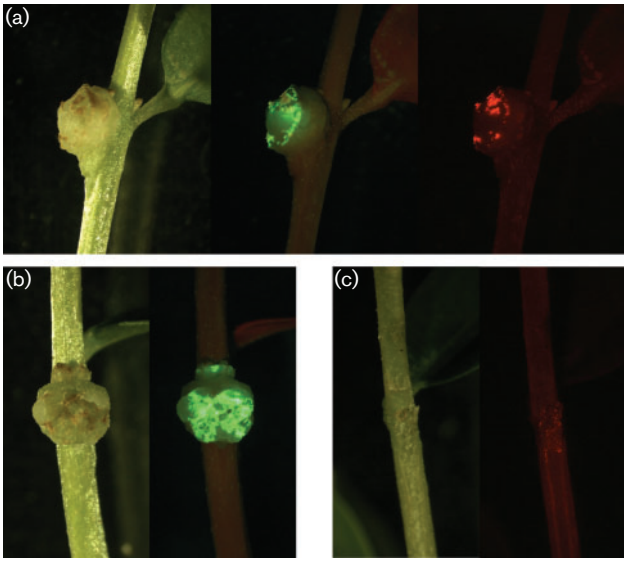

Fig. 1. Stereoscopic epifluorescence microscopy of (a) co-inoculated olive knots, and single inoculations with (b) *Pseudomonas savastanoi* pv. *savastanoi*–GFP and (c) *E. toletana*–DsRedExpress at 28 days p.i. Each image was acquired without a filter, with a GFP filter and/or with a RFP filter. Knot development and *Pseudomonas savastanoi* pv. *savastanoi*–GFP cell localization were similar to the single inoculation, whilst *E. toletana*–DsRedExpress cells were detected in different regions of the knot, always co-localizing with *Pseudomonas savastanoi* pv. *savastanoi*–GFP cells.

This indicated that the presence of *E. toletana* does not interfere with the preferred positioning within the knot of *Pseudomonas savastanoi* pv. *savastanoi*. The number of c.f.u. was measured at 0 and 28 days p.i. (Fig. 3). These results further corroborated the observations reported by Hosni *et al.* (2011) that in the presence of *Pseudomonas savastanoi* pv. *savastanoi*, c.f.u. numbers of *E. toletana* increased dramatically compared with single inoculations in adult 1-year-old olive plants, suggesting that observations in micropropagated olive plants can be correlated with what occurs in adult plants.

Pseudomonas savastanoi pv. *savastanoi* and *E. toletana*: *in silico* analysis of possible metabolic complementarity/exchanges

The previous report of AHL signal sharing and mutualistic behaviour as well as results shown here on strict co-localization of *Pseudomonas savastanoi* pv. *savastanoi* and *E. toletana* prompted us to analyse the recently published genomes of *Pseudomonas savastanoi* pv. *savastanoi* and *E. toletana* for possible metabolic complementarity and/or exchange. This is in view of the fact that both species grow more in the olive knot when both are present, indicating probable metabolic benefits [in the model used here using plantlets, only *E. toletana* grows more, whereas when using

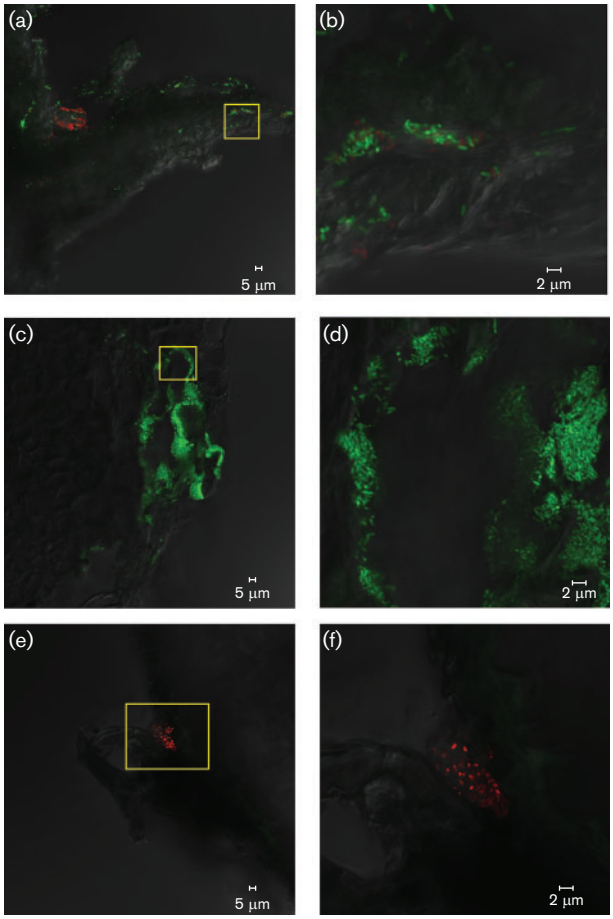

Fig. 2. CLSM images of transversal vibratome sections from (a) olive knots co-inoculated with *Pseudomonas savastanoi* pv. *savastanoi*–GFP and *E. toletana*–DsRedExpress, (c) inoculated with *Pseudomonas savastanoi* pv. *savastanoi*-GFP alone and (e) with *E. toletana*-DsRedExpress alone at 28 days p.i. Images were acquired with a ×63 objective. (b, d, f) Magnifications of highlighted area from (a), (c) and (e), respectively. Whilst *Pseudomonas savastanoi* pv. *savastanoi*–GFP could be found at different regions of the olive knot, *E. toletana*–DsRedExpress could only be found mixed with *Pseudomonas savastanoi* pv. *savastanoi*–GFP cells.

1-year-old olive plants in 60-day-old olive knots, they both grow more as reported by Hosni *et al.* (2011)]. We have performed an analysis on the metabolic potential of the two genomes via the reconstruction of metabolic pathways. This was achieved by feeding the annotated draft genome sequences of the two species separately (*Pseudomonas savastanoi* pv. *savastanoi* and *E. toletana*) and merged into Pathological (version 16.5) to predict their metabolic pathways. Reconstruction of predicted pathways from *Pseudomonas savastanoi* pv. *savastanoi* (SavCyc), *E. toletana* (TolCyc) and merged genomes (SavtolCyc) was made by matching all fed annotated enzymes with a database of enzymes with known function in order to predict possible single reactions that could be assembled into pathways to be tested experimentally (Karp *et al.*, 2010).

After creating the predicted pathways, the merged SavtolCyc was used to highlight all the new pathways that could emerge by joining the enzymes present in the two separate genomes. By evidencing all the reactions not shared between SavtolCyc/SavCyc and SavtolCyc/TolCyc on the cellular overview panel, an interactive visual method to track all singular contributions given by the two single bacterial species to the pathways was possible. Interestingly, several plant-related compounds, including shikimate, sucrose and salicylate (Fig. 4), were evidenced as their predicted degradation pathways were only complete when the genomes of the two species were combined. The degradation benefits of these aromatic compounds by bacterial consortia could be relevant since these phenolics are found commonly in plants. The presence of both *E. toletana* and *Pseudomonas savastanoi* pv. *savastanoi* could allow them to more efficiently degrade these compounds and utilize them as carbon sources or possibly to detoxify them as they could be toxic compounds if found at high concentrations. In addition, as salicylates and phenols are involved in the plant defence response in plant/pathogen interactions (Loake & Grant, 2007), olive/*Pseudomonas savastanoi* pv. *savastanoi* included (Roussos *et al.*, 2002), it is possible to hypothesize that the increased knot size we documented when *Pseudomonas savastanoi* pv. *savastanoi* and *E. toletana* were co-inoculated in olive plants (Hosni *et al.*, 2011) is due to the collaborative bacterial degradation of these plant defence compounds.

We performed growth tests on sucrose and salicylic acid of *Pseudomonas savastanoi* pv. *savastanoi* and *E. toletana* both as single and mixed cultures in minimal medium as described in Methods. It was established that *Pseudomonas savastanoi* pv. *savastanoi* could not grow on salicylic acid and sucrose as unique carbon sources (data not shown), confirming the *in silico* data described above. Similarly, *E. toletana* also could not grow in either sucrose or salicylic acid; this was partly in accordance with *in silico* metabolic profiles as *E. toletana* was predicted to utilize sucrose as a unique carbon source. We also performed mixed inoculations of *E. toletana* and *Pseudomonas savastanoi* pv. *savastanoi* with either sucrose or salicylic acid as the sole energy source as described in Methods. With salicylic acid, we did not observe any growth or transformation (as determined by HPLC analysis of spent supernatants) of the aromatic acid when both species were co-inoculated (data not shown). In minimal medium with sucrose, we observed similar results, i.e. no growth when using a mixed inoculum of *E. toletana* and *Pseudomonas savastanoi* pv. *savastanoi*. These initial binary growth tests did not evidence metabolic complementarity as indicated by the *in silico* analysis; the reason for this is unknown currently.

Identification of olive knot bacterial communities via metagenomics

Several bacterial species have been isolated from olive knots using standard culturing methods, possibly indicating the

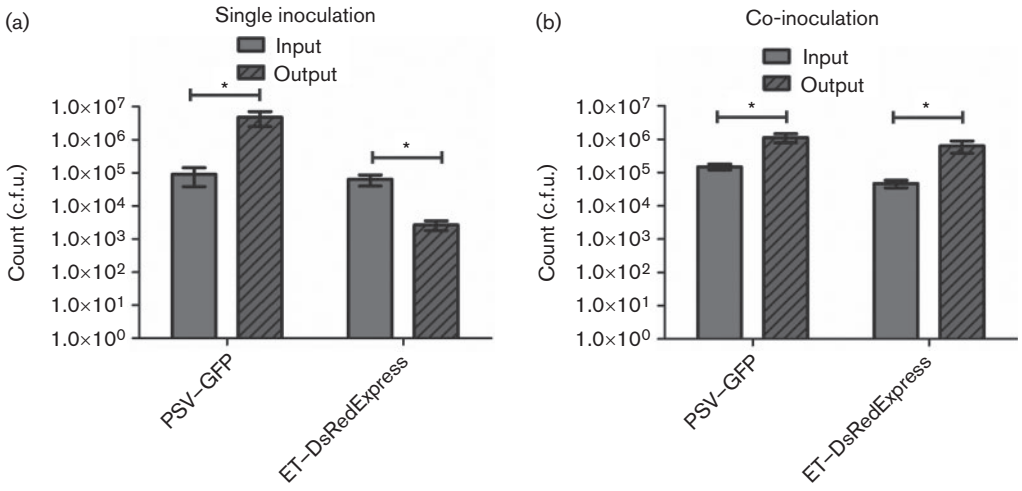

Fig. 3. Counts (c.f.u.) per inoculation site from (a) single and (b) co-inoculations using *Pseudomonas savastanoi* pv. *savastanoi* (PSV)–GFP and *E. toletana* (ET)–DsRedExpress. Gray bars represent number of cells used for inoculations and grey stripped bars represent c.f.u. retrieved from the inoculation site at 28 days p.i. The number of c.f.u. from the output (28 days p.i.) of *E. toletana*–DsRedExpress when co-inoculated with *Pseudomonas savastanoi* pv. *savastanoi*–GFP was more than two orders of magnitude higher than in single inoculations. Bars indicate means ± SD (n=3). Statistical significance was calculated using Student's *t*-test (*$P \leq 0.05$).

presence of a multispecies bacterial community within the olive knot (Moretti *et al.*, 2011; Ouzari *et al.*, 2008; Rojas *et al.*, 2004); many of these isolates belong to the genera *Erwinia* and *Pantoea*. It was of interest here to perform an exhaustive high-throughput analysis of the bacterial population inside olive knots since to our knowledge it has never been performed. Nine olive knots belonging to three different varieties of olive trees were collected from five regions of Italy, and a metagenomics approach based on the amplification and sequencing of the hypervariable 16s rRNA regions V1/V3 was used as described in Methods.

The data indicated rich and diverse bacterial life in this niche. We wish to note that the olive knot material was not sterilized prior to DNA purification as knots are porous and *Pseudomonas savastanoi* pv. *savastanoi* is known to also colonize intercellular spaces very near the surface. It is therefore possible that some of the bacterial species identified could be living on the surface of the olive knot as epiphytes. Among all bacterial 16S rRNA sequences retrieved, the gammaproteobacteria class was by far the most represented, accounting for up to 90 % of the total bacterial population (Table S1). Unsurprisingly, *Pseudomonas savastanoi* pv. *savastanoi* makes up almost 50 % of the bacterial load; the other most abundant bacteria belong to the *Pantoea* genera (Fig. 5) and, interestingly, *Pantoea agglomerans* has long been known to be commonly found in or associated with olive knots (Hosni *et al.*, 2011; Ouzari *et al.*, 2008; Quesada *et al.*, 2007; Savastano, 1886). The abundance of other genera showed some distinct features in every knot; however, among the different samples, a common core of bacterial genera was evident composed of *Clavibacter*, *Curtobacterium*, *Enterobacter*, *Erwinia*, *Hymenobacter*, *Kineococcus*, *Pectobacterium* and *Sphingomonas* (Fig. 5). The geographical position of extraction seems to have little effect on the common core; however, for genera that are underrepresented such as *Vibrio*, their abundance is greater in samples from the south of Italy.

DISCUSSION

Olive knot disease has thus far been studied poorly, mainly focusing on the causal agent *Pseudomonas savastanoi* pv. *savastanoi* (Marchi *et al.*, 2009; Matas *et al.*, 2009; Pérez-Martínez *et al.*, 2008, 2010; Ramos *et al.*, 2012; Rodríguez-Moreno *et al.*, 2009; Scortichini *et al.*, 2004; Surico *et al.*, 1985). The description of several virulence factors (Hosni *et al.*, 2011; Iacobellis *et al.*, 1994; Matas *et al.*, 2009; Matas *et al.*, 2012; Pérez-Martínez *et al.*, 2010; Ramos *et al.*, 2012; Rodríguez-Moreno *et al.*, 2008, 2009; Rodríguez-Palenzuela *et al.*, 2010; Rojas *et al.*, 2004; Surico *et al.*, 1985) and the normal localization on the intercellular space of the parenchymal tissue as a biofilm structure are, to our knowledge, the main recent discoveries (Rodríguez-Moreno *et al.*, 2009).

We reported previously that harmless *E. toletana* can colonize the knot in the presence of *Pseudomonas savastanoi* pv. *savastanoi* and demonstrated sharing of AHL QS signals as one of the interactions on the knot microenvironment (Hosni *et al.*, 2011). In addition, co-inoculation of *Pseudomonas savastanoi* pv. *savastanoi* with *E. toletana* resulted in increased knot size. Interestingly, this synergism was also observed when the AHL QS *luxI* AHL

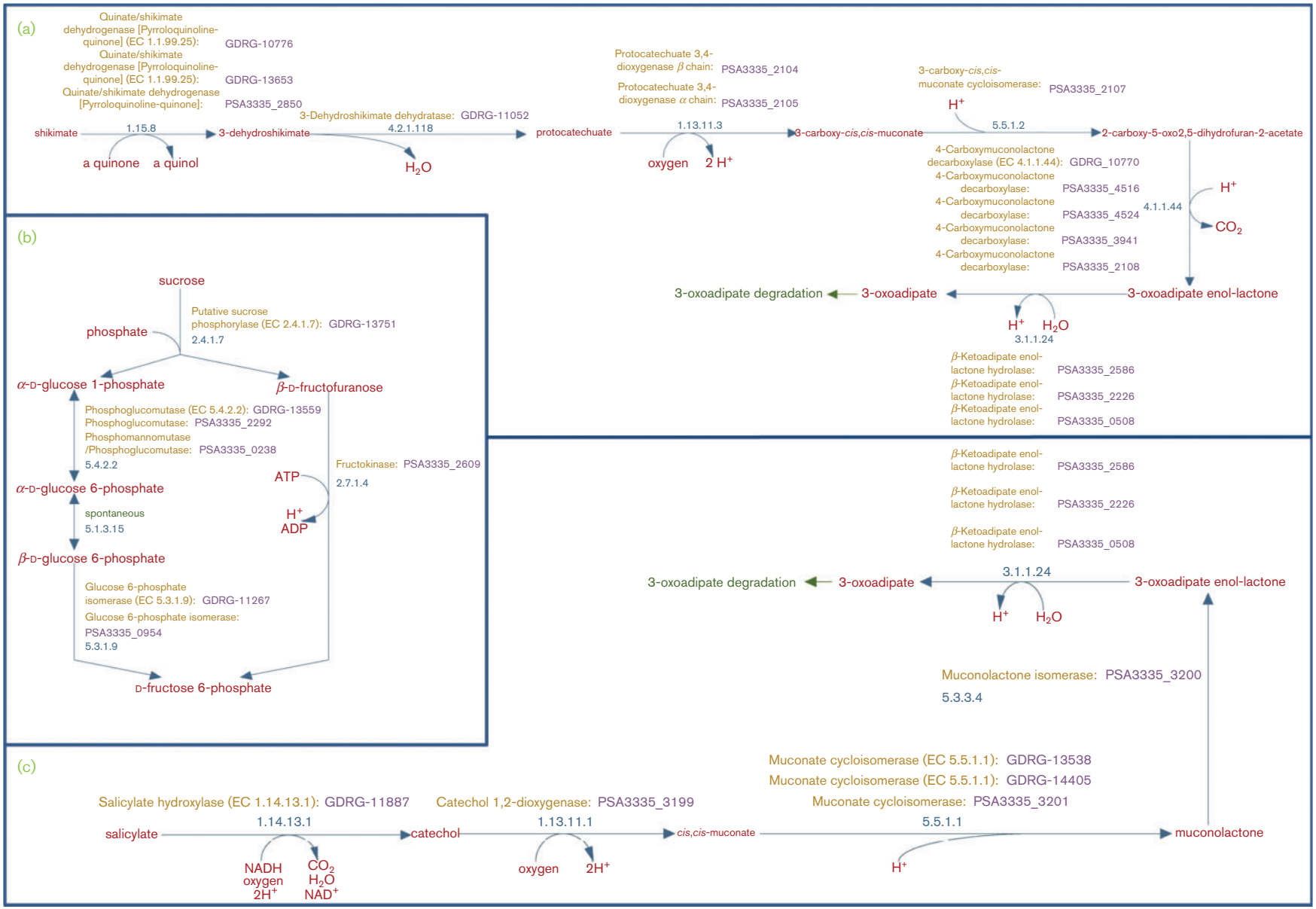
(a)
Quinate/shikimate dehydrogenase [Pyrroloquinoline-quinone] (EC 1.1.99.25): GDRG-10776
Quinate/shikimate dehydrogenase [Pyrroloquinoline-quinone] (EC 1.1.99.25): GDRG-13653
Quinate/shikimate dehydrogenase [Pyrroloquinoline-quinone]: PSA3335_2850
shikimate
1.15.8
a quinone
a quinol
3-dehydroshikimate
3-Dehydroshikimate dehydratase: GDRG-11052
4.2.1.118
H_2O
protocatechuate
Protocatechuate 3,4-dioxygenase β chain: PSA3335_2104
Protocatechuate 3,4-dioxygenase α chain: PSA3335_2105
1.13.11.3
oxygen
2 H^+
3-carboxy-cis,cis-muconate
3-carboxy-cis,cis-muconate cycloisomerase: PSA3335_2107
H^+
5.5.1.2
2-carboxy-5-oxo2,5-dihydrofuran-2-acetate
4-Carboxymuconolactone decarboxylase (EC 4.1.1.44): GDRG_10770
4-Carboxymuconolactone decarboxylase: PSA3335_4516
4-Carboxymuconolactone decarboxylase: PSA3335_4524
4-Carboxymuconolactone decarboxylase: PSA3335_3941
4-Carboxymuconolactone decarboxylase: PSA3335_2108
4.1.1.44
H^+
CO_2
3-oxoadipate enol-lactone
3-oxoadipate
3-oxoadipate degradation
H^+
H_2O
3.1.1.24
β-Ketoadipate enol-lactone hydrolase: PSA3335_2586
β-Ketoadipate enol-lactone hydrolase: PSA3335_2226
β-Ketoadipate enol-lactone hydrolase: PSA3335_0508
(b)
sucrose
phosphate
Putative sucrose phosphorylase (EC 2.4.1.7): GDRG-13751
2.4.1.7
α-D-glucose 1-phosphate
β-D-fructofuranose
Phosphoglucomutase (EC 5.4.2.2): GDRG-13559
Phosphoglucomutase: PSA3335_2292
Phosphomannomutase /Phosphoglucomutase: PSA3335_0238
5.4.2.2
α-D-glucose 6-phosphate
ATP
H^+
ADP
Fructokinase: PSA3335_2609
2.7.1.4
spontaneous
5.1.3.15
β-D-glucose 6-phosphate
Glucose 6-phosphate isomerase (EC 5.3.1.9): GDRG-11267
Glucose 6-phosphate isomerase: PSA3335_0954
5.3.1.9
D-fructose 6-phosphate
β-Ketoadipate enol-lactone hydrolase: PSA3335_2586
β-Ketoadipate enol-lactone hydrolase: PSA3335_2226
β-Ketoadipate enol-lactone hydrolase: PSA3335_0508
3-oxoadipate degradation
3-oxoadipate
3.1.1.24
3-oxoadipate enol-lactone
H^+
H_2O
Muconolactone isomerase: PSA3335_3200
5.3.3.4
(c)
Muconate cycloisomerase (EC 5.5.1.1): GDRG-13538
Muconate cycloisomerase (EC 5.5.1.1): GDRG-14405
Muconate cycloisomerase: PSA3335_3201
5.5.1.1
Salicylate hydroxylase (EC 1.14.13.1): GDRG-11887
1.14.13.1
salicylate
NADH
oxygen
2H^+
CO_2
H_2O
NAD^+
catechol
Catechol 1,2-dioxygenase: PSA3335_3199
1.13.11.1
oxygen
2H^+
cis,cis-muconate
H^+
muconolactone

Fig. 4. Graphical representations of complementary metabolic pathways between *Pseudomonas savastanoi* pv. *savastanoi* and *E. toletana*. Codes for genes encoded by *Pseudomonas savastanoi* pv. *savastanoi* possess the prefix PSA, whilst codes for genes encoded by *E. toletana* possess the prefix GDRG. In the pathways presented for the degradation of shikimate (a), sucrose (b) and salicylate (c), there are reactions that could only be catalysed by one of the species, meaning that the absence of one of the two species would impair the complete mineralization of these compounds.

synthase mutant of *E. toletana* was used, indicating that most likely signal sharing was not the only interaction taking place between *E. toletana* and *Pseudomonas savastanoi* pv. *savastanoi* (Hosni *et al.*, 2011). The localization of *E. toletana* in relation to *Pseudomonas savastanoi* pv. *savastanoi* during knot development could provide insights on possible mechanisms that play a role in the interaction. By using epifluorescence stereoscopic microscopy and CLSM, we observed that *E. toletana* was consistently in the vicinity of *Pseudomonas savastanoi* pv. *savastanoi*, possibly meaning that *E. toletana* requires this close proximity with *Pseudomonas savastanoi* pv. *savastanoi* for its persistence and growth in the olive knot. This closeness is in line with AHL signal sharing observed previously to be taking place between *Pseudomonas savastanoi* pv. *savastanoi* and *E. toletana* in the olive knot (Hosni *et al.*, 2011); AHLs of *E. toletana* can therefore easily diffuse into *Pseudomonas savastanoi* pv. *savastanoi*. In addition, close proximity can result in community signalling by cell contact and/or facilitated sharing of metabolites. *Pseudomonas savastanoi* pv. *savastanoi* cells actually form biofilm structures in the olive knot

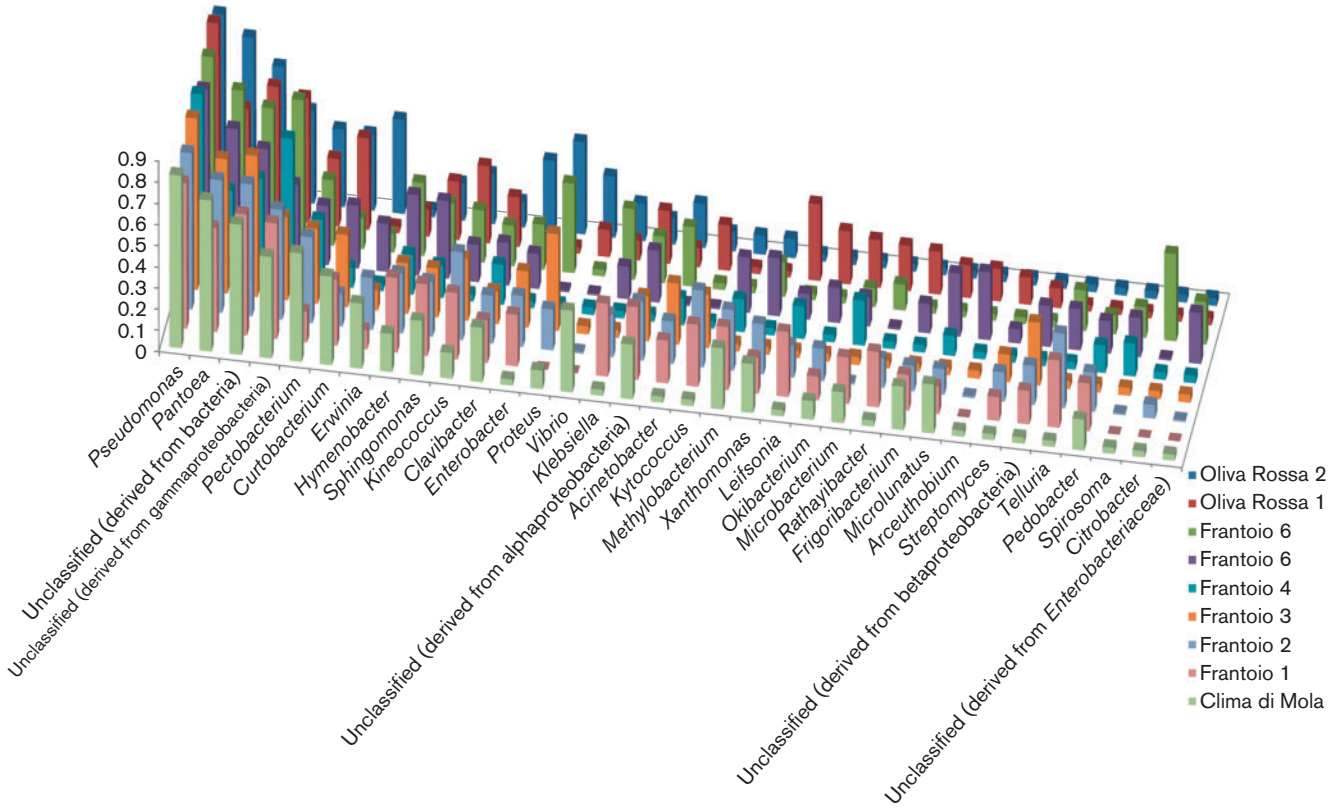

Fig. 5. Graphical representation of bacterial abundance determined from the metagenomics studies of nine olive knots. Different colours are assigned to each of the nine samples and the organization of the key follows the same order as the samples on the graph (from bottom to top). Genera *Pseudomonas* and *Pantoea* are clearly the main constituents of these communities. *Pectobacterium*, *Curtobacterium*, *Kineococcus*, *Sphingomonas*, *Clavibacter* and *Hymenobacter* compose a group that is less abundant if compared with *Pseudomonas* and *Pantoea*, but these genera are found consistently in all samples. Although *Erwinia*, *Proteus*, *Enterobacter*, *Acinetobacter*, *Klebsiella*, *Kytococcus*, *Methylobacterium*, *Xanthomonas* and *Leifsonia* are not present in all samples, the abundance of these genera in some samples is significant. A considerable number of sequences could not be assigned to any genera with accuracy. Data were normalized according to the MG-RAST manual.

(Rodríguez-Moreno *et al.*, 2009), thus this close proximity of *E. toletana* during knot formation suggests that mixed biofilms most probably occur, and this could be more advantageous for both species via facilitating diffusion of metabolites and signals, possibly resulting in a more stable biofilm.

It is believed that metabolic sharing/complementarity is one of the features that allows the formation of stable bacterial consortia (Egland *et al.*, 2004; Kim *et al.*, 2008). For example, the diffusion of metabolites can be transformed by one species that can then be further utilized by the neighbouring species, resulting in a mutualistic interaction (Egland *et al.*, 2004; Kim *et al.*, 2008; Ramsey *et al.*, 2011). We have evaluated this possibility between *E. toletana* and *Pseudomonas savastanoi* pv. *savastanoi* using an *in silico* approach. By predicting all the metabolic pathways that each of the two organisms were able to perform individually, we were able to determine incomplete pathways due to the absence of key enzymes on one genome that could be completed by the presence of these given enzymes on the genome of the second species. Possible degradation pathways of several plant-related aromatic compounds, some of which are associated with plant defence, were only possible *in silico* when the two genomes were joined. Compounds such as salicylate, shikimate and sucrose are examples that could only be mineralized by the dual-species community. We have tested possible metabolic complementarity using growth tests in liquid and solid media using salicylic acid and sucrose. Under the conditions we tested, we could not detect binary growth of *Pseudomonas savastanoi* pv. *savastanoi* and *E. toletana*, providing evidence for metabolic sharing/complementarity in the mineralization of these compounds. It could be that under the conditions we tested it was not possible to initiate such an interaction that takes place *in planta*. Future studies need to focus in this direction using all the possible compounds revealed by the *in silico* analysis that could be transformed using metabolic sharing. It is also possible that the Pathway Tools analysis overpredicts pathways and that this information needs to be validated carefully.

The metagenomics studies proved that apart from *Pseudomonas savastanoi* pv. *savastanoi*, there was a dominance of *Pantoea* throughout all nine samples; the presence of *Pantoea agglomerans* on olive knots has been extensively described and its role in knot development remains unclear (Hosni *et al.*, 2011; Marchi *et al.*, 2006). These results indicate that the enrichment of *Pantoea* in the knot environment is an important aspect that merits further attention. It was surprising to see the presence of so many different genera in the olive knot; the consensus of genera present in the different olive knots could indicate a community structure present in the olive knot that could have evolved together with *Pseudomonas savastanoi* pv. *savastanoi*. Our studies and observations with *E. toletana* could be then applicable to other species, and most probably also to multispecies studies involving more than two bacterial species. *Clavibacter*, *Curtobacterium*, *Hymenobacter*, *Kineococcus*, *Proteus* and *Sphingomonas* were present in almost all samples, and to our knowledge they have never been reported in the olive knot. The descriptions of species within these genera being able to tolerate high concentrations of copper (Bagwell *et al.*, 2010), facilitating the mineralization of polycyclic aromatic compounds (Manickam *et al.*, 2012) or even associated with fungi that degrades decaying matter (Kamei *et al.*, 2012) also show diverse biological roles that could aid the maintenance of the disease. Another interesting observation is that alpha diversity seems to be related directly to the geographical location from where the sample was collected (data not shown). Samples from the south of Italy (Clima di Mola, and Oliva Rossa 1 and 2) show a higher diversity when compared with samples from central Italy (Frantoio 1–6). This might be due to the difference of mean temperature and humidity (Teviotdale & Krueger, 2004) or possibly the susceptibility of distinct cultivars of olive trees (Penyalver *et al.*, 2006). Even though a core group of bacterial genera seems to be present in all samples, a large part of the community present in the nine different samples shows considerable variation in abundance. Importantly, however, the phylogenetic variation present among the samples might not necessarily reflect on the genetic pool (Burke *et al.*, 2011). It is possible that major roles in community interactions are played by the genera that are found in all samples (e.g. *Pantoea*), whilst the other bacteria present in only some or even one of the samples might be recruited in response to some specific traits (e.g. cultivar) or by diverse environmental conditions.

In summary, we shown that *Pseudomonas savastanoi* pv. *savastanoi* and *E. toletana* co-localize during knot development, and the presence of *Pseudomonas savastanoi* pv. *savastanoi* is essential for the maintenance of *E. toletana* cells on olive knots. This is a clear example of harmless and beneficial organisms teaming up in a disease (Venturi & da Silva, 2012). The close proximity of *E. toletana* and *Pseudomonas savastanoi* pv. *savastanoi* in the knot indicates that they are most probably interacting via a variety of mechanism that we have discussed. Using *in silico* analysis, we found compounds that could be shared *in planta*, possibly improving the stability of the community. Metagenomics sequencing revealed that some genera are commonly found associated with the olive knot, nevertheless high bacterial diversity occurs among different knots, and this could be related to environmental factors and/or cultivars of *O. europaea*. This study opens new possibilities on the *Pseudomonas savastanoi* pv. *savastanoi*/*E. toletana* interaction and presents a valid model to study multispecies interactions in a bacterial disease.

ACKNOWLEDGEMENTS

D. P. D. S. is funded by an ICGEB fellowship. We thank Giulia Devescovi, Giuliano Degrassi and Iris Bertani for interest and constant discussion. This study was supported partially by Spanish

Plan Nacional I+D+i (grant AGL2011-30343-C02-01) from the Ministerio de Economía y Competitividad (MINECO), co-financed by FEDER.

REFERENCES

Bagwell, C. E., Hixson, K. K., Milliken, C. E., Lopez-Ferrer, D. & Weitz, K. K. (2010). Proteomic and physiological responses of *Kineococcus radiotolerans* to copper. *PLoS ONE* **5**, e12427.

Burke, C., Steinberg, P., Rusch, D., Kjelleberg, S. & Thomas, T. (2011). Bacterial community assembly based on functional genes rather than species. *Proc Natl Acad Sci U S A* **108**, 14288–14293.

Caspi, R., Altman, T., Dreher, K., Fulcher, C. A., Subhraveti, P., Keseler, I. M., Kothari, A., Krummenacker, M., Latendresse, M. & other authors (2012). The MetaCyc database of metabolic pathways and enzymes and the BioCyc collection of pathway/genome databases. *Nucleic Acids Res* **40**, D742–D753.

Driver, J. A. & Kuniyuki, A. (1984). *In vitro* propagation of paradox wallnut rootstock. *HortScience* **19**, 507–509.

Duan, K., Dammel, C., Stein, J., Rabin, H. & Surette, M. G. (2003). Modulation of *Pseudomonas aeruginosa* gene expression by host microflora through interspecies communication. *Mol Microbiol* **50**, 1477–1491.

Egland, P. G., Palmer, R. J., Jr & Kolenbrander, P. E. (2004). Interspecies communication in *Streptococcus gordonii–Veillonella atypica* biofilms: signaling in flow conditions requires juxtaposition. *Proc Natl Acad Sci U S A* **101**, 16917–16922.

Hosni, T., Moretti, C., Devescovi, G., Suarez-Moreno, Z. R., Fatmi, M. B., Guarnaccia, C., Pongor, S., Onofri, A., Buonaurio, R. & Venturi, V. (2011). Sharing of quorum-sensing signals and role of interspecies communities in a bacterial plant disease. *ISME J* **5**, 1857–1870.

Human Microbiome Project Consortium (2012). Structure, function and diversity of the healthy human microbiome. *Nature* **486**, 207–214.

Iacobellis, N. S., Sisto, A., Surico, G., Evidente, A. & DiMaio, E. (1994). Pathogenicity of *Pseudomonas syringae* subsp. *savastanoi* mutants defective in phytohormone production. *J Phytopathol* **140**, 238–248.

Kamei, I., Yoshida, T., Enami, D. & Meguro, S. (2012). Coexisting *Curtobacterium* bacterium promotes growth of white-rot fungus *Stereum* sp. *Curr Microbiol* **64**, 173–178.

Karp, P. D., Paley, S. M., Krummenacker, M., Latendresse, M., Dale, J. M., Lee, T. J., Kaipa, P., Gilham, F., Spaulding, A. & other authors (2010). Pathway Tools version 13.0: integrated software for pathway/genome informatics and systems biology. *Brief Bioinform* **11**, 40–79.

Kim, H. J., Boedicker, J. Q., Choi, J. W. & Ismagilov, R. F. (2008). Defined spatial structure stabilizes a synthetic multispecies bacterial community. *Proc Natl Acad Sci U S A* **105**, 18188–18193.

Koch, B., Jensen, L. E. & Nybroe, O. (2001). A panel of Tn*7*-based vectors for insertion of the *gfp* marker gene or for delivery of cloned DNA into Gram-negative bacteria at a neutral chromosomal site. *J Microbiol Methods* **45**, 187–195.

Kolenbrander, P. E., Palmer, R. J., Jr, Periasamy, S. & Jakubovics, N. S. (2010). Oral multispecies biofilm development and the key role of cell–cell distance. *Nat Rev Microbiol* **8**, 471–480.

Korgaonkar, A., Trivedi, U., Rumbaugh, K. P. & Whiteley, M. (2013). Community surveillance enhances *Pseudomonas aeruginosa* virulence during polymicrobial infection. *Proc Natl Acad Sci U S A* **110**, 1059–1064.

Kovach, M. E., Elzer, P. H., Hill, D. S., Robertson, G. T., Farris, M. A., Roop, R. M., II & Peterson, K. M. (1995). Four new derivatives of the broad-host-range cloning vector pBBR1MCS, carrying different antibiotic-resistance cassettes. *Gene* **166**, 175–176.

Kuramitsu, H. K., He, X., Lux, R., Anderson, M. H. & Shi, W. (2007). Interspecies interactions within oral microbial communities. *Microbiol Mol Biol Rev* **71**, 653–670.

Lambertsen, L., Sternberg, C. & Molin, S. (2004). Mini-Tn*7* transposons for site-specific tagging of bacteria with fluorescent proteins. *Environ Microbiol* **6**, 726–732.

Loake, G. & Grant, M. (2007). Salicylic acid in plant defence – the players and protagonists. *Curr Opin Plant Biol* **10**, 466–472.

Maldonado-González, M. M., Prieto, P., Ramos, C. & Mercado-Blanco, J. (2013). From the root to the stem: interaction between the biocontrol root endophyte *Pseudomonas fluorescens* PICF7 and the pathogen *Pseudomonas savastanoi* NCPPB 3335 in olive knots. *Microb Biotechnol* **6**, 275–287.

Manickam, N., Bajaj, A., Saini, H. S. & Shanker, R. (2012). Surfactant mediated enhanced biodegradation of hexachlorocyclohexane (HCH) isomers by *Sphingomonas* sp. NM05. *Biodegradation* **23**, 673–682.

Mansfield, J., Genin, S., Magori, S., Citovsky, V., Sriariyanum, M., Ronald, P., Dow, M., Verdier, V., Beer, S. V. & other authors (2012). Top 10 plant pathogenic bacteria in molecular plant pathology. *Mol Plant Pathol* **13**, 614–629.

Marchi, G., Sisto, A., Cimmino, A., Andolfi, A., Cipriani, M. G., Evidente, A. & Surico, G. (2006). Interaction between *Pseudomonas savastanoi* pv. *savastanoi* and *Pantoea agglomerans* in olive knots. *Plant Pathol* **55**, 614–624.

Marchi, G., Mori, B., Pollacci, P., Mencuccini, M. & Surico, G. (2009). Systemic spread of *Pseudomonas savastanoi* pv. *savastanoi* in olive explants. *Plant Pathol* **58**, 152–158.

Matas, I. M., Pérez-Martínez, I., Quesada, J. M., Rodríguez-Herva, J. J., Penyalver, R. & Ramos, C. (2009). *Pseudomonas savastanoi* pv. *savastanoi* contains two *iaaL* paralogs, one of which exhibits a variable number of a trinucleotide (TAC) tandem repeat. *Appl Environ Microbiol* **75**, 1030–1035.

Matas, I. M., Lambertsen, L., Rodríguez-Moreno, L. & Ramos, C. (2012). Identification of novel virulence genes and metabolic pathways required for full fitness of *Pseudomonas savastanoi* pv. *savastanoi* in olive (*Olea europaea*) knots. *New Phytol* **196**, 1182–1196.

Maurice, C. F., Haiser, H. J. & Turnbaugh, P. J. (2013). Xenobiotics shape the physiology and gene expression of the active human gut microbiome. *Cell* **152**, 39–50.

Meyer, F., Paarmann, D., D'Souza, M., Olson, R., Glass, E. M., Kubal, M., Paczian, T., Rodriguez, A., Stevens, R. & other authors (2008). The metagenomics RAST server – a public resource for the automatic phylogenetic and functional analysis of metagenomes. *BMC Bioinformatics* **9**, 386.

Mitri, S., Xavier, J. B. & Foster, K. R. (2011). Social evolution in multispecies biofilms. *Proc Natl Acad Sci U S A* **108** (Suppl 2), 10839–10846.

Moretti, C., Hosni, T., Vandemeulebroecke, K., Brady, C., De Vos, P., Buonaurio, R. & Cleenwerck, I. (2011). *Erwinia oleae* sp. nov., isolated from olive knots caused by *Pseudomonas savastanoi* pv. *savastanoi*. *Int J Syst Evol Microbiol* **61**, 2745–2752.

Ouzari, H., Khsairi, A., Raddadi, N., Jaoua, L., Hassen, A., Zarrouk, M., Daffonchio, D. & Boudabous, A. (2008). Diversity of auxin-producing bacteria associated to *Pseudomonas savastanoi*-induced olive knots. *J Basic Microbiol* **48**, 370–377.

Passos da Silva, D., Devescovi, G., Paszkiewicz, K., Moretti, C., Buonaurio, R., Studholme, D. J. & Venturi, V. (2013). Draft genome sequence of *Erwinia toletana*, a bacterium associated with olive knots caused by *Pseudomonas savastanoi* pv. *savastanoi*. *Genome Announc* **1**, e00205-13.

Penyalver, R., García, A., Ferrer, A., Bertolini, E., Quesada, J. M., Salcedo, C. I., Piquer, J., Pérez-Panadés, J., Carbonell, E. A. & other authors (2006). Factors affecting *Pseudomonas savastanoi* pv. *savastanoi* plant inoculations and their use for evaluation of olive cultivar susceptibility. *Phytopathology* **96**, 313–319.

Pérez-Martínez, I., Zhao, Y., Murillo, J., Sundin, G. W. & Ramos, C. (2008). Global genomic analysis of *Pseudomonas savastanoi* pv. *savastanoi* plasmids. *J Bacteriol* **190**, 625–635.

Pérez-Martínez, I., Rodríguez-Moreno, L., Lambertsen, L., Matas, I. M., Murillo, J., Tegli, S., Jiménez, A. J. & Ramos, C. (2010). Fate of a *Pseudomonas savastanoi* pv. *savastanoi* type III secretion system mutant in olive plants (*Olea europaea* L.). *Appl Environ Microbiol* **76**, 3611–3619.

Quesada, J. M., García, A., Bertolini, E., López, M. M. & Penyalver, R. (2007). Recovery of *Pseudomonas savastanoi* pv. *savastanoi* from symptomless shoots of naturally infected olive trees. *Int Microbiol* **10**, 77–84.

Quesada, J. M., Penyalver, R., Pérez-Panadés, J., Salcedo, C. I., Carbonell, E. A. & López, M. M. (2010). Dissemination of *Pseudomonas savastanoi* pv. *savastanoi* populations and subsequent appearance of olive knot disease. *Plant Pathol* **59**, 262–269.

Ramos, C., Matas, I. M., Bardaji, L., Aragón, I. M. & Murillo, J. (2012). *Pseudomonas savastanoi* pv. *savastanoi*: some like it knot. *Mol Plant Pathol* **13**, 998–1009.

Ramsey, M. M., Rumbaugh, K. P. & Whiteley, M. (2011). Metabolite cross-feeding enhances virulence in a model polymicrobial infection. *PLoS Pathog* **7**, e1002012.

Rodríguez-Moreno, L., Barceló-Muñoz, A. & Ramos, C. (2008). *In vitro* analysis of the interaction of *Pseudomonas savastanoi* pvs. *savastanoi* and *nerii* with micropropagated olive plants. *Phytopathology* **98**, 815–822.

Rodríguez-Moreno, L., Jiménez, A. J. & Ramos, C. (2009). Endopathogenic lifestyle of *Pseudomonas savastanoi* pv. *savastanoi* in olive knots. *Microb Biotechnol* **2**, 476–488.

Rodríguez-Palenzuela, P., Matas, I. M., Murillo, J., López-Solanilla, E., Bardaji, L., Pérez-Martínez, I., Rodríguez-Moskera, M. E., Penyalver, R., López, M. M. & other authors (2010). Annotation and overview of the *Pseudomonas savastanoi* pv. *savastanoi* NCPPB 3335 draft genome reveals the virulence gene complement of a tumour-inducing pathogen of woody hosts. *Environ Microbiol* **12**, 1604–1620.

Rojas, A. M., de Los Rios, J. E., Fischer-Le Saux, M., Jimenez, P., Reche, P., Bonneau, S., Sutra, L., Mathieu-Daudé, F. & McClelland, M. (2004). *Erwinia toletana* sp. nov., associated with *Pseudomonas savastanoi*-induced tree knots. *Int J Syst Evol Microbiol* **54**, 2217–2222.

Roussos, P. A., Pontikis, C. A. & Tsantili, E. (2002). Root promoting compounds detected in olive knot extract in high quantities as a response to infection by the bacterium *Pseudomonas savastanoi* pv. *savastanoi*. *Plant Sci* **163**, 533–541.

Savastano, L. (1886). Les maladies de l'olivier, et la tuberculose en particulier. *C R Acad Agric Fr* **CIII**, 103–114.

Schroth, M. N., Osgood, J. W. & Miller, T. D. (1973). Quantitative assessment of the effect of the olive knot disease on olive yield and quality. *Phytopathology* **63**, 1064–1065.

Scortichini, M., Rossi, M. P. & Salerno, M. (2004). Relationship of genetic structure of *Pseudomonas savastanoi* pv. *savastanoi* populations from Italian olive trees and patterns of host genetic diversity. *Plant Pathol* **53**, 491–497.

Sessitsch, A., Hardoim, P., Döring, J., Weilharter, A., Krause, A., Woyke, T., Mitter, B., Hauberg-Lotte, L., Friedrich, F. & other authors (2012). Functional characteristics of an endophyte community colonizing rice roots as revealed by metagenomic analysis. *Mol Plant Microbe Interact* **25**, 28–36.

Stolyar, S., Van Dien, S., Hillesland, K. L., Pinel, N., Lie, T. J., Leigh, J. A. & Stahl, D. A. (2007). Metabolic modeling of a mutualistic microbial community. *Mol Syst Biol* **3**, 92.

Surico, G., Iacobellis, N. S. & Sisto, A. (1985). Studies on the role of indole-3-acetic acid and cytokinins in the formation of knots on olive and oleander plants by *Pseudomonas syringae* pv. *savastanoi*. *Physiol Plant Pathol* **26**, 309–320.

Teviotdale, B. L. & Krueger, W. H. (2004). Effects of timing of copper sprays, defoliation, rainfall, and inoculum concentration on incidence of olive knot disease. *Plant Dis* **88**, 131–135.

Venturi, V. & da Silva, D. P. (2012). Incoming pathogens team up with harmless 'resident' bacteria. *Trends Microbiol* **20**, 160–164.

Wang, Z., Klipfell, E., Bennett, B. J., Koeth, R., Levison, B. S., Dugar, B., Feldstein, A. E., Britt, E. B., Fu, X. & other authors (2011). Gut flora metabolism of phosphatidylcholine promotes cardiovascular disease. *Nature* **472**, 57–63.

Young, J. (2004). Olive knot and its pathogens. *Australas Plant Pathol* **33**, 33–39.

Edited by: W. Achouak

MPMI Vol. 27, No. 5, 2014, pp. 424–436. http://dx.doi.org/10.1094/MPMI-07-13-0206-R

e-Xtra*

Translocation and Functional Analysis of *Pseudomonas savastanoi* pv. *savastanoi* NCPPB 3335 Type III Secretion System Effectors Reveals Two Novel Effector Families of the *Pseudomonas syringae* Complex

Isabel M. Matas,[1] M. Pilar Castañeda-Ojeda,[1] Isabel M. Aragón,[1] María Antúnez-Lamas,[2,3] Jesús Murillo,[4] Pablo Rodríguez-Palenzuela,[2,3] Emilia López-Solanilla,[2,3] and Cayo Ramos[1]

[1]Instituto de Hortofruticultura Subtropical y Mediterránea "La Mayora", Universidad de Málaga-Consejo Superior de Investigaciones Científicas (IHSM-UMA-CSIC), Área de Genética, Facultad de Ciencias, Campus Teatinos s/n, E-29010 Málaga, Spain; [2]Centro de Biotecnología y Genómica de Plantas (CBGP), Universidad Politécnica de Madrid-Instituto Nacional de Investigación y Tecnología Agraria y Alimentaria, Parque Científico y Tecnológico de la UPM, Campus de Montegancedo, 28223 Pozuelo de Alarcón, Madrid; [3]Departamento de Biotecnología. Escuela Técnica Superior de Ingenieros Agrónomos, UPM. Avda, Complutense S/N, 28040, Madrid; [4]Departamento de Producción Agraria, ETS Ingenieros Agrónomos, Universidad Pública de Navarra, 31006 Pamplona, Spain

Submitted 26 July 2013. Accepted 28 November 2013.

***Pseudomonas savastanoi* pv. *savastanoi* NCPPB 3335 causes olive knot disease and is a model pathogen for exploring bacterial infection of woody hosts. The type III secretion system (T3SS) effector repertoire of this strain includes 31 effector candidates plus two novel candidates identified in this study which have not been reported to translocate into plant cells. In this work, we demonstrate the delivery of seven NCPPB 3335 effectors into *Nicotiana tabacum* leaves, including three proteins from two novel families of the *P. syringae* complex effector super-repertoire (HopBK and HopBL), one of which comprises two proteins (HopBL1 and HopBL2) that harbor a SUMO protease domain. When delivered by *P. fluorescens* heterologously expressing a *P. syringae* T3SS, all seven effectors were found to suppress the production of defense-associated reactive oxygen species. Moreover, six of these effectors, including the truncated versions of HopAA1 and HopAZ1 encoded by NCPPB 3335, suppressed callose deposition. The expression of HopAZ1 and HopBL1 by functionally effectorless *P. syringae* pv. *tomato* DC3000D28E inhibited the hypersensitive response in tobacco and, additionally, expression of HopBL2 by this strain significantly increased its competitiveness in *N. benthamiana.* DNA sequences encoding HopBL1 and HopBL2 were uniquely detected in a collection of 31 *P. savastanoi* pv. *savastanoi* strains and other *P. syringae* strains isolated from woody hosts, suggesting a relevant role of these two effectors in bacterial interactions with olive and other woody plants.**

Current address for I. M. Matas: Instituto de Agrobiotecnología, CSIC-UPNA-Gobierno de Navarra, Universidad Pública de Navarra, Campus Arrosadía, 31192 Mutilva, Spain.

Corresponding author: C. Ramos; Telephone: +34-95213 1955; Fax: +34-95213 2001; E-mail: crr@uma.es

*The *e*-Xtra logo stands for "electronic extra" and indicates that six supplementary tables and one supplementary figure are published online.

Type III secretion system (T3SS) effectors (T3E) delivered by bacterial pathogens are key elements for establishing infection. In bacterial plant pathogens, these proteins primarily interfere with the plant immune system at two main defense layers: pathogen-associated molecular pattern (PAMP)-triggered immunity (PTI) and effector-triggered immunity (ETI) (Chisholm et al. 2006; Jones and Dangl 2006). Because there is an overlap between these two layers of immunity, T3E may target PTI, ETI, or both (Boller and Felix 2009; Katagiri and Tsuda 2010). Examples include the *Pseudomonas syringae* effector AvrPtoB, which has been demonstrated to suppress both PTI and ETI (de Torres et al. 2006; Lin et al. 2006). The production of reactive oxygen species (ROS) is one of the earliest cellular responses associated with plant immunity (Doke 1983). ROS can directly strengthen the host cell wall (Bradley et al. 1992; Huckelhoven 2007) and are important signals that mediate defense gene activation (Levine et al. 1994; Torres and Dangl 2005). Moreover, this oxidative burst is associated with the hypersensitive response (HR), a localized response at the site of pathogen attack characterized by the induction of programmed cell death (Mur et al. 2008) that limits pathogen spread.

The growing availability of bacterial genomes and the evolution of bioinformatics tools have revolutionized the discovery of novel plant pathogen effectors. Genome-wide searches for motifs shared by known T3E have recently revealed a repertoire of these proteins in plant bacterial pathogens, including *P. syringae* and related pathogens (Collmer et al. 2009; Lindeberg 2012; Lindeberg et al. 2008). The *P. syringae* complex, which encompasses up to 10 *Pseudomonas* spp. and 60 *P. syringae* pathovars (Young 2010), has become a model for a systems-level exploration of effector repertoires and their functions in biotrophic pathogenesis. T3E proteins of *P. syringae* and related plant pathogens are generically known as Hrp outer proteins (hops) (Lindeberg et al. 2005). Over 60 effector families, whose expression is transcriptionally activated by the alternative σ factor HrpL (Xiao and Hutcheson 1994), are currently defined in the *P. syringae* pangenome. Currently, three *P. syringae* strains—*P. syringae* pv. *tomato* DC3000 (Alfano and Collmer 1996), *P. syringae* pv. *phaseolicola* 1448A (Jackson et

al. 1999) and *P. syringae* pv. *syringae* B728a (Hirano and Upper 2000)—prevail as model systems for identifying and functionally analyzing protein effectors. Each strain provides a different perspective on the complex interactions of this pathogen with herbaceous plants. Comparisons of T3E gene repertoires within a phylogenetic context has elucidated the molecular basis of host specialization and host range evolution in fully or partially sequenced *P. syringae* pathovars (Baltrus et al. 2011, 2012; Lindeberg 2012; Lindeberg et al. 2012). However, a molecular mechanism governing *P. syringae* pathovar adaptation to woody hosts remains undefined.

P. savastanoi pv. *savastanoi* NCPPB 3335 causes olive knot disease and is a model bacterium to study the molecular basis of disease production and tumor formation in woody hosts (Ramos et al. 2012). As previously established for several *P. syringae* strains (Cunnac et al. 2009; Mansfield 2009), *P. savastanoi* pv. *savastanoi* NCPPB 3335 T3SS is required for infection establishment and knot formation on olive plants (Matas et al. 2012; Pérez-Martínez et al. 2010). Additionally, bioinformatics analysis of the draft genome sequence of NCPPB 3335 identified 30 putative T3E in this pathogen, 19 of which were more than 65% similar to previously described effectors based on their amino acid identity (Rodríguez-Palenzuela et al. 2010). Furthermore, sequencing of the three-plasmid complement of this strain revealed that two of these T3E genes, *hopAF1* and *hopAO1*, are encoded in plasmids (Bardaji et al. 2011). A later revision of this genome sequence discarded three of the previously identified nonhomologous T3SS and identified four new candidate effectors in NCPPB 3335: AvrPto1, HopAT1, HopAZ1, and AvrRpm2 (Ramos et al. 2012) (Hop Database). Among these 31 T3E candidates, only two are homologs of *P. syringae* T3E with a previously demonstrated enzymatic function (i.e., HopAO1, a protein tyrosine phosphatase [Underwood et al. 2007], and HopAB1, an E3 ubiquitin ligase [Janjusevic et al. 2006]). Moreover, translocation of effector proteins into plant cells through the T3SS has not been reported to date for *P. savastanoi* pv. *savastanoi* or any other *P. syringae* pathovar of woody hosts.

In this work, we searched for additional *P. savastanoi* pv. *savastanoi* NCPPB 3335 T3E candidates on the basis of protein-domain similarity to known plant-pathogen effectors. A group of selected candidates was further analyzed in relation to their translocation into plant cells and their inhibition of plant defense responses. In this study, we demonstrated the translocation of seven Hop-Cya fusions through the *P. savastanoi* pv. *savastanoi* T3SS, including three novel T3E of the *P. syringae* complex, which belong to two new effector families; that is, HopBK (HopBK1) and HopBL (HopBL1 and HopBL2).

RESULTS

Bioinformatics prediction of novel T3E in the *P. savastanoi* pv. *savastanoi* NCPPB 3335 genome.

We started with the set of candidate effector genes identified previously in the *P. savastanoi* pv. *savastanoi* NCPPB 3335 genome (Rodríguez-Palenzuela et al. 2010) and later updated (Ramos et al. 2012). In addition, we searched specifically for NCPPB 3335 proteins with pfam domains (The Pfam Database) already found in known T3E (details below and in Supplementary Table S1). Two novel candidate T3E (AER-0000509 and

Table 1. Putative type III effectors identified in the *Pseudomonas savastanoi* pv. *savastanoi* NCPPB 3335 genome[a]

ID-ASAP	Locus tag	Pfam[b]	Name	Reference	Homolog[c]	Reference
AER-0005350	PSA3335_1360	PF11725	avrE1	Ramos et al. 2012	+	Badel et al. 2006, Vinatzer et al. 2006
AER-0005727	PSA3335_5082	PF11592	avrPto1	Ramos et al. 2012	+	Vinatzer et al. 2006
AER-0005728	**PSA3335_5091**	**None**	**avrRpm2**	**Ramos et al. 2012**	**nd**	**…**
AER-0002657	**PSA3335_5065**	**None**	**HopA1**	**Rodríguez-Palenzuela et al. 2010**	**+**	**Chang et al. 2005**
AER-0000274	**na**	**None**	**HopAA1**	**Ramos et al. 2012**	**–**	**Chang et al. 2005**
AER-0004725	PSA3335_2333	PF09046	HopAB1	Rodríguez-Palenzuela et al. 2010	+	Chang et al. 2005, Vinatzer et al. 2006
AER-0000741	PSA3335_4315	PF15457	HopAE1	Rodríguez-Palenzuela et al. 2010	+	Vinatzer et al. 2006
AER-0000968	PSA3335_1469	None	HopAF1	Ramos et al. 2012	+	Chang et al. 2005
AER-0003643	PSA3335_1477	None	HopAF1-2#	Rodríguez-Palenzuela et al. 2010	+	Chang et al. 2005
AER-0001776	PSA3335_2927	PF00150	HopAH2	Rodríguez-Palenzuela et al. 2010	+	Zumaquero et al. 2010
AER-0000610	PSA3335_0875	PF14566	HopAO1#	Rodríguez-Palenzuela et al. 2010	+	Chang et al. 2005
AER-0005024	PSA3335_4684	None	HopAS1	Rodríguez-Palenzuela et al. 2010	+	Vencato et al. 2006
AER-0005726	PSA3335_5084	None	HopAT1′	Ramos et al. 2012	+^	Chang et al. 2005
AER-0000625	PSA3335_5031	PF10791	HopAU1	Rodríguez-Palenzuela et al. 2010	+	Vencato et al. 2006
AER-0001017	**PSA3335_1783**	**None**	**HopAZ1**	**Ramos et al. 2012**	**nd**	**…**
AER-0000696	**PSA3335_2068**	**PF13974**	**HopBK1**	**Rodríguez-Palenzuela et al. 2010**	**nd**	**…**
AER-0000509	**PSA3335_0157**	**PF02902**	**HopBL1**	**This study**	**nd**	**…**
AER-0003844	**PSA3335_4544**	**PF02902**	**HopBL2**	**This study**	**nd**	**…**
AER-0004681	PSA3335_4805	None	HopD1	Rodríguez-Palenzuela et al. 2010	+	Chang et al. 2005
AER-0000629	PSA3335_0852	None	HopG1	Rodríguez-Palenzuela et al. 2010	+	Chang et al. 2005
AER-0000168	PSA3335_4509	PF00226	HopI1	Rodríguez-Palenzuela et al. 2010	+	Chang et al. 2005; Vinatzer et al. 2006
AER-0005351	PSA3335_1358	None	HopM1′	Rodríguez-Palenzuela et al. 2010	+	Badel et al. 2003; Vinatzer et al. 2006
AER-0004680	PSA3335_4804	PF01156	HopQ1	Rodríguez-Palenzuela et al. 2010	+	Chang et al. 2005
AER-0004685	PSA3335_4809	None	HopR1	Rodríguez-Palenzuela et al. 2010	+	Chang et al. 2005; Schechter et al. 2006
AER-0003015	PSA3335_2327	PF13485	HopV1	Rodríguez-Palenzuela et al. 2010	+	Schechter et al. 2004
AER-0003833	PSA3335_5066	None	HopW1′	Rodríguez-Palenzuela et al. 2010	+	Chang et al. 2005; Zumaquero et al. 2010
AER-0000344	**PSA3335_5061**	**None**	**HP0344**	**Rodríguez-Palenzuela et al. 2010**	**nd**	**…**
AER-0000393	**PSA3335_1416**	**None**	**HP0393**	**Rodríguez-Palenzuela et al. 2010**	**nd**	**…**
AER-0001113	**PSA3335_0894**	**PF07090**	**HP1113**	**Rodríguez-Palenzuela et al. 2010**	**nd**	**…**
AER-0001936	PSA3335_3242	None	HP1936	Rodríguez-Palenzuela et al. 2010	nd	…
AER-0002597	PSA3335_0106	PF15184	HP2597	Rodríguez-Palenzuela et al. 2010	nd	…
AER-0002714	**PSA3335_2804**	**PF01565**	**HP2714**	**Rodríguez-Palenzuela et al. 2010**	**nd**	**…**
AER-0003934	**PSA3335_1247**	**None**	**HP3934**	**Rodríguez-Palenzuela et al. 2010**	**nd**	**…**

[a] Bold indicates effectors for which translocation was analyzed in this study; # = plasmid-encoded genes, ′ = putative pseudogenes, nd = not determined, na = not available, and ^ = translocation tested for HopAT1 of *P. syringae* pv. *tomato* DC3000 but not for HopAT1′.
[b] Accession number for the corresponding protein families at the pfam database.
[c] Homolog translocated in *P. syringae.*

AER-0003844) were found, both containing the domain PF02902. This domain, which belongs to the Ulp1 protease family with SUMO protease activity, has been associated with several known effector proteins in pathogenic bacteria of the genus *Xanthomonas*, such as XopD (Kay and Bonas 2009). The final set of 33 candidate *P. savastanoi* pv. *savastanoi* NCPPB 3335 effectors is listed in Table 1, which includes these two novel putative T3E. Based on the translocation, functional, and phylogenetic analysis of these proteins shown below, and taking into account the guidelines for a unified nomenclature of T3E in the plant pathogen *P. syringae* proposed by Lindenberg and associates (2005), hereafter these T3E are called HopBL1 (AER-0000509) and HopBL2 (AER-0003844) (Table 1; Supplementary Table S2).

Translocation assay of T3E candidates revealed novel effectors in *P. savastanoi.*

Of the 33 candidate *P. savastanoi* pv. *savastanoi* NCPPB 3335 T3E, 12 were selected for further analysis (Table 1). These candidates included the three proteins with a *P. syringae* homolog for which plant-cell translocation has not been demonstrated to date (AvrRpm2, HopAA1, and HopAZ1). Additionally, we selected seven of the 10 hypothetical T3E identified in the genome of *P. savastanoi* pv. *savastanoi* NCPPB 3335 that are not present in *P. syringae* pv. *phaseolicola* 1448A, its closest relative that infects herbaceous plants for which there is a closed genome. The selection also included AER-0003934, which harbors a homolog in the genome of 1448A, and HopA1 (AER-0002657). With the exception of the *hopA1* gene,

Table 2. Occurrence of consensus Hrp-box sequences upstream of type III secretion system effector genes from *Pseudomonas savastanoi* pv. *savastanoi* NCPPB 3335

Gene name	Hrp-box position[a]	Hrp-box sequence
Consensus[b]	…	B**GGAAC**YHNNNNNNNNNNNNNNN**CCAC**NH**AG**
avrPto1	–69 to –39	T**GGAAC**CGACCTGCCCCCGATGA**CCAC**TC**AG**
avrRpm2	–474 to –444	T**GGAAC**CAAATATGTAGTTATGGT**CAC**TCAC
hopAA1	–193 to –163	T**GGAAC**CGTCAACGGATCCGGGA**CCAC**ACA**G**
hopAZ1	–124 to –94	T**GGAAC**CTCTCCTCAATGAGTTG**CCAC**TCAC
hopBK1	–218 to –197	A**GG**TGCGCCGGGGTTATGACGAGG**CCAC**GGTG
hopBL1	–244 to –214	T**GGAAC**CTAATCGCTGGAGAGGC**CTAC**TAAT
hopBL2	–412 to –383	A**GGAA**TTTAAGCTCGATAGTTG**CCAC**AGTC
HP0344	–184 to –155	G**GCAAG**GCGCCTGCACCTAGAG**CCAC**AAC**G**
HP0393	–56 to –26	A**GGAAC**CCGGCCCACGCAAGTGGA**CAC**CCG**G**
HP1113	–84 to –55	T**GAAAC**CCTTTTGATCGACAAC**CCAC**GCC**G**
HP2714	–82 to –53	A**GGAC**CCGGTAGTTTTCGCAAT**CCG**C**G**ACC
HP3934	–483 to –451	T**GGAAC**CTGTTCAATGTGCTGTCGG**CAC**CCGC
hopA1	…	na

[a] Coordinates are with respect to the annotated start codon of the coding sequence.
[b] Consensus Hrp box sequence (Fouts et al. 2002). Conserved sequences are highlighted in bold; na = not available in the draft genome sequence of *P. savastanoi* pv. *savastanoi* NCPPB 3335.

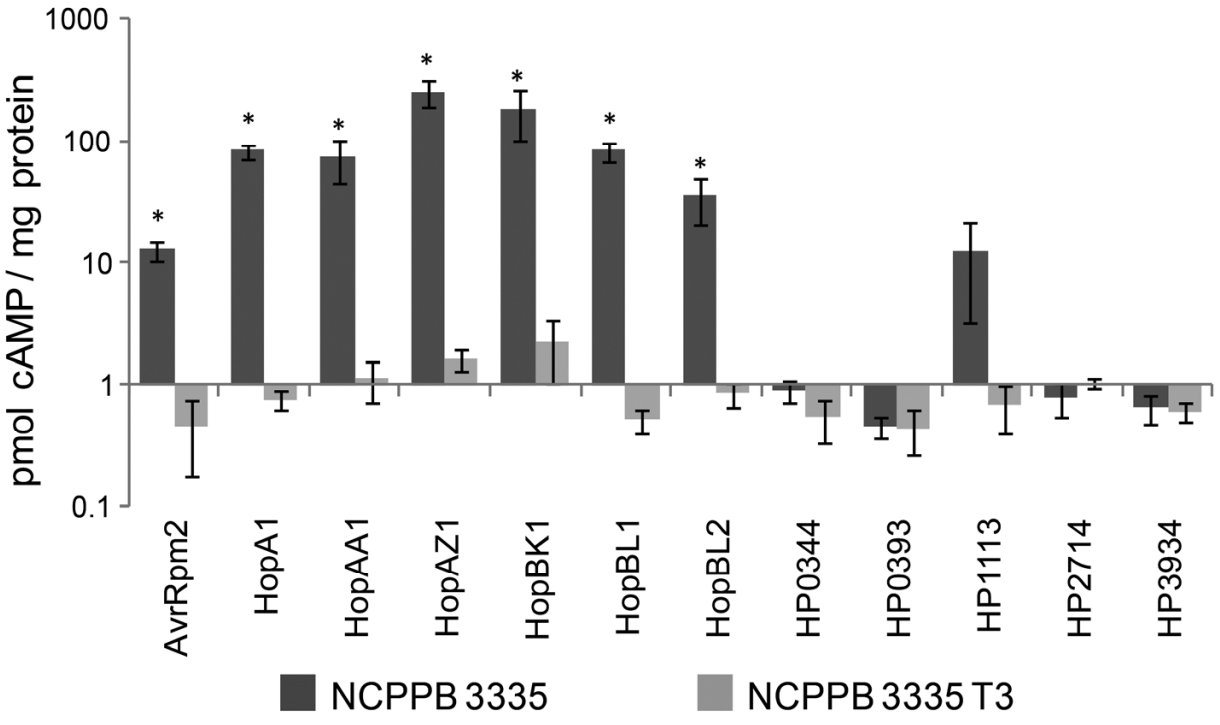

Fig. 1. Translocation assay of candidate *Pseudomonas savastanoi* pv. *savastanoi* NCPPB 3335 type III secretion system (T3SS) effectors (T3E) in *Nicotiana tabacum* var. Newdel plants by the NCPPB 3335 T3SS. Calmodulin- and Cya-dependent production of cAMP was used to measure the translocation of T3E-Cya fusions into plant cells. *N. tabacum* plants were inoculated with *P. savastanoi* pv. *savastanoi* NCPPB 3335 or NCPPB 3335-T3 (T3SS mutant) expressing the indicated Hop-Cya fusions from pCPP3234 derivatives. T3E are denoted by their corresponding names. Values represent the mean and standard error for samples obtained in triplicate; similar results were obtained in multiple experiments. Asterisks indicate significant differences (P = 0.05) between the cAMP levels obtained for the NCPPB 3335 and NCPPB 3335-T3 strains.

whose upstream region is not available in the draft genome sequence of *P. savastanoi* pv. *savastanoi* NCPPB 3335 (Rodríguez-Palenzuela et al. 2010), an identifiable Hrp box (Fouts et al. 2002) was found in the 500 nucleotides upstream of the start codon of the other 11 T3E candidates (Table 2).

To determine whether the selected candidate effectors were T3SS substrates that could translocate into plant cells, we constructed pCPP3234 derivatives (Supplementary Table S3) expressing fusions of *Bordetella pertussis* adenylate cyclase (Cya) to the C terminus of full-length T3E. This system, which is based in cyclic AMP (cAMP) production exclusively in the presence of eukaryotic calmodulin, has been widely used for analyzing the translocation of *P. syringae* T3E (Casper-Lindley et al. 2002; Schechter et al. 2004; Sory and Cornelis 1994).

Nicotiana tabacum leaves were infiltrated with either *P. savastanoi* pv. *savastanoi* NCPPB 3335 or the strain NCPPB 3335-T3, a T3SS mutant derived from wild-type NCPPB 3335 (Pérez-Martínez et al. 2010), expressing each of the 12 constructed Cya fusions. Significant differences in cAMP production between the wild-type strain and the T3SS mutant strain were observed in seven of the 12 candidate T3E tested—AvrRpm2, HopA1, HopAA1, HopAZ1, HopBK1 (the first described member of a novel effector family of the *P. syringae* complex), HopBL1, and HopBL2 (Fig. 1)—indicative of their translocation through the *P. savastanoi* pv. *savastanoi* T3SS. Notably, HopA1 was translocated by *P. savastanoi* pv. *savastanoi* in tobacco (Fig. 1), as expected because its homolog in *P. syringae* pv. *tomato* DC3000 has been shown to be translocated into *Arabidopsis* leaves (Chang et al. 2005).

HrpL-dependent expression of novel *P. savastanoi* T3E.

To unveil the HrpL-dependent expression of the three hypothetical proteins identified here as novel T3E of the *P. syringae* complex (HopBK1, HopBL1, and HopBL2), a Δ*hrpL P. savastanoi* pv. *savastanoi* NCPPB 3335 mutant was constructed. As previously described for the *P. savastanoi* pv. *savastanoi* NCPPB 3335-T3 (Pérez-Martínez et al. 2010), the NCPPB 3335 Δ*hrpL* mutant was unable to elicit an HR in *N. tabacum* plants (Fig. 2A) or form knots in lignified olive plants (Fig. 2B). The expression of the *hopBK1*, *hopBL1*, and *hopBL2* genes was analyzed using quantitative reverse-transcription polymerase chain reaction (qRT-PCR) with both the wild type and the NCPPB 3335 Δ*hrpL* mutant. In addition, the expression of the *avrRPto1* gene and the *iaaM* gene (encoding tryptophan monooxygenase, involved in the biosynthesis of indoleacetic acid) was also tested as positive and negative controls, respectively. Under noninducing conditions (cells grown in King's B [KB] medium), the expression of the *hopBK1*, *hopBL1*, and *hopBL2* genes was comparable in the Δ*hrpL* mutant and the wild-type strain (*data not shown*). However, 6 h after the transfer of bacterial cells to Hrp-inducing medium, the expression of all three genes and the expression of the *avrPto1* gene decreased (0.002- to 0.4-fold) in the Δ*hrpL* mutant compared with the wild type, demonstrating an expression dependency on HrpL. As expected for the negative control, no reduction in the expression of the *iaaM* gene was observed under the same conditions (Fig. 2C).

Distribution of HopBK1, HopBL1, and HopBL2 T3E among *P. savastanoi* pv. *savastanoi* and related strains.

To study the conservation of the three new *P. savastanoi* pv. *savastanoi* NCPPB 3335 effectors among strains from the *P. syringae* complex, their protein sequences were used as queries to perform BLASTp searches against the nonredundant protein sequence database. The results revealed that HopBL1 and HopBL2 are similar to XopD of *Xanthomonas* spp. and infrequent within the *P. syringae* complex. Conversely, HopBK1 is present in *P. syringae* pathovars *tomato*, *actinidae*, *aceris*, *oryzae*, *syringae*, and *lachrymans* (Fig. 3A and B).

The *hopBK1*, *hopBL1*, and *hopBL2 P. savastanoi* pv. *savastanoi* NCPPB 3335 T3E genes were used as probes in dot-blot hybridizations to ascertain their distribution among a collection of 31 *P. savastanoi* pv. *savastanoi* strains isolated in different countries and among a selection of *P. syringae* strains isolated from either woody or herbaceous hosts. The strains used in this assay are presented in Supplementary Table S4. These three effector genes were present in most of the *P. savastanoi* pv. *savastanoi* strains, two strains of *P. savastanoi* pv. *nerii* (2 and 519), and in strains *P. syringae* pv. *eriobotryae* CFBP 2343, pv. *morsprunorum* CFBP 2116, and pv. *myricae* CFBP 2897 (Fig. 3C). The *hopBK1* gene was not detected in six *P. savastanoi* pv. *savastanoi* strains (CFBP 71, CFBP 1670, CFBP 1746, IMC-1, IVIA 1624-1b, and NCPPB 1479), *P. syringae* pv. *dendropanacis* CFBP 3226, and pv. *mori* CFBP 1642. Furthermore, *hopBL1* and *hopBL2* were absent in *P. syringae* pv. *glycinea*

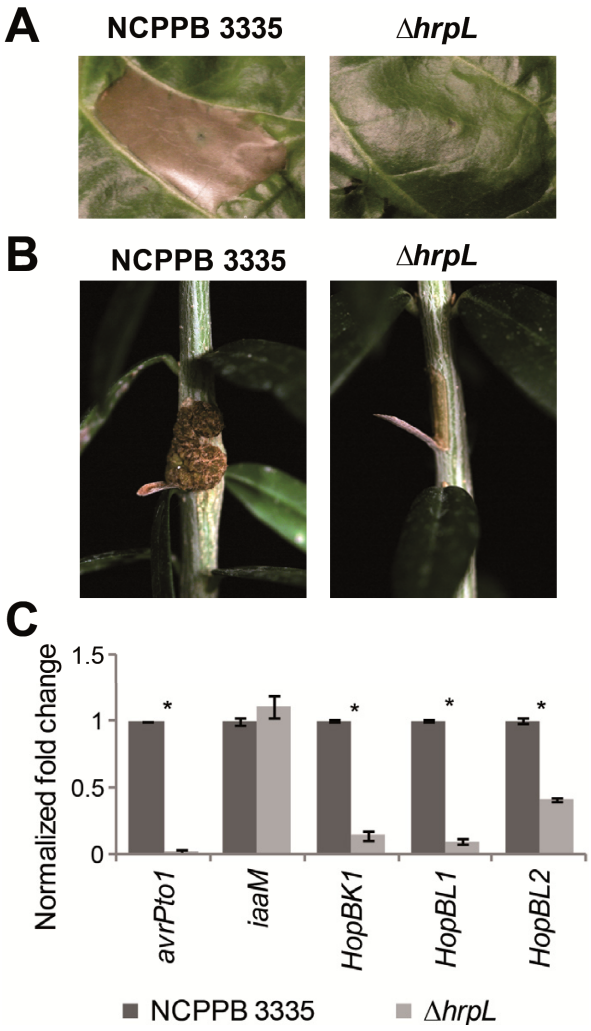

Fig. 2. HrpL-dependent expression of the *Pseudomonas savastanoi* pv. *savastanoi* NCPPB 3335 novel type III secretion system effectors (T3E). **A,** Hypersensitive response of *Nicotiana tabacum* var. Newdel leaves 24 h after infection with *P. savastanoi* pv. *savastanoi* NCPPB 3335 or NCPPB 3335 Δ*hrpL*. **B,** Symptoms induced in lignified olive plants 90 days after inoculation with NCPPB 3335 or NCPPB 3335 Δ*hrpL*. **C,** Quantitative reverse-transcription polymerase chain reaction with the indicated *P. savastanoi* pv. *savastanoi* NCPPB 3335 T3E genes in NCPPB 3335 Δ*hrpL* versus NCPPB 3335 at 6 h after transfer to Hrp-inducing medium. The fold change was calculated after normalization using the *gyrA* gene as an internal control. Results represent the means from three independent experiments. Error bars represent the standard deviation.

PG4180, pv. *lachrymans* CFBP 1644, pv. *sesami* CFBP 1671, and pv. *tomato* PT23 (Fig. 3C). The widespread distribution of these three effectors among strains of *P. savastanoi* pv. *savastanoi* suggests that they might be important for the interaction with olive. However, their patchy distribution among pathovars infecting woody hosts indicate that they are not universally essential for the infection of woody plants and that their effect might be dependent on the particular pathosystem.

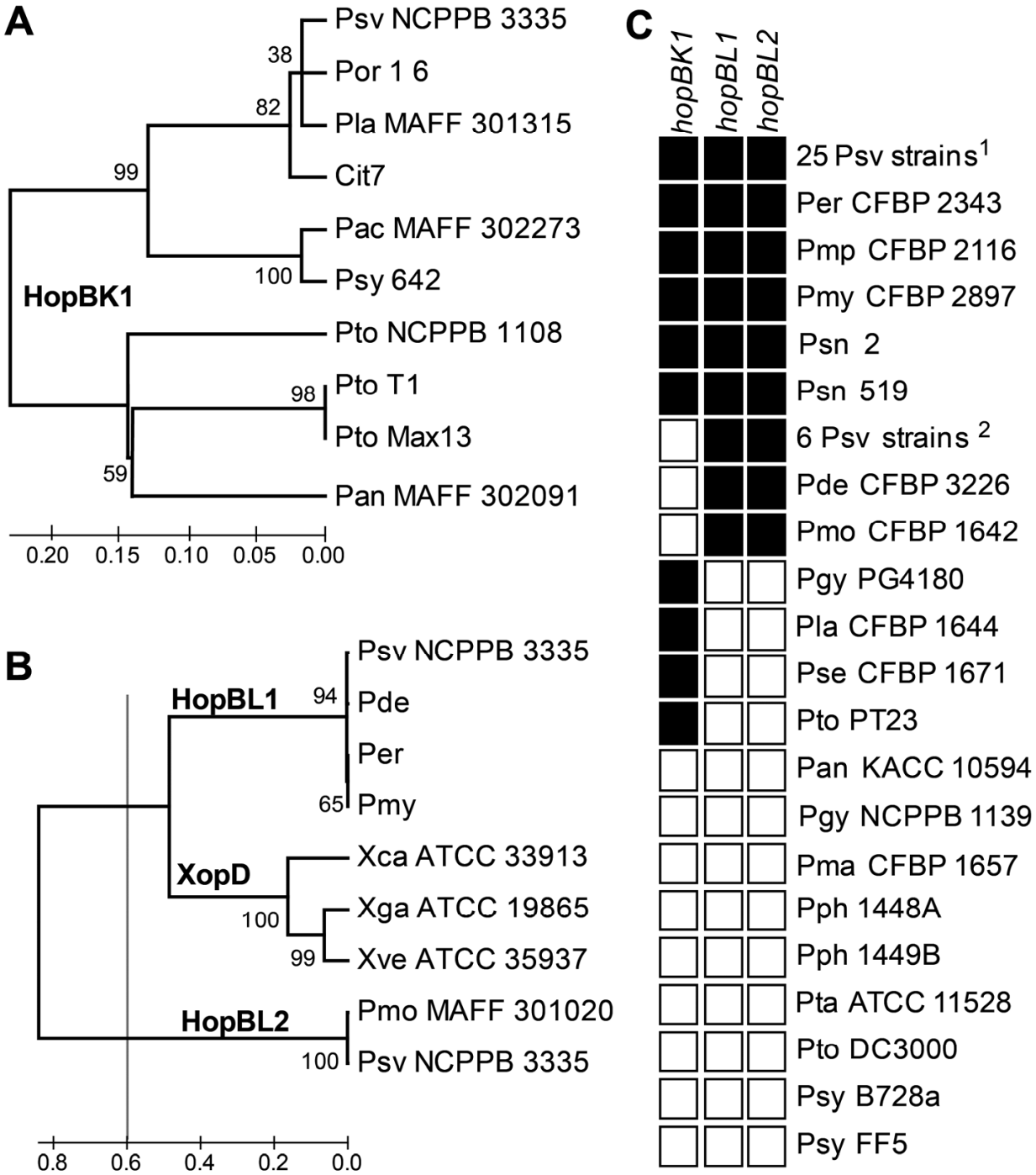

Fig. 3. Distribution and phylogeny of HopBK1, HopBL1 and HopBL2 among pathovars of the *Pseudomonas syringae* complex. Unrooted neighbor-joining tree of **A,** HopBK1 and **B,** HopBL1 and HopBL2 proteins from strains of the *P. syringae* complex. HopBK1 is widely distributed in *P. syringae* pv. *actinidiae*, with at least two alleles showing 94% amino acid identity, although only a single strain is shown for clarity. Similar or identical topologies were obtained by maximum likelihood. Bootstrap percentage values (10,000 repetitions) are shown on the branches and evolutionary distances are given in units of amino acid substitutions per site. **C,** Distribution of the novel *P. savastanoi* pv. *savastanoi* NCPPB 3335 type III secretion system effector genes *hopBK1*, *hopBL1*, and *hopBL2* among a collection of strains from the *P. syringae* complex isolated from woody and herbaceous plant hosts. A colony blot analysis was performed using the indicated gene probes. Strains are indicated by their pathovar abbreviation. Black and white squares represent the presence or absence, respectively, of strong hybridization signals with the indicated effectors for each strain analyzed. Superscript 1 indicates 25 strains of *P. savastanoi* pv. *savastanoi*: B15.00, C1.01, C2.01, C3.01, CFBP 1020, CFBP 2074, DAPP-PG722, IMC-2, ITM 317, IVIA 1628-3, IVIA 1629-1a, IVIA 1637-a, IVIA 1637-B3, IVIA 1649-1, IVIA 1651-C15, IVIA 1657-A2, IVIA 1657-B8, IVIA 2733-1a, IVIA 2743-3, NCPPB 64, NCPPB 1342, NCPPB 1344, NCPPB 1506, NCPPB 3335, and PVFi-1; and superscript 2 indicates six strains of *P. savastanoi* pv. *savastanoi*: CFBP 71, CFBP 1670, CFBP 1746, IMC-1, IVIA 1624-1b, and NCPPB 1479.

P. savastanoi pv. *savastanoi* NCPPB 3335 encodes truncated versions of HopAA1 and HopAZ1.

The occurrence of premature stop codons and transposon disruptions is common in T3E across the *P. syringae* phylogeny. Although these variants are generally considered to be functionless pseudogenes, the functional significance of these truncated alleles remains unresolved (Baltrus et al. 2011). The *P. syringae hopAA1* and *hopAZ1* families contain alleles of vastly different lengths. The truncated version of *hopAA1* encoded by *P. savastanoi* pv. *savastanoi* NCPPB 3335 (189 amino acids) harbors a single nucleotide insertion within codon 188 relative to the full-length *hopAA1-1* allele of *P. syringae* pv. *tomato* DC3000 (486 amino acids). Truncations of the *hopAA1* gene have also been identified in *P. syringae* pvs. *phaseolicola* and *actinidiae* (Fig. 4). On the other hand, *P. savastanoi* pv. *savastanoi* NCPPB 3335 also contains a truncated version of *hopAZ1*, encoding a polypeptide of 122 amino acids lacking the C-terminal domain of the HopAZ1 versions encoded by other *P. syringae* pathovars (Fig. 4). The truncated versions of the *hopAA1* and *hopAZ1* genes encoded by *P. savastanoi* pv. *savastanoi* NCPPB 3335 were included in the plant bioassays described below, in order to determine their functionality during plant infection.

Heterologous expression of *P. savastanoi* T3E in the nonpathogen *P. fluorescens* 55 expressing a cloned *P. syringae* Hrp system.

T3E activities interfere with the innate immunity response of the plant at different levels. ROS production and callose deposition upon pathogen recognition are early plant defense responses. To test the ability of the seven *P. savastanoi* pv. *savastanoi* T3E identified here—AvrRpm2, HopA1, HopAA1, HopAZ1, HopBK1, HopBL1, and HopBL2—to attenuate these responses, we expressed their corresponding genes (pCPP5040 derivatives) in *P. fluorescens* 55 (pLN18), which heterologously expresses a *P. syringae* T3SS, thus enabling the delivery of effector proteins into plant cells at levels characteristic of a natural infection (Jamir et al. 2004; Lopez-Solanilla et al. 2004; Oh et al. 2010; Rodríguez-Herva et al. 2012). For this purpose, *N. tabacum* leaves were used. PAMPs displayed by *P. fluorescens* 55 generate a PTI response in inoculated plants, which is increased by the pLN18-encoded T3SS, as indicated by a higher ROS level than that induced by *P. fluorescens* 55 without a T3SS (Oh et al. 2010). The ROS levels, determined by 3,3′-diaminobenzidine (DAB) staining, were significantly reduced by the expression of each of the seven T3E compared with the control strain *P. fluorescens* 55 (pLN18) harboring an empty vector (Tukey test; $P \leq 0.01$) (Fig. 5A and B). Moreover, with the exception of HopA1, all the other T3E significantly reduced the levels of callose deposition compared with the control strain (Tukey test; $P \leq 0.01$) (Fig. 5C and D). These results suggest that these T3E interfere with the early responses associated with plant immunity.

Heterologous expression of *P. savastanoi* T3E in the functionally effectorless polymutant *P. syringae* pv. *tomato* DC3000D28E.

To further analyze the individual roles of the *P. savastanoi* pv. *savastanoi* T3E when confronting the plant immune system, we constructed derivatives of the *P. syringae* pv. *tomato* DC3000D28E strain expressing each of the seven effectors from the pCPP5040 plasmid. DC3000D28E is a polymutant of the model pathogen *P. syringae* pv. *tomato* DC3000 that harbors deletions in all 28 well-expressed effector genes. Thus, DC3000D28E is considered to be functionally effectorless but otherwise wild type in planta. Although the wild-type strain DC3000 induces an ETI-like rapid plant cell death in *N. benthamiana* and *N. tabacum*, DC3000D28E has a reduced ability to induce this response and seems to elicit plant defenses that are T3SS-dependent and additional to basal PTI (Cunnac et al. 2011). This elicitation is explained by the fact that DC3000D28E has the wild-type complement of T3SS helper proteins (except HrpW1), and several of these proteins can elicit plant defenses and induce an HR response (Cunnac et al. 2011; Kvitko et al. 2007). Therefore, this strain is an excellent tool to investigate the role of heterologous effectors in amenable systems, such as *N. benthamiana* and *N. tabacum*. DC3000D28E derivatives expressing the selected T3E were compared with DC3000D28E regarding their ability to elicit cell death in *N. tabacum* at two different inoculum levels, which were chosen to exceed the threshold typically needed to elicit cell death associated with ETI. Neither the polymutant strain DC3000D28E nor the derivatives expressing *P. savastanoi* pv. *savastanoi* T3E incited the HR response typical of the wild-type strain DC3000 at a bacterial dose of 2×10^7 CFU/ml. However, with 10× more bacteria (2×10^8 CFU/ml), the polymutant strain stimulated an ETI-like response after 48 h of inoculation, which was partially or completely inhibited by the expression of the *P. savastanoi* pv. *savastanoi* proteins HopAZ1 and HopBL1, respectively (Fig. 6A and B). These results suggest that these two effectors participate in the inhibition of the plant defense response associated with the onset of programmed cell death.

The DC3000D28E strain has been shown to grow better in planta when coinoculated with a strain that is able to suppress plant immunity, such as DC3000ΔhopQ1-1 (Cunnac et al. 2011). Therefore, this strain is considered an excellent tool for testing the ability of individual T3E to restore bacterial growth or to induce specific plant responses. To investigate the effect of the seven *P. savastanoi* pv. *savastanoi* T3E on the ability of DC3000D28E to colonize *N. benthamiana*, competition assays between the polymutant strain (DC3000D28E) and each derivative expressing the selected T3E were conducted. *N. benthamiana*

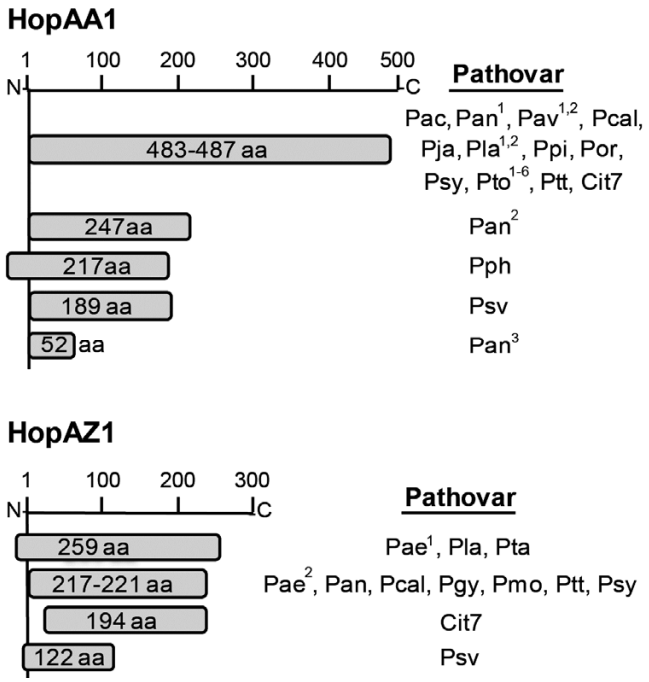

Fig. 4. Schematic map of HopAA1 and HopAZ1 alleles with variable protein length from the *Pseudomonas syringae* complex. Strains are indicated by their pathovar abbreviation. Superscript numbers indicate different strains or ortholog genes; aa = amino acids residues encoded by the corresponding genes.

iana leaves were infiltrated with a mixed inoculum (1:1) of DC3000D28E and each of the derivatives and, after 6 days, bacteria were recovered and viable cells were determined. The results presented in Figure 6C are expressed as the competition indices (CI) of the derivatives expressing each of the *P. savastanoi* pv. *savastanoi* T3E relative to the DC3000D28E strain. Interestingly, the expression of *P. savastanoi* pv. *savastanoi* HopBL2 in DC3000D28E significantly increased the competitiveness of the strain, which was reflected in a CI value (HopBL2/DC3000D28E) of 21.1. Expression of HopAA1 also increased the competitiveness of the strain, although at a lower level (CI = 2.6) than HopBL2. These results suggest that these effectors inhibit plant defense responses.

DISCUSSION

The recent availability of complete and draft genome sequences for several *P. syringae* and *P. savastanoi* pathovars and the relevant advances in the development of bioinformatics tools led to a comprehensive catalog of candidate effector repertoire for 19 different strains (Baltrus et al. 2011). Given that only nine new effector families were identified after the latest comparative genome-sequence analysis, the *P. syringae* complex effector super-repertoire may be nearly complete with 57 effector families (Baltrus et al. 2011; Lindeberg et al. 2012). However, novel candidate effectors identified using these strategies should be functionally characterized in the context of a unified model for a two-layered immune system in plants (Block and Alfano 2011; Lindeberg et al. 2012). To that end, in this study, we demonstrated that the Hrp T3SS mediated the delivery into plant cells of seven *P. savastanoi* pv. *savastanoi* NCPPB 3335 effectors, including HopA1; three T3E for which translocation into plant cells has not been demonstrated for any other *P. syringae* strain (AvrRpm2, HopAA1, and HopAZ1); and three novel T3E (HopBK1, HopBL1, and HopBL2) from two new effector families of the *P. syringae* complex (HopBK and HopBL) (Fig. 1). Moreover, we demonstrated that the expression of these three genes encoding novel T3E was transcriptionally dependent on HrpL.

Translocation assays based on Cya reporters were designed for use in herbaceous plants and require injection of bacterial suspensions expressing T3E-Cya fusions into fully expanded

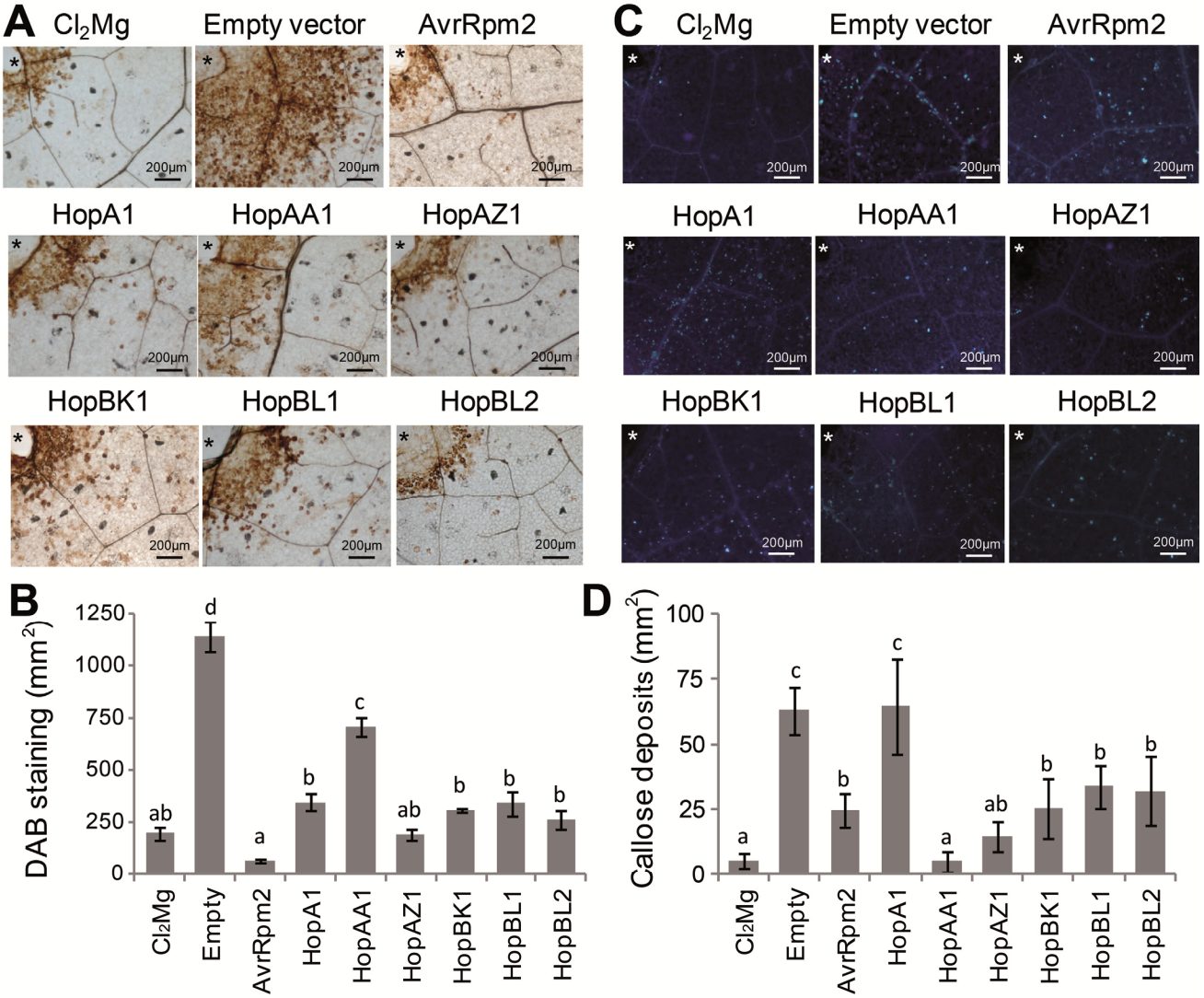

Fig. 5. 3,3′-Diaminobenzidine (DAB) staining and callose deposition in *Nicotiana tabacum* var. Xanthi leaves. Plants were challenged with *Pseudomonas fluorescens* 55 (pLN18) harboring the pCPP5040 empty vector or the vectors expressing the indicated *P. savastanoi* pv. *savastanoi* NCPPB 3335 type III secretion system effectors. **A,** The DAB signal was quantified 4 h after infection and **B,** represented in a histogram. **C,** The callose deposition was assessed using aniline blue staining, quantified 12 h after infection, and **D,** represented in a histogram. Asterisks in A and C indicate inoculation zones. For histograms, data are means ± standard error of the mean for at least five replicas; bars topped with the same letter represent values that are not significantly different using one-way analysis of variance followed by post-hoc comparisons using the Tukey test.

upper leaves. However, adapting this assay to study the interaction of bacterial effectors with a woody plant such as olive has been limited by two main restrictions, both due to secondary wall thickenings of the host. First, inoculating the olive plant stem with bacteria requires artificially wounding the plant material, a process that induces complex plant defense mechanisms (Conrath 2011); and, second, visualizing the damaged stem tissue after bacterial inoculation is complex. For these reasons, translocation assays of T3E through the *P. savastanoi* pv. *savastanoi* T3SS were performed in *N. tabacum*, a nonhost plant of this pathogen (Pérez-Martínez et al. 2010). Cya has been used as a reporter to study T3SS-mediated translocation of effector proteins by animal- and plant-pathogenic bacteria (Schechter et al. 2004). This system has been optimized in host and nonhost plants with the well-studied effector protein AvrPto from *P. syringae* pv. *tomato*. The translocation of several DC3000 candidate T3E has been assessed using this Cya reporter, which induces cAMP accumulation in tomato or *N. benthamiana* after effectors are delivered by the *P. fluorescens* 55, which expresses a *P. syringae* Hrp system (Schechter et al. 2004). Our results demonstrated that several *P. savastanoi* pv. *savastanoi* NCPPB 3335 effector proteins were translocated. However, we cannot exclude that the negative results obtained for some of the other candidate proteins tested were due to the induction of an HR response in *N. tabacum*, which impedes cAMP accumulation.

The *P. syringae* pangenome includes only four effector families that are considered core members of the effector superrepertoire: AvrE, HopI, HopM1, and HopAA (Baltrus et al. 2011; Lindeberg et al. 2012). Candidate effectors from all four families were identified in the genome of *P. savastanoi* pv. *savastanoi* NCPPB 3335 (Table 1). Our in silico survey also demonstrated that the three novel T3E identified here (HopBK1, HopBL1, and HopBL2) are present in only a few *P. syringae* strains (Fig. 3A and B). In contrast, dot-blot hybridization analysis revealed that these three T3E were present in most *P. savastanoi* pv. *savastanoi* strains (Fig. 3C). Interestingly, *hopBL1* and *hopBL2* were detected in all *P. savastanoi* pv. *savastanoi* strains analyzed and in other *P. syringae* strains isolated from woody hosts, suggesting a relevant role for these effectors in the interaction of *P. syringae* and *P. savastanoi* with certain woody plants. However, this association did not occur with *hopBK1*, because it was not present in all *P. savastanoi* strains analyzed and was also detected in diverse *P. syringae* pathovars associated with herbaceous plants.

The vast majority of the *P. syringae* pv. *tomato* DC3000 T3E have been demonstrated to suppress ETI and many can also suppress PTI, suggesting that numerous T3E exert multiple activities or, alternatively, that common T3E targets are utilized in pathways needed for ETI, PTI, or both (Guo et al. 2009). Our results indicate that the seven *P. savastanoi* pv. *savastanoi* NCPPB 3335 T3E shown to translocate in this study, including the truncated versions of HopAA1 and HopAZ1, interfered with early responses associated with plant defense. In addition, we demonstrated that HopAZ1 and HopBL1 also inhibited the ETI-like response incited by DC3000D28E in tobacco.

Although all the tested effectors significantly reduced ROS production, expression of HopA1 in *P. fluorescens* 55 did not significantly reduce callose deposition under the conditions

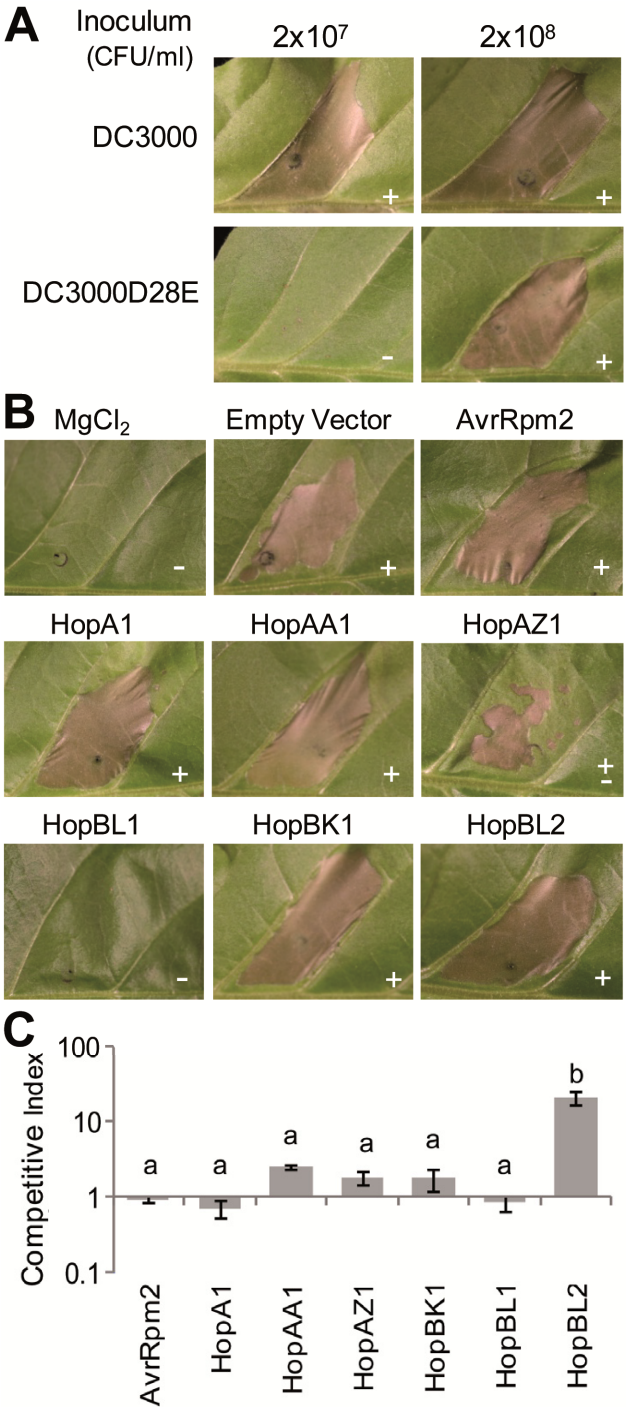

Fig. 6. Delivery of *Pseudomonas savastanoi* pv. *savastanoi* type III secretion system effectors (T3E) by functionally effectorless *P. syringae* pv. *tomato* DC3000D28E in *Nicotiana* leaves. **A,** Cell death response in *Nicotiana tabacum* var. Newdel leaves 48 h after inoculation with *P. syringae* pv. *tomato* strains DC3000 (wild type) or DC3000D28E cells suspended in $MgCl_2$ and adjusted to the indicated densities (in CFU/ml). **B,** Cell death response in *N. tabacum* var. Newdel leaves 48 h after inoculation with *P. syringae* pv. *tomato* DC3000D28E cells suspended in $MgCl_2$ carrying pCPP5040 (empty vector) derivatives expressing the indicated *P. savastanoi* pv. *savastanoi* NCPPB 3335 T3E adjusted to 2×10^8 CFU/ml. Cell death response: + = positive, – = null, and ± = partial. Each experiment was repeated at least three times with similar results. **C,** Competition assays in *N. benthamiana* leaves between *P. syringae* pv. *tomato* DC3000D28E and each of its transformants carrying pCPP5040 derivatives expressing the indicated *P. savastanoi* pv. *savastanoi* T3E. Competition indices (CI) were normalized with respect to the CI obtained for DC3000D28E versus DC3000D28E expressing the empty vector (pCPP5040). Values are the mean ± standard error of the mean of three replicates demonstrating typical results from three independent experiments; bars topped with the same letter represent values that are not significantly different using one-way analysis of variance followed by post-hoc comparisons using the Tukey test.

tested. The secretion of HopA1 via the T3SS in *P. syringae* pv. *syringae* 61 requires the ShcA chaperone (van Dijk et al. 2002). Although a ShcA protein homolog has been annotated in the draft genome of *P. savastanoi* pv. *savastanoi* (AER-0002589), the expression analysis of this effector in this study did not include the NCPPB 3335 ShcA. Thus, we cannot exclude that this protein chaperone may also be necessary for full secretion and in planta activity of HopA1 in *P. savastanoi*. Conversely, HopA1 from *P. syringae* pv. *syringae* 61 has been demonstrated to elicit an HR in tobacco when expressed in *P. fluorescens* (Alfano and Collmer 1996). In agreement with these authors, HopA1 expression in DC3000D28E did not suppress the HR response incited by DC3000D28E in tobacco.

DC3000D28E has been demonstrated to be suitable for testing the ability of T3E to restore bacterial growth and induce plant responses (Cunnac et al. 2011). Although the expression of *P. savastanoi* pv. *savastanoi* HopBL2 in DC3000D28E did not inhibit the ETI-like response induced at high cell doses by DC3000D28E in *N. tabacum*, HopBL2 expression in this strain significantly increased its competitiveness in *N. benthamiana* (Fig. 6C). Significant DC3000D28E growth restoration in *N. benthamiana* due to the expression of single DC3000 effectors was demonstrated for only AvrPto and AvrPtoB; however, neither other effectors such as HopM1 nor a set of several conserved effectors displayed this effect. Conversely, single DC3000 effectors promoted growth when combined with other effectors in DC3000D28E (Cunnac et al. 2011). Thus, our results suggest that the *P. savastanoi* pv. *savastanoi* HopBL2, which harbors a C-terminal XopD-like SUMO protease domain (Kim et al. 2011), and HopBL1 might be involved in the inhibition of the initial perception of pathogens. More specifically, XopD has been recently demonstrated to suppress the ethylene production required for anti-*Xanthomonas euvesicatoria* immunity (Kim et al. 2013). Although the current knowledge of specific T3E functions is limited, our results suggest that the seven *P. savastanoi* T3E analyzed here inhibited PTI, whereas HopAZ1 and HopBL1 also inhibited the ETI-like response. Moreover, and although truncated T3E are generally considered as functionless pseudogenes, our results also demonstrate that the N-terminal region of the truncated versions of HopAA1 and HopAZ1 encoded by *P. savastanoi* pv. *savastanoi* NCPPB 3335 (Fig. 4; Supplementary Table S5) are able to interfere with responses associated with plant defense (Figs. 5 and 6). Although no function has been yet established for the HopAZ and HopAA T3E families, *P. syringae* pv. *avellanae* HopAZ1 is a promising candidate for modulating hazelnut host specificity (O'Brien et al. 2012). On the other hand, deletion of *hopAA1-1* in *P. syringae* pv. *tomato* significantly reduced the formation of necrotic speck lesions in tomato leaves (Munkvold et al. 2009). Moreover, HopAA1 has been demonstrated to attenuate the innate immunity in *Arabidopsis* (Li et al. 2005).

In summary, bioinformatics prediction of proteins belonging to the Ulp1 protease family revealed two novel T3E (HopBL1 and HopBL2) encoded in the genome of *P. savastanoi* pv. *savastanoi* NCPPB 3335, yielding a final set of 33 T3E candidates in this strain. We demonstrated here that seven of these proteins, including HopBK1, HopBL1, and HopBL2, were translocated into the plant cell via the NCPPB 3335 T3SS and interfered with early responses associated with plant defense. In addition, we demonstrated that HopAZ1 and HopBL1 also inhibited the ETI-like response. Collectively, our results revealed the existence of two novel effector families of the *P. syringae* complex, of which HopBL1 and HopBL2 appear to be specific for *P. syringae* and *P. savastanoi* strains isolated from woody hosts. Future studies should focus on elucidating the precise mechanisms and targets of these and other effectors that are included in the *P. syringae* pangenome and that specifically participate in the infection of woody plants.

MATERIALS AND METHODS

Bioinformatics analysis.

Bioinformatics-based predictions of novel candidate T3E in the genome of *P. savastanoi* pv. *savastanoi* NCPPB 3335 (ASAP Database) were performed by searching for specific protein families corresponding to known T3E that have been previously demonstrated in either *P. syringae*, *Xanthomonas* spp., or *Ralstonia* spp. Positive hits were further analyzed for the presence of N-terminal sequence features and potential HrpL boxes in the promoter sequences (500 nucleotides upstream of the start codon), as previously described (Rodríguez-Palenzuela et al. 2010). Novel candidate T3E meeting both criteria were selected for further investigation.

Sequence alignment using Muscle, determination of the optimal amino acid substitution model, and phylogenetic tree construction were performed using MEGA5 (Tamura et al. 2011). Neighbor-joining and maximum-likelihood phylogenetic trees of the individual protein sequences were generated using MEGA5 with the optimal model (John-Taylor-Thornton model) and the option of complete deletion to eliminate positions containing gaps. Confidence levels for the branching points were determined using 10,000 bootstrap replicates.

Bacterial strains, plasmids, and growth conditions.

Pseudomonas and *Escherichia coli* strains were grown at 28 and 37°C, respectively, using Luria-Bertani (LB) medium (Miller 1972), KB medium (King et al. 1954), or super optimal broth medium (Hanahan 1983). Solid and liquid media were supplemented, when required, with the following antibiotics for the *Pseudomonas* or *E. coli* strains: ampicillin (Ap) at 300/100, gentamicin (Gm) at 10/10, spectinomycin (Sp) at 7/50, and kanamycin (Km) at 10/50 µg/ml. Expression plasmids were generated using Gateway cloning technology (Invitrogen Corp., Carlsbad, CA, U.S.A). Using this system, an open reading frame without a stop codon cloned in an entry vector can be transferred by recombination into a destination vector, creating an in-frame fusion. Entry vectors were constructed by cloning PCR products, amplified with specific primer pairs (Supplementary Table S6), into the plasmid pENTR/SD/D-TOPO (Invitrogen Corp.). DNA sequencing using the universal primers T7 and M13-20 confirmed the absence of mutations in the cloned DNA fragments. Expression clones were constructed by combining the pENTR plasmids with the desired expression vector and the LR clonase. The recombination reactions were performed as suggested by the manufacturer (Invitrogen Corp.). Two Gateway-compatible expression vectors were used: i) pCPP3234, a derivative of the broad host-range vector pVLT35 that employs a *tac* promoter to express insert genes and generates hybrid proteins with a C-terminal Cya fusion for T3SS translocation studies (Schechter et al. 2004); and ii) pCPP5040, a derivative of the broad-host-range vector pML123 (Labes et al. 1990), which expresses inserted genes from the *nptII* promoter and generates protein products with a C-terminal HA tag for expression in *Pseudomonas* spp.

A *P. savastanoi* pv. *savastanoi* NCPPB 3335 *hprL* mutant was constructed using the pIAC4-Km plasmid. First, DNA fragments of approximately 1.2 kb, corresponding to the 5′ and 3′ flanking regions of the NCPPB 3335 *hrpL* gene, were amplified using three rounds of PCR with NCPPB 3335 genomic DNA as a template and primers that included an *Eco*RI site and the T7 primer sequence, as previously described

(Zumaquero et al. 2010). The resulting product was A/T cloned into pGEM-T and fully sequenced to discard mutations on flanking genes. Following sequencing, the resulting plasmid (pIAC4) was tagged with the *nptII* Km-resistance gene obtained from pGEM-T-KmFRT-*Eco*RI, yielding pIAC4-Km. For marker-exchange mutagenesis, the pIAC4-Km plasmid was electroporated into NCPPB 3335, as described previously (Pérez-Martínez et al. 2007). Transformants were selected on LB medium containing Km, and the resulting colonies were replica plated onto LB-Ap plates to assess whether each transconjugant integrated the plasmid into the chromosome (Ap^R) or engaged in allelic exchange (Ap^S). Southern blot analyses, using both *nptII* and *hrpL* as probes, were used to confirm that allelic exchange occurred at a single position and at the correct site within the genome.

Translocation assay of *P. savastanoi* pv. *savastanoi* NCPPB 3335 T3E candidates.

Translocation assays were performed as previously described by Schechter and collaborators (2004). This method is based on the construction of fusion proteins between identified T3E and the calmodulin-dependent Cya reporter domain. Electrocompetent *P. savastanoi* pv. *savastanoi* NCPPB 3335 and NCPPB 3335-T3 cells were transformed with Cya fusions, as previously described (Choi et al. 2006). Sp^R transformants were tested by PCR using a forward primer designed specifically for each T3E gene and a reverse primer annealing to the *cya* gene (primer Cya-R135). Cya assays were performed in *N. tabacum* var. Newdel plants, as previously described (Schechter et al. 2004). *P. savastanoi* pv. *savastanoi* NCPPB 3335 and NCPPB 3335-T3 transformants carrying plasmids expressing T3E-Cya fusions were scraped off of the LB plates, washed twice, and resuspended to an optical density at 600 nm (OD_{600}) of 0.5 (approximately 10^8 CFU/ml) in 5 mM morpholinoethanesulfonic acid (pH 5.5) and 100 µM isopropyl-thiogalactopyranoside (IPTG). Cell suspensions were injected into the fully expanded upper plant leaves using a 1-ml syringe. Leaf disks were collected at 6 h postinoculation with a 10-mm inner-diameter cork borer, frozen in liquid nitrogen, ground to a powder, and suspended in 250 µl of 0.1 M HCl. The samples were incubated at –20°C overnight, and cAMP levels were determined using a 1:100 dilution of the samples and the Correlate-EIA cAMP immunoassay kit according to the manufacturer's directions (Assay Designs, Inc., Ann Arbor, MI, U.S.A.). The protein content of each sample was determined using the Pierce BCA protein-assay kit (Thermo Scientific, Rockford, IL, U.S.A.).

The Cya activity of the Cya fusion proteins expressed in *E. coli* XL1Blue from pCPP3234 derivatives were assayed as previously reported (Schechter et al. 2004). Bacterial cells were grown in 5 ml of LB medium containing 100 µM IPTG to an OD_{600} of 0.6 to 0.8. The culture was centrifuged, and the pellet was washed and resuspended in sonication buffer (20 mM Tris-HCl [pH 8.0] and 10 mM $MgCl_2$). The bacteria were sonicated with a microtip for 2 min, and the cellular debris was pelleted by centrifugation. Cya activity was determined in the presence or absence of bovine calmodulin (Calbiochem, Darmstadt, Germany) by using 5 µl of each lysate (Sory and Cornelis 1994). cAMP was quantified in bacteria as described above for the leaf samples. Every Cya hybrid protein exhibited calmodulin-dependent Cya activity in *E. coli* XL1Blue lysates, indicating that all of them could induce cAMP accumulation in planta. The in vitro activity of all the Cya fusions without significant differences in cAMP production in planta between the wild-type *P. savastanoi* pv. *savastanoi* NCPPB 3335 and its T3SS mutant (strain NCPPB 3335-T3) is illustrated in Supplementary Figure S1.

Plant bioassays.

The *N. benthamiana* and *N. tabacum* (var. Newdel and var. Xanthi) plants used in this study were 5 to 7 and 4 to 6 weeks old, respectively. The plants were grown with a photoperiod of 16 h of light and 8 h of darkness with day and night temperatures of 26 and 22°C, respectively. Bacterial suspensions in 10 mM $MgCl_2$ were inoculated into plant leaves using a blunt syringe. Assays with derivatives of *P. fluorescens* 55 (pLN18) were performed by injecting a bacterial suspension (5×10^7 CFU/ml) into *N. tabacum* var. Xanthi leaves using a blunt syringe. The injected areas were lightly marked on the back of the leaves. The bacterial inoculum levels differed among experiments. The bacterial levels in planta were determined by cutting three leaf disks with a boring tool (inner diameter of 10 mm) and placing the plant material in 1 ml of 10 mM $MgCl_2$. The disks were completely homogenized and the resulting suspensions, containing the bacteria, were diluted and plated on LB-Sp plates (DC3000D28E) or LB-Sp-Gm plates (transformants containing pCPP5040 derivatives). *N. tabacum* var. Newdel plants were used for the HR assays. The leaves were infiltrated with bacterial suspensions (10^7 and 10^8 CFU/ml) of *P. syringae* pv. *tomato* DC3000D28E or its derivatives harboring plasmids expressing each of the different *P. savastanoi* pv. *savastanoi* T3E. The generated symptoms, scored 48 h after inoculation, were captured with a high-resolution digital camera (Nikon DXM 1200; Nikon Corporation, Tokyo).

For competition assays, the *N. benthamiana* leaves were inoculated with mixed suspensions containing equal CFU (approximately 10^4 CFU/ml) of *P. syringae* pv. *tomato* DC3000D28E and each of its transformants carrying pCPP5040 derivatives expressing *P. savastanoi* pv. *savastanoi* T3E. Input and ouput pools assayed 1 and 6 h after inoculation, respectively, were plated onto LB-Sp and LB-Sp-Gm to select for DC3000D28E and the transformants with pCPP5040 derivatives, respectively. A CI was calculated by dividing the output ratio (CFU transformant:CFU DC3000D28E) by the input ratio (CFU transformant:CFU DC3000D28E). CI of the transformant strains expressing *P. savastanoi* pv. *savastanoi* T3E versus DC3000D28E were normalized with respect to the CI obtained for DC3000D28E (pCPP5040). The CI presented in Figure 6 represent the mean of three replicates demonstrating typical results from three independent experiments. The results were statistically analyzed using one-way analysis of variance (ANOVA) followed by post-hoc comparisons using the Tukey test. Statistical analysis of the results obtained for CI revealed significant differences (F [7/41] = 17,273, $P \leq$ 0.0001).

Olive plants derived from seed germinated in vitro (originally collected from an 'Arbequina' plant) were micropropagated, rooted, and maintained as previously described (Rodríguez-Moreno et al. 2008, 2009). To analyze the pathogenicity of the *P. savastanoi* pv. *savastanoi* NCPPB 3335 Δ*hrpL* mutant in 1-year-old olive explants (woody plants), micropropagated olive plants were transferred into soil and maintained in a glasshouse at 27°C with a relative humidity of 58% under natural daylight. The plant stems were wounded and infected with approximately 10^6 CFU of *P. savastanoi* pv. *savastanoi* as previously described (Penyalver et al. 2006; Pérez-Martínez et al. 2007). Morphological changes, scored at 90 days postinoculation, were captured with a high-resolution digital camera (Nikon DXM 1200).

Detection of ROS production and callose deposition.

ROS production was observed after DAB staining (Thordal-Christensen et al. 1997) 4 h after inoculation with *P. fluorescens* 55 (pLN18) derivatives. Bacterial suspensions (10^8 CFU/ml) were inoculated into *N. tabacum* var. Xanthi leaves using a blunt

syringe. Small pieces of tobacco leaves cut from around the injection area were placed into a syringe and stained by vacuum infiltration of a freshly prepared 1 mg/ml solution of DAB (Sigma-Aldrich D-8001; Sigma-Aldrich, Inc., St. Louis) in 8 mM HCl, pH 3.8. Chlorophyll was removed by submerging the leaves into a solution of ethanol/lactic acid/glycerol (3:1:1 [vol/vol/vol]) at 60°C and stored overnight at room temperature on water-soaked filter paper. At least 10 biological replicates from each specimen were mounted on slides in a 50% glycerol (vol/vol) solution and observed with a Nikon Eclipse E800 microscope (Nikon Corporation) under bright field. DAB staining produces an intensely brown precipitate at the sites of ROS production, which were next to the infection zone.

Callose deposition samples were developed 12 h after inoculation and stained as described previously (Guo et al. 2009). Chlorophyll was removed in 95% (vol/vol) ethanol from small pieces of tobacco leaves, which were cut from around the injection area, and staining was performed in a 0.02% (wt/vol) solution of aniline blue (number 415049; Sigma-Aldrich, Inc.) in 150 mM potassium phosphate, pH 9, for 1 h in the dark. At least 10 biological replicates from each specimen were mounted in 50% (vol/vol) glycerol on glass slides. Observations were conducted under UV-light excitation using the filter UV-2[a] (EX 330-380, DM 400; BA 420) on a Nikon Eclipse E 800 microscope (Nikon Corporation).

ROS production and callose deposition were quantified as previously described (Rodríguez-Herva et al. 2012), with slight modifications. Up to four snapshots of each specimen from equivalent areas surrounding the wound (inoculation zone) were captured with a Nikon DXM1200 camera using the Nikon ACT-1 2.70 software. The same settings and a final magnification of ×40 were applied to all the samples. After calibrating all the images using the scale bar included in each picture, DAB staining and aniline blue fluorescence were quantified using the program Visilog 6.3 (Noesis, Les Ulis, France). For this purpose, the characteristic brown color of the DAB precipitate and the specific blue fluorescence of callose deposition (Fig. 5) were separated by color deconvolution using the i_classification command. Then, the stained areas were quantified and the results were expressed in square millimeters. Five to six images per assay were analyzed, and statistical analyses were performed using one-way ANOVA followed by post-hoc comparisons using the Tukey test. Statistical analysis of the results obtained for ROS production and callose deposition revealed significant differences (F [8/44] = 59.12, $P \leq 0.0001$ and F [8/44] = 24.33, $P \leq 0.0001$, respectively).

Colony blots.

To fix total DNA from the colonies, overnight cultures of *Pseudomonas* strains grown on LB microtiter plates were transferred onto nylon membranes placed on LB agar plates using a 48-pin replicator (Sigma-Aldrich, Inc.). Total DNA from the bacterial colonies was denatured on the membranes by alkaline lysis by placing a Whatman 3 MM paper soaked in denaturing solution (0.4 M NaOH) for 15 min on top of the colonies. The membranes were neutralized twice for 15 min in 1 M NaCl and 0.5 M Tris, pH 7.2, then washed twice for 10 min in 2× SSC (1× SSC is 0.15 M NaCl plus 0.015 M sodium citrate). Finally, the DNA was cross-linked by UV fixation (Vilber Lourmat, Eberhardzell, Germany). DNA probes were amplified and labeled by PCR using primers and digoxigenin (DIG)-dNTPs from the Dig labeling mix kit (Roche Applied Science, Mannheim, Germany), and the appropriate pENTRY plasmid as the DNA template. Hybridization was performed at 65°C using the DIG Nucleic Acid Detection Kit (Roche Applied Science), following the manufacturer's instructions.

qRT-PCR assays.

Pure cultures of the wild-type *P. savastanoi* pv. *savastanoi* NCPPB 3335 and its Δ*hrpL* mutant were grown overnight in KB medium at 28°C. The cells were diluted in fresh KB medium and incubated with shaking at 28°C to an OD_{600} of 0.5. The sample was split into two. One half was pelleted and frozen (for noninducing condition) and the other half was pelleted, washed twice with 10 mM $MgCl_2$, and resuspended in the same volume of Hrp-inducing medium (Huynh et al. 1989) supplemented with 5 mM mannitol and 0.0006% ferric citrate (Roine et al. 1997; Sambrook and Russell 2001). After 6 h of incubation, the cells were pelleted and processed for RNA isolation using TriPure Isolation Reagent (Roche Applied Science) according to the manufacturer's instructions, except that the TriPure was preheated at 65°C, the lysis step was performed at 65°C, and BCP (Molecular Research Center, Cincinnati, OH, U.S.A.) was used instead of chloroform. Total RNA was treated with the RNAeasy kit (Qiagen GmbH, Hilden, Germany), as detailed by the manufacturer. The RNA concentration was determined spectrophotometrically and its integrity was assessed by agarose gel electrophoresis. DNA-free total RNA was retrotranscribed to cDNA using the cDNA Reverse Transcription kit (Applied Biosystems, Foster City, CA, U.S.A.) and random hexamers. The primer efficiency tests, qRT-PCRs, and confirmation of the specificity of the amplification reactions were performed as described previously (Vargas et al. 2011). The relative transcript abundance was calculated using the ΔΔ cycle-threshold (Ct) method (Livak and Schmittgen 2001). Transcriptional data were normalized to the housekeeping gene *gyrA* using the Roche LightCycler 480 Software and are presented as the fold change in expression compared with the expression of each gene in the wild-type strain. The relative expression ratio was calculated as the difference in qPCR threshold cycles (ΔCt = Ctgene of interest – CtgyrA). One PCR cycle represents a twofold difference in template abundance; therefore, fold-change values were calculated as $2^{-\Delta\Delta Ct}$, as previously described (Pfaffl 2001; Rotenberg et al. 2006). qRT-PCRs were performed in triplicate.

ACKNOWLEDGMENTS

This study was supported by Spanish Plan Nacional I+D+i grants AGL2011-30343-C02-01, AGL2011-30343-C02-02, and AGL2012-32516 from the Ministerio de Economía y Competitividad (MINECO), co-financed by FEDER, and by the grant P08-CVI-03475 from the Junta de Andalucía, Spain. I. M. Matas, I. M. Aragón, and M. P. Castañeda-Ojeda were supported by the Ramón Areces Foundation (Spain) and by FPU and FPI fellowships from the MINECO, respectively. We thank M. Vega Sánchez for excellent assistance with image analysis for quantifying ROS production and callose deposition, L. Santín (University of Malaga, Spain) for statistical analysis of data, and A. Barceló and I. Imbroda (IFAPA, Churriana, Spain) for micropropagating the olive plants.

LITERATURE CITED

Alfano, J. R., and Collmer, A. 1996. Bacterial pathogens in plants: Life up against the wall. Plant Cell 8:1683-1698.

Badel, J. L., Nomura, K., Bandyopadhyay, S., Shimizu, R., Collmer, A., and He, S. Y. 2003. *Pseudomonas syringae* pv. *tomato* DC3000 HopPtoM (CEL ORF3) is important for lesion formation but not growth in tomato and is secreted and translocated by the Hrp type III secretion system in a chaperone-dependent manner. Mol. Microbiol. 49:1239-1251.

Badel, J. L., Shimizu, R., Oh, H. S., and Collmer, A. 2006. A *Pseudomonas syringae* pv. *tomato avrE1/hopM1* mutant is severely reduced in growth and lesion formation in tomato. Mol. Plant-Microbe Interact. 19:99-111.

Baltrus, D. A., Nishimura, M. T., Romanchuk, A., Chang, J. H., Mukhtar, M. S., Cherkis, K., Roach, J., Grant, S. R., Jones, C. D., and Dangl, J. L. 2011. Dynamic evolution of pathogenicity revealed by sequencing and comparative genomics of 19 *Pseudomonas syringae* isolates. PLoS

Pathog. 7:e1002132. Published online.
Baltrus, D. A., Nishimura, M. T., Dougherty, K. M., Biswas, S., Mukhtar, M. S., Vicente, J., Holub, E. B., and Dangl, J. L. 2012. The molecular basis of host specialization in bean pathovars of *Pseudomonas syringae*. Mol. Plant-Microbe Interact. 25:877-888.
Bardaji, L., Pérez-Martínez, I., Rodríguez-Moreno, L., Rodríguez-Palenzuela, P., Sundin, G. W., Ramos, C., and Murillo, J. 2011. Sequence and role in virulence of the three plasmid complement of the model tumor-inducing bacterium *Pseudomonas savastanoi* pv. *savastanoi* NCPPB 3335. PLoS One 6:e25705. Published online.
Block, A., and Alfano, J. R. 2011. Plant targets for *Pseudomonas syringae* type III effectors: Virulence targets or guarded decoys? Curr. Opin. Microbiol. 14:39-46.
Boller, T., and Felix, G. 2009. A renaissance of elicitors: Perception of microbe-associated molecular patterns and danger signals by pattern-recognition receptors. Annu. Rev. Plant Biol. 60:379-406.
Bradley, D. J., Kjellbom, P., and Lamb, C. J. 1992. Elicitor- and wound-induced oxidative cross-linking of a proline-rich plant cell wall protein: A novel, rapid defense response. Cell 70:21-30.
Casper-Lindley, C., Dahlbeck, D., Clark, E. T., and Staskawicz, B. J. 2002. Direct biochemical evidence for type III secretion-dependent translocation of the AvrBs2 effector protein into plant cells. Proc. Natl. Acad. Sci. U.S.A. 99:8336-8341.
Chang, J. H., Urbach, J. M., Law, T. F., Arnold, L. W., Hu, A., Gombar, S., Grant, S. R., Ausubel, F. M., and Dangl, J. L. 2005. A high-throughput, near-saturating screen for type III effector genes from *Pseudomonas syringae*. Proc. Natl. Acad. Sci. U.S.A. 102:2549-2554.
Chisholm, S. T., Coaker, G., Day, B., and Staskawicz, B. J. 2006. Host-microbe interactions: Shaping the evolution of the plant immune response. Cell 124:803-814.
Choi, K. H., Kumar, A., and Schweizer, H. P. 2006. A 10-min method for preparation of highly electrocompetent *Pseudomonas aeruginosa* cells: Application for DNA fragment transfer between chromosomes and plasmid transformation. J. Microbiol. Methods 64:391-397.
Collmer, A., Schneider, D. J., and Lindeberg, M. 2009. Lifestyles of the effector rich: Genome-enabled characterization of bacterial plant pathogens. Plant Physiol. 150:1623-1630.
Conrath, U. 2011. Molecular aspects of defence priming. Trends Plant Sci. 16:524-531.
Cunnac, S., Lindeberg, M., and Collmer, A. 2009. *Pseudomonas syringae* type III secretion system effectors: Repertoires in search of functions. Curr. Opin. Microbiol. 12:53-60.
Cunnac, S., Chakravarthy, S., Kvitko, B. H., Russell, A. B., Martin, G. B., and Collmer, A. 2011. Genetic disassembly and combinatorial reassembly identify a minimal functional repertoire of type III effectors in *Pseudomonas syringae*. Proc. Natl. Acad. Sci. U.S.A. 108:2975-2980.
de Torres, M., Mansfield, J. W., Grabov, N., Brown, I. R., Ammouneh, H., Tsiamis, G., Forsyth, A., Robatzek, S., Grant, M., and Boch, J. 2006. *Pseudomonas syringae* effector AvrPtoB suppresses basal defence in *Arabidopsis*. Plant J. 47:368-382.
Doke, N. 1983. Involvement of superoxide anion generation in the hypersensitive response of potato tuber tissues to infection with an incompatible race of *Phytophthora infestans* and to the hyphal wall components. Physiol. Plant Pathol. 23:345-357.
Fouts, D. E., Abramovitch, R. B., Alfano, J. R., Baldo, A. M., Buell, C. R., Cartinhour, S., Chatterjee, A. K., D'Ascenzo, M., Gwinn, M. L., Lazarowitz, S. G., Lin, N. C., Martin, G. B., Rehm, A. H., Schneider, D. J., van Dijk, K., Tang, X., and Collmer, A. 2002. Genomewide identification of *Pseudomonas syringae* pv. *tomato* DC3000 promoters controlled by the HrpL alternative sigma factor. Proc. Natl. Acad. Sci. U.S.A. 99:2275-2280.
Guo, M., Tian, F., Wamboldt, Y., and Alfano, J. R. 2009. The majority of the type III effector inventory of *Pseudomonas syringae* pv. *tomato* DC3000 can suppress plant immunity. Mol. Plant-Microbe Interact. 22:1069-1080.
Hanahan, D. 1983. Studies on transformation of *Escherichia coli* with plasmids. J. Mol. Biol. 166:557-580.
Hirano, S. S., and Upper, C. D. 2000. Bacteria in the leaf ecosystem with emphasis on *Pseudomonas syringae*-a pathogen, ice nucleus, and epiphyte. Microbiol. Mol. Biol. Rev. 64:624-653.
Huckelhoven, R. 2007. Cell wall-associated mechanisms of disease resistance and susceptibility. Annu. Rev. Phytopathol. 45:101-127.
Huynh, T. V., Dahlbeck, D., and Staskawicz, B. J. 1989. Bacterial blight of soybean: Regulation of a pathogen gene determining host cultivar specificity. Science 245:1374-1377.
Jackson, R. W., Athanassopoulos, E., Tsiamis, G., Mansfield, J. W., Sesma, A., Arnold, D. L., Gibbon, M. J., Murillo, J., Taylor, J. D., and Vivian, A. 1999. Identification of a pathogenicity island, which contains genes for virulence and avirulence, on a large native plasmid in the bean pathogen *Pseudomonas syringae* pathovar *phaseolicola*. Proc. Natl. Acad. Sci. U.S.A. 96:10875-10880.
Jamir, Y., Guo, M., Oh, H. S., Petnicki-Ocwieja, T., Chen, S., Tang, X., Dickman, M. B., Collmer, A., and Alfano, J. R. 2004. Identification of *Pseudomonas syringae* type III effectors that can suppress programmed cell death in plants and yeast. Plant J. 37:554-565.
Janjusevic, R., Abramovitch, R. B., Martin, G. B., and Stebbins, C. E. 2006. A bacterial inhibitor of host programmed cell death defenses is an E3 ubiquitin ligase. Science 311:222-226.
Jones, J. D., and Dangl, J. L. 2006. The plant immune system. Nature 444:323-329.
Katagiri, F., and Tsuda, K. 2010. Understanding the plant immune system. Mol. Plant-Microbe Interact. 23:1531-1536.
Kay, S., and Bonas, U. 2009. How *Xanthomonas* type III effectors manipulate the host plant. Curr. Opin. Microbiol. 12:37-43.
Kim, J. G., Taylor, K. W., and Mudgett, M. B. 2011. Comparative analysis of the XopD type III secretion (T3S) effector family in plant pathogenic bacteria. Mol. Plant Pathol. 12:715-730.
Kim, J. G., Stork, W., and Mudgett, M. B. 2013. *Xanthomonas* type III effector XopD desumoylates tomato transcription factor SlERF4 to suppress ethylene responses and promote pathogen growth. Cell Host Microbe 13:143-154.
King, E. O., Ward, M. K., and Raney, D. E. 1954. Two simple media for the demonstration of pyocyanin and fluorescin. J. Lab. Clin. Med. 44:301-307.
Kvitko, B. H., Ramos, A. R., Morello, J. E., Oh, H. S., and Collmer, A. 2007. Identification of harpins in *Pseudomonas syringae* pv. *tomato* DC3000, which are functionally similar to HrpK1 in promoting translocation of type III secretion system effectors. J. Bacteriol. 189:8059-8072.
Labes, M., Puhler, A., and Simon, R. 1990. A new family of RSF1010-derived expression and lac-fusion broad-host-range vectors for gram-negative bacteria. Gene 89:37-46.
Levine, A., Tenhaken, R., Dixon, R., and Lamb, C. 1994. H_2O_2 from the oxidative burst orchestrates the plant hypersensitive disease resistance response. Cell 79:583-593.
Li, C., Potuschak, T., Colon-Carmona, A., Gutierrez, R. A., and Doerner, P. 2005. *Arabidopsis* TCP20 links regulation of growth and cell division control pathways. Proc. Natl. Acad. Sci. U.S.A. 102:12978-12983.
Lin, N. C., Abramovitch, R. B., Kim, Y. J., and Martin, G. B. 2006. Diverse AvrPtoB homologs from several *Pseudomonas syringae* pathovars elicit Pto-dependent resistance and have similar virulence activities. Appl. Environ. Microbiol. 72:702-712.
Lindeberg, M. 2012. Genome-enabled perspectives on the composition, evolution, and expression of virulence determinants in bacterial plant pathogens. Annu. Rev. Phytopathol. 50:111-132.
Lindeberg, M., Stavrinides, J., Chang, J. H., Alfano, J. R., Collmer, A., Dangl, J. L., Greenberg, J. T., Mansfield, J. W., and Guttman, D. S. 2005. Proposed guidelines for a unified nomenclature and phylogenetic analysis of type III Hop effector proteins in the plant pathogen *Pseudomonas syringae*. Mol. Plant-Microbe Interact. 18:275-282.
Lindeberg, M., Myers, C. R., Collmer, A., and Schneider, D. J. 2008. Roadmap to new virulence determinants in *Pseudomonas syringae*: Insights from comparative genomics and genome organization. Mol. Plant-Microbe Interact. 21:685-700.
Lindeberg, M., Cunnac, S., and Collmer, A. 2012. *Pseudomonas syringae* type III effector repertoires: Last words in endless arguments. Trends Microbiol. 20:199-208.
Livak, K. J., and Schmittgen, T. D. 2001. Analysis of relative gene expression data using real-time quantitative PCR and the 2–ΔΔCT method. Methods 25:402-408.
Lopez-Solanilla, E., Bronstein, P. A., Schneider, A. R., and Collmer, A. 2004. HopPtoN is a *Pseudomonas syringae* Hrp (type III secretion system) cysteine protease effector that suppresses pathogen-induced necrosis associated with both compatible and incompatible plant interactions. Mol. Microbiol. 54:353-365.
Mansfield, J. W. 2009. From bacterial avirulence genes to effector functions via the hrp delivery system: An overview of 25 years of progress in our understanding of plant innate immunity. Mol. Plant Pathol. 10:721-734.
Matas, I. M., Lambertsen, L., Rodríguez-Moreno, L., and Ramos, C. 2012. Identification of novel virulence genes and metabolic pathways required for full fitness of *Pseudomonas savastanoi* pv. *savastanoi* in olive (*Olea europaea*) knots. New Phytol. 196:1182-1196.
Miller, J. H. 1972. Experiments in Molecular Genetics. Cold Spring Harbor Laboratory, Cold Spring Harbor, NY, U.S.A.
Munkvold, K. R., Russell, A. B., Kvitko, B. H., and Collmer, A. 2009. *Pseudomonas syringae* pv. *tomato* DC3000 type III effector HopAA1-1 functions redundantly with chlorosis-promoting factor PSPTO4723 to produce bacterial speck lesions in host tomato. Mol. Plant-Microbe Interact. 22:1341-1355.

Mur, L. A., Kenton, P., Lloyd, A. J., Ougham, H., and Prats, E. 2008. The hypersensitive response; the centenary is upon us but how much do we know? J. Exp. Bot. 59:501-520.

O'Brien, H. E., Thakur, S., Gong, Y., Fung, P., Zhang, J., Yuan, L., Wang, P. W., Yong, C., Scortichini, M., and Guttman, D. S. 2012. Extensive remodeling of the *Pseudomonas syringae* pv. avellanae type III secretome associated with two independent host shifts onto hazelnut. BMC Microbiol. 12:141.

Oh, H. S., Park, D. H., and Collmer, A. 2010. Components of the *Pseudomonas syringae* type III secretion system can suppress and may elicit plant innate immunity. Mol. Plant-Microbe Interact. 23:727-739.

Penyalver, R., García, A., Ferrer, A., Bertolini, E., Quesada, J. M., Salcedo, C. I., Piquer, J., Pérez-Panades, J., Carbonell, E. A., Del Rio, C., Caballero, J. M., and López, M. M. 2006. Factors affecting *Pseudomonas savastanoi* pv. *savastanoi* plant inoculations and their use for evaluation of Olive cultivar susceptibility. Phytopathology 96:313-319.

Pérez-Martínez, I., Rodríguez-Moreno, L., Matas, I. M., and Ramos, C. 2007. Strain selection and improvement of gene transfer for genetic manipulation of *Pseudomonas savastanoi* isolated from olive knots. Res. Microbiol. 158:60-69.

Pérez-Martínez, I., Rodríguez-Moreno, L., Lambertsen, L., Matas, I.M., Murillo, J., Tegli, S., Jiménez, A.J., and Ramos, C. 2010. Fate of a *Pseudomonas savastanoi* pv. *savastanoi* type III secretion system mutant in olive plants (*Olea europaea* L.). Appl. Environ. Microbiol. 76:3611-3619.

Pfaffl, M. W. 2001. A new mathematical model for relative quantification in real-time RT-PCR. Nucleic Acids Res. 29:e45.

Ramos, C., Matas, I. M., Bardaji, L., Aragón, I. M., and Murillo, J. 2012. *Pseudomonas savastanoi* pv. *savastanoi*: Some like it knot. Mol. Plant Pathol. 13:998-1009.

Rodríguez-Herva, J. J., González-Melendi, P., Cuartas-Lanza, R., Antúnez-Lamas, M., Rio-Alvarez, I., Li, Z., López-Torrejon, G., Díaz, I., Del Pozo, J. C., Chakravarthy, S., Collmer, A., Rodríguez-Palenzuela, P., and López-Solanilla, E. 2012. A bacterial cysteine protease effector protein interferes with photosynthesis to suppress plant innate immune responses. Cell Microbiol. 14:669-681.

Rodríguez-Moreno, L., Barceló-Muñoz, A., and Ramos, C. 2008. In vitro analysis of the interaction of *Pseudomonas savastanoi* pvs. savastanoi and nerii with micropropagated olive plants. Phytopathology 98:815-822.

Rodríguez-Moreno, L., Jiménez, A. J., and Ramos, C. 2009. Endopathogenic lifestyle of *Pseudomonas savastanoi* pv. *savastanoi* in olive knots. Microb. Biotechnol. 2:476-488.

Rodríguez-Palenzuela, P., Matas, I. M., Murillo, J., López-Solanilla, E., Bardaji, L., Pérez-Martínez, I., Rodríguez-Moskera, M. E., Penyalver, R., López, M. M., Quesada, J. M., Biehl, B. S., Perna, N. T., Glasner, J. D., Cabot, E. L., Neeno-Eckwall, E., and Ramos, C. 2010. Annotation and overview of the *Pseudomonas savastanoi* pv. *savastanoi* NCPPB3335 draft genome reveals the virulence gene complement of a tumour-inducing pathogen of woody hosts. Environ. Microbiol. 12:1604-1620.

Roine, E., Saarinen, J., Kalkkinen, N., and Romantschuk, M. 1997. Purified HrpA of *Pseudomonas syringae* pv. *tomato* DC3000 reassembles into pili. FEBS (Fed. Eur. Biochem. Soc.) Lett. 417:168-172.

Rotenberg, D., Thompson, T. S., German, T. L., and Willis, D. K. 2006. Methods for effective real-time RT-PCR analysis of virus-induced gene silencing. J. Virol. Methods 138:49-59.

Sambrook, J., and Russell, D. 2001. Molecular Cloning: A Laboratory Manual. Cold Spring Harbor Laboratory Press, Cold Spring Harbor, NY, U.S.A.

Schechter, L. M., Roberts, K. A., Jamir, Y., Alfano, J. R., and Collmer, A. 2004. *Pseudomonas syringae* type III secretion system targeting signals and novel effectors studied with a Cya translocation reporter. J. Bacteriol. 186:543-555.

Schechter, L. M., Vencato, M., Jordan, K. L., Schneider, S. E., Schneider, D. J., and Collmer, A. 2006. Multiple approaches to a complete inventory of *Pseudomonas syringae* pv. *tomato* DC3000 type III secretion system effector proteins. Mol. Plant-Microbe Interact. 19:1180-1192.

Sory, M. P., and Cornelis, G. R. 1994. Translocation of a hybrid YopE-adenylate cyclase from *Yersinia enterocolitica* into HeLa cells. Mol. Microbiol. 14:583-594.

Tamura, K., Peterson, D., Peterson, N., Stecher, G., Nei, M., and Kumar, S. 2011. MEGA5: Molecular evolutionary genetics analysis using maximum likelihood, evolutionary distance, and maximum parsimony methods. Mol. Biol. Evol. 28:2731-2739.

Thordal-Christensen, H., Zhang, Z., Wei, Y., and Collinge, D. B. 1997. Subcellular localization of H_2O_2 in plants, H_2O_2 accumulation in papillae and hypersensitive response during barley-powdery mildew interaction. Plant J. 11:1187-1194.

Torres, M. A., and Dangl, J. L. 2005. Functions of the respiratory burst oxidase in biotic interactions, abiotic stress and development. Curr. Opin. Plant Biol. 8:397-403.

Underwood, W., Zhang, S., and He, S.Y. 2007. The *Pseudomonas syringae* type III effector tyrosine phosphatase HopAO1 suppresses innate immunity in *Arabidopsis thaliana*. Plant J. 52:658-672.

van Dijk, K., Tam, V. C., Records, A. R., Petnicki-Ocwieja, T., and Alfano, J. R. 2002. The ShcA protein is a molecular chaperone that assists in the secretion of the HopPsyA effector from the type III (Hrp) protein secretion system of *Pseudomonas syringae*. Mol. Microbiol. 44:1469-1481.

Vargas, P., Felipe, A., Michan, C., and Gallegos, M. T. 2011. Induction of *Pseudomonas syringae* pv. *tomato* DC3000 MexAB-OprM multidrug efflux pump by flavonoids is mediated by the repressor PmeR. Mol. Plant-Microbe Interact. 24:1207-1219.

Vencato, M., Tian, F., Alfano, J. R., Buell, C. R., Cartinhour, S., DeClerck, G. A., Guttman, D. S., Stavrinides, J., Joardar, V., Lindeberg, M., Bronstein, P. A., Mansfield, J. W., Myers, C. R., Collmer, A., and Schneider, D. J. 2006. Bioinformatics-enabled identification of the HrpL regulon and type III secretion system effector proteins of *Pseudomonas syringae* pv. *phaseolicola* 1448A. Mol. Plant-Microbe Interact. 19:1193-1206.

Vinatzer, B. A., Teitzel, G. M., Lee, M. W., Jelenska, J., Hotton, S., Fairfax, K., Jenrette, J., and Greenberg, J. T. 2006. The type III effector repertoire of *Pseudomonas syringae* pv. *syringae* B728a and its role in survival and disease on host and non-host plants. Mol. Microbiol. 62:26-44.

Xiao, Y., and Hutcheson, S. W. 1994. A single promoter sequence recognized by a newly identified alternate sigma factor directs expression of pathogenicity and host range determinants in *Pseudomonas syringae*. J. Bacteriol. 176:3089-3091.

Young, J. M. 2010. Taxonomy of *Pseudomonas syringae*. J. Plant Pathol. 92:S1.5-S1.14.

Zumaquero, A., Macho, A. P., Rufian, J. S., and Beuzón, C. R. 2010. Analysis of the role of the type III effector inventory of *Pseudomonas syringae* pv. *phaseolicola* 1448a in interaction with the plant. J. Bacteriol. 192:4474-4488.

AUTHOR-RECOMMENDED INTERNET RESOURCES

ASAP database: www.genome.wisc.edu/tools/asap.htm
Junta de Andalucía website: www.juntadeandalucia.es
Pfam database: pfam.sanger.ac.uk
Pseudomonas syringae genome resources home page: www.pseudomonas-syringae.org

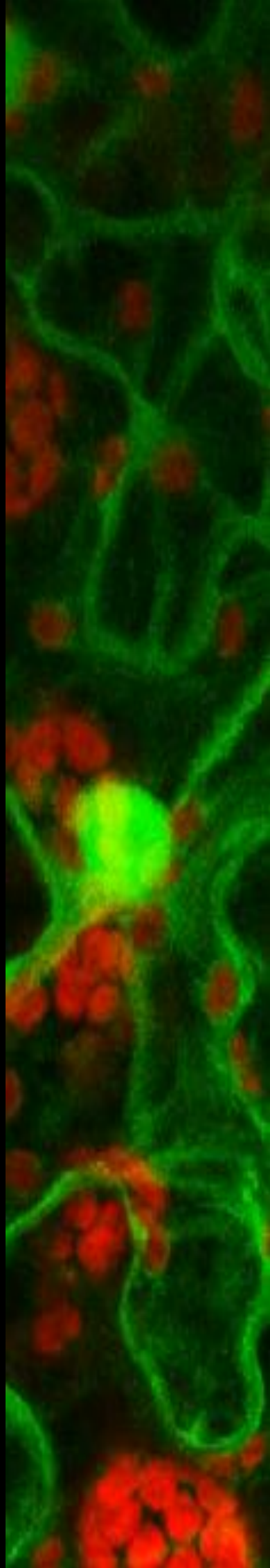

Instituto de Hortofruticultura Subtropical y Mediterránea "La Mayora" (IHSM-UMA-CSIC)
Universidad de Málaga
Área de Genética